# Session 5:

# Application studies and implementation aspects

# Coupled human-environment system approaches to desertification: linking people to pixels

E. F. Lambin[a], H. Geist[a], J. F. Reynolds[b,c], D. M. Stafford-Smith[d]

[a] University of Louvain, Louvain-la-Neuve, Belgium
[b] Division of Environmental Science and Policy, Nicholas School of the Environment and Earth Science
[c] Department of Biology, Phytotron Bldg., Duke University, Durham, NC 27708-0340, USA
[d] CSIRO Sustainable Ecosystems, Centre for Arid Zone Research, CSIRO, Alice Springs, Australia

## 1 INTRODUCTION

The definition of desertification used by the Convention to Combat Desertification (CCD) makes it clear that whilst biophysical components of ecosystems and their properties are involved (e.g., soil erosion, loss of vegetation), the interpretation of change as 'loss' is dependent upon the integration of these components within the context of the socio-economic activities of human beings. The CCD's definition of desertification explicitly focuses on the linkages between humans and their environments that affect human welfare in arid and semi-arid regions.

Unfortunately, the CCD definition of desertification is not amenable to easy quantification, especially as a single number or synthetic index. Most estimates of desertification are derived solely from either biophysical factors (e.g., soil erosion, loss of plant cover, change in albedo) or socio-economic factors (decreased production, economic loss, population movements, etc), but rarely both types simultaneously.

This paper is divided in two parts: a first part provides the rationale for approaching desertification by integrating biophysical and socio-economic data, and a second part discusses methodologies to achieve that integration, by linking remote sensing data with household survey data.

## 2 THE CAUSES OF DESERTIFICATION

Land degradation in drylands is still poorly documented and its causes are hardly understood [4]. On the one hand, proponents of single-factor causation suggest various primary causes, such as irrational or unwise land mismanagement by nomadic pastoralists and growing populations in fragile semi-arid ecosystems. On the other hand, desertification has been attributed to multiple causative factors that are specific to each locality, revealing no distinct pattern. There has also been a great deal of debate on whether the causes of desertification lie in the socio-economic or biophysical spheres (human-induced land degradation *versus* climate-driven desiccation).

Geist and Lambin [2] carried out a worldwide review of the causes of desertification based on 132 carefully selected case studies. Their aim was to generate a general understanding of the proximate causes and underlying driving forces of desertification, including cross-scalar interactions of causes and feedbacks, while preserving the descriptive richness of these case studies. Results showed that desertification is driven by a limited suit of recurrent core variables, with identifiable regional patterns of causal factor synergies.

At the proximate level, desertification is best explained by the combination of multiple social and biophysical factors, rather than by single variables. Dominating the broad clusters of proximate factors is the combination of agricultural activities, increased aridity, extension of infrastructure, and wood extraction (or related extractional activities), with clear regional variations. In particular, agricultural activities and increased aridity are associated together.

At the underlying level, desertification is also best explained by regionally distinct combinations of multiple, coupled social and biophysical factors, and drivers acting synergistically rather than by single-factor causation. A recurrent and robust broad factor combination implies the interplay of climatic factors leading to reduced rainfall, agricultural growth policies, newly introduced land use technologies, and malfunct land tenure arrangements which are no longer suited to contemporary dryland ecosystem management.

It is mostly the interactions between multiple causal factors that lead to desertification. A frequent pattern of causal interactions stems from the necessity for water-related infrastructures that are associated with the expansion of irrigated croplands and pastures. Typically, newly introduced irrigation infrastructures induce accelerated in-migration of farm workers into drylands, and often stir more commercial-industrial developments as well as the

growth of human settlements and related service economies. Irrigation infrastructure is often nested in a system of larger infrastructure extension related to regional economic growth. Commonly, road extension paves the way for the subsequent extension of irrigation, and (semi)urban land uses. In the developing world, underlying these proximate factors are national policies aimed at consolidating territorial control over remote, marginal areas, and attaining self-sufficiency in food and clothing, with rice and cotton being the key irrigated crops.

## 3 CONSEQUENCES OF DESERTIFICATION

Desertification is only a problem if it threatens the short- or long-term welfare of users of affected ecosystems. Actually, the definition of what is a significant change in environmental conditions depends on the uses to which the environment is put [7]. Since natural resources are only one of many elements that make up livelihoods, which exist in very complex environmental, social and political milieux, the impacts of desertification can only be evaluated in their social context [13]. Empirical measures of land degradation must therefore be linked to socio-economic variables that represent how people collect information to evaluate threats to their natural resources, human behaviours and motivation with respect to resource management, and the capacity of land managers to respond to potential threats through their access to technology, social and economic resources and their risk-avoidance strategies [5, 12].

From the socio-economic point of view, most consequences of desertification (especially in pastoral systems) are a direct result of the decline in 'productivity' or the capacity of the land to support plant growth and animal production. During early stages of desertification such losses are compensated by the social resilience of the local human populations, especially in developing countries, or by economic inputs from government [47]. However, when certain thresholds are crossed, social resilience or government subsidies may not be enough to compensate for the loss of productivity, and this fuels a battery of socio-economic changes that range from modifications in trade promoted by lower agricultural production to large population migrations [1]. Biophysical and socio-economic indicators need always to be associated for any meaningful evaluation of the severity, for a given stakeholder, of land degradation.

## 4 INTEGRATED APPROACH TO DESERTIFICATION

The simultaneous assessment of biophysical and socio-economic drivers and consequences of desertification has been recognized as one of the most challenging topics for further research. Stafford Smith and Reynolds [9] proposed the Dahlem Desertification Paradigm (DDP) that is unique in two ways: it attempts to capture the multitude of interrelationships within human-environment systems that cause desertification within a single, synthetic framework; and it is testable, which ensures that it can be revised and improved upon. The DDP consists of nine assertions, which embrace a hierarchical view of land degradation and highlight key linkages between socio-economic and biophysical systems at different scales.

The monitoring of desertification is an increasingly important development in the management of dryland areas. The establishment of long-term and rigorous monitoring programs is an effective way to assess the status of natural resources and the evolution of desertification processes. The challenge is to monitor not just biophysical indicators but the coupled human-environment system as a whole. This requires methods to link biophysical data to socio-economic data on land managers, to capture the varying capacity of local agents to cope and respond to a decline in land productivity.

Informal monitoring by land managers tends to focus on those factors that they perceive readily and that vary from day to day as a result of the variable external environment – i.e., "fast" variables such as rainfall, grass growth, animal condition, market prices [7]. However, there is a growing acceptance that a small number of "slow" variables act as the critical determinants in human-environment systems [3]. Monitoring systems of desertification should therefore be designed around these slow variables – e.g., shrub encroachment, cropland expansion, change in land tenure, opening of new export markets for agricultural products.

## 5 LINKING PEOPLE TO PIXELS

Recent studies demonstrated the complementarity of remote sensing and socio-economic survey data for understanding causes, processes and impacts of land-use/land-cover changes. Creating a direct link between spatially-explicit land cover information, as derived by remote sensing, and information on land-use change processes requires the development of new methods and models which are merging landscape data with data on human behaviour [6]. Several studies combined socio-economic household survey data and remote sensing data to better understand processes of land-use change. One of the major challenges of merging these data from heterogeneous sources concerns the definition of the appropriate spatial observation units, i.e., the appropriate level

of aggregation of information derived from the domains of social phenomena and natural environment [25]. In remote sensing, the spatial unit of observation is not directly associated to any unit of observation in the social sciences, e.g. individuals, households or communities.

Rindfuss et al. [8] provide an in-depth discussion of the methodological and practical problems in designing a study linking household and remotely sensed data, including issues of ephemeral households, boundaries of farms and villages, prospective or retrospective study designs, differences in sampling between land-to-people or people-to-land approaches, connection with households through land use or land ownership, plot and pixel size mismatch, sample size, etc. One of the most difficult problems is the difficulty to protect the identity of surveyed households, for obvious confidentiality reasons, once their plots have been georeferenced. Releasing survey data with geographic coordinates associated with the plots used or owned by every household is tantamount to disclosing the identity of the respondent households [8].

## 6 THE CHALLENGES OF LINKING PEOPLE TO PIXELS IN DRYLANDS

Land use is drylands is characterised by a number of features that make the fine scale linking of socio-economic and remote sensing data particularly difficult: extensive agriculture (including pastoralism) practiced over large plots with fuzzy boundaries and communal ownership; often complex and flexible tenure arrangements regulating land access across space and time; mixture of natural vegetation and managed rangelands or croplands (e.g., tree cultivation); multifunctional landscapes (e.g., grazing in crop fields after the harvest); mobility of households and their livestock in transhumant or nomadic farming systems: households move across the landscape in search of forage and water, in the face of environmental uncertainty and seasonal fluctuations; large inter-annual variability in climatic conditions; and risk-avoidance land use strategies that can only be understood by adopting a long-term perspective, cutting across several climatic cycles.

A few pioneer studies have taken place in rangelands. They have combined socio-economic with remote sensing data following different approaches: (i) socio-economic survey to explain or supplement observed patterns of land-cover change; (ii) overlay of spatially-explicit socio-economic and land cover data, and proximity analyses; (iii) interpretation of spatial patterns of land use in terms of land use practices; or (iv) joint statistical analysis of spatially-explicit household survey and land cover data

## 7 CONCLUSION

The above paper has first provided compelling reasons for an integration of biophysical and socio-economic variables to assess desertification status. This is related to the nature, causes and consequences of desertification. It then discussed new methodologies linking remote sensing data to household survey data to achieve this goal. These methodologies have still to be widely developed and applied to land use in drylands, which poses particularly difficult challenges.

Understanding complex human-environment dynamics in drylands requires moving beyond simple map overlay approaches. Remote sensing can add to the broader human ecological analysis and spatial analysis must be informed by the more complete understanding of causal connections uncovered by detailed field work [10]. Remote sensing is just one step in a broader, more comprehensive methodology.

## ACKNOWLEDGEMENT

This paper has greatly benefited from ideas developed within several workshops of the Land-Use and Cover Change (LUCC) project.

## REFERENCES

[1] FERNANDEZ, R.J., ARCHER, E.R.M., ASH, A.J., DOWLATABADI, H., HIERNAUX, P.H.Y., REYNOLDS, J.F., VOGEL, C.H., WALKER, B.H., AND WIEGAND., T., 2002: Degradation and recovery in socio-ecological systems: A view from the household/farm level. Pages 297-323. In: REYNOLDS J.F. AND STAFFORD SMITH, D.M. (EDS.): Global Desertification: Do Humans Cause Deserts? (Dahlem Workshop Report 88), ed.. Berlin: Dahlem University Press.
[2] GEIST, H.J. AND LAMBIN., E.F., 2004: Dynamic causal patterns of desertification. *Bioscience* 54, pp. 817-829
[3] GUNDERSON, L.H., HOLLING, C.S., 2002: Panarchy: understanding transformations in human and natural systems. Island Press, Washington, D.C.
[4] LAMBIN, E.F., GEIST, H.J. AND LEPERS, E., 2003: Dynamics of land-use and land-cover change in tropical regions. *Annual Review of Environment and Resources* 28, pp. 205-241.
[5] LAMBIN E.F., 2005: Conditions for sustainability of human-environment systems: information, motivation, and capacity. Global Environmental Change, in press.

[6] LIVERMAN, D., MORAN, E.F., RINDFUSS, R.R. AND STERN, P.C. (EDS.), 1998: People and pixels: linking remote sensing and social science. National Acadamy Press, Washington, D.C.
[7] LYNAM, T. AND STAFFORD SMITH, M., 2003: Monitoring in a complex world: seeking slow variables, a scaled focus and speedier learning. In: ALLSOPP, N., PALMER, A..R.., MILTON, S.J., KIRKMAN, K.P., KERLEY, G.I.H., HURT, C.R.. AND BROWN, C.J. (eds.): Proceedings of the VIIth International Rangelands Congress. Durban, pp. 617-629.
[8] RINDFUSS, R.R., S.J. WALSH, V. MISHRA, J. FOX AND G.P. DOLCEMASCOLO, 2003: Linking household and remotely sensed data: Methodological and practical problems. In: People and the environment: Approaches for linking household and community surveys to remote sensing and GIS, eds. J. Fox, R.R. Rindfuss, S.J. Walsh and V. Mishra, pp. 1-29. Boston, Dordrecht, London: Kluwer Academic Publishers.
[9] STAFFORD SMITH, D.M. AND J.F. REYNOLDS, 2002: The Dahlem Desertification Paradigm: A new approach to an old problem. In: Global Desertification: Do Humans Cause Deserts? Eds. J.F. Reynolds and M. Stafford Smith. Dahlem University Press, Berlin, Germany
[10] TURNER, D.T., 2003: Methodological reflections on the use of remote sensing and geographic information science in human ecological research. *Human Ecology* 31 (2), pp. 255-279.
[11] VOGEL, C.H. AND J. SMITH, 2002: Building social resilience in arid ecosystems. In: Global Desertification: Do Humans Cause Deserts? Eds. J.F. Reynolds and M. Stafford Smith, pp. 149-166. Dahlem University Press, Berlin, Germany
[12] WARREN, A., BATTERBURY S. AND OSBAHR H., 2001: Soil erosion in the West African Sahel: a review and an application of a “local political ecology” approach in South West Niger. Global Environmental Change 11, pp. 79-95.
[13] WARREN, A. 2002. Land degradation is contextual. *Land Degradation & Development* 13, pp. 449-459.

# What is Desert*Net?
# Scientific networking to combat desertification

M. Akhtar-Schuster[a], C. Martius[b], A. Rieser[c]

[a] Biocentre Klein Flottbek and Botanical Garden, University of Hamburg, Germany, email: makhtar-schuster@botanik.uni-hamburg.de
[b] Center for Development Research (ZEF), University of Bonn, Germany
[c] Agricultural Sciences and Resource Management in the Tropics and Sub-tropics (ARTS), University of Bonn, Germany

## ABSTRACT

Drylands make up 41% of the global land surface, and a third of the human population (status 2000) lives in these drought-, and desertification-prone areas (Millennium Ecosystem Assessment, 20051). The MA (2005) estimates with medium certainty (65-85% probability) that approximately 10-20% of the drylands - thus, between 6 million and 12 million km²! - are already degraded. 10 years after the ratification of the UN Convention to Combat Desertification (UNCCD), desertification is still proceeding at an alarming rate. In many dryland countries rural households are affected to the extent that the deterioration of natural resources has led to increased poverty, conflicts and human displacement. The four scenarios developed by the MA underscore that desertified areas are likely to increase, whereby poverty and unsustainable land use systems in future will remain the driving forces for triggering desertification. It seems to be necessary to develop new bonds of co-operation and synergies between scientific disciplines, politics, the economic sector, development agencies and affected communities in order to halt the deterioration of productive lands. The German Scientific Network to Combat Desertification (Desert*Net, www.desertnet.de) was founded as an interdisciplinary network that serves as an interface for communication and knowledge transfer to prevent and combat desertification.

**Keywords**: Desertification, interdisciplinarity, participation, scientific networking

## 1 INTRODUCTION

Solving today's ecological and socio-economic problems in drylands cannot be undertaken without the integration of science at all levels of policy making for sustainable development. Besides identifying the problem on the basis of mostly mono-disciplinary excellence, the eminent problem of desertification also requires a more marked and stronger commitment of science towards finding mechanisms to rehabilitate or to restore degraded lands, and to actively examine cost-efficient and implementable prevention strategies. Where land use rights, and thus the regulation or non-regulation of human activities in the utilisation of natural resources are concerned, integrated science is required in order to create tools for preventing and combating desertification. Desert*Net member institutes are very active in the areas of identifying the causes and effects of desertification, rehabilitation and sustainable development in drylands. However, in order to be grounded and achieve multiplier effects, these scientific tools must be firmly embedded in the local realities of the affected areas. Besides the interdisciplinary approach to combat and/or to prevent desertification, science requires a stronger stakeholders' involvement. Thus, a strong commitment for participation processes is indispensable for research on sustainable development.

## 2 THE STRUCTURE AND AIMS OF DESERT*NET

Desert*Net's expertise is based on an interdisciplinary group of scientists with long-term field and laboratory experience in basic and applied research on desertification in over 40 countries. The major aims of the German Scientific Network to Combat Desertification (Desert*Net) are to support bilateral and multilateral activities for sustainable land use systems in degraded areas of developing or transition countries. Desert*Net closely co-operates with the United Nations Convention to Combat Desertification (UNCCD). E.g., in 2002 member institutes of Desert*Net organized the meeting of the UNCCD's Committee on Science and Technology (CST) in Hamburg. The organisation of national and international conferences, workshops and exhibitions partly together with the

[1] Millennium Ecosystem Assessment, (2005): Ecosystems and human well-being: Desertification synthesis. http://www.maweb.org/en/Products.aspx.

UNCCD secretariat in Bonn have enhanced public and media awareness on desertification and have also sensitised the public that desertification is not only "their" problem but also controlled by the consumer habits and policies of the ´North´. This network scientifically supports innovative research concepts which are feasible and applicable. Member institutes of Desert*Net co-operate with countries affected by or prone to desertification in the line of technical and methodological training, scientific knowledge transfer and applied field research.

## 3 CREATING POLICY-RELEVANT MECHANISMS IN DESERT*NET

The addressees of this network also lie beyond the scientific community. They are found in development agencies (governmental and non-governmental), ministries and local communities. Much of the existing research for sustainable development, however, does not reach the level of policy making. In order to strengthen the dialogue between science and development agencies, Desert*Net is at present developing a science plan on research for development. The science plan delineates an agenda with concrete deliverables which have to be delivered in a defined time that will support the implementation of the UNCCD.

In order to pool, analyse and disseminate best practice options for sustainable development in drylands, and to strengthen the dialogue between science and policy level, the German Desert*Net together with scientists from Belgium1 and France2 have started organizing a European network. The Declaration of the European Desert*Net outlines the major aims of the European Desert*Net (see below), and invites interested parties – individuals and institutions - from all European countries to join this network.

In July 2005 in Potsdam, within the French-German Workshop for Strengthening Bilateral Research for sustainable development, the French Ministry of Education and Research (Ministère de l'education nationale, de l' enseignement supérieur et de la recherche) and the German Ministry of Education and Research (Bundesministerium für Bildung und Forschung) invited French and German scientists working in drylands to develop joint activities in the fields of biodiversity and desertification: The interactive role of (a) the change of biodiversity and (b) desertification processes in a context of degradation and of sustainable use of natural resources. The meeting showed numerous possibilities for future co-operation in the fields of biodiversity and desertification. Currently, complementary projects exist in both countries. It was proposed to merge specific projects, especially in the fields of methods and standards. Thus, joint initiatives can be developed by close partnership of already existing programmes. Additional initiatives are proposed for innovative approaches and joint visibility. For instance, socio-political topics and also scientific structures with high political implication were highlighted for bilateral co-operation. Measures for strengthening structures for the continuous exchange and transfer of scientific knowledge at all scientific levels were discussed. Finally, it was proposed to develop small working groups in order to further elaborate future co-operation on the identified topics. The German DesertNet and the French CSFD volunteered to monitor the progress.

1 Belgian Expert Group on Desertification to support Ministry for Development Cooperation

2 Comité Scientifique Français de la Désertification (CSFD)

## European DESERT*NET

## DECLARATION
## FOR A EUROPEAN NETWORK FOR RESEARCH ON DESERTIFICATION

Mitigating the effects of drought, combating desertification and alleviating poverty in drylands are challenges whose importance should be sufficiently recognized within the context of global environmental changes and sustainable development.

We, members of European interdisciplinary groups of scientists, active in basic and applied research on land degradation/desertification, directly related to poverty alleviation, intend to coordinate our activities in view of possible collaboration at national and international level.

Our major objectives are:

- To **identify and analyse the pressing problems** with regard to drought, land degradation/desertification and poverty;
- To review **the state of the art** of European scientific knowledge and know-how concerning this global problem;
- To identify, through networking, **success stories and best practices** resulting from scientific research, and to create multipliers and accelerators for their implementation;
- To identify gaps and develop **innovative basic research** in these areas;
- To develop **applied research** in view of its use in arid, semi-arid and dry sub-humid areas, thereby focusing on users' needs, interdisciplinarity and integration;
- To strengthen and support **European research capacities** in order to promote scientific cooperation;
- To structure and facilitate the **communication and transfer** of know-how and technologies within the European DESERTNET and towards affected countries;
- To establish and intensify **linkages with research partners** inside and outside Europe;
- To stimulate **application of appropriate research findings** in the drylands through participatory processes, involving civil society, NGOs and CBOs;
- To establish a **mechanism for effective and successful policy advice** and for **public awareness raising**.

For this purpose, the European DESERTNET is open to all European scientists wanting to join our association and collaborate with us. We support the UN environmental conventions, in particular the UN Convention to Combat Desertification (UNCCD). We intend to strengthen the cooperation with its scientific body, the Committee on Science and Technology (CST) and are open to collaborate with all other UNCCD panels or groups, in need of scientific input. We are also looking forward to collaboration with international organisations, programmes and agencies in need of scientific information or advice. We are prepared to put our knowledge and understanding to the service of combating desertification and creating sustainable livelihoods in drylands through sound scientific work.

First Signatories

Mariam Akhtar-Schuster, Marc Bied-Charreton, Murielle Eyletters, Norbert Jürgens, Christopher Martius
Willem Van Cotthem
Bonn, 24th June 2005

# Application of Remote Sensing Techniques and GIS for Land Degradation Monitoring at Pilot Scale in the Syrian Coastal Areas

M. Al-Abed[a]

[a] General Organization of Remote Sensing (GORS), P.O.Box 12586, Damascus, Syria, email: ibrahim5@scs-net.org

## ABSTRACT

The issue of land resources conservation is strongly felt in Syria like in most other Mediterranean Countries. The present study is focusing on two pilot areas in the Syrian coastal area for further intensive investigation on the dominant erosion process and evaluation trends, determination of final criteria and procedures for consideration of socio-economic parameters, determination of priority areas for investigated pilot areas, identification of remedial measures, and development of draft recommendations. The detailed analysis at this pilot scale lead to finalizing the descriptive erosion maps and priority maps for both areas based on using remote sensing techniques and the erosion risk map developed at the reconnaissance scale. The final soil erosion maps provide useful tools for the knowledge and interpretation of the erosion processes that are present in the pilot areas as well as they are a planning tool for the erosion control.

**Keywords:** remote sensing, GIS, land degradation, hot spots, descriptive erosion map, priority map

## 1 INTRODUCTION

The present study is part of the documentation of the results of the EU LIFE THIRD Countries regional project "Improving Coastal Land Degradation Monitoring in Lebanon and Syria" and describes the development in Syria of PAP/RAC-MAP-UNEP[1] Erosion Mapping and Management Programme.

The coastal landscape in Syria is the result of interactions between human activities and natural environment. The soil is the essential component interfacing these relationships, and consequently has become deeply affected. Among the natural factors which influence this phenomenon, precipitation, land relief, and vegetation cover offer conditions which are particularly unfavourable. However, in last decades, more favourable socio-economic circumstances have led to substantial decrease in the traditional erosive agents, and the government paid considerable attention to the problem, resulting in the restoration of a considerable number of forests.

The Kurdaha and Sheikh Bader areas were selected as the pilot areas for the application in Syria of the common consolidate methodology of Mapping of Rainfall-Induced Erosion processes in the Mediterranean Coastal Area. Consequently, this will form Syria contribution to the overall PAP/RAC-MAP-UNEP Erosion Mapping and Management Programme.

## 2 LOCATION OF THE STUDY AREA

The coastal region is located in the northwestern part of Syria bordered in the west by the Mediterranean Sea of coastline of about 220 km. The region can be viewed as a major natural resource and "transitional" in character, linking the Mediterranean Sea with arid zones of the interior Syria and the Arab world.

The coastal region of Syria covers about 4190 km2 (2%) of the national territory. The region is divided into two main districts; Latakia district in the north with 2300 km2 total area and Tartous district in the south with 1900 km2 area. Unfortunately, due to lack of time and fund all the detailed analysis activities was implemented up to 800 meters above sea level.

Two pilot areas were identified in the coastal region of Syria; the first pilot area is Kurdaha and the other is Sheikh Bader. The two pilot areas were selected based on a number of criteria chosen to allow the selection of the most representative areas for the whole Syrian coastal region. These criteria include: eco-geological conditions,

[1] PAP/RAC: Priority Actions Program/ Regional Activity Center; MAP: Mediterranean Action Plan; UNEP: United Nations Environment Program.

dimensional aspects, physical and geomorphological conditions, socio-economics, political, strategic and logistical criteria, and availability of information.

The Kurdaha area is located in the center to northern part of the coastal mountains, about 30 km southeast of Latakia with a total area of 40040 hectare. It is bordered by the Ghab-rift in the east and the Syrian coastal plain in the west. The second pilot area is Sheikh Bader with a total area of 20279 hectare. The detailed analysis activities was executed in these two pilot areas up to 800 meters only due to the project limitations. Thus, the generated maps are up to this altitude only and don't cover the entire real areas of Kurdaha and Sheikh Bader. Consequently, the filed investigation has been done on 235 Km2 in Kurdaha area instead of 400.40 Km2 (the total area), and on 188 Km2 in Sheikh Bader area instead of 200.79 Km2 (the total area).

Relevant features of these two pilot areas are: great variety of ecosystems, great human pressure, land abandonment, large areas are affected by soil erosion processes, and socio-economic condition of the regions in economic recession, except for the partially flat and gently sloping lands where agriculture is developed.

## 3 MAPPING METHODOLOGY AND RELATED FIELD WORK

Topographic maps at 1:50000 scale, and Landsat7-ETM image taken in March 2001, have been used for the executing of the project. The project activities, which have been completed in about 30 months, consist of image interpretation, land surveys and field work, as well as office work. The investigations of soil erosion in the pilot areas were carried out using modern remote sensing techniques and modern methods of mapping of erosion processes with the aid of Geographic Information System, GIS, modified to suit the conditions in the Mediterranean zone.

Mapping of water erosion in Kurdaha and Sheikh Bader areas was assessed according to the common consolidate methodology of Mapping of Rainfall-Induced Erosion processes in the Mediterranean Coastal Area, (PAP/RAC, 1997). The method is based on elaboration of the GIS in accordance with the criteria and standards for elaboration of Landsat image and maps with scale 1:50000, using ArcGIS, Arcview, Spatial Analyst as well as ERDAS program packages. These programmes allow working out of numerous maps in digital form, and carrying out overlay and connection with databases.

The descriptive approach consists of the application of the above mentioned methodology to the polygons of the erosion status map resulting from the first phase (predictive approach). Two procedures are used for such application: image interpretation, and field observation. Easily identifiable by image interpretation are wastelands (rock outcrops, stony or sandy areas) and some type of afforestations and plantations. Furthermore, field observations and erosion process identification procedures consist of two steps:

***Step 1:*** Defining the grade of erosion risks/potentials and causative erosive agents for stable/ stabilized environments:

The procedure only applies to stable, non erosion affected areas which are defined as showing very view or no evidence sign of erosion, with well developed top soil and good soil structure; these areas are usually unused or very lightly/suitably used by man: either the present vegetation cover is adequate and/or topographic and soil conditions prevent erosion. Different types of stable and/or rehabilitated areas are identified according to their use, management and grade of erosion risk: the erosion risk ranges from 0 to 3. In most cases, the main erosion risk causative agents are easily identifiable; they might be indicated by extra codes.

***Step 2:*** identifying and defining the type of dominant erosion processes and its relative intensity and evolutive trend for unstable environments:

The procedure only applies on unstable areas which are affected by one or several erosion processes ranging from slight to moderate and sever degradation which for each specific process can be assessed in relative terms of instability (depth of gullies, volume of removed soil), or extension of space affected (localized, dominant or generalized). In total, about 391 sites have been described using GPS[1] devices, among them 210 sites in Kurdaha area and the rest 181 sites in Sheikh Bader area. For each site the geographical location as well as the erosion situation has been identified with the Type, Grade of Risk and Causative Agents for the Stable Area, and with the Type, Grade of Extent and Expansion Trend for Unstable Areas.

[1] GPS: Global Positioning System

## 4 DESCRIPTION OF DESCRIPTIVE EROSION MAP

Based on the field description and investigation the Descriptive Erosion Maps for Kurdaha area and Sheikh Bader area were finalized, as shown in **Map 1** and **Map 2.**

Most of the areas of *Kurdaha* include stable and stabilized zones which are not affected by active erosion. According to the Kurdaha descriptive erosion map, the total area of the lands having little to high erosion risk spread over 170 km$^2$ and account for 42 % of Kurdaha total area and form 72% of the area up to 800m with the main causative agents belong to human activity and topography. While 16 % of the total area (27% up to 800m) is covered by unstable zones in which bad land management, sheet and gully erosion are active.

The stable areas with low to moderate erosion risk form about 23% of the total surface area, the stable areas with no erosion risk form about 8% of the total area, the stable areas with high erosion risk 12%, and the areas in critical state account for 0.3 % of the total area.

The "Multiple process due to bad land management" is the predominant form of unstable area and form 8% of the total area (14% up to 800m). This category is present in the southern and southeastern parts. Sheet erosion is the second predominant form of erosion and spread over 6% of the total area (9% up to 800m). Mainly, the sheet erosion occur in the northwestern and southeastern parts. The southern part of Kurdaha city is dominated by unstable situation with gully erosion 1.6% of the total area where the individual gullies is the dominant type.

It is remarkable that managed areas with agricultural use extend over 18% of Kurdaha total area with low to moderate risk is the dominant instability risk grade. This category located mainly in western flat areas. The unmanaged areas with potential for forestry use only account for 9% of the total area, the low to moderate risk grade account for 6.5%, this area spread mainly in the eastern parts of Kurdaha, **Map 1** (Kurdaha descriptive erosion map). The codes on the polygons of the map, multiple digits and letters, correspond to the legend of descriptive phase.

While for *Sheikh Bader*, according to data obtained from the mapping activities using the predictive approach, the erosion status in Sheikh Bader is rather worse than that of Kurdaha area. About 38% of Sheikh Bader total area is fall under the category unstable areas in which bad land management and sheet erosion are predominant. While the stable areas account for 54% of Sheikh Bader total area. As for Kurdaha stable areas, the main causative agents belong to human activity and topography. About 27% of the total area (17% covered by dominant type) is affected by bad land management and thus classified under unstable areas category. The main reason for this classification is that erosion processes are active due to presence of partly destroyed terraces or abandoned terraces over large parts of Sheikh Bader district in particular in the northwestern parts. About 10% of the total area is affected by sheet erosion in the north and northwestern areas.

The dominant types of stable areas in the region, mainly in northern and northeastern parts, are unmanaged areas with potential for forestry use only (18% of the total area), unmanaged areas with agriculture potential (12% of the total area) located in the southern parts, and managed areas with agriculture potential (10%) in the southern east and eastern parts, **Map 2 (**Sheikh Bader descriptive erosion map). The codes on the polygons of the map, multiple digits and letters, correspond to the legend of descriptive phase..

## 5 IDENTIFICATION AND PRIORITISATION OF FUTURE INTERVENTION AREAS (HOT SPOTS)

Successful land degradation control is based on the efficient use of available resources and therefore needs the establishment of clear priorities for both identification and planning of future interventions in the framework of control programmes. In order to facilitate this task, a prioritisation procedure was developed, integrating the results of the physical assessment and related descriptive mapping with the aggravating socio-economic conditions and further considering actual and potential land use values according to different views, notably the perception of the local population, established national policies and assessment of potential for forestry, agricultural use and other land use forms. For the different criteria, a rating grid from 1 (lowest possible score) to 3 (highest possible score was applied.

In total for Kurdaha area, about 8.49 % (19.95 km$^2$) of the assessed area fall into the *high priority class* whereas 29.53 % (69.39 km$^2$) were classified as medium priority areas and 61.03 % (143.4 km$^2$) as low priority areas. The high priority areas in Kurdaha area were identified as unstable areas showing active erosion processes such as: dominant multi process due to bad land management because the terraces are either degraded, partly-destroyed, broken, collapsed or abandoned terraces, dominant gully networks, and dominant sheet erosion. In the *medium priority class*, the stable areas form 12.26 % (28.78 km$^2$) of the whole assessed area. These areas mainly comprise rehabilitated areas by means of terraces and a high instability risk. A smaller part is managed areas with

agricultural use with a high instability risk, and some areas are potential for forestry use only with high instability risk. Also some non-used wastelands with a high instability risk fall into the medium priority class. With regard to unstable areas, small proportion has been identified as medium priority (17.27 % of the whole assessed area, i.e. 40.58 $km^2$). These areas showing active erosion processes with different degrees of instability risk such as: localized gully networks, localized and dominant rill erosion, sheet erosion, multi process due to bad land management because the terraces are either degraded, partly-destroyed, broken, or abandoned terraces, and individual quarry. In the *low priority classes*, the stable areas are dominant (59.84 % of the whole assessed area, i.e. 140.65 $km^2$). These areas include all types of stability conditions as shown in the above table. While the unstable areas account for small proportion which is 1.19 % (2.75 $km^2$) of the whole area. The priority classes for Kurdaha can be illustrated in **Map 3** (Kurdaha priority map).

For Sheikh Bader area, about 16.17 % (30.39 $km^2$) of the assessed area fall into the high priority class whereas 39.88 % (74.91 $km^2$) were classified as medium priority areas and 42.53 % (79.92 $km^2$) as low priority areas. In the *high priority classes* in Sheikh Bader area, the unstable areas are dominant and showing two unstable conditions: dominant multi process due to bad land management due to the terraces are either degraded, partly-destroyed, broken, collapsed or abandoned terraces, and dominant sheet erosion. In the *medium priority class*, the stable areas form 15.26 % of the whole assessed area, i.e. 28.68 $km^2$). These areas mainly comprise all types of stable areas with exception for stable non-used wastelands. With regard to unstable areas, larger proportion has been identified as medium priority and account for 24.62 % of the whole assessed area, i.e. 46.23 $km^2$). These areas showing mainly two dominant unstable conditions, sheet erosion and multi process due to bad land management with varying degrees of instability risk. In the *low priority classes*, the stable areas form about 42.53 % (79.92 $km^2$) of the whole area. These areas include all types of stability conditions as shown in the above table. The above mentioned priority classes for Sheikh Bader area can be illustrated in **Map 4** (Sheikh Bader priority map).

Field data show that, for all those areas, erosion processes are much more active not only where no conservation practices are applied but also where such practices are not maintained. Furthermore, degraded or partly-destroyed terraces may cause or even accelerate intensive erosion processes, therefore, maintenance interventions such as repairing partially-collapsed terraces seem to have the same importance as the application of new land management measures.

## 6 MANAGEMENT RECOMMENDATIONS FOR PILOT AREAS

Effective land degradation control consists of site-specific land management and related remedial measures. This goal require identification of specific intervention areas, their type of problems and grade of priority, and the selection of remedial measures to be applied; specification of institutional and administrative arrangements, including local contributions, and participation modalities at both decisional and implementation levels; and monitoring indicators for on-going activities and potential environment impacts.

After identification of the intervention areas, the remedial measures to be applied have been discussed in detail including general recommendations for their application in the two pilot areas. In summary, **for stable areas** the preventive measures needed should emphasis on forest management and forest treatment, construction of terraces, applying contour tillage, installation of anti-erosive structures mainly check dams, and applying drainage control and land consolidation measures on active erosion processes to minimize disturbance of highly susceptible areas. While, the curative measures to be applied for the stable intervention areas should emphasis on the education of the rural community to the importance of forestland and land management, execution of reclaiming projects, and construction of fire break lines. **For the unstable areas**, the curative measures to be applied should be directed to construction of water outlets and rural roads, provide financial aids and training to rural population, and applying reforestation programs and forest management activities. While, the protective measures needed for the unstable intervention areas show the importance of two main procedures; instruct and educate the local people to the importance of forest lands and land management as well as execution of reclaiming projects.

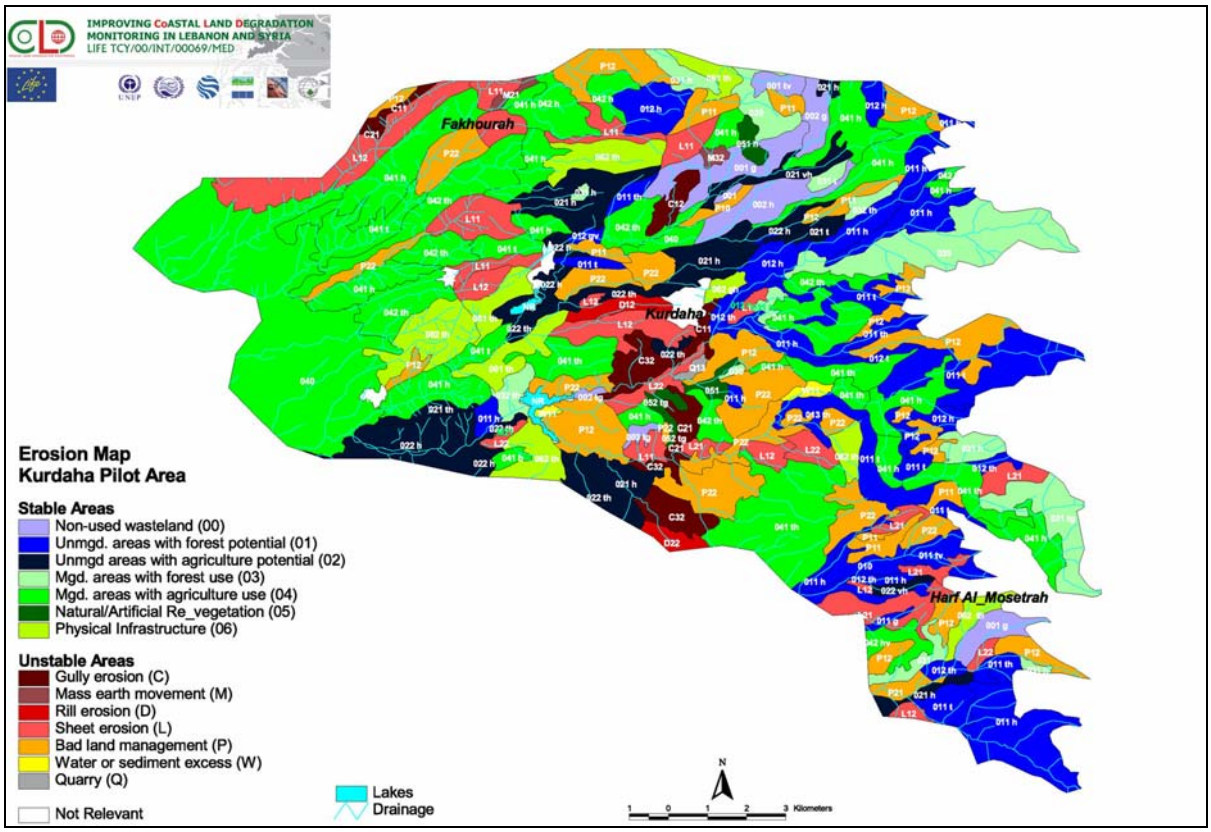


**Map 1.** Kurdaha descriptive erosion map.

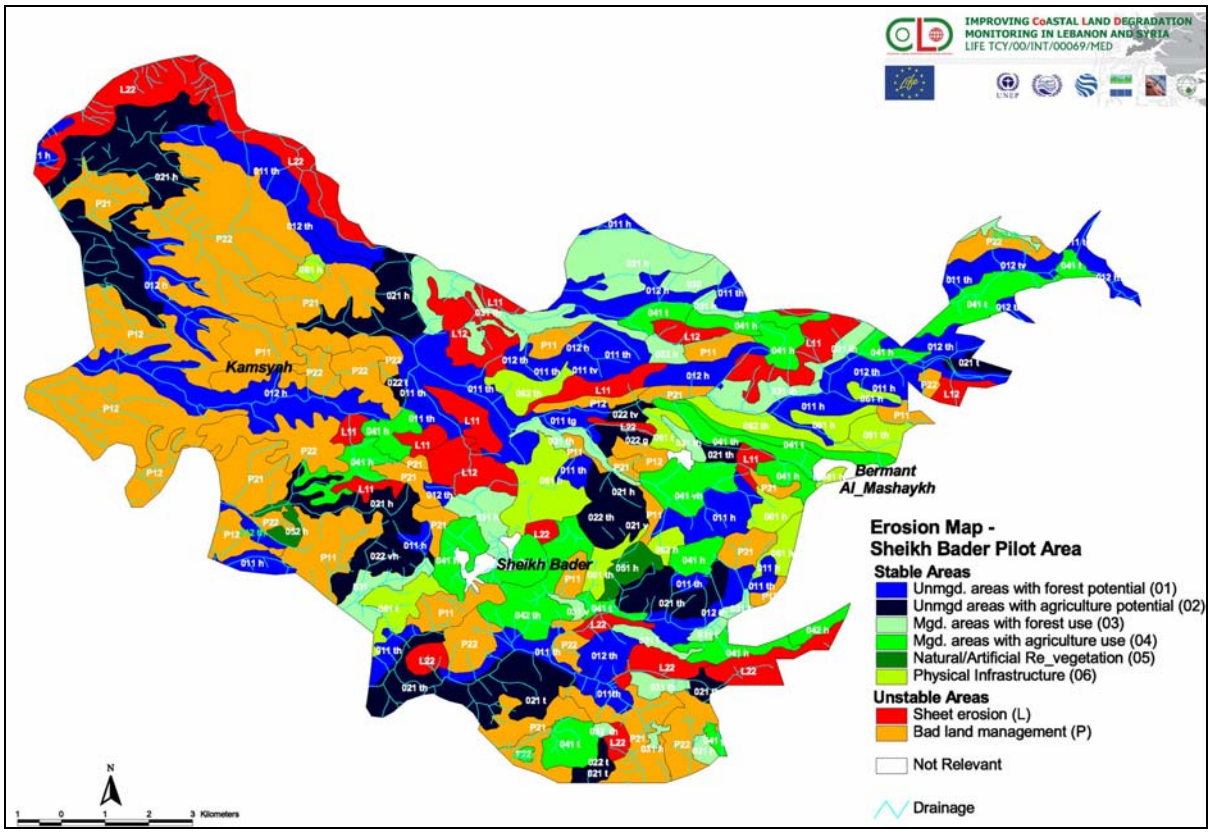


**Map 2.** Sheikh Bader descriptive erosion map.

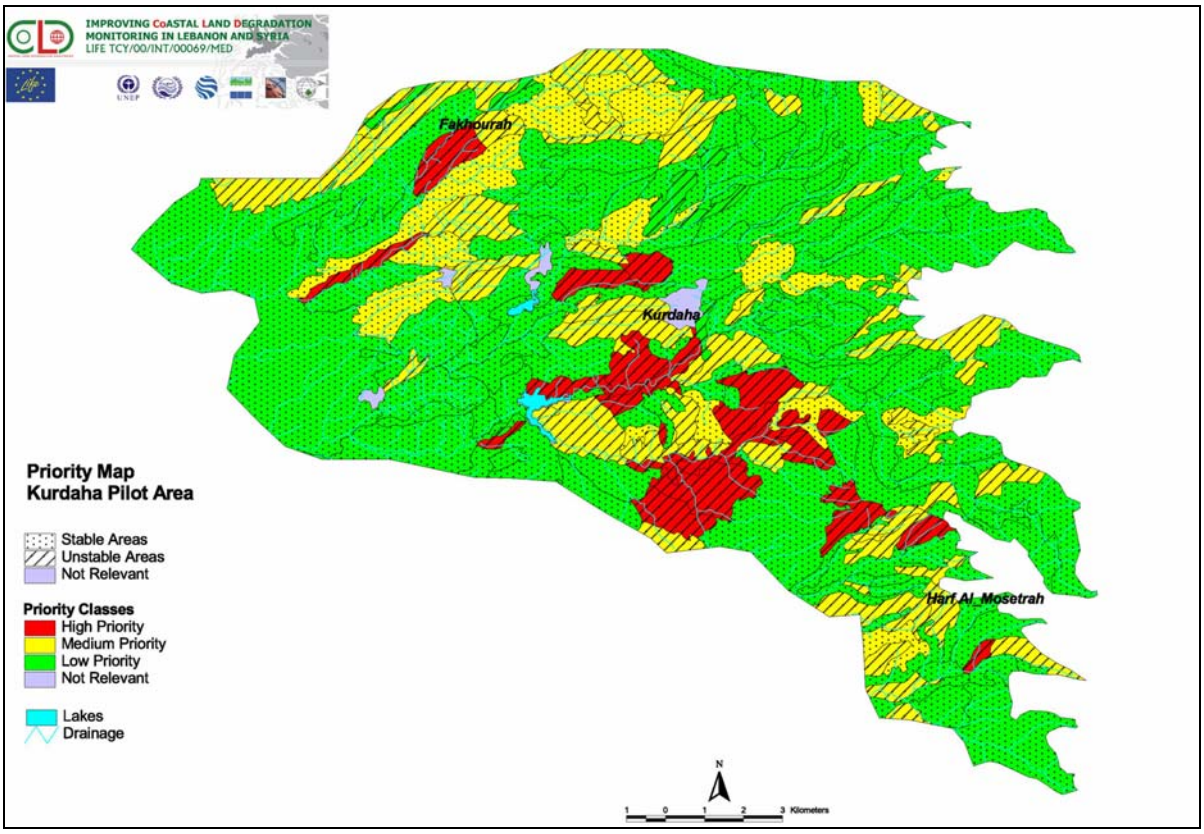


**Map 3.** Kurdaha priority map.

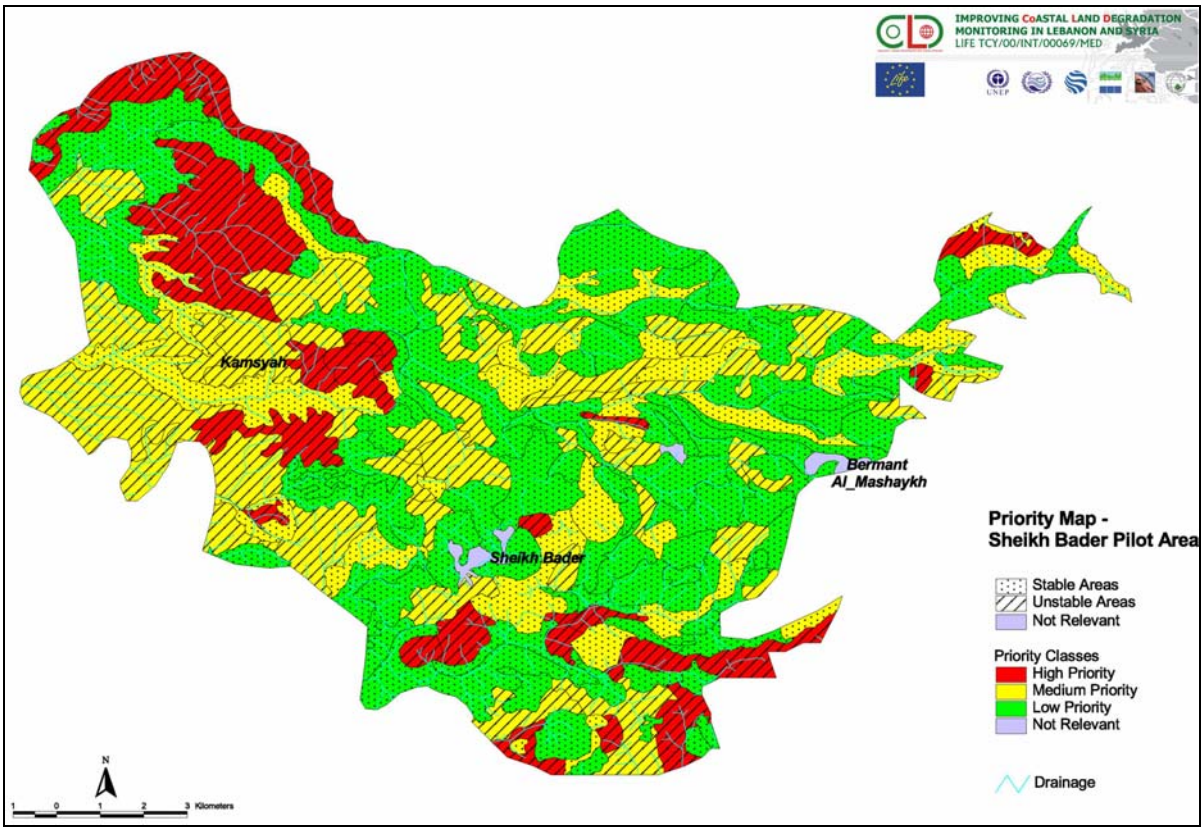


**Map 4.** Sheikh Bader priority map.

# Arab network of the remote sensing centers for desertification monitoring and assessment

W. F. Erian[a]

[a] The Arab Center for the Studies of Arid Zones and Dry Lands – ACSAD, Damascus, Syria
email: erian@acsad.org; Tel: 963 11 (5743039 / 5743087); Fax: 963 11 5743063

## ABSTRACT

The main mission of ACSAD is to face the challenge imposed by the arid and semi-arid environments which are characterized by fragile farming systems, through the provision of scientific and applied data and advanced techniques in a way that allows large-scale implementation of tasks of the agricultural and social development and the optimum exploitation of the renewable natural resources in the arid areas. Supporting Arab countries for implementing the UNCCD, including monitoring, assessment and rehabilitation, considered to be an important role for ACSAD. For Achieving ACSAD role in monitoring and assessment of desertification, a partnership with German technical cooperation (GTZ) was started to undertaken the following tasks:

- Establish Regional Early Warning systems (REWs)
- Establish Desertification Monitoring and Assessment (ADMAnet),
- Standardize, and harmonize ADMAnet member's in applying RS/ GIS techniques, and recent approaches related to DMA.

Since 2003 ACSAD started to collaborate with the Remote Sensing, Department University of Trier. This cooperation provided technical support and training courses in the fields of DMA and early warning, exploration and development of joint research activities, connected with desertification and exchange of knowledge and materials in the fields of contemporary issues on desertification aiming at supporting the establishment of a regional desertification monitoring system at the current stage and a national one at later stage.

The participation in the network shall bind the members to close cooperation towards a defined objective, promote their resources and support their efforts in the fields of dynamic operations for desertification and drought monitoring and assessment by using the space sciences technologies. Syrian General Organization for Remote Sensing (GORS), the Egyptian National Authority for Remote Sensing and Space Sciences (NARSS), the Lebanese National Centre for Remote Sensing (NCRS), the General Authority of Remote sensing in Sudan (GARS) are the founders of ADMAnet, besides other potential members such as, the Royal Geographic Jordanian Centre (RGJC) of Jordan, the Royal Center for Remote Sensing (RCRS), The Libya Mapping of Natural Resources for Agricultural Use and Planning Project and other Arab national remote sensing centers. ADMAnet has open-ended membership for all the accepted Arab countries which ratified the UNCCD.

**Key words:** Desertification Monitoring and Assessment, ADMAnet, Land Degradation, LADA, Hot Spots, GLCN, and Time Series analysis.

## 1 BACKGROUND AND CONTEXT

The drylands (arid, semi-arid, and dry sub-humid zones) cover worldwide 52 million km$^2$, more than one third of the globe's land area. The natural resources in the dryland areas (water, soil, and vegetation) are facing unprecedented degradation threats.

World Atlas of Desertification by UNEP (1992) sets the limits of Aridity Index based on the annual precipitation/potential evapotranspiration (P/PET) between 0.05 and 0.65. Dry lands are home to nearly 2 billion people (herdsmen and small-scale farmers, and urbanized lifestyles in growing urban centers).

**Table 1:** Limits of Aridity Index based on the annual precipitation / potential evapotranspiration (P/PET).

| Aridity Index | | Extent (million km$^2$) | % | Population (million) | % |
|---|---|---|---|---|---|
| **Hyper-arid deserts** | (P/PET < 0.2) | 8.1 | 10.9 | 95 | 1.6 |
| **Arid dryland** | (0.05 < P/PET < 0.2) | 14.1 | 18.8 | 275 | 4.7 |
| **Semi-arid drylands** | (0.02 < P/PET < 0.5) | 15.9 | 21.2 | 966 | 16.5 |
| **Dry sub-humid drylands** | (<0. 5 < P/PET < 0.65) | 7.1 | 9.5 | 637 | 10.8 |
| **Drylands total** | (0. 05 < P/PET < 0.65) | 37.1 | 49.5 | 1868 | 32.0 |

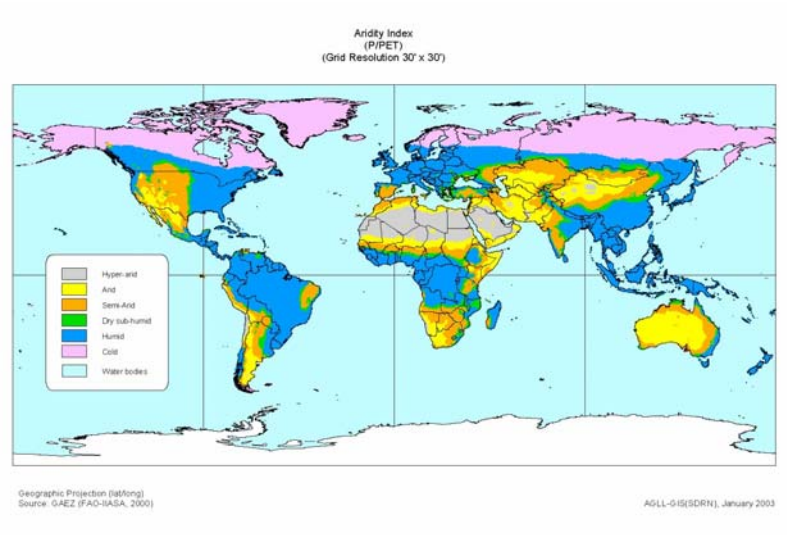


**Figure 1.** Aridity Index based on the annual P/PET.

Most of the West Asia and North Africa (WANA) region, where, the Arab countries are located, falls within the arid and semi-arid zones and is considered one of the most fragile ecosystem regions worldwide, FAO (1996), receiving an average annual rainfall of up to 400 mm with a growing season of 60-120 days.

The rural sector is an important contributor to the economies of most WANA countries as agriculture employs between 20-40 % of the labor force, and contributes 20-30 % of the Gross Domestic Product (GDP) on average. The drylands support the livelihoods of 60 % of the total population living in WANA region in spite of their limited resources. However, the degradation of natural resources (land, water and vegetation) has seriously affected the agricultural production capacities of the WANA countries, with severe repercussions on economic growth, food security and poverty alleviation. According to the recently revised World Bank Environmental Strategy for Middle East and North Africa (MENA), the cumulative impact of land degradation is estimated to cost about US$ 1.15 billion a year in lost agricultural productivity.

The causes of resource degradation and its subsequent impact on the agricultural production capacity of the WANA region entail various aspects. In addition to recurrent droughts and high variability in rainfall, which cause drylands to be progressively more vulnerable to climatic changes, intensive forms of land use, including over-grazing, excessive irrigation, and intensive tillage and cropping have also been identified as factors. Additionally, primary causes of land degradation are policy and institutional distortions or failures on the part of the public or the government and inadequate government policies

The main causes of the core problem are the absence of planning for appropriate land use and the corresponding lack of closer ties among control mechanisms. These mechanisms are necessary in particular for providing the necessary current data and information on the various activities and their impacts at the national and supranational levels. Furthermore, the institutional structures responsible for steering and coordinating activities need to be strengthened.

The core problem manifests itself, inter alia, in an accelerated deforestation, inappropriate use of grazing land and inefficient utilization of the available water resources. These combined impacts lead to accelerated soil

degradation, which, in turn, exacerbates the increasing marginalization of the population, impacting first and foremost on rural dwellers, especially women. These factors reveal a considerable potential for social conflict, with the result that the region is becoming increasingly crisis-prone.

As a consequence of the core problem, the sustainable development of the countries affected is severely impaired.

## 2 ACSAD ROLE IN DESERTIFICATION MONITORING AND ASSESSMENT

The Arab Center for the Studies of Arid Zones and Dry Lands (ACSAD) was established in Damascus, Syria in 1968. ACSAD is a specialized Arab organization working within the framework of the League of Arab States with the objective of unifying the Arab efforts which aim to develop the scientific agricultural research in the arid and semi-arid areas, help in the exchange of information and experience and make use of scientific progress and modern agricultural techniques in order to increase the agricultural production.

The main mission of ACSAD is to face the challenge imposed by the arid and semi-arid environments which are characterized by fragile farming systems through the provision of scientific and applied data and advanced techniques in a way that allows the large-scale implementation of the tasks of the agricultural and social development and the optimum exploitation of the renewable natural resources in the arid areas.

Supporting Arab countries for implementing the UNCCD, including monitoring, assessment and rehabilitation, considered to be an important role for ACSAD. For Achieving ACSAD role in monitoring and assessment of desertification, a partnership with German technical cooperation (GTZ) was started to undertaken the following tasks:

- Establish Regional Early Warning system (REWs)
- Establish Desertification Monitoring and Assessment (ADMAnet),
- Standardize, and harmonize ADMAnet member's in applying RS/ GIS techniques, and recent approaches related to DMA.

### 2.1 ACSAD / REWs

Monitoring, assessment and early warning systems (EWs) for desertification and drought need to integrate not only geo/biophysical parameters but also climatic, geomorphological, human and socio-economic factors. The effective desertification monitoring also needs to take into account spatio-temporal characteristics of drought and desertification processes. Thus DMA should incorporate and integrate the spatio-temporal characteristics, the active processes, and the nature and severity of the phenomenon. In order to monitor and assess in time and space, a baseline needs to be defined. One suggestion is the Desertification Status Map (DSM) which should depict the spatial characteristic of the land, its status of degradation, and also identify the involved processes and their severity.

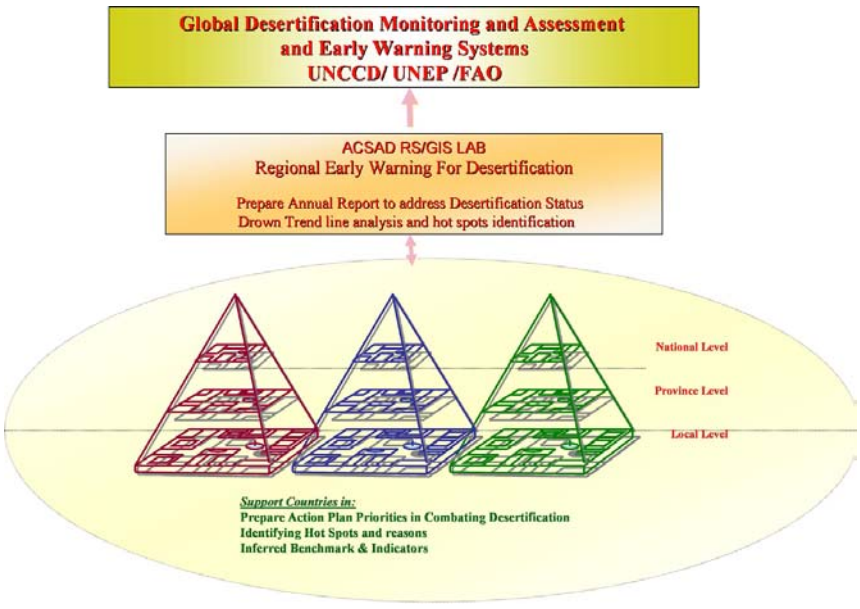


**Figure 2.** Desertification Monitoring and Assessment in Different Levels.

The steps toward the establishment of ACSAD / REWs for desertification started in 2003. The system product is an annual report to address the global and the national levels. The report will describe the annual changes on the vegetation cover and its trend line. Studies to be carried out on the national level

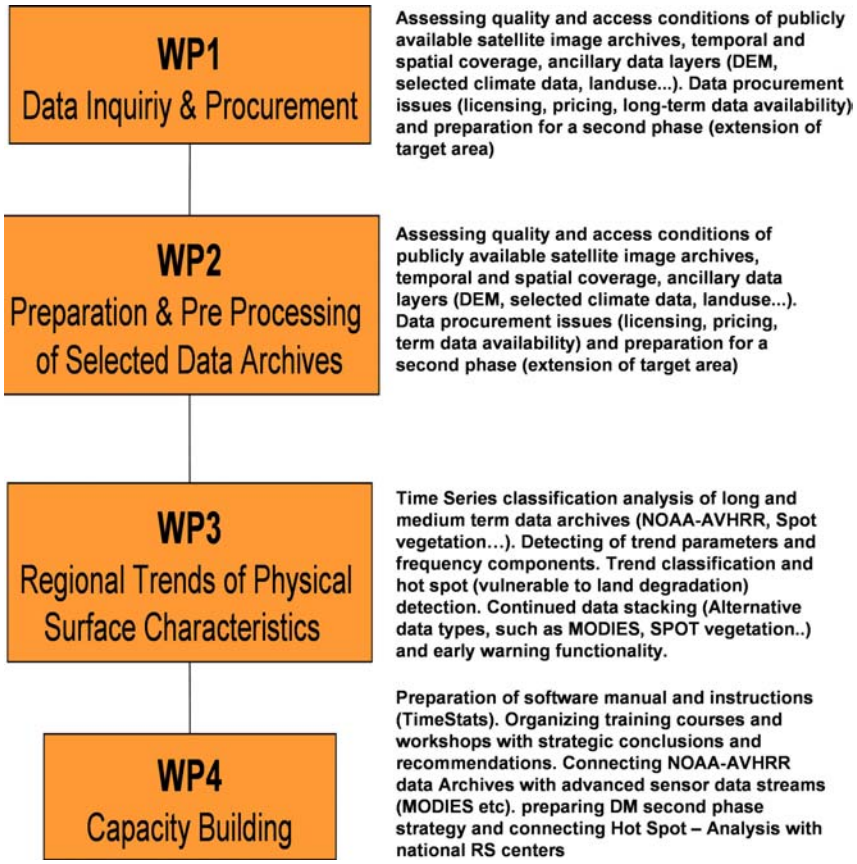


**Figure 3.** ACSAD/University of Trier DM implementation components.

to identify the reasons of change and whether we could consider it a hot spot or bright spots. The relationship between ACSAD and the global and national levels is shown in figure (2).

The analysis of land degradation /desertification processes and dynamics on regional scale (8 km /1 km-grid) depends on long term data sets covering the whole region. The initial backbone component to be established by ACSAD should hence comprise a regional assessment module. This should primarily be based on existing remote sensing data archives with moderate spatial, but high temporal, resolution (i.e., weekly or decadal integrals with roughly 1 km spatial resolution). These archives should cover a long time span (of at least 10-15 years) to enable the identification of environmental changes that occurred in the past. But this needs to be complemented with an appropriate updating strategy (continued data stream of up-to-date satellite data, supplied by national or international space data processing centers (i.e. NASA, ESA, SPOT VEGETATION, …,etc)).

### 2.1.1 Steps to achieve Regional Early warning

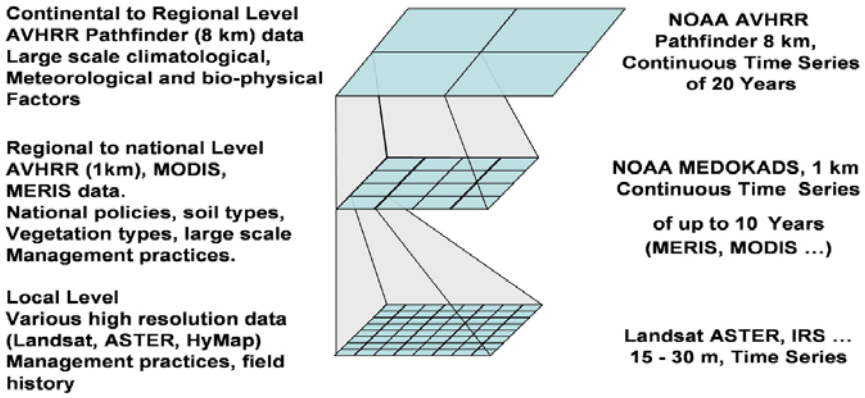


**Figure 4.** Recommended spatial resolution at different DM levels.

Since 2003 ACSAD started to collaborate with the Remote Sensing Department, University of Trier. This cooperation provided technical support and training courses in the fields of DMA and early warning, exploration and development of joint research activities, connected with desertification and exchange of knowledge and materials in the fields of contemporary issues on desertification aiming at supporting the establishment of a regional desertification monitoring system at the current stage and a national one at later stage. The agreed upon steps for achieving REWs are shown in figure (3). The recommended spatial resolution at different DM Levels is shown in figure (4).

### 2.1.2 Preliminary Regional Early warning obtained Results

The trend model used in the TimeStats software package is illustrated after Udelhoven [8] as follows:

$$NDVI_t = \alpha + \beta_1 \cdot t + \left( \sum_{i=1}^{NoOfLags} \beta_i NDVI_{t-i} \right) + \left( \sum_{j=1}^{NoOfX} \sum_{k=1}^{NoOfLags} \beta_{jk} X_{jk} \right) + \left( \sum_{m=1}^{NoOfHarm} a_m \cos 2\pi \frac{1}{P_m} \cdot t + b_m \sin 2\pi \frac{1}{P_m} \cdot t \right) + \varepsilon$$

| Constant | linear trend | stochastic component | external variables | Periodic components (cycles, long-periodical trends | white-noise |
|---|---|---|---|---|---|

Significance of the regression coefficient (t-test) in a linear trend model applied to annual NDVI Pathfinder data (1982 – 1999) is shown in figure (5), after [8]. The related significance describes the likelihood that the actual regression coefficient of non-parametric trend models equal zero.

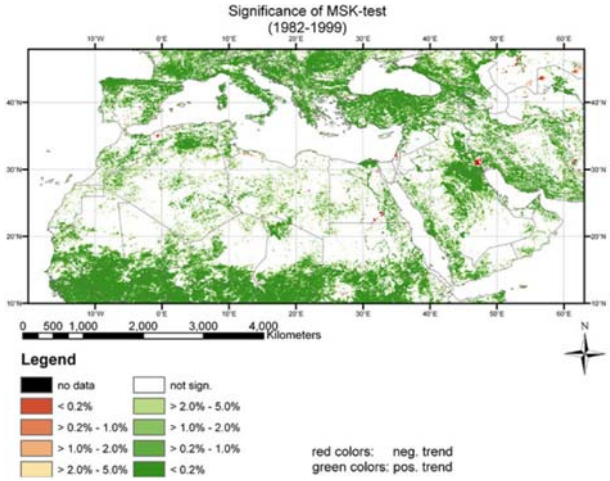


**Figure 5.** Significance of linear trend analysis.

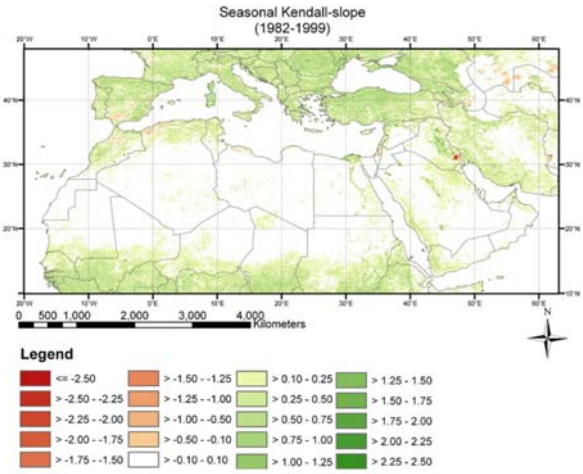


**Figure 6.** Modeled absolute NDVI changes (Jan. 1982 – Dec. 1999).

The modeled absolute NDVI changes (Dec. 1999 – Jan. 1982) using a complete trend model including linear and non-linear terms is shown in figure (6), after [8].

Appling the trend model used in the TimeStats software package to NOAA-AVHRR – MEDOKADS archive of Freie University in Berlin or to the SPOT vegetation archive will put ACSAD in the position to issue "Early Warning Signals" whenever significant deviations from long-term (average) conditions are detected in the region. Once more, the verification and more detailed analysis of such events will be done on a more detailed level of scale through the national counterparts of ACSAD.

## 2.2 Arab Centers of Remote Sensing, Desertification Monitoring, and Assessment Network , ADMAnet

In order to secure more detailed level of monitoring and assessment studies, through ACSAD national counterparts in addition to the detection and identification of "desertification hot spots" and harmonizing the efforts between the Arab national bodies of remote sensing centers, ACSAD called for the establishment of ADMAnet.

The participation in the network shall bind the members to close cooperation towards a defined objective, promote their resources and support their efforts in the fields of dynamic operations for desertification and drought monitoring and assessment by using the space sciences technologies. Syrian General Organization for Remote Sensing (GORS), the Egyptian National Authority for Remote Sensing and Space Sciences (NARSS), the Lebanese National Centre for Remote Sensing (NCRS), the General Authority of Remote sensing in Sudan (GARS) are the founders of ADMAnet, besides other potential members such as, the Royal Geographic Jordanian Centre (RGJC) of Jordan, the Royal Center for Remote Sensing (RCRS), The Libya Mapping of Natural Resources for Agricultural Use and Planning Project and other Arab national remote sensing centers. ADMAnet has open-ended membership for all the accepted Arab countries, which ratified the UNCCD.

### 2.2.1 ADMAnet Main Goals and Objectives

ADMAnet main goal is to provide a scientific and programmed mechanism for decision makers for a better and sustainable management to preserve the land cover by a comprehensive long term monitoring of the Arab area. For achieving this ultimate goal the following objectives were defined:

- To establish a permanent regional network between the national Centers for Remote Sensing to implement the new programming technologies based on the space studies, and related to the realities on earth for the desertification process monitoring and assessment in the Arab region.
- To promote and build the institutional capacities of regional early warning system.
- To share and manage information relevant to desertification monitoring and assessment.
- To develop a framework including monitoring several factors of geophysical, economic and social dimensions of the desertification problem considering mutual relations between DMA and EWS.
- To establish a coordinated regional database for assessing the expansion of desertification and the influence of the economic and social factors.
- To adopt a coordinated regional plan of work to face the risks of desertification and the loss of natural resources and to assess the interaction of the land and climate with a coordinated regional monitoring.
- To link the national institutions with the similar ones in order to achieve the objectives on the regional and national levels.

ACSAD will play its role to coordinate between ADMAnet members for achieving the defined objectives with link to its mandate and role in the region as shown in figure (7).

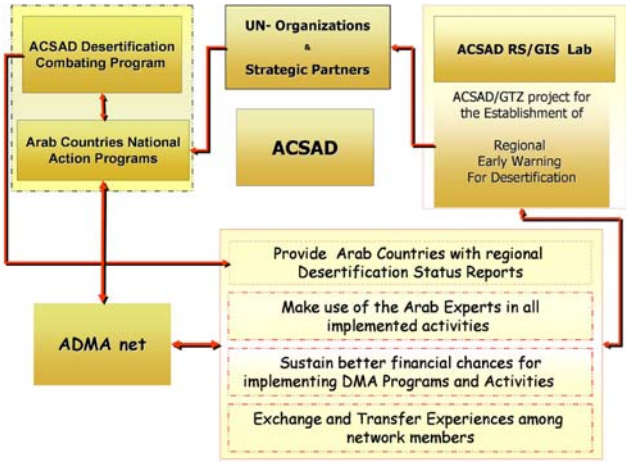


**Figure 7.** ACASD/ADMAnet links with desertification monitoring.

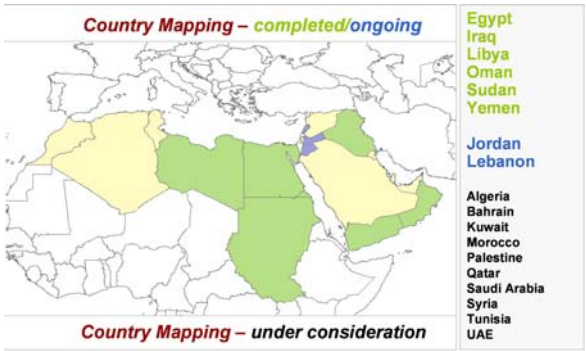


**Figure 8.** The current status of the GLCN project within the Arab region.

## 2.3 Standardize and Harmonize ADMAnet member's application RS/ GIS techniques related to DMA

For the Assessment of desertification status it is important to standardize, and harmonize ADMAnet member's application of RS/ GIS techniques related to DMA and in producing relevant scales of mappings including, layers such as: agro-climatic regions, land-use/ land-cover maps, and land degradation hot spots and bright spots. Accordingly, ACSAD established a strategic partnership with three main UN partners

### 2.3.1 UNCCD/TPN1 Activities in ASIA

There still exist strong needs for ACSAD involvements in West Asia for establishing a baseline for monitoring desertification at the sub-regional level. the first cut desertification status map of the Asian region has been prepared under its thematic programme network (TPN1) and presented during the UNCCD/CRIC3 [9] meeting. UNCCD/TPN1 member countries in ASIA and ACSAD have also come up with a commonly accepted benchmarks and indicators.

### 2.2.2 FAO/UNEP Land Cover Classification System (LCCs)

GLCN is based on the success of the Africover project to develop a digital geo-referenced database on land cover and a geographic referential for the whole of Africa including:

geodetical homogeneous referential, toponomy, roads and hydrography, FAO/UNEP [1].

Land cover assessment and monitoring of its dynamics are essential requirements for the sustainable management of natural resources and for environmental protection. They provide the foundation for environmental, food security and humanitarian programmes that are crucial in fulfilling the mandates of many UN, international and national institutions. Current monitoring programmes, however, have no access to reliable or comparable baseline land cover data. Therefore, the implementation of a global programme using a fully harmonized approach is essential to increase the reliability of land cover information for a large user community. Responding to this need, FAO and UNEP have jointly developed a Global Land Cover Network (GLCN). The FAO/UNEP /LCCS is the only universally applicable classification system in operational use at present. It enables a comparison of land cover classes regardless of data source, economic sector or country. Most other land cover classification systems are single-purpose systems, tailored to requirements of a specific project or based on a sectorial approach, FAO/UNEP (2004). The League of Arab States (LAS) is represented in the Global Land Cover Network GLCN project by ACSAD. The Current Status of the GLCN Project Within the Arab Region is shown in figure (8), after [6].

### 2.2.3 FAO/UNEP Land Degradation Assessment of Drylands LADA Programme

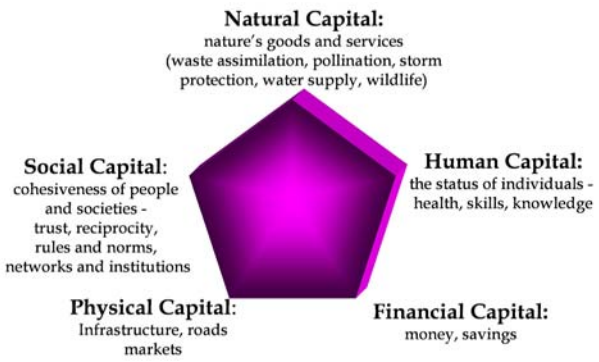


**Figure 8.** The current status of the GLCN project within the Arab region.

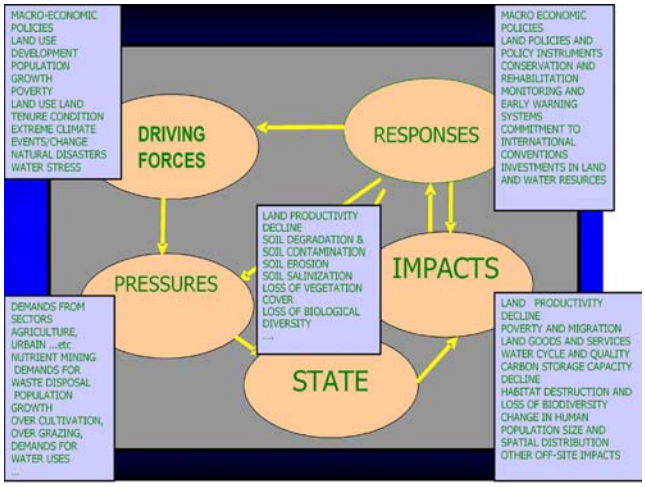


**Figure 9.** Measuring complexity.

ACSAD started to cooperate with LADA development activities led by FAO in both tools and methods to assess and quantify the nature, extent, severity and impacts of land degradation on ecosystems, watersheds and river basins, carbon storage and biological diversity at a range of spatial and temporal scales within the Arab region . ACSAD is interested in building the national and regional capacity to analyze, design, plan and implement interventions to mitigate land degradation and establish sustainable land use and management practices. FAO/UNEP LADA programme agreed to cooperate technically with ACSAD as a regional agency for the implementation of LADA. The same steps of LADA will be followed to develop standardized and improved methods for dryland degradation assessment within the Arab region. Using these methods, it will assess the National and regional baseline condition of land degradation with a view to highlighting the areas at greatest risk. Accordingly ACSAD organized together with FAO/RNE on July 2004 in Damascus a regional workshop for promoting LADA programme in Western Asia and the Near East.

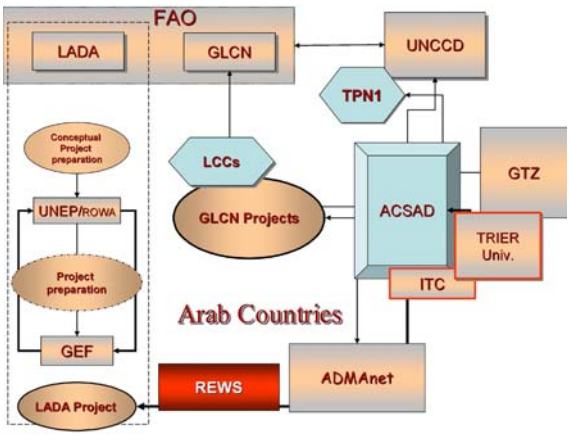


**Figure 10.** ACASD partners for implementing DMA.

LADA follows a participatory, decentralised, country-driven and integrated approach and makes ample use of participatory rural appraisals, expert assessment, remote sensing, modelling and other modern means of data generation, networking and communication technologies for share of information at national and international levels [5]. The key elements of the approach are

participation and inclusion of the different perception of LD, combination of expert assessment & local knowledge and the use of adapted assessment tools for specific environments. ACSAD's role will also extend to harmonizing approaches like measuring all of the capitals of rural livelihood, shown in figure (8) and measuring complexity as shown in figure (9). ACSAD Partners for implementing a regional project concerning DMA, figure (10). Those partners will contribute by supporting the implementation. In the light of UNEP/ROWA's role in implementing UNCCD in the sub-region, the project on "LADA implementation in West Asia" will be supported within the framework of the SRAP. It was mentioned that strong country support is needed in order to implement projects within the sub-region in West Asia., Loulou, [7]. Accordingly, ACSAD is preparing a regional project for LADA implementation. By the end of the project ACSAD will have developed in a close cooperation with FAO LADA programme and UNCCD/TPN1 the following:

- Standardised methodological framework to address the process of dryland degradation,
- Regional baseline degradation assessments completed.
- Contributing to the Guidelines for dryland degradation assessment preparation efforts, and

These regional baseline assessments will be (from existing information sources) to identify priority 'hot spots' where the potential impacts on ecosystems is severe.

## REFERENCES

[1] FAO, 1996: Agro-ecological Zoning Guidelines. FAO Soils Bulletin No. 73, 78 pp. Rome: Food and Agriculture Organization of the UN.
[2] FAO/UNEP, 2002: Proceedings of the FAO/UNEP Expert Consultation on Strategies for Global Land Cover Mapping and Monitoring. Artimino, Florence, Italy.
[3] FAO/UNEP, 2004: Land Cover Classification System. Classification concepts and user manual, Environment and Natural Resources Series No. 8.
[4] HAMDALLAH, G., 2004: A Regional Perspective to Land Degradation in the Near East. LADA Regional Workshop, ACSAD, Damascus (July 25-28 '2004).
[5] KOOHAFKAN, P., 2004: Regional Workshop for Promoting LADA Programme in Western Asia and the Near East, organized by ACSAD and FAO/RNE, Damascus, Syria
[6] LATHAM J.S., 2005: The Global Land Cover Network and the Relevancy of Harmonized Land Cover. GLCN, Sharm El Sheikh, Egypt.
[7] LOULOU, A.R., 2005: First Regional Consultation Meeting on the Abu Dhabi Initiative for Implementation of the Priority Activities for the Regional Action Programme (RAP). Abu Dhabi, United Arab Emirates
[8] UDELHOVEN, T., 2005: Time-series analysis using the 8 km AVHRR PAL and the 1 km MEDOKADS data archives. Training Workshop on Land Degradation Monitoring System Regional to Local Level, ACSAD, Damascus
[9] UNCCD/CRIC3, 2005: Panel Session on Desertification Monitoring and Assessment. Bonn, Germany.
[10] UNEP, 1992: World Atlas Of Desertification. Edited by L. R. Oldman.

# Forest fire hazard mitigation in Lebanon using remote sensing and GIS

G. Faour[a], R. Bou Kheir[a], A. Darwish[b], A. M. Kobeissi[b], M. Ayoub[b]
[a] National Council for Scientific Research - Remote Sensing Center, Lebanon,
email: gfaour@cnrs.edu.lb
[b] Greenline Association, Beirut, Lebanon
[c] Islamic University, Faculty of Engineering, Beirut, Lebanon

## ABSTRACT

Land degradation processes are widespread in the Mediterranean region resulting from mismanagement of land and water resources. They can also be related to progressive drought under changing climatic conditions. Among these processes, forest fires constitute the most serious economic and life-threatening natural disaster in Lebanon. This research was conducted in the context of defining a strategy for combating forest fire in the country. It deals with two major phases. The first concerns the forest fire Database Management System (DBMS) for data observation on a systematic basis during 20 years (1983-2003.) It covers all information related to fires such as specific location, duration, burnt area, fuel types, climatic and human related causes, closest civil defense centers, etc. This database defines the historical and spatial forest fire occurrence that was used as an input in the designed model to produce forest fire risk map of Lebanon. The second phase consists of building a new integrated approach to forest fire mitigation aiming at predicting forest fire at national (whole country) and local (five pilot areas) levels. The constructed model was produced using GIS combining the influencing factors, i.e. vegetal cover, fuel type, slope gradient, slope aspect, evapotranspiration and number of occurrence of forest fires. The produced fire risk maps describe the potentiality of fire at long-term depending on static factors. Therefore, they provide policy-makers, including an effective tool for allocation and prioritization of endangered areas for fire prevention and control. They can be considered as a solid base for generating short-term fire risk maps to reduce the occurrence of accidental fires.

**Keywords:** forest fire, modelling, GIS, remote sensing, Lebanon, Mediterranean region

## 1 INTRODUCTION

Over the last decades, forest fires and other wildfires have increased dramatically in the Mediterranean region, becoming larger and more severe than in past fire episodes. In the early 1990's, over 2.5 million ha have been burnt by more than 260 000 fires in the five principal European countries bordering the Mediterranean Sea (Portugal, Spain, France, Italy, and Greece) [1]. In Lebanon, fires represent a major threat being related to natural and human causes. The natural ones are mainly represented through extreme global climatic conditions, particularly the dry hot summers that frequently coincide with high temperatures and speed wind directions. In addition, the inadequate agricultural practices (cleaning fields using fire), the indigenous knowledge of the local people on the importance of biodiversity conservation, the lack of the Lebanese law's enforcement prohibiting fire use and the scarcity of adequate equipment to protect against the fast widespread of forest fires can increase to a large extent the occurrence and propagation of forest fires.

Forestry service reports indicate that 1200 ha of natural forests are burnt every year in Lebanon. The burnt area has increased to around 1600 ha during 1998 and 1999. Resultant effects of forest fires are extremely serious and dramatic. In most burnt areas, the damage and decrease of vegetation cover during dry summer periods is followed by violent rainstorms, during which the unprotected topsoil is subject to severe erosion processes destroying the productive value of the land. The increasing frequency and intensity of fires can threat to a large extent the floristic species diversity in Lebanon, even those plant communities (e.g. maquis, garrigue, some pine communities) which have been adapted to naturally-occurring fires or are depending on fires to maintain themselves. In fact, the floristic richness of the country was estimated in 1973 at 2600 plant species [2] comprising a total number of 311 endemic species. At actual time, 12% of these species (312) was counted, from which 212 species having an economic value and are characterized as medicinal plant species or edible crops [3]. Thus, fires can lead to a general loss of the remaining species. Forest fires impacts can be seen also over a whole river catchment level where the excessive loss of vegetation from the ecosystem severely affects the landscape touristic view, and thus drives a mechanism of sometimes irreversible environmental damage. The potential loss of life and property is considered also the most harmful negative consequence of widespread forest fires. This led to the necessity of a fast acting in order to

preserve and upgrade remaining forest communities. All the conducted solutions until actual time (defense civil centers, municipalities, ministries, non governmental associations, etc…) reveal useful but insufficient and should be tackled by constructing a forest fire Database Management System (DBMS) that can be of extreme importance for modelling the forest fire vulnerability.

The recent availability of the powerful data processing technique "Geographic Information System (GIS)" coupled with satellite imagery has increased the opportunities of tackling the problems of fire spatial variability. The potential benefit of GIS and Remote Sensing in monitoring fires has been demonstrated in many studies [4, 5, 6]. Several fire risk indices exist nowadays in the Mediterranean region, but they differ referring to the input variables, to the time scale for use (long-term and short-term "dynamic" indices) but also the update and goal of the derived products [7, 8, 9]. In addition most of them even pointing out to problematic areas, they include a major disadvantage consisting of a big subjectivity in the selection and weighting of the used variables. In this context, a GIS fire model is proposed allowing predictions of both present and future risks depending on past fires (objective approach) occurring in Lebanon. Fire occurrence is mapped at different levels of scaling, i.e. 1.100,000 (whole country) and 1.20,000 (fragile areas) and rated in terms of severity. It is computed before the fire season (pre-crisis phase) and provides useful information for the improvement of preparedness for forest fire fighting.

## 2 STUDY AREA

Lying on the eastern side of the Mediterranean Sea, Lebanon is divided into six mohafazats or governates (Beirut, North, South, Nabatieh, Mount Lebanon and Bekaa). These mohafazats are subdivided into 26 cazas, regrouping 1580 cadastral zones. In spite of its limited area (10 452 km$^2$), its geomorphologic structure is diversified. Its landforms fall into four parallel belts that run from northeast to southwest as follows (Fig. 1): a narrow coastal plain (< 100 m altitude) along the Mediterranean shore, the massive Lebanese Mountains (between 100 and more than 1500 m) (often referred to locally as Mount Lebanon), a fertile intermountain (between mountains) basin called the Bekaa valley, and the ridges of the Anti-Lebanon's Mountains (900-1500 m), shared with Syria. Natural vegetation cover occupies the largest portion of Lebanon (concentrated mainly in Mount Lebanon), with 33% dedicated to grass lands and 23% to wooded lands. These latter comprise dense and clear coniferous trees (pines, cedars, fir, cypress and juniper) (3.31%), broadleaves trees (oaks and other types) (5.58%) and mixed trees (2.25%) as well as scrubland (11.86%). Agricultural lands are less widespread than natural vegetation, covering 32%.

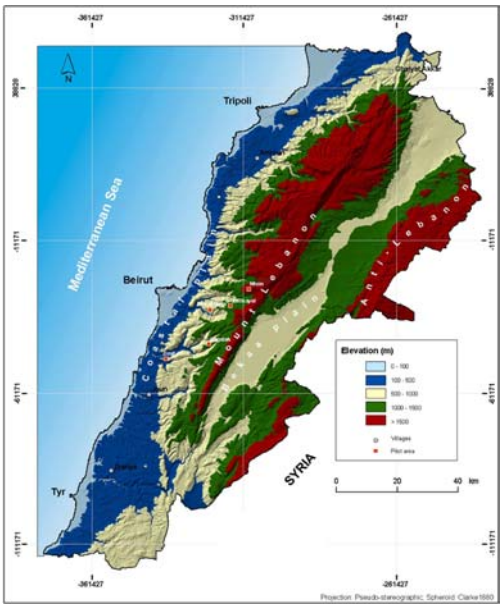


**Figure 1.** Geomorphological map of Lebanon.

Annual precipitation rate ranges in Lebanon between 700 mm on the coastal plain and 1400 mm over the crests of Mount Lebanon (average 1050 mm/year). The rainy period is from October to March reaching its climax often in January. Therefore, dryness period is relatively long, constituting a water stress for vegetation. Similarly, mean yearly temperatures are a function of altitude and decrease regularly with it: 20º to 21 ºC on the coast; 15 ºC at 900 m altitude; 12 ºC at 1800 m and 5 ºC at 2700 m. The highest temperatures are registered in August exceeding 35º C per day in the Bekaa valley.

In addition to the whole country, five fragile areas have been studied at much more detailed scale (1.20,000). All of them were located in Mount Lebanon, i.e. Mtein (El-Matn caza), Dmit (Chouf caza), Ramlieh (Aley caza), Qornayel (Baabda caza) and Ras El-Matn (Baabda caza) (Fig. 1). They were chosen because they are classically known to include local sites that have been experienced high frequency of fires that affect mainly pine forests which are considered to be economically valuable F since they are used in oriental food industry. They represent less than 1% of the total area in Lebanon.

## 3 MATERIAL AND METHODS

### 3.1 Fire database

The characterization of forest fires is based on the creation of a wide database spread on 20 years. Then, a statistical and spatial analysis (under GIS) was accomplished allowing a precise and appropriate determination of fire occurrence conditions in Lebanon.

### 3.1.1 Collection of forest fire archives

Compilation of data during 20 years (1983-2003) describing the number and the exact time of forest fires per year, the areas burnt and the fuels affected was a very hard issue. In fact, the data was spread between many institutions like the Lebanese Civil Defense and the Ministries of Environment and Agriculture. We made use also of available newspapers that are describing wide and important forest fires. The forest fire archive of the Lebanese Civil Defense is recent dating from two years ago (2002 and 2003) while that of the Ministries of Environment and Agriculture archive is represented by reports compiling forest fire information for 4 years (1994-98) and for 6 years (1996-2002), respectively. All the available collected archive was indefinite, not classified, not homogeneous, unorganized and presented on a paper form.

### 3.1.2 Data conversion and management

The data was stored and handled in the computer into tables regrouping the following information: location of forest fire occurrence, starting and ending date and time of a given forest fire, the name of the nearest civil defense center, and forest fuels as described in the collected archives. Meteorological data (temperature '◦C', humidity '%', wind direction and wind speed 'km/h') were also added in the fire database allowing correlating fire occurrence with different climatic conditions. These data were managed using Microsoft Access program to create a forest fire DataBase Management System (DBMS). Common database operations such as query, filtering, statistical analysis, etc…..were carried out on original input data to prepare them at the successive computation.

### 3.1.3 Collected fire archive GIS and statistics

The managed fire data under Access was analyzed and several statistical relations were created, i.e. number of fires per fuel, per location (mohafazat, casa and cadastral zone) and per date, relation between fire duration and fuel type, relation between climatic conditions and fire ignition, and relation fire occurrence and urbanization from one side and forest cover from the other side. These relations were then converted digitally using the GIS system.

## 3.2 Identification of burnt areas

This solid database was also extremely useful in the determination of areas affected by fires since 20 years. To delineate the exact contour of each burnt area, several satellite images were collected and treated. The choice of these images was based on several criteria, i.e. the availability, date of acquisition, covering of most affected areas and dependence on satellites with fine spatial resolutions. Thus, the whole country was covered by two scenes of Landsat TM (30 m) and ETM+ (15 m) satellite images acquired in October 1986 and 2000, respectively. As well, a SPOT-5 (5 m) satellite image was acquired for Mount-Lebanon (the most affected by fires) and five IKONOS images (1 m) for the five pilot areas. SPOT-5 and IKONOS images were taken in October 2003. The acquiring date (October) was chosen in order to detect the eventual decreasing of the green biomass and plant cover at the end of the vegetation season. All images were ortho-rectified using a Digital Elevation Model (DEM) with 10 m resolution. A mosaicking was applied on the two scenes of Landsat TM and ETM+ images. An amelioration of the spatial resolution was made by merging Landsat ETM+, SPOT-5 and IKONOS images with the panchromatic band of each satellite.

Visual photo-interpretation of the resulting images assisted by the collected database on forest fires has allowed detecting burnt areas. Several spectral confusions were reported in many studies using Landsat TM images between the burnt areas and non covered zones, specifically water bodies, urban regions and bare soils from one side [10, 11, 12] and shadowed areas from the other side [12, 13]. For that, in addition to historical data, land cover maps were used to minimize these confusions. The first one (1.50,000) was established by FAO (1990) [14] from SPOT-HRV (20 m) images acquired in October 1987 and the second (1.20,000) issued from the visual interpretation of indian panchromatic images with very high resolution IRS (5.8 m) acquired in 1998 [15]. The obtained burnt areas map was then intersected using GIS with some of the factors influencing fire propagation, allowing therefore the calculation of their relative weights.

## 3.3 Fire vulnerability

Several factors affect the behaviour of forest fires, resulting in complex spatial patterns after each fire. Five are considered in this study showing a close interrelationship with the fire phenomenon, i.e. vegetal cover, fuel type, slope gradient, slope aspect and evapotranspiration. In addition, past fire events (20 recorded available years) were integrated also in the model designed for the whole country for better evaluating the future fire risk occurrence.

### 3.3.1 Vegetal cover

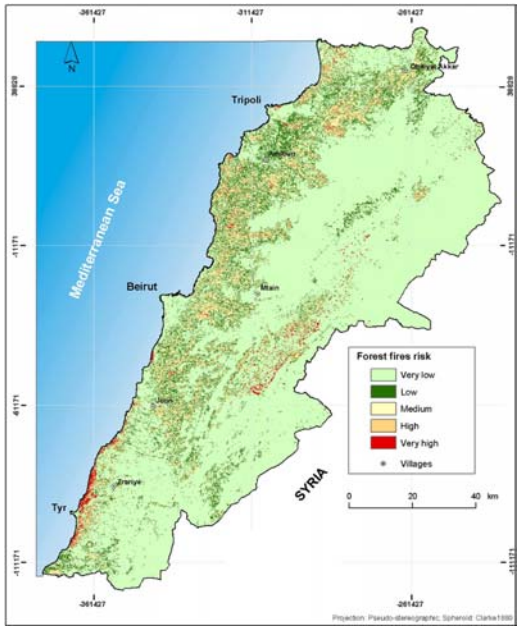


**Figure 2.** NDVI map of Lebanon.

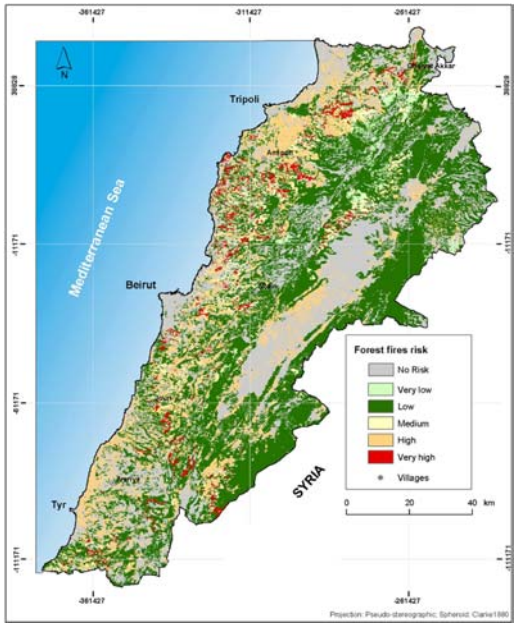


**Figure 3.** Land cover/use fire vulnerability map.

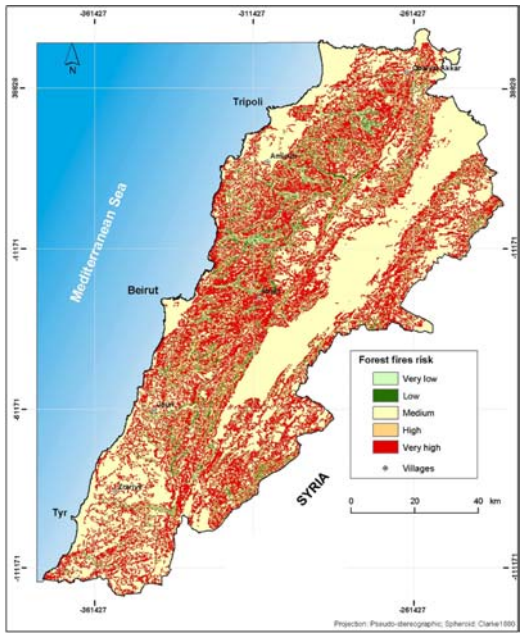


**Figure 4.** Slope gradient fire vulnerability map.

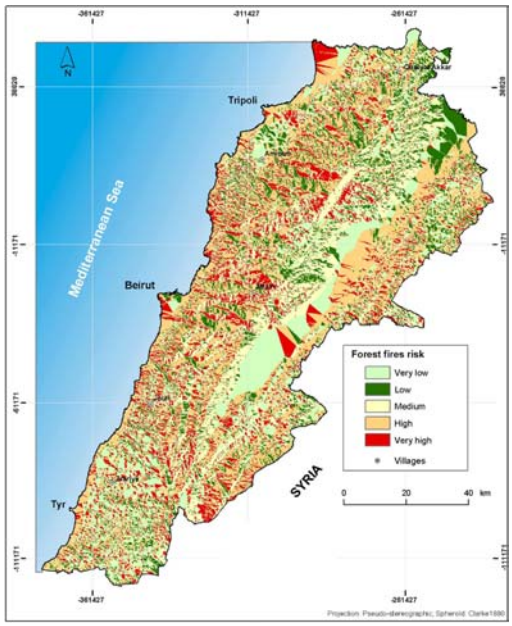


**Figure 5.** Slope aspect fire vulnerability map.

The vegetal cover or relative biomass is considered as an important factor in the extension of fire. It was determined by calculating the NDVI (Normalized Difference Vegetation Index) from a Landsat TM image (30 m spatial resolution) when the whole country is considered (Fig. 2) and from a SPOT-5 satellite image (5 m) for the five pilot areas. An increase of NDVI is supposed to be in relation with the increase of fire risk.

### 3.3.2 Fuel type

Forest fuels are energy sources responsible for the ignition, propagation and consolidation into crown fires due to their spatial distribution. Various plant species have a different sensitivity towards fire. Each fuel or vegetable type burns more or less quickly than the others. For that, a determination of the different land cover/use modes covering Lebanon was done by referring to the available map produced at a scale of 1:20,000 [15]. It was updated in this

study using IKONOS satellite images with very high spatial resolution (1 m) acquired in 2003. Classifying these modes in function of their sensitivity to fire was established depending on a statistical calculation of the fire occurrence probability in Lebanon for the period extending between 1983 and 2003. The obtained numbers of fires per fuel type were converted to percentages or ratios (weights) (Fig. 3).

### 3.3.3. Slope gradient

Slope gradient is considered an indicator of forest density, and on steep slopes, forests are dense implying a high probability of fire extension. It was derived from digital elevation models (DEM) with different resolutions, i.e. 50 m (whole country) and 10 m (pilot areas). Considering the histogram of equalization between distribution of slope gradient and the corresponding number of pixels, the slope gradient was divided into five different classes depending on the area studied (whole country or pilot areas). The overlapping using GIS of derived slope maps with burnt areas map has allowed the calculation of fires percentage in each slope class (Fig. 4).

### 3.3.4 Slope aspect

Aspect, within the topographic variables, was selected because it is related to the amount of solar illumination the vegetation receives, which influences both the type of fuels and their moisture condition. Moreover, areas exposed to sun show a higher aptitude to forest fire due to the resulted high temperature. The DEMs with 50 m and 10 m size were also used to divide the studied areas into four classes of slope exposure (N-E, E-W, S-W and W-N). Based on the number of forest fires on each slope aspect class, weights were calculated (Fig. 5).

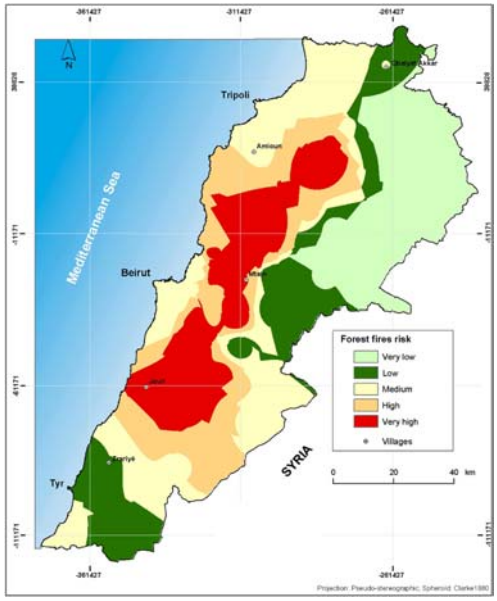


**Figure 6.** Evapotranspiration fire vulnerability map.

### 3.3.5 Evapotranspiration

It is assumed that the dryer the vegetation is, the more prone it is to be burnt. Since it is difficult and costly to directly estimate the vegetation water content, surrogate variables are used to estimate it. This is often done through the use of meteorological variables, or through the use of vegetation indices computed from remotely sensed data. Calculation of evapotranspiration is in close relation with meteorological data, specifically the temperature. Once the temperature is high, evaporation and transpiration will be very high implying a dryness natural vegetation cover, and thus indicating a high probability of forest fire extension. In Lebanon, five classes of evapotranspiration sensitivity having an interval of about 200 mm/year were considered by dividing the available digital evapotranspiration map [16] ranging from 785 mm/year to 1836 mm/year. This map was intersected with the burnt areas map to determine evapotranspiration sensitivity classes (Fig. 6).

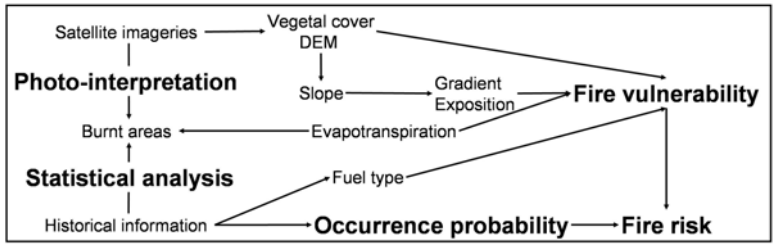


**Figure 7**. Organigramm showing the different steps of the study.

## 3.4 Modelling fire risk

The designed models were produced by combining using ArcGIS software the considered influencing factors (Fig. 7). For that, all the produced factorial maps were converted into raster format with different grid sizes, i.e. 50 m (whole country) and 10 m (pilot areas). The final value of each cell in the forest risk maps at 1.100,000 cartographic scale (whole country) and 1.20,000 (pilot areas) was calculated by multiplying the values of the factors described above divided by 6 (5 natural factors + past fire occurrence). The maximum normalized values obtained (values ranging 1-2) pointed up the very high forest risked areas. This range was further divided into six fire risk classes from no risk to very high risk using the natural break method.

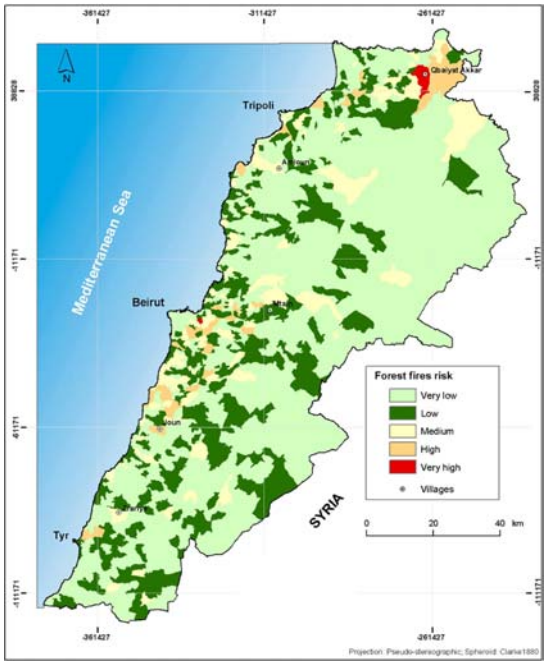


**Figure 8.** Fire occurrence map.

## 4 RESULTS AND DISCUSSION

During the analysis of past fires' archive, we have found that fire data collected by the Lebanese centers during the years of 2002 and 2003 were more accurate than those considered per other sources, especially because of the war period (1975-1990) imposing other concerns.

### 4.1 Forest fire occurrence per fuel type

Thicket is the most fuel type affected by fires during 20 years (1983-2003). It is followed by olives for 2002 and 2003. Herbs are replaced by fruit trees between 1983 and 2001. Meanwhile, in spite of the reduced number of fires attacking pine and oak forests, their limited coverage aggravates the risk to a critical point.

### 4.2 Forest fire geographical distribution

Analysing the collected fire data on 20 years (1983-2003) indicates that the majority of fires are occurring in Mount Lebanon mohafazat (40 of fires), followed successfully by North (24%), South (19%), Bekaa (10%) and finally by Nabatieh mohafazat (7%). No forest fires were noted in Beirut due to the absence of green areas. Mount Lebanon is known as the richest mohafazat in forests and the most attractive place for tourists. A map was produced describing the number of fires per cadastral zone for 20 years (1983-2003) (Fig. 8). This map allows detecting areas highly affected by fires and those without any risk of fire propagation. It seems beneficial to municipalities managing therefore fires at earliest stage. Six different classes of fires' occurrence were taken and determined using natural breaks method. The number of fires can reach 95 per cadastral zone during 20 years. The areas occupied by each class can be summarized as follows: no fires (29% of the total area of Lebanon), very low "1-9 fires" (49%), low "10-18 fires" (13%), medium "19-32 fires" (8%), high "33-53 fires" (0.27%) and very high occurrence "54-95 fires" (0.4%). This map indicates that 71% of the country is affected by one fire at least during 20 years, demonstrating the necessity of acting to limit the propagation of this problem and restraint its propagation. The five pilot areas used in this project are affected by different numbers of fires during 20 years, i.e. Mtein (15 fires), Dmit (17), Ramlieh (6), Qornayel (29) and Ras El-Matn (20).

### 4.3 Fires timing

The analysis of the collected fire data for 2002 and 2003 indicates that fires can occur between June and October of each year with a high frequency during August and September (25 to 27% of the fires occurred). The highest percentage of fires is falling between 12 and 18 p.m. with a mean start time approximately equal to 14 p.m., on which the sun is highly rising. The mean duration for each fire oscillates between 2 hours and 5 days. Cypress forests are the most affected during long time (5 days), followed by thicket and oak forests (2 days approximately). In addition, all fires develop equally for all days of the week indicating that leisure activities during the week-end are not aggravating fires.

**Table 1.** Matrix relating the number of fires and climatic conditions (temperature and wind velocity).

| **Number of fires** | | **Wind velocity (km/h)** | | | | |
|---|---|---|---|---|---|---|
| | | < 15 | 15-20 | 20-25 | 25-30 | > 30 |
| **Température (◦C)** | < 27 | 4 | 37 | 168 | 186 | 250 |
| | 27-28 | 8 | 60 | 193 | 197 | 250 |
| | 28-30 | 5 | 71 | 421 | 494 | 539 |
| | > 30 | 1 | 85 | 443 | 580 | 728 |

### 4.4 Causes of forest fire occurrence

We have analyzed also the probable causes of fire occurrence. These can be related to climatic or anthropic conditions. The increase of the number of fires coincides with an increase of the temperature coupled with a strong wind (Table 1). If one of these climatic parameters is high only, few fires will occur. 50% of fires produce if the

temperature is superior to 28 ◦C and if wind velocity is more than 25 km/hours. The number of fires increases also with the increase of the humidity, i.e. 76% of fires is produced at a relative humidity superior to 70%.

The overlapping between land use map and fire occurrence map at the level of cadastral zone (Fig. 8) allows formulating certain hypotheses: 1) a high concentration of fires is observed visually in the hills and mountainous areas close to Beirut agglomeration and on the coast. This indicates a strong link between urbanization and forest fires. 2) This relation do not seem having the same intensity everywhere. We can distinguish for example another region, the forested hills and mountains of Akkar in the North, where the frequency of fires seems equally important, while the urbanization level is lower than the coast even though the urban is denser, particularly with a dispersed habitat.

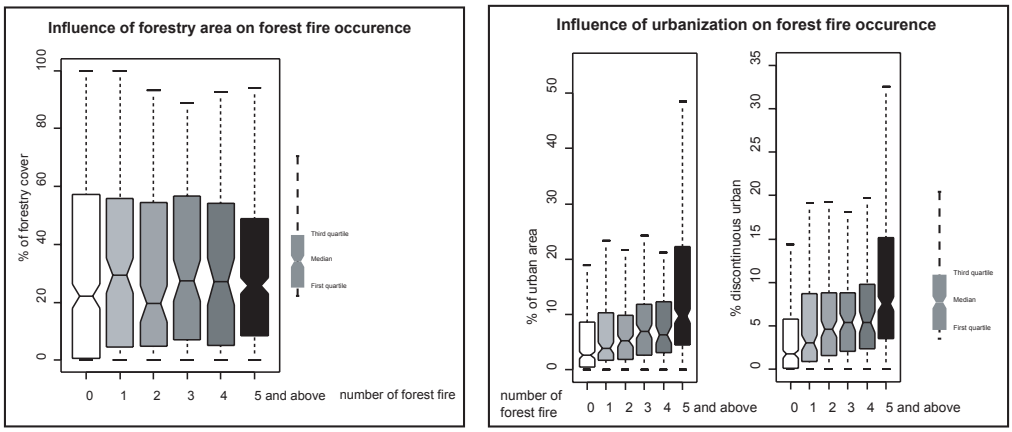


**Figure 9.** Influence of forestry area and urbanization on fire occurrence.

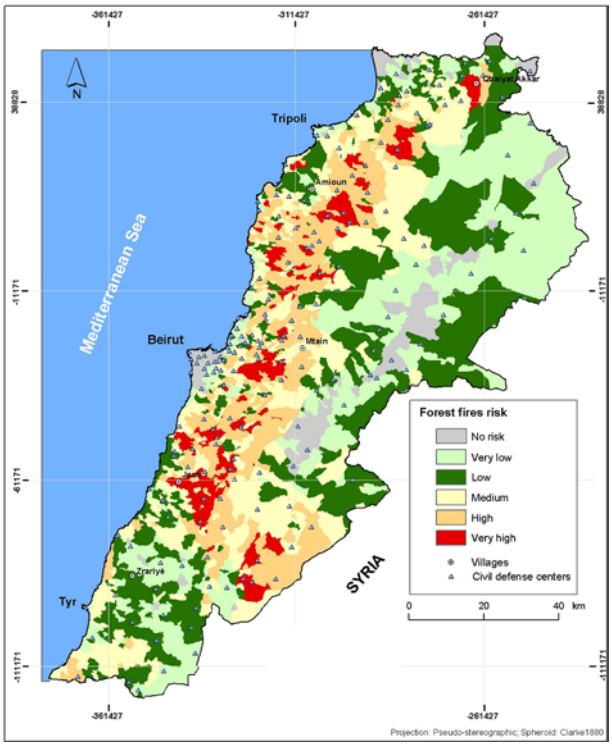


**Figure 10**. National fire risk map of Lebanon.

A third region appears in the South, where the urbanization is relatively high but dispersed. The second hypothesis indicates that fires intensity is linked to disperse urban in forested areas. To validate these hypotheses, 5 populations of cadastral zones were constructed in function of the produced number of fires, i.e. 0, 1, 2, 3, 4 and 5 $^{+}$. It appears that fire occurrence presents a strong link with the problematic of urbanization, if we consider dispersed or continuous urban (Fig. 9).

## 4.5 National forest fire risk map

The intersection of the factors affecting the fire behaviour together had led to produce the national fire risk map of Lebanon (Fig. 10). A good portion of Lebanon is affected by a medium risk (28%), which can become high or very high if no appropriate management of resources is taken place. High and very high fire risk classes are covering 575 km$^2$, representing 5.5% of the total area of Lebanon. They are mainly located on the southern slopes of western Mount Lebanon chain, which are covered by broadleaf and coniferous forests. They are also observed in North Lebanon, especially in Qbayat area (Akkar). The coastal strips (Beirut mainly), barren rocky areas specifically in Anti-Lebanon mountains as well as bare lands of the Bekaa valley are not showing a fire risk. Grasslands largely widespread in South Lebanon as well as horticultural areas and open agricultural fields of the major productive regions (Bekaa and Akkar plains) are belonging to low risk class (31%).

Five other fire maps were also produced at 1.20,000 scale covering the following pilot areas, i.e. Mtein, Dmit, Ramlieh, Qornayel and Ras El-Matn.

## 5 CONCLUSION

The obtained forest fire risk maps can be used in assigning in tactical decisions on prioritizing fires for initial attack. They give an indication of forest fires at long-term and they will be utilized by policy-makers to protect suffering from fires. More work is required to better quantify values and risks, as well as suppression capability. The incorporation of a spatial climate model would improve fire behaviour predictions. In addition, instead of using only the worst case fire weather, it would be useful to examine the wildfire threat associated with multiple-year fire weather conditions to determine how many days fall in each wildfire threat class during an average fire season on a spatial daily basis.

## ACKNOWLEDGMENTS

This research is part of a project held among the Association for Forest Development and Conservation (AFDC-Lebanon), Green Line Association (GLA-Lebanon) and the National Center of Remote Sensing (NCRS-Lebanon). It has been supported by the European Commission (EC Life) as a part of an important work asking for the assessment and monitoring of forest fires in the Mediterranean region. For that, we express all our thanks to the responsibles of both associations and European Union.

## REFERENCES

[1] VARELA, J., ARIAS, J.E., SORDO, I. AND TARELA, A., 2003: Multicriteria decision analysis for forest fire risk assessment in Galicia, Spain. 4th International Workshop on Remote Sensing and GIS applications to forest fire management: Innovative concepts and methods in fire danger estimation, 5-7/6/2003, Ghent University, Belgium.

[2] ZOHARY, M., 1973: The geobotanical foundation of the Middle East. Vol. 1. Gustave Fisher Verlag, Amsterdam.

[3] TALHOUK, S.N., ZURAYK, R. AND KHURI, S., 2001: Conservation of the coniferous forests of Lebanon: past, present and future prospects. Oryx, 35(3), pp. 206-215.

[4] KAUFMAN, Y.J., JUSTICE, C.O. AND SETZER, A.W., 1998: Potential global fire monitoring from EOS-MODIS. Journal of Geophysical Research, 103, pp. 3221-3225.

[5] SAN MIGUEL-AYANZ, J., ANNONI, A. AND SCHMUCK, G., 1998: The use of satellite imagery for retrieval of information on wildfire damage in Mediterranean landscapes. Proceedings of ERIM'98, International Symposium on Remote Sensing of Environment: Information for sustainability, 8-12/9/1998, Tromsö, Norway, pp. 758-762.

[6] MITRI, G.H. AND GITAS, I.Z., 2004: A semi-automated object oriented model for burned area mapping in the Mediterranean region using Landsat-TM imagery. International Journal of Wildland Fire, 13, pp. 367-376.

[7] BECK, J.A. AND MULLER, C., 1991: The inception and development of decision support systems for forest fire management in Western Australia. In: Daniel, T.C. and Ferguson, I.S., (eds). Integrating Research on Hazards in Fire-Prone Environments - Proceedings of the U.S. Australia Workshop, Melbourne 1989.

[8] FINNEY, M., 1995: FARSITE. Fire area simulator. User's guide and technical documentation. Version 1.0. System for Environmental Management. Missoula MT.

[9] CHUVIECO, E., DESHAYES, M., STACH, N., COCERO, D., RIANO, D., 1999: Short-term fire risk: foliage moisture content estimation from satellite data. In: Chuvieco, E., ed. "Remote sensing of large wildfires in the European Mediterranean basin". Springer-Verlag, New York, pp. 17-38.

[10] PEREIRA, J.M.C., 1992: Burned area mapping with conventional and selective principal component analysis. Revista Portuguesa de Geografia, 27, pp. 63-78.

[11] SILJESTRÖM, P. AND MORENO, A., 1995: Monitoring burnt area by principal component analysis of multitemporal data. International Journal of Remote Sensing, 16(9), pp. 1577-1587.

[12] CAETANO, M.S., MERTES, L., CADETE, L. AND PEREIRA, J.M.C., 1996: Assessment of AVHRR data for characterising burned area and post-fire vegetation recovery. EARSeL Advances in Remote Sensing, 4(4), pp. 124-134.

[13] PEREIRA, M.C., CHUVIECO, E., BEUDOIN, A. AND DESBOIS, N., 1997: Remote sensing of burned areas: a review. In: Chuvieco, E. "A review of remote sensing methods for the study of large wildland fires". Departamento de Geografia, Universidad de Alcala, pp. 127-184.

[14] Land cover/use maps of Lebanon at 1.50,000. FAO.

[15] Land cover/use maps of Lebanon at 1.20,000. National Council for Scientific Research and Ministry of Agriculture (Lebanon).

[16] Evapotranspiration map of Lebanon at 1.200,000. Climatic Atlas of Lebanon. Ministry of public affairs.

# Steppic areas dynamics and agropastoral systems viability in the Jeffara region (Southern Tunisia)

A. Hanafi[a], D. Genin[b], V. Simonneaux[c]

[a] Institut de Recherche Pour le Développement (IRD) - Tunisie, BP 434, El Menzah - Tunisie, Tél: +216 71 750 009, fax: +216 71 750 254, email: ali_hanafi@yahoo.fr;
[b] Laboratoire Population - Environnement - Développement, Centre St Charles, 3 Place V. Hugo, 13003 Marseille, Cedex 3 - France,
[c] Programme SudMed - Centre Geber, Université Cadi Ayyad, B.P. 2390 Marrakech - Maroc

## ABSTRACT

The Jeffara is an arid region of Southern Tunisia characterised by the fragility of its environment and the scarcity of its natural resources (water, soil and vegetation). Following the political, economic and social transformations (independence, demographic explosion, sedentarisation, land privatisation…) occurring notably during the past fifty years, this region has been subjected to an important spatial dynamics affecting its rural areas, its traditional land uses and especially its steppic vegetation. The analysis of this dynamics on a thirty-year period was possible thanks to two satellite images covering the area (Landsat/MSS of 1972 and SPOT/PXI of 1998) that were completed by a field data collection. Results showed (i) an important fragmentation and encroachment on the steppe areas and (ii) a general decrease of their surface of about 38% to the benefit of agricultural lands (olives orchards and irrigated perimeters) that increases of about 617%. The residual steppes presented also (iii) high qualitative variations in term of floristic composition and cover, which were discussed regarding their ecological significance. The drastic land use dynamics observed in the region highlighted transformations of the traditional agropastoral systems, which turned from a subsistence-oriented activity characterised by a spatio-temporal flexibility in the use of natural resources and diversified farms, into a more market-oriented systems with more specialised farms and intensification in the uses of natural resources, particularly regarding soils and water. This situation led to an enhancement of the global rural livelihood, but also induced high disparities between farms, and the emergence of new environmental, economical and social risks, which cast doubts on the viability in the middle and long term of the present production systems.

**KEYWORDS:** Satellite images, Steppe , Land use / Land cover, Degradation, Agropastoral production systems, Viability, Desertification, Southern Tunisia.

## 1 INTRODUCTION

Since the sixteenth, the Tunisian Arid Lands have been submitted to important territorial dynamics that have led to the disturbance of ecosystems' equilibrium and degradation of natural resources. The environment degradation has especially been remarkable in the steppic vegetation. The demographic explosion and the acceleration of the privatisation of collective areas, accompanied by the government policies in favour of rural settlement, are main factors for the quantitative and qualitative regression of the steppes and thereafter the decline of extensive grazing and an important agricultural intensification based on the spatial extension of orchards. Nowadays, natural resources, especially vegetation and soil, play less and less their role in the environment protection against desertification risks. The weak adaptation of the contemporaneous agropastoral systems accelerated the deterioration of the natural resources and generated a landscape more and more constituted by invading cultivated sectors with residual steppes of low pastoral value.

## 2 STUDY AREA

The study was conducted in the Jeffara region, a characteristically areas of the Tunisian arid lands, located in the Tunisian south-eastern of the Country. This region is morphologically diversified, constituted by a part of the Matmata mountains in the south-west and the west, a calcareous crusted piedmont, and a sandy central plain separated from the gypseous crusted coastal plain by a set of calcareous crusted foothills. This landscape ends to the north-east and the east by a set of closed salty depressions on the border of the Mediterranean Sea. The bioclimat is defined as Mediterranean lower Arid (Q = 15-20) with winter rains and summer droughts. The mean annual rainfall is around 150-200mm with a high interannual variability (with an average of 2 rainy years of 5). Therefore, surface water resources are limited, and underground water is important but slightly salty. Soils are generally poor in

organic materials and nitrogen. The human occupation is very ancient and nowadays conforms a rural society submitted to deep socio-economical mutations [1].

## 3 LAND USE / LAND COVER DYNAMICS BETWEEN 1972 AND 1998

### 3.1 DIACHRONIC SURVEY OF LAND USE / LAND COVER DYNAMICS

Using two satellite images, a Landsat MSS image of 1972 and a SPOT/XS of 1998), we mapped the land use / land cover dynamics in the Jeffara region between 1972 and 1998. The SPOT/XS image was first *georeferenced*, using *ENVI 3.4* software, on the basis of the Tunisian topographic map at 1/200.000 scale - Gabès paper. Then, the Landsat/MSS image was geo-referenced based on the SPOT/XS image allowing a good superposition of the two images. In order to have the same spatial resolution for the two images, the Landsat/MSS image was resampled from 80m/80m to 20m/20m.

Using Unsupervised Classification, the two images were classified in 30 classes in order to discriminate the maximum of objects on the field. This technique was preferred to Supervised Classification because spectral definition of classes was very heterogeneous and difficult to describe by field sampling. Conversely, our good empirical knowledge of the area allowed us to interpret rather easily the classes obtained. A post-classification was then achieved on the two images allowing to merge the classes with the same meaning.

After this processing, the two images and their classifications were integrated into a GIS. Based on classes mixture and texture differences, we visually interpreted landscape units on the images using a combination of information sources, including topographic features, geomorphological units, soil characteristics and the spatial extent of the vegetation units. Referring to several field data collections achieved in 2001, we established a pre-map of the contemporaneous landscape units. To have the same pre-map in 1972, we referred to previous cartographic documents and bibliography [2], [3], [4], [5]. The result of this work showed big landscape heterogeneity what didn't facilitate the diachronic analysis. Therefore, we simplified the representation in the main units based on the spatial dominance of steppes or crops (Table 1, fig. 1 and2):

**Table 1:** Main landscape units of the Jeffara region

| | **Steppes** | **Crops** | **Urban** |
|---|---|---|---|
| **Pure or greatly dominant steppe** | > 90 | < 10 | - |
| **Pure or greatly dominant crops** | 60-90 | 10-40 | - |
| **Steppe - Crops mosaics** | 10-40 | 60-90 | - |
| **Crops - Steppe mosaics** | < 10 | > 90 | - |
| **Urban Agglomerations** | - | - | 100 |

The superposition of the maps, thanks to the GIS, allowed to establish the map of land use / land cover dynamics between 1972 and 1998. The 1972-1998 period has especially been characterised by a drastic decrease of the steppe areas of about 19.000ha (-38%) of the total area of the pure steppe found in 1972 (fig.3, Table 2). This decrease occurred mainly in the 70's at the expense of the piedmonts supporting the *Artemisia*

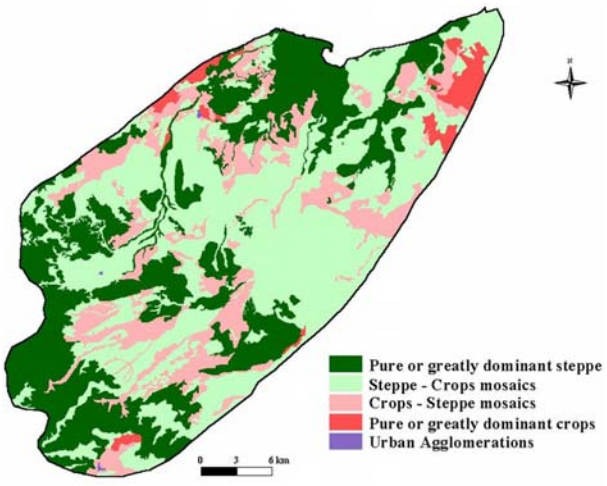


**Figure 1.** Spatial distribution of landscape units in the Jeffara region in 1972.

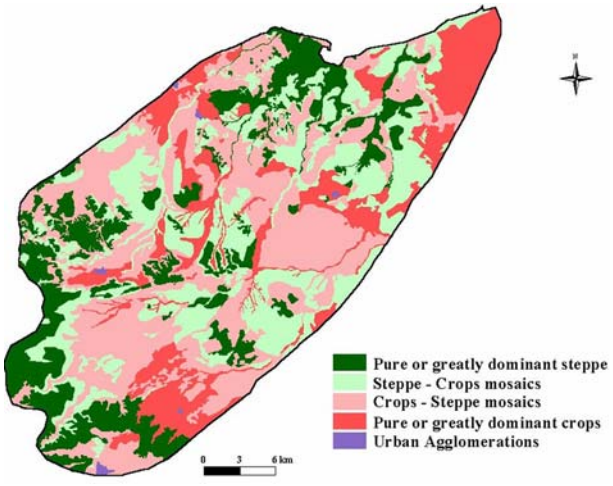


**Figure 2.** Spatial distribution of landscape units in the Jeffara region in 1998.

*herba-alba* & *Hammada scoparia* steppes (35% of the lost 19.000ha), the sandy *Rhanterium suaveolens* steppes (26%) and of the wadi beds *Ziziphus lotus* & *Retama raetam* steppes (18%) [6].

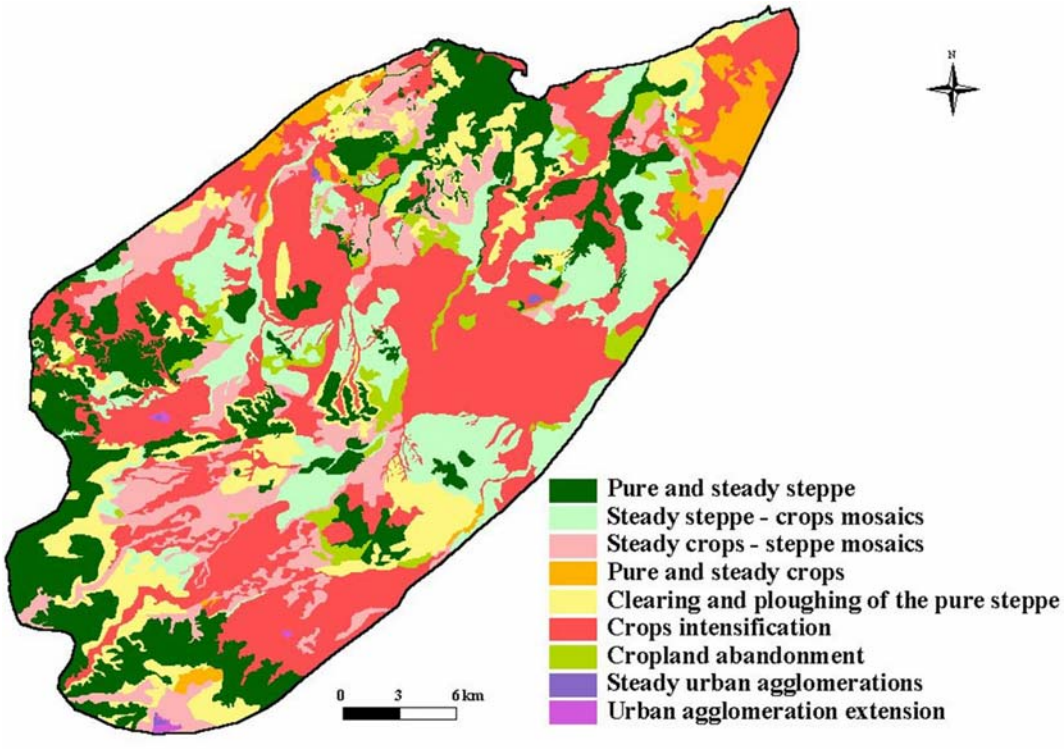


**Figure 3.** Land use / Land cover spatial dynamics in the Jeffara between 1972 and 1998.

**Table 2.** Land use / Land cover quantitative dynamics in the Jeffara between 1972 and 1998

| Landscape units | Area in 1972 (ha) | Area in 1998 (ha) | % |
|---|---|---|---|
| **Pure or greatly dominant steppe** | 50 210 | 30 957 | - 38,3 |
| **Steppe - Crops mosaics** | 73 212 | 40 998 | - 44,0 |
| **Crops - Steppe mosaics** | 26 501 | 49 396 | 86,4 |
| **Pure or greatly dominant crops** | 4 539 | 32 562 | 617,3 |
| **Urban Agglomerations** | 450 | 1 000 | 122,1 |
| **Total** | 154 913 | 154 913 | |

*Source*: Hanafi, in prep.

The collective land privatisation and the steppes area decrease are correlated to an important increase of croplands. Table 2 shows an increase of the pure or greatly dominant crops of about 28.000ha (617%) between 1972 and 1998. Crops spread first, over the piedmonts and the wadi beds, and later on sandy plains. Wadi beds steppes lost in this period about 91% of their area to the benefit of crops. In the sandy steppes, this loss was about 38%. In the 1970-1980 period, agriculture expansion has been based on olive trees plantation combined to dry cereal cropping. In the 90's, it has been characterised by the extension of irrigated perimeters especially private ones. In spite of their weak spatial extension (1ha on average per exploitation), the irrigated perimeters increased a lot during this period reaching more then 120 exploitations in 2002, and occupying about 350ha [7].

## 3.2 An Environment always threatened by desertification

At a vegetation scale and since a long time, the Jeffara has experienced many waves of natural vegetation cutting to the benefit of cropping. However, this phenomenon has especially been important since the 60's due to an important population dynamics (demographic increase, extra-agricultural incomes investment in agriculture). The acceleration of the collective land privatisation, the various government encouragements and the agricultural

activity mechanisation permitted the dismantling of crusts, the increase of water and soil harvesting techniques, particularity in plains, and therefore, the plantation of trees. Nowadays, the result of this dynamics is a heterogeneous landscape characterised by a mosaic of many vegetation units overlapped with many cropping units. Perennial plant cover decreased in all vegetation units from about 20-30% to about 10-15% on average in thirty years [6]. The different units are henceforth characterised by floristic homogeneity due to the extension of post-cultivated species and the dominance of unpalatable ones (*Astragalus armatus ssp. tragacanthoides*, *Cleome amblyocarpa*, *Peganum harmala*…) due to overgrazing. The main result of these floristic changes is the decrease of biodiversity and the reduction of vegetation role in the protection of soil against wind deflation. Human activities are today the main causes of this phenomenon and of ecosystems equilibrium disturbance.

At a landscape scale, traditional agropastoral systems were adapted to the peculiarities of rainfall (drought and variability) and topography (wadi beds). Many water harvesting techniques (*jessour*, *tabias*[1]…) have been made mainly within wadi beds, allowing a rational extension of arid agricultural types (cereal cropping, orchards). However, the intensification of natural resources uses particularly at the end of the 70's and the beginning of the 80's, increased desertification processes in the Jeffara region [8]. This phenomenon has been especially conditioned by a succession of several very dry years (1976-77, 1979-80, 1982-83…) and by government policies more oriented toward urban agglomerations than rural environment [9] and encouraging land privatisation [8]. Relatively abandoned by the government, the rural environment has been thereafter, abandoned by the farming population whose life conditions were difficult. This situation was the main cause of migration toward national urban agglomerations, Libya and Europe. As a consequence, soil and water harvesting techniques was abandoned and landscape, very degraded, was therefore exposed to desertification. At the end of the 80's and the beginning of the 90's, massive intervention of the different social actors (Government, rural population, scientists...), has limited desertification extension.

Nowadays, new cereal cropping and olive trees plantation are developing, especially on sandy plains threatening the region by the return of desertification processes. Clearing and ploughing to the benefit of cropping decreases first vegetation cover, and then, increases the risk of wind erosion. These phenomena lead to sand dunes accumulation especially along roads and around urban agglomerations and farming exploitations. Hence, desertification remains always a preoccupying problem in several sectors of the Jeffara region. It will be able to start again if the social actors don't rationalise natural resources uses and control land use dynamics. Today, preventing the region against the return of this phenomenon should pass by a better understanding of the socio-economic problems of the farming population in order to assure their sustainable development without compromising regeneration and conservation of natural resources.

## 4 THE CONTEMPORANEOUS AGROPASTORAL PRODUCTION SYSTEMS: TYPOLOGY, IMPACTS ON LAND USE DYNAMICS AND VIABILITY

### 4.1 TYPOLOGY OF AGROPASTORAL SYSTEMS

Using data from a pervious socio-economic survey achieved in 2002 on 609 households, we intended to define a typology of the main agropastoral systems found in the region. Among households surveyed, 535 had an agricultural and/or pastoral activity and were differentiated on the basis of 3 categories of quantitative and qualitative variables, which were subdivided in 52 modalities [6]. The variables are (i) socio-economic (household chief age, household size, number of domestic employees in the household, household main source of the monetary incomes, part of agricultural income / total income, household monetary income level and household external employment), (ii) related to agricultural activity (total areas farmed by the household, % of area occupied by orchard, possession of irrigated perimeters, use of agricultural inputs in the exploitation) and (iii) related to pastoral activity (household herd size, dominant animal species, part of steppe in herd alimentation, herd mobility)

From this dataset, our aim was to define a typology in order to figure out the major agropastoral systems. This was achieved by the use of multivariate analyses (*Multiple Correspondences Factorial Analysis, Hierarchical Ascending Classification, Typology*…) thanks to the *Statbox* software. These analyses highlighted 7 agropastoral production systems. The use of households coordinates in GIS allowed on one hand, to map these production systems, and on the other hand, to superpose this map with the one of land use dynamics to see the relation between the agropastoral production systems on the landscape changes during about thirty years.

[1] The *tabias* and the *Jessour* are a small water harvesting techniques (elevations of soil trained in wadi beds), conceived in the South Tunisian mountains to keep the water and soil excess coming from impluviums and their exploitation for agriculture. A *Jesser* (singular) is composed by an impluvium, the wadi bed and the soil elevation also locally called *tabia* or *katra* [10].

Results showed a diversification of the contemporaneous agropastoral systems comparing to the previous ones [11], [12]. The 7 types identified here are:

- The subsistence small agro-pastoralists
- The young agro-pastoralists in phase of production growing
- The small cultivators
- The big cultivators
- The small precarious pastoralists
- The big agro-pastoralists
- The big pastoralists.

A more detailed description of these types can be found in Genin et al. (2003) [13]. More diversified then before [11], these agropastoral systems are also characterised by their specialisation, the intensification of their uses of the limited natural resources and their market orientation. The result of these changes is the reduction of their flexibility and their complementarity not only between agro-pastoral activities but also between farms [6].

## 4.2 IMPACTS OF AGROPASTORAL SYSTEMS ON LAND USE DYNAMICS

The superposition of these different agropastoral production systems with land use / land cover data (fig. 4) showed a localisation of the exclusively agricultural systems between wadi beds, on sandy plains and on crusted foothills and plains which are not necessarily appropriate to cropping [14].

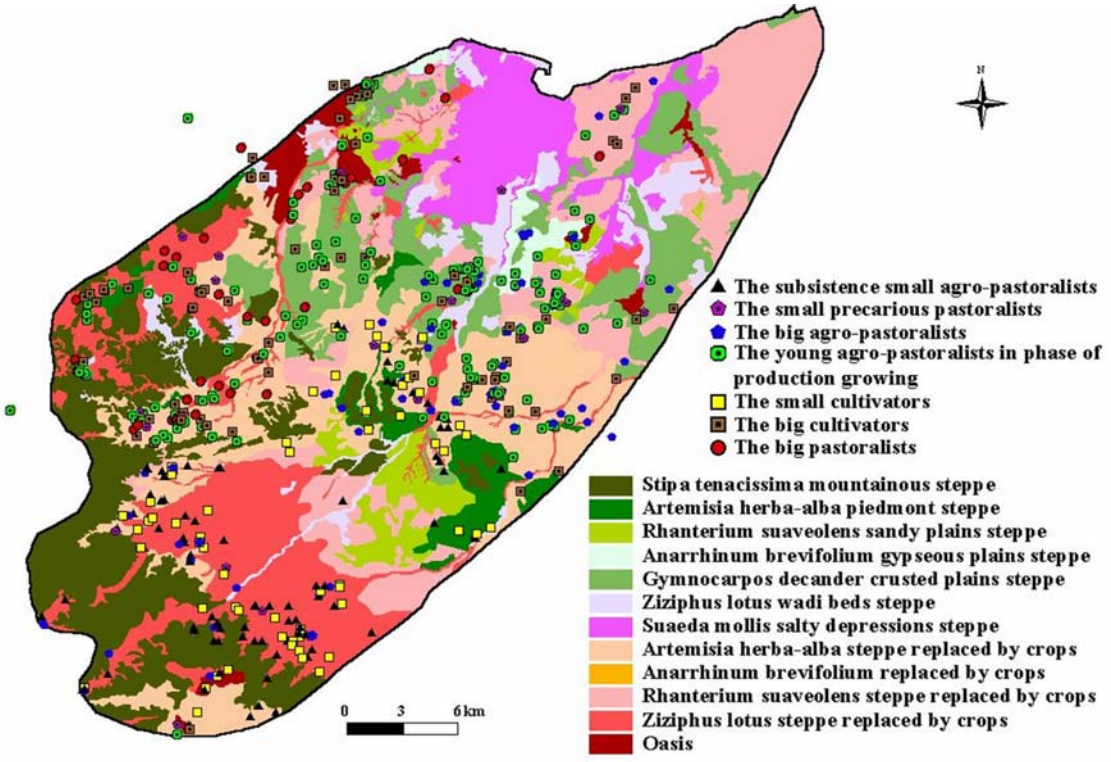


**Figure 4.** Impact of agropastoral production systems on land use / land cover dynamics in the Jeffara region.

It is the case of young agro-pastoralists in phase of production growing (characterised by young households chiefs, the possession of about 10 to 20ha dominated by orchards, a relatively high monetary income coming mainly from the extra-agricultural activities) who are mainly localised on crusted and sandy plains. The investigation showed that a large part of their income is invested in the agricultural activity particularly in olive tree plantation.

## 4.3 AGROPASTORAL PRODUCTION SYSTEMS VIABILITY

The socio-economic changes occurred in the region generated some transformations in landscape occupation: a deep reduction of the traditional adaptive uses of the spatio-temporal heterogeneity of natural resources such as herd mobility, roving agriculture, mountains agriculture with jessour systems and related ones; a higher dependency on foreign inputs and resources which led to deep changes in the structure and functioning of agropastoral systems. These changes can be highlighted by some specialisation and intensification at the farm household level. Consequently, we observed a higher pressure on land utilisation, and particularly the most sensitive areas to desertification. The case of olive orchard development observed during the three past decades is particularly significant of the environmental and socio-economical threatening dynamics observed in the region. It can be considered as a "green desertification". Indeed, these new cropping areas are often extremely stony and characterised by marginal soils. Therefore, Water Use Efficiency is very limited and trees roots present an important development deficits [13]. In this situation, the development of orchards is submitted to strong environmental constraints (strong droughts). The production of olive is of this fact, often weak (18,5 kg of olives per tree on average), with very high inter-annual variability (42 kg/tree in 1991 and only 3,8 kg/tree in 2002) [ODS, 2003 cited by 13]. Indeed, the recent dry period (1999-2002) has shown the difficulties of this type of agriculture. It was especially striking for the almond-trees of which the death rate by drying out reached 60% [ODS, 2003 cited by 13]. These losses were particularly localised in areas not appropriate to cropping activities (crusted areas with very degraded soils and limited water reserves…).

The second type of cropping extension is the irrigated perimeters. They are usually of small sizes because of the limited financial means of the majority of the farmers. The weak soil fertility and level of agricultural input and the water salinity contributed to limit this cropping type. In addition to these limitations, we must mention the pressure that water resources undergo by the other social actors and economic sectors (urban agglomerations, tourism in Jerba island…). This situation exposed the region to many socio-economic inequalities linked to water access modalities [7]. The scarcity of this resource and the inequalities in its distribution, are sometimes threatening for the irrigated perimeters productions (tomato, pepper and melon…) in the case of coercive climatic conditions (ex: the *sirocco*, hot and dry wind, blowing during spring).

Finally, dynamics observed in the Jeffara region also led to a reduction of livestock husbandry importance in agropastoral households, which was in the past the pillar of rural livelihood. This evolution effectively has to be related to the decrease of rangeland areas, but also to changes in perception on ways of life and to low incentives from public rural policies for extensive livestock husbandry. However, due to a high flexibility linked with animal mobility, with the possibility to sell and buy easily animals, and with the opportunity to economically valorise marginal lands, extensive livestock production is viewed as a sound strategy to spread risks, particularly in arid zones [15], [16]. In the Jeffara region, agro-pastoralists are more and more attracted to intensify their livestock production, by purchasing feeds from outside the region, and are less awared on the importance of integrity of rangelands and on their rational management. This situation could partly explain the poor status of rangelands in the region.

## 5 CONCLUSION

This work demonstrates how satellite imagery may help monitoring landscape changes occurring in arid areas. Because of the poor discrimination of land cover classes induced by a high spectral heterogeneity due to heterogeneous physical and anthropic conditions, classical classification techniques alone don't allow an accurate land cover mapping. Instead, we showed that a limited image processing (automatic classification), followed by a visual interpretation of the resulting map, may help mapping diachronic changes.

Agropastoral systems dynamics found in the Jeffara induce many disturbances in traditional balance between the human use of natural resources and land use / land cover. The result of these interactions and evolutions is an heterogeneous landscape formed by a mosaic of steppes and crops units used by some agropastoral systems sometimes not well adapted to environmental specificities' of the region and thus highly sensitive to environmental and/or socio-economical events which can lead to threaten their viability. Nowadays, the human population of the Jeffara region requires an improvement of its life conditions. This will go through diversification of socio-economical activities, including the maintenance and development of the agropastoral sector based on the adaptation of agropastoral activities to the highly limiting constraints of this arid region, and on the conservation of landscapes against the risks of desertification. This choice is not only socio-economic but also environmental, and encompassed in a global perspective of sustainable development of rural societies.

## ACKNOWLEDGMENTS

This work was funded by the Institut de Recherche pour le Développement (IRD) in Tunisia between 2001 and 2003, in the frame of the JEFFARA project, managed jointly by IRD, the Institut des Régions Arides (Médenine – Tunisia) and the Commissariats Régionaux de Dévelopment Agricole of Médenine and Gabès. We thank all participants in this project for their helps and their fruitful contributions.

## REFERENCES

[1] SGHAIER, M. & GENIN, D., (COORD., 2003) : La désertification dans la Jeffara (Sud-Est tunisien) : Pratiques et usages des ressources, techniques de lutte et devenir des populations rurales. Rapport scientifique de synthèse, Programme JEFFARA, IRA/IRD/CRDA Médenine et Gabès, 148p.

[2] LE HOUEROU H.N., 1969: La végétation de la Tunisie steppique (avec références au Maroc, à l'Algérie et à la Libye). Annales de l'INRAT, vol. 42, fasc. 5, Tunis, 622p. annexes, carte couleur h.t.

[3] LE FLOC'H E., 1973: Étude des parcours du Sud tunisien. I- Carte phyto-écologique de Oglat Merteba et Mareth. Annales de l'INRAT, vol. 46, fasc. 5, 96p, cartes 1/100.000, annexes.

[4] LE FLOC'H E., 1975: Carte phyto-écologique, coupure spéciale Médenine au 1/100.000 INRAT/FAO, Projet Parcours Sud TUN/69/001. Notice, 33p, carte.

[5] BENDALI F., 1978: Dynamique de la végétation et mobilité du sable en Jeffara tunisienne. Thèse Doct., Univ. Languedoc, Montpellier, 243p.

[6] HANAFI A., in prep. : Végétation et systèmes de production agro-pastoraux au nord de la Jeffara tunisienne: Recherche sur les relations dynamiques. Thèse Doct., Univ. Tunis, FSHST.

[7] PALLUAULT S., 2003: Les périmètres irrigués privés dans la plaine de la Jeffara (sud-est tunisien): de nouvelles opportunités face à la rareté de l'eau ? Mémoire de DEA, Univ. Paris X, Nanterre, (IRD-IRA), 150p.

[8] AUCLAIR L., CHAIZE AUCLAIR M., DELAITRE E., SIMONNEAUX V., 1999 : Mutations Foncières et Désertification dans le Sud Tunisien, le Cas de Menzel Habib. Symposium international « Jardin Planétaire », Chambéry, France, 14-18 Mars 1999.

[9] MZABI H., 1993: La Tunisie du sud-est : géographie d'une région fragile, marginale et dépendante. Thèse Doct. d'État, Univ. Tunis, FSHST, Tunis, 658p.

[10] BONVALLOT J., 1979: Comportement des ouvrages de petite hydraulique dans la région de Médenine (Tunisie du Sud) au cours des pluies exceptionnelles de mars 1979. Cah. ORSTOM, Sér. Sci. Hum., Vol. XVI, pp : 233-249.

[11] NASR N., 1993: Systèmes agraires et organisations spatiales en milieu aride : Cas d'El Ferch et du Dahar de Chenini-Guermessa (Sud-Est tunisien). Thèse Doct., Univ. Paul Valéry – Montpellier III, 271p.

[12] RAHMOUNE L., 1998: Dynamique des systèmes agraires du Sud-Est tunisien (cas de la presqu'île de Jorf). Mémoire DEA, Univ. Paris X-INA PG, 96p.

[13] GENIN D., ATTIA W., CIALDELLA N., HANAFI A. & OULED BELGACEM A., 2003: La désertification dans la Jeffara, Sud-Est tunisien : Ressources pastorales et dynamiques des usages agropastoraux. Rapport scientifique final du thème 1, Programme Jeffara, IRA/IRD, 89p.

[14] HANAFI A., GENIN D. & OULED BELGACEM A., 2004: Steppes et systèmes de production agro-pastorale dans la Jeffara tunisienne : Quelles relations dynamiques ? Cah. Options Médit., Vol. 62 : « Réhabilitation des pâturages et des parcours méditerranéens », FAO-CIHEAM-IRA, pp : 223-226.

[15] ORSKOV E.R., VIGLIZZO E.F., 1994. The role of animal in spreading farmers' risks: a new paradigm for animal science. Outlook on agriculture, 23: 81-89.

[16] ABAAB A., GENIN D., 2004. Politiques de développement agropastoral au Maghreb: Enseignements pour de nouvelles problématiques de recherche-développement. In: Picouet M., Sghaier M., Genin D., Abaab A., Guillaume H., Elloumi M. (eds.), Environnement et sociétés rurales en mutation: approches alternatives. Coll. Latitudes 23, IRD Editions, Paris, pp. 341-358.

# The use of geoinformation processing to illuminate the dimensions of land use and land cover change in the Zamfara Reserve, northwest Nigeria

A. Hof[a], B.S. Malami[b] and B. Rischkowsky[c]

[a] Department of Geography, Ruhr University Bochum, Universitaetsstrasse 150, D-44780 Bochum, Germany, email: angela.hof@rub.de
[b] Department of Animal Science, Usmanu Danfodiyo University Sokoto, Nigeria
[c]Department of Livestock Ecology, Justus Liebig University Giessen, Germany

## ABSTRACT

The paper uses Remote Sensing and geoinformation processing to assess long-term land use/land cover change in a context of poor data and (geo-) information. It thereby addresses the question whether the estimates of a widespread degradation of natural vegetation derived from local scale studies correspond to findings at the landscape scale. Past land cover conversions in a common access resource area in northern Nigeria were reconstructed and the current pattern of natural grasslands was assessed from MODIS land cover (SDS-01) and MODIS Vegetation Continuous Fields (VCF) thematic datasets. In situ measurements of the vegetation parameters herbaceous biomass, leaf mass (foliage) and aerial cover of the woody layer were combined with a SAVI image of Landsat ETM+ data (1999) for a stratification of the study area into sparsely to densely vegetated grasslands. The results show that land degradation in terms of deforestation and prevalence of barren land is less drastic than estimates from previous studies had suggested. Half of the grasslands in the study area are slightly degraded with a dry matter per hectare productivity comparable to fallows and open access rangeland in drier northeastern Nigeria.

**Keywords:** Land use and land cover change, Nigeria, grasslands, dry matter productivity, forest/grazing reserves.

## 1 INTRODUCTION

In Nigeria, overgrazing and deforestation are considered to be the major causes of human-induced land degradation with 44% of the drylands estimated to be at risk from desertification [1]. However, existing regional-to-global scale data on rapid land cover change do not depict the Nigerian drylands as present-day desertification hot spot [2]. Rural and urban population and markets in northern Nigeria are growing and the extent of agricultural land in the Nigerian drylands expanded drastically from the 1970s to the 1990s, mostly at the expense of woodland and grassland [3]. Land use/cover change research in northern Nigeria has focused on village and farming systems [4]. The ecological bearing of cultivation encroachment and related changes in the extent and productive capacity of common access rangelands have received little attention. This case study uses the Zamfara Reserve as an example for a common access resource and delivers baseline data against which future changes can be assessed.

The case study area (Figure 1) is a regionally important transhumance corridor in the northern Nigerian drylands and a locally vital common access grazing resource [5, 6]. The reserve is located in the transitional bioclimatic zone between the Sub-Sahelian and the northern Sudanian sector and long-term average annual rainfall ranges from 650 mm in the north to 850 mm in the very south. The vegetation of the Zamfara Reserve has been described as undifferentiated Sudanian savanna woodland with a tree canopy cover of 5 to 8% and more than 90% shrub/grassland cover [7].

Today's Zamfara Reserve (2219 km$^2$) was demarcated in 1957 but most of the area had been *de jure* a forest reserve and *de facto* a grazing reserve since 1919. The reserve includes four legal farming enclaves, Dumburum, Shamushalle, Tsabre and Aja, and is surrounded by farming communities outside. With this setting, the competition for land between cropping and grazing has always been an issue. In 1960, Zamfara and part of the neighbouring Runka forest reserve became pilot grazing reserve schemes in northern Nigeria. Although the status as grazing reserve has never been gazetted, the Zamfara Reserve was included in the large range management schemes funded and managed by the United States Agency for International Development from 1961 to 1972 and then handed over to the local governments. The paradox was that the Grazing Reserve Law (1965) aimed at sedentarisation of pastoralist producers whereas the Forestry Law (Forestry Ordinance of 1957, as cited in [5]) did not permit land clearing to enlarge the cropping area that was allocated to the farming enclaves before 1960.

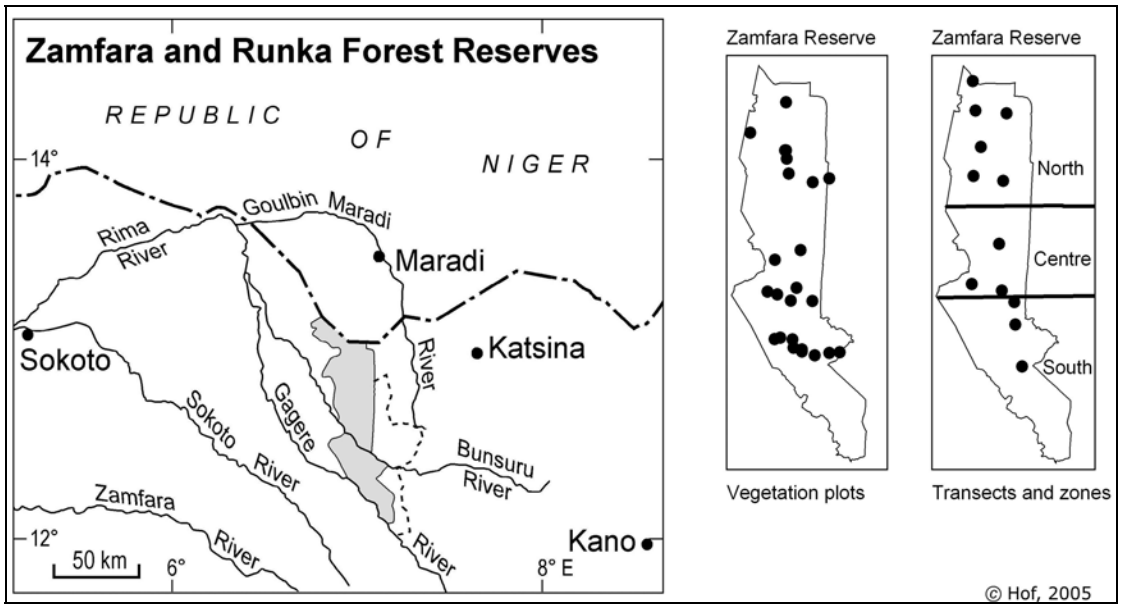


**Figure 1.** The location of the study area and the vegetation ground measurement locations.

Land degradation in the reserve and the risk of desertification were identified as problems in the late 1980s. From 1988 to 1994, the Desert Reclamation Project and the subsequent EEC-financed Sokoto Environmental Protection Programme (SEPP) aimed at improved resource management and environmental protection in the reserve. Research carried out in the 1990s considered agricultural expansion, overgrazing and fuel wood extraction as major land degradation problems [7, 8]. Based on sample areas in the Zamfara Reserve it was estimated that between 1962 and 1994 the tree density had been reduced by 50%, that 70-85% of the vegetation had been removed and 6.7% of the rangeland had been appropriated for cultivation [8].

Like elsewhere in the Sahelo-Sudanian zone, the contemporary competition for land between cropping and grazing is driven by increasing human and livestock populations. Total stocking density measured as tropical livestock unit (TLU) on natural range increased from 0.73 TLU $ha^{-1}$ in 1993 to 0.93 TLU $ha^{-1}$ in 2003 (22%). The corresponding increase in the livestock population on crop fields was 1.04 to 1.27 TLU $ha^{-1}$ (18%). District population density at the western fringe of the reserve ranged from 74 to 114 people/$km^2$ based on Gridded Population of the World version 2 data for 1995 [9]. Population density in the four enclaves of the reserve enclaves ranges from 100 to 460 people/$km^2$ [6].

The objective of the present paper is to assess the long-term rate and extent of land cover conversion for cultivation and to inventory the grasslands vegetation cover in the reserve using remotely sensed data and thematic geodatasets. This analysis is complemented by a transect analysis of grasslands vegetation resources and productivity along the north to south rainfall gradient in the reserve. The paper addresses the question whether the estimates of widespread loss of natural vegetation derived from local scale studies correspond to contemporary grasslands cover, pattern and productivity at the landscape scale.

## 2 MATERIAL AND METHODS

The long-term rate and extent of land cover conversion in terms of cropland expansion was mapped for the period of 1965 to 1999. The dry season remotely sensed data used included historical CORONA satellite photographs (4 November 1965) digital Landsat 4 TM images (23 February 1988), SPOT 3 HRV XS colour-infrared (07 November 1994) film positives at scale 1:400,000 and digital Landsat 7 ETM+ images (19 October 1999). The CORONA and SPOT XS film positives were scanned with a Vexcel Imaging UltraScan 5000 at 20 µm resolution. The scans were then co-registered in ERDAS IMAGINE to the two Landsat 7 ETM+ scenes 189-51 and 189-52 covering the reserve, and nearest-neighbour resampled into UTM projection (zone 32 North, WGS84). The contrast between the rangeland and cropland areas was sufficient for visual image interpretation [10] based on different pattern and texture (panchromatic CORONA) and tone and colour of pixels (SPOT and Landsat colour-composites). Location, situation and association [10] were also important guidelines for identifying cultivated land and determining the extent of the area. Visual image interpretation of the October 1999 Landsat imagery was supported by 794 GPS records collected in situ along cropland boundaries in 2000.

With a focus on grazing resources, the shrub/grassland areas were extracted and inventoried from digital geoinformation datasets collected at coarse to medium spatial resolution. Grasslands were extracted from the 1-km MODIS SDS-01 land cover product of 2001 (IGBP classification system) [11]. From the grasslands areas the mapped cropland areas (1999) were masked. The mask excluding cropland areas and land covers other than grasslands was applied to the 500-m MODIS Vegetation Continuous Fields (VCF) dataset of 2001 [12]. The resulting three layers of individual 500m raster cells represent the contribution of tree, herbaceous and bare cover to total grasslands ground cover. The early dry season Landsat ETM+ images (19 October 1999) provided higher spatial resolution data on the distribution of grasslands land cover. In addition to cropland, barren land, riparian woodland and watercourses were masked to extract the grasslands. Completely bare ground was derived from the built-up area index [13] applied to the Landsat ETM+ data. Due to their spectral contrast compared to all other land covers, riparian woodland and associated watercourses were clustered into distinct spectral classes by an unsupervised ISODATA classification and subsequently masked from the dataset. The remaining pixels represented the grasslands. The Soil Adjusted Vegetation Index (SAVI, [14]) was calculated for these pixels. SAVI is a measure of vegetation greenness, and by correlation, a surrogate measure of vegetation cover and biomass [10, 14].

This analysis of thematic and remotely sensed data was complemented by 24 vegetation ground measurements on aerial tree and shrub cover estimates according to the Zürich-Montpellier method of vegetation survey [15] (Figure 1). In addition, an in situ assessment of grasslands vegetation resources and productivity was carried out from 2000 to 2001. Tree and shrub density, crown cover, leaf mass, and herbaceous biomass were measured on twelve 1-km transects (Figure 1). The transects span a distance of 77 kilometres and were all placed in the grasslands land cover class as identified by the masked Landsat ETM+ dataset. Six transects were located in the northern zone which encompasses half of the grasslands in the reserve and receives 650-700 mm rainfall. Three transects each were placed in the central and southern zone which receive 800-850 mm rainfall (Figure 1).

On each transect (Figure 1), the herbaceous layer was sampled with twelve 1 $m^2$ sampling quadrates placed at random. In each quadrate, plant species cover was estimated at the first sampling and plants were subsequently clipped, air dried and weighed to estimate herbaceous biomass production from the early wet (May-July) to the late dry season (February-April). Shrubs (woody plants <5 m height) were recorded on the first 200 m of the transects using 4 circular 0.5 ha-plots at intervals of 50 m. Trees (woody plants >5 m height) were recorded in 4 circular 1 ha-plots at 250 m intervals. The tree crowns were measured with a pole, and basal circumference with a measuring tape. The height, large and perpendicular crown diameters of shrubs were measured with a measuring tape, while base diameter was taken at 20 cm above the ground using a Vernier calliper. Tree and shrub foliage mass were estimated using specific regressions between foliage mass and height, trunk circumference and crown area for different species [16].

Mean SAVI values of pixels in a buffer generated according to varying size of the total 36 sampling plots were calculated in ArcGIS and related with vegetation parameters. The strongest positive interrelation was found between SAVI and aerial tree and shrub cover and for the transect plots, between SAVI and herbaceous or total biomass. Relative to the plots' mean SAVI values they were grouped into sparsely (9), medium (8) and densely vegetated plots (19). The respective mean SAVI values were used as guideline to stratify the SAVI image of grasslands into densely, medium and sparsely vegetated areas. Zonal statistics from the MODIS VCF layers were calculated in ArcGIS for the three zones and the three grasslands strata.

## 3 RESULTS AND DISCUSSION

The expansion of agricultural land in the study area is divided into two categories: the increase of enclave farmland and cropland encroachment outside of the four designated farming enclaves. Cropland encroachment is driven by farming communities at the western fringe of the reserve. However, both types of cropland expansion particularly affect the southern parts of the reserve (Figure 2).

Including encroachment at the western fringe (Figure 2), cropland in the Zamfara Reserve increased from 0.9% to 8.3% of the total area within 34 years (Table 1). Rate and extent of encroachment clearly outweighs the expansion of the enclaves' farmland (Table 1). Moderate increase of enclave farmland by 1.9% annually between 1965 and 1988 was followed by accelerated expansion at 10.5% annually (1988-1994) and slowed down to 3.1% annually (1994-1999). In contrast, cropland encroachment was most drastic between 1965 and 1988 but the increase after 1965 and annual rates of 8.7% (1988-1994) and 7.5% (1994-1999) exceeded farmland expansion. Except for the period 1988-1994, the annual increase of enclave farmland tallies with annual population increase estimates for the northern Nigerian drylands and annual rates of change in cropland in other Sudano-Sahelian countries [3, 17]. In comparison, the rate of cropland encroachment is extremely high and especially the expansion phase of 1988-1994 is evidently related to subsequent land allocations which ex post facto legalised clearing at the expense of the common rangeland [6, 8].

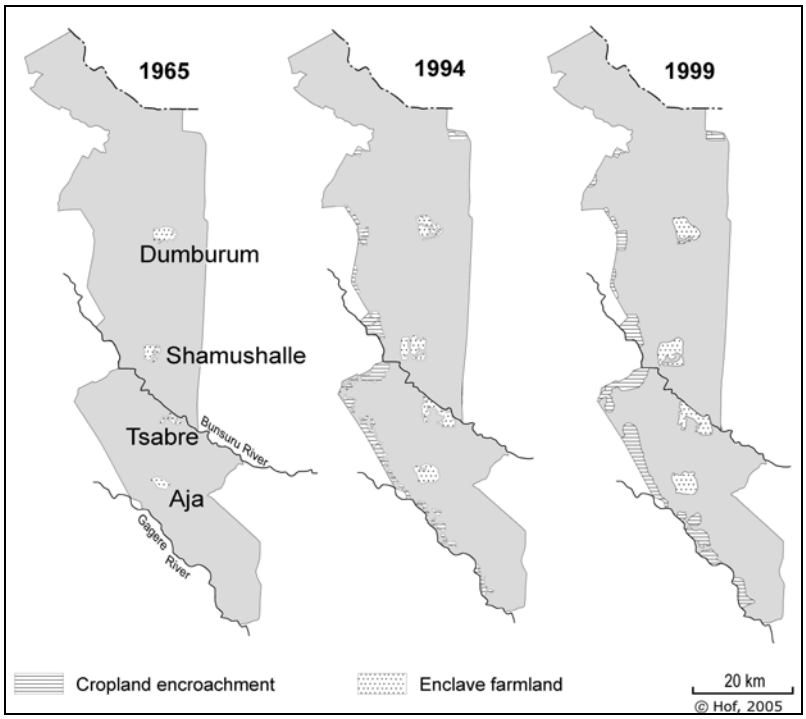


**Figure 2.** Long-term cropland expansion in the Zamfara Reserve.

The MODIS-SDS 01 derived land cover inventory confirms that grasslands are the dominant land cover [7], covering 87.8% of the study area (Figure 3). MODIS VCF derived statistics on the tree, herbaceous and bare ground cover of these grasslands by zone show that tree cover increases and bare cover decreases from north to south. The pattern of herbaceous ground cover does not show such an obvious spatial trend (Table 2). The zonal SAVI statistics convey considerable heterogeneity of vegetation cover and biomass in the grasslands of each zone (Table 2). Only 7% of the grasslands were classified as completely barren land in terms of the built-up area index [13].

**Table 1.** Long-term cropland expansion in the Zamfara Reserve (hectares).

| **Year mapped** | **1965** | **1988/90** | **1994** | **1999** |
|---|---|---|---|---|
| **Enclave farmland** | 2096 | 3224 | 5881 | 6850 |
| **Cropland encroachment** | 0 | 5039 | 8314 | 11950 |
| **Encroachment (% of total cropland)** | 0 | 60.9 | 58.6 | 63.6 |
| **Cropland surface cover (%)** | 0.9 | 3.7 | 6.3 | 8.3 |

**Table 2.** Zonal statistics for MODIS VCF data and SAVI within the three zones of the reserve.

| **Zone** | **Tree cover** | | **Herbaceous cover** | | **Bare ground cover** | | **SAVI** | |
|---|---|---|---|---|---|---|---|---|
| | ----------[%]---------- | | | | | | | |
| | **mean** | **STD** | **mean** | **STD** | **mean** | **STD** | **mean** | **STD** |
| **North** | 1 | 0.7 | 69.5 | 27.5 | 16.9 | 10.2 | 0.24 | 0.16 |
| **Centre** | 1.5 | 1.9 | 59.7 | 38.5 | 9.8 | 8.4 | 0.25 | 0.20 |
| **South** | 3.3 | 3.4 | 63.1 | 37.7 | 7.5 | 7.1 | 0.23 | 0.18 |

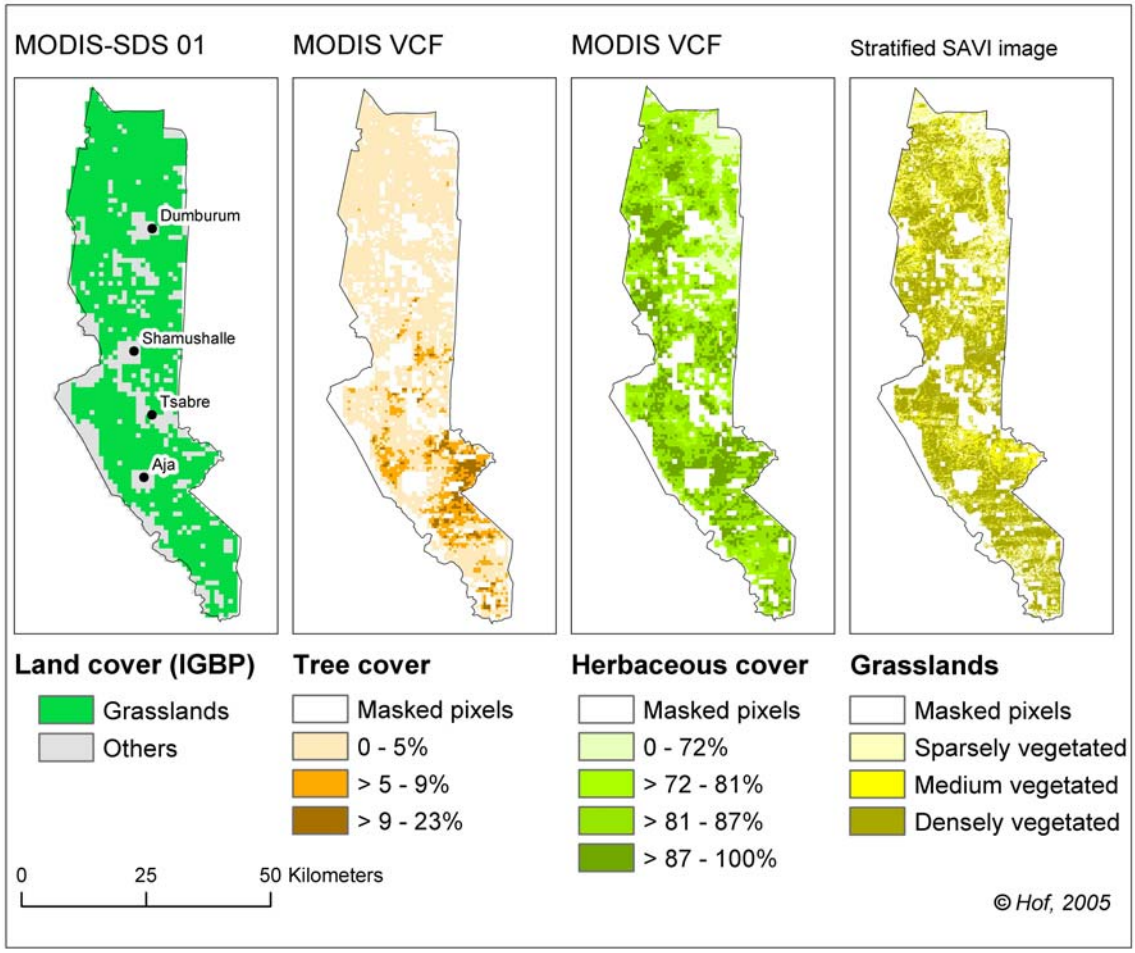


**Figure 3.** Extent of grasslands cover and composition of grasslands ground cover in the study area.

The results of the transect analysis showed that increasing density of woody plants occurs along the north-south rainfall gradient. The mean density of trees increases from north (16 trees $ha^{-1}$) to the centre (17 trees $ha^{-1}$) and south of the reserve (25 trees $ha^{-1}$). Mean shrub densities exhibit the same trend but increase more markedly from north (102 shrubs $ha^{-1}$) to centre (122 shrubs $ha^{-1}$) and south (154 shrubs $ha^{-1}$). The results of the transect analysis confirmed the MODIS VCF data, showing that the mean cover of trees and shrubs increases from north to south in the reserve (Table 2, Table 3). Across the three zones of the reserve, the central zone had the highest mean herbaceous biomass and foliage mass (Table 3). This result contradicts the assumption that vegetation productivity in the reserve increases with increasing rainfall north to south. The results on foliage mass indicate wider crowns and more mature woody plants in the centre of the reserve despite the rainfall gradient. Considering that the dynamics of the woody vegetation span more extended timescales than those of the herbaceous communities, these results contradict the deforestation and land degradation scenario evoked in other local scale studies [8, 15].

Judged by productivity, measured as dry matter (DM) per hectare in a season with average rainfall (2000-2001), the natural grasslands of the reserve can be described as slightly degraded rangeland. The productivity of the woody vegetation foliage ranges from 333 to 510 kg DM $ha^{-1}$ and is in the range of the 350 kg DM $ha^{-1}$ reported for open Sahel Savanna Woodland in northeast Nigeria with only 400 mm mean annual rainfall [4]. The mean total biomass (1606 kg DM $ha^{-1}$) from the herbaceous layer and woody foliage is slightly higher than the mean of 1408 kg DM $ha^{-1}$ reported for fallows and common access rangeland in a drier northeastern Nigerian location with only 360 mm rainfall in the survey year [4]. The mean herbaceous biomass of 1259 kg DM $ha^{-1}$ (STD 173) in the study area is only as much as the herbaceous biomass measured in the northeastern open Sahel Savanna Woodland [4]. The mean density of 138 woody plants $ha^{-1}$ (data not shown) is rather low if compared with a mean density of 538 woody plants per hectare for a forest reserve in the Kano Closed Settled Zone (CSZ) with 700 mm annual rainfall [4]. Nevertheless, the values for the Zamfara Reserve are twice as high as mean woody plant densities for unprotected shrubland in the Kano CSZ [4].

**Table 3.** Mean cover of trees and shrubs and annual mean biomass of the three zones of the reserve.

| Zone | Tree cover | | Shrub cover | | Herbaceous Biomass | | Foliage mass | |
|---|---|---|---|---|---|---|---|---|
| | ----------[%]---------- | | | | ----------[kg DM ha-1]---------- | | | |
| | mean | STD | mean | STD | mean | STD | mean | STD |
| North | 2.4 | 1.7 | 2.9 | 1.6 | 1138b | 228 | 310 | 132 |
| Centre | 5.6 | 3.2 | 5.0 | 4.4 | 1457a | 308 | 509 | 375 |
| South | 7.3 | 5.3 | 3.5 | 2.4 | 1183b | 205 | 380 | 12 |

Means within the same column with different superscript differ significantly ($p<0.05$).

The stratified SAVI image of Landsat 7 ETM+ data (19 October 1999) reflects the same general pattern of vegetation cover in the study area as the MODIS VCF tree and herbaceous ground cover layers (Figure 3). The MODIS VCF data resolve the contribution of woody vegetation to total biomass and clearly show that grasslands with high tree cover only occur in the south of the reserve, east of Aja enclave (Figure 3). This is consistent with the results of the ground measurements. The contribution of dense, medium and sparse grasslands vegetation cover to total grasslands cover by zone (Table 4) tallies with the MODIS VCF data (Table 2) and the observation that the central zone is endowed with the highest biomass (Table 3).

**Table 4.** Composition of grasslands in three zones of the reserve**.**

| | Grassland composition within zones (% of grasslands in zone area) | | |
|---|---|---|---|
| Stratum/zone | North | Centre | South |
| Sparse | 15.7 | 7.5 | 8.1 |
| Medium | 37.3 | 25.4 | 29.4 |
| Dense | 47.0 | 67.1 | 62.5 |
| Total | 100 | 100 | 100 |

There was a clear positive interrelation between SAVI values and aerial tree ($r=0.5$) and shrub cover ($r=0.3$) measured at the 24 plots (Figure 1) and SAVI values and mean total and mean herbaceous biomass ($r=0.6$) measured at the 12 transects (Figure 1). The vegetation parameters and SAVI values for the three grasslands strata show that the dense grasslands stratum is differentiated by higher woody cover which adds up with the mean herbaceous biomass of 1343 kg DM $ha^{-1}$ (STD 253) to the much higher total biomass (Table 5). The sparse grasslands have lower woody cover (Table 5) and lower mean total herbaceous biomass of 1016 kg DM $ha^{-1}$ (STD 79) than the medium vegetated grasslands with 1149 kg DM $ha^{-1}$ (STD 142). In terms of total biomass (Table 5), the results show that about 55% of the grasslands in the study area (Figure 3) are only as productive as fallows and common access rangeland in a drier northeastern Nigerian location with 360 mm rainfall in the survey year [4].

**Table 5.** Vegetation and productivity parameters for three grasslands strata**.**

| Stratum (% of total) | Aerial woody cover* | | Woody crown cover | | Total biomass | | SAVI | |
|---|---|---|---|---|---|---|---|---|
| | ----------[%]---------- | | | | [kg DM ha-1] | | | |
| | mean | STD | mean | STD | mean | STD | mean | STD |
| | 15.7 | 5.5 | 6.1 | 4.2 | 1374.0 | 257.1 | 0.17 | 0.06 |
| Medium (22.8) | 16.4 | 9.2 | 6.4 | 5.1 | 1398.5 | 343.6 | 0.27 | 0.04 |
| Dense (45.2) | 32.8 | 13.1 | 8.9 | 5.5 | 1765.3 | 309.1 | 0.42 | 0.06 |

Data source: *[15].

Given the positive but weak interrelation between SAVI and cover parameters and SAVI and biomass, the vegetation and productivity parameters (Table 5) indicate a trend but are not necessarily representative for the respective grasslands stratum.

## 4 CONCLUSIONS

The north to south increase of woody vegetation indicated by the vegetation ground measurements is less clear in the land cover inventory based on remotely sensed data and thematic geodatasets. At the landscape scale the northern zone of the reserve is differentiated from the zones to the south by a higher contribution of bare ground and sparse grasslands to total land cover. The ground measurement results suggest that increasing grassland productivity cannot be inferred from higher rainfall or higher woody cover in thematic geodatasets.

The present results from both ground measurements and remote sensing do not support the claims of local scale studies that deforestation and removal of vegetation have led to widespread land degradation in the reserve. The results tally with earlier descriptions of land cover [7] and cropland extent [8] in the reserve. Increasing land use pressure on shrinking grasslands may aggravate the subtle modifications within the grasslands cover class that are indicated by the contemporary low dry matter per hectare productivity of the grasslands. With medium resolution remote sensing data like Landsat, such changes are hardly detectable [18]. The rate and extent of cropland expansion pinches the rangeland which is at the same time the production basis of an increasing number of transhumant and local livestock-keepers and provides forest products such as fuel wood and timber. Further ground measurements under variable rainfall amounts and in areas stratified *a priori* by synoptic remote sensing data are needed to scale up from the local to the landscape scale.

## ACKNOWLEDGMENTS

We are grateful to DG XII of the European Union for funding the research under the INCO-DC programme “Development of pastoral and agropastoral livelihood systems in West Africa.” (Contract No. ERB IC18-CT98-0280). We also thank our colleagues from Usmanu Danfodiyo University and the people in the Zamfara Reserve for their kind cooperation.

## REFERENCES

[1] FAO TERRASTAT database http://www.fao.org/ag/agl/agll/terrastat/#terrastatdb accessed 4/21/2005 5:10 PM.

LEPERS, E., LAMBIN, E.F., JANETOS, A.C., DEFRIES, R., ACHARD, F., RAMANKUTTY, N. AND SCHOLES, R.J., 2005: A synthesis of information on rapid land cover change for the period 1981-2000. *Bioscience* 55 (2), pp. 115-124.

MORTIMORE, M., 2000: Hard questions for ‘pastoral development’: a northern Nigerian perspective. In: Tielkes, E., Schlecht, E. and Hiernaux, P. (eds.): Elevage et gestion de parcours au Sahel, implications pour le développement, pp. 101-114. Grauer, Stuttgart.

MORTIMORE M., HARRIS, F.M.A. AND TURNER, B., 1999: Implications of land use change for the production of plant biomass in densely populated Sahelo-Sudanian shrub-grasslands in north-east Nigeria. *Global Ecol. Biogeogr.* 8, pp. 243-256.

HOFFMANN, I., 2004: Access to Land and Water in the Zamfara Reserve. A Case Study for the Management of Common Property Resources in Pastoral Areas of West Africa. *Hum. Ecol.* 32 (1), pp. 77-105.

HOF, A., ADDY, L. AND RISCHKOWSKY, B., 2003: Degradation of Natural Resources or Necessary Intensification of Land Use to Sustain a Growing Number of Users? - The case of the Zamfara Reserve, Northwest Nigeria. In: Proceedings Deutscher Tropentag 2003: Technological and Institutional Innovations for Sustainable Rural Development. Göttingen, October 8-10, 2003. http://www.tropentag.de/2003/abstracts/full/206.pdf

RIM (Resource Inventory and Management Limited), 1991: Woody Vegetation Cover and Wood Volume Assessment in Northern Nigeria. Report for the Federal Government of Nigeria. RIM, St. Helier, UK.

ARCA, 1995: Forest Reserve Study: Ruma Kukar Janjarai and Zamfara Forests. Final Report, Vol. 1. The Environment: Present Conditions and Degradation Factors. Vol. 2. Conservation-based Development Framework. Katsina Arid Zone Programme, Nigerian National Planning Commission. ARCA Consulting, Rome.

CIESIN, IFPRI AND WRI (eds.), 2000: Gridded Population of the World, Version 2. http://sedac.ciesin.columbia.edu/plue/gpw accessed 2/21/2005 2:10 PM

JENSEN, J.R., 2000: Remote Sensing of the Environment. An Earth Resource Perspective. Prentice Hall, Upper Saddle River, NJ.

BOSTON UNIVERSITY, 2004: MOD12Q1 V004 Land Cover Product (SDS 01 Land_Cover_Type_1). http://duckwater.bu.edu/lc/mod12q1.html#af. Accessed 7/01/2004 1:22 PM.

HANSEN, M.; DEFRIES, R.; TOWNSHEND, J.R.; CARROLL, M.; DIMICELI, C. AND SOHLBERG, R., 2003: 500m MODIS Vegetation Continuous Fields: Tree Cover, Bare Cover, Herbaceous Cover. Version: 1.0. University of Maryland; Department of Geography; the Global Land Cover Facility: College Park, Maryland.
ZHA, Y., GAO, J. AND NI, S., 2003: Use of normalized difference built-up index in automatically mapping urban areas from TM imagery. *Int. J. Remote Sens.* 24 (3), pp. 583-594.
HUETE, A.R., 1988: A Soil-adjusted Vegetation Index (SAVI). *Remote Sens. Environ.* 25 (3), pp. 295-309.
KÜPPERS, K., 1998: Evaluation of the ligneous strata of the vegetation of Zamfara Reserve, North-West Nigeria. In: Hoffmann, I. (ed.) Prospects of pastoralism in West Africa. Giessener Beiträge zur Entwicklungsforschung, Reihe I, Band 25, pp. 41-47. Tropeninstitut Justus Liebig Universität, Giessen, Germany.
CISSE, M.I., 1980: Production fourragère de quelques arbres sahéliens: relations entre la biomasse foliaire maximale et divers paramètres physiques. In: Le Houérou, H.N. (ed.), Les fourrages ligneux en Afrique. Etat actuel des connaissances, pp. 203 - 208. ILCA, Addis Ababa.
STÉPHENNE, N. AND LAMBIN, E.F., 2001: A dynamic simulation model of land-use changes in Sudano-sahelian countries of Africa (SALU). *Agric. Ecosystems Environ.* 85 (1-3), pp. 145-161.
LAMBIN, E.F., 1999: Monitoring Forest Degradation in Tropical Regions by Remote Sensing: Some Methodological Issues. *Global Ecol. Biogeogr.* 8 (3-4), pp. 191-198.

# Asian regional Desertification mapping objectives and methodologies

J. Hongbo[a] and M. Hong[a]

[a]Chinese Academy of Forestry, Beijing 100091, China,
email: mahong@forestry.ac.cn

## ABSTRACT

The proposed Asian Regional Desertification Status Map will serve users at national, regional and international levels for understanding causes and progress of desertification and ecosystem vulnerability to desertification and land degradation. By applying remote sensing techniques to the Asian regional, the applied study of satellite image in desertification monitoring and assessment is conducted. The desertification status map of Asia now have been completed the first raw map, the benchmarks and indicator system and classification system is raised, and its working process is described.

**Keywords:** Desertification, Regional level, land degradation, MODIS, Indicator system

## 1 INTRODUCTION

Desertification Status Map is one of the most useful and visible reference for the prognosis of desertification and for planning preventive or combative measures against it by showing the causes and dynamics of desertification with respect to the process itself and environmental vulnerability to desertification. Before practically starting desertification mapping a series of technical aspects that are related to the scale, the minimum map able unit, classification system, projection system, datum, accuracy, map composition and format should be clarified.

Technically, preparation of desertification mapping includes availabilities of the prescription of mapping standard, relevant data and technological capacity. It is necessary to collect some information from the involved countries, such as availabilities of climatic data and national maps for the purpose of desertification monitoring.

The delivered questionnaire is expected to provide necessary information on these issues. The desertification mapping is moved forward by forming a framework of regional desertification mapping. The main technical details were discussed and defined in the "Thematic Programme Network on Desertification Monitoring &Assessment (TPN1)"meeting in 2003.

The general objective is to put forth to TPN1 member countries a common set of benchmarks and indicators (B&I) system for desertification monitoring and assessment (DMA) in Asian region for comments and suggestions. The B&I system, once finalized based on the comments and suggestions from the member countries, could be used for DMA for the Asian region.

Based on the B&I adopted, the Chinese Academy of Forestry undertook the work of developing the Desertification Status Map of Asia in 2004,and has now completed its first raw map.

## 2 BENCHMARKS

According to the opinion from General Assembly of the Intergovernmental Negotiating Committee for the Elaboration of UNCCD, Tenth Session, New York, 6-17 January 1997: "Benchmarks are used to develop correlations between various parameters and to provide a baseline for monitoring at the local, national and regional levels."

Benchmarks are the baselines that serve as the starting point for evaluation and monitoring and thus provides a point of reference from which the land starts to degrade/improve. Benchmarks are standards against which decertified land can be compared in order to determine degradation trends. The benchmarks are also used to quantify the severity/degree of degradation. Different benchmarks are to be established for different agro climatic regions and different land uses.

Benchmarks can be determined by identifying non-degraded land ecosystems (representative sites) under the same agro climatic zone and natural conditions. The benchmarks can also be established based on existing researches, historical data and field investigation.

# 3 INDICATOR SYSTEM

The proposed indicator system includes four aspects: pressure, state, desertification impact and implementation.

## 3.1 Pressure indicators

Characterize driving forces both natural and man-made, affecting the status of natural resources and leading to desertification. Pressure indicators are used to assess desertification trends and make an early warning for desertification. Natural indicators describe natural factors, mainly climatic conditions, natural disasters, which promote the occurrence and development of desertification. Non-natural indicators describe the pressure on land/ecosystems leading to land degradation from human activities.

## 3.2 State indicators

Characterize the status of natural resources including land. The physical and biological features of desertified land ecosystem are the main factors to be considered. Physical indicators describe the land characteristics, physical and chemical properties of soil and hydrological features of the land ecosystem. Biological indicators are used to describe biological characteristics of the land ecosystem.

## 3.3 Impact indicators

Desertification impact indicators are used to evaluate the effects of desertification on human beings and environment.

## 3.4 Implementation indicators

Implementation indicators are used to assess the actions taken for combating desertification and to assess its impacts on natural resources and human beings. Such impacts refer to improvements of socio-economic and natural conditions.

# 4 ASIAN REGIONAL DESERTIFICATION STATUS MAPPING

## 4.1 Methodologies

### 4.1.1 Data

MODIS (or Moderate Resolution Imaging Spectra-radiometer) is a key instrument aboard the Terra (EOS AM) and Aqua (EOS PM) satellites. Terra's orbit around the Earth is timed so that it passes from north to south across the equator in the morning, while Aqua passes south to north over the equator in the afternoon. Terra MODIS and Aqua MODIS are viewing the entire Earth's surface every 1 to 2 days, acquiring data in 36 spectral bands, or groups of wavelengths. These data will improve our understanding of global dynamics and processes occurring on the land, in the oceans, and in the lower atmosphere. **4.1.2 Image processing**

500-meter resolution satellite image (band 1~7) was acquired in 2003, by the Moderate resolution Imaging Spectroradiometer (MODIS). Image Processing and mapping by Asian Thematic Programme Network on Desertification Monitoring &Assessment (TPN1).

The MODIS Image Processing have been done on the ENVI and ERDAS Image Processing system. The Projection system is Albers Conical Equal Area, to keep the data in continuity and systematizing. The Albers Conical Equal Area projection is mathematically based on a cone that is conceptually secant on two parallels. There is no areal deformation. This projection produces very accurate area and distance measurements in the middle latitudes. Thus, Albers Conical Equal Area is well-suited to countries or continents where north-south depth is about 3/5 the breadth of east-west and used for thematic maps.

Parameter detail:

Latitude of 1st standard: 15° 00' 00" N

Latitude of 2nd standard: 47° 00' 00" N

Longitude of central meridian: 90° 00' 00" N

Longitude of origin of projection: 0.0

Datum: WGS 84 (World Geodetic System);

Band combination: 4,3,2

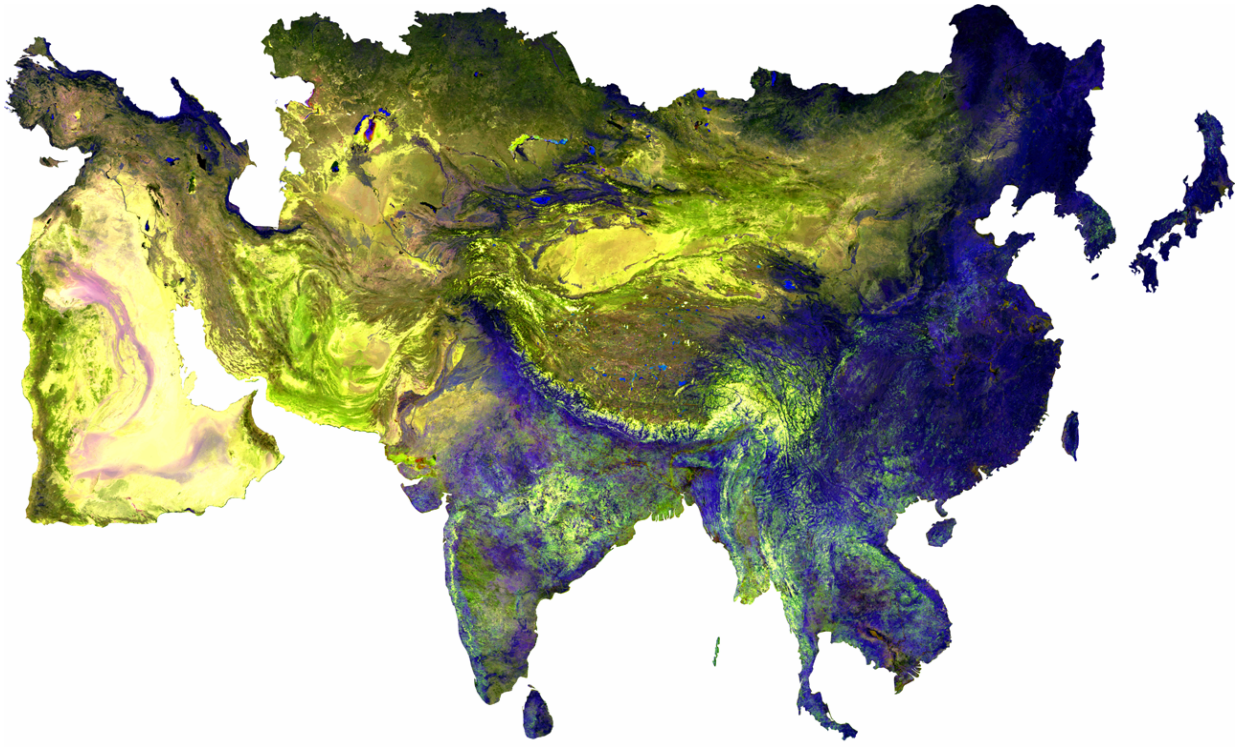

**Figure 1.** The MODIS Image in Asian regional.

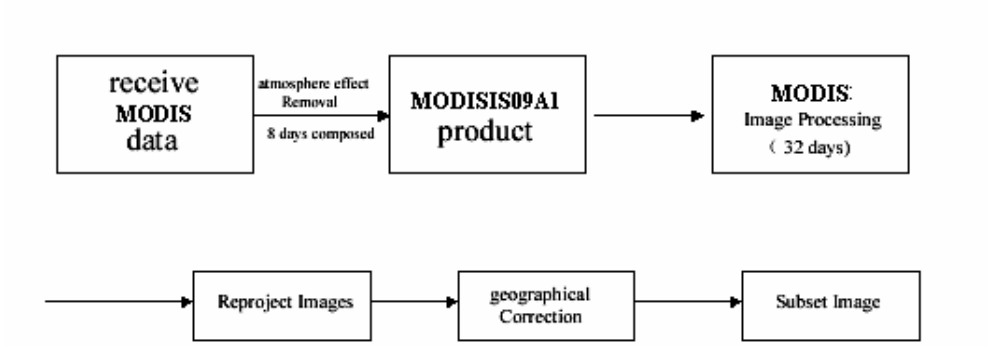


**Figure 2.** MODIS Image Processing flow chart.

### 4.1.3 Classification system

Multispectral classification process the sorting of pixels into a finite number of individual classes, the Land use map is a classified image, showing vegetation, bare land, pasture, urban, etc. In order to confirm the land use classification system in the project area, the guideline should be set up. Land resources and land use (Land resources character, specialty and the land use pattern) to reflect the actuality of land resources and land use. The precision in classification, classify investigating to the land resource by using remote sensing technology. Every indicator in the classification system must be reached the anticipated precision of MODIS data. Adapted the land resources investigatation in large-scale using remote sensing technology.

According to the guideline, the classification system is established:

level 1: land use

level 2: processes of degradation

level 3: severity of degradation

The detail as follow:

- Land use: Farmland; Forest; Meadow; Water; construction; have not utilized land;
- Forest and Meadow: In accordance with the land use pattern, the characteristic of land coverage, the management prescription of land resources, the secondly class is for Meadow and Forest;
- Farmland;
- Water;
- Urban, factory, inhabitation;
- Sandy land, Gobi, salinization-alkalization land;

To classify desertification degree, the basal land use pattern were used as the evaluate indicator, and to evaluate the degree of desertification respectively. The dictators include: forest, Meadow, Farmland, otherwise. For farmland, the classification was in accordance with the surface features of the project area, and the crop reflects to the depth and homogeneity of the image. For forest, Meadow and otherwise, the NDVI indices (The Normalized Difference Vegetation Index) method were adopted.

Indices are used to create output images by mathematically combining the DN values of different bands. It is used extensively in vegetation analyses to bring out small differences between various vegetation classes. In many cases, judiciously chosen indices can highlight and enhance difference, which cannot be observed in the display of the original color bands. The Normalized Difference Vegetation Index (NDVI) is a combination of addition, subtraction, and division (eq. 1, 2):

$$\text{Vegetation Index} = \text{IR-R} \quad (1)$$

$$\text{NDVI} = (\text{IR-R})/ (\text{IR+R}) \quad (2)$$

### 4.1.4 Classification

Supervised Classification, it is usually appropriate when the user wants identify relatively few classes, and when the user can identify distinct, homogeneous regions that represent each class. On some regions that the objects in a feature space are obvious, the pattern recognition skills and a knowledge of the data to help the system determine the statistical criteria for data classification.

About the rest, the classes are determined by spectral distinctions that are inherent in the data, and than define the class. Unsupervised classification enables to define many classes easily, and identify classes that are not in contiguous, easily recognize regions.

Unsupervised Classification uses the ISODATA clustering method (Iterative Seif-Organizing Data Analysis Technique), and uses spectral distance as in the sequential method, but interactively classifies the pixels, redefines the criteria for each class, and classifies again.

### 4.1.5 Classify result


**Figure 3.** The Asian Regional Desertification Status Map.

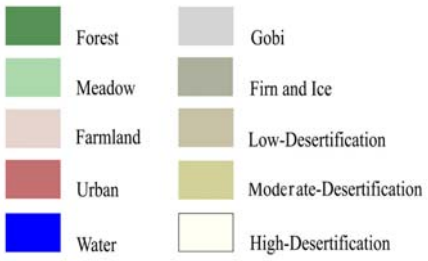


**Table 1.** Classify result.

| | **Classification** | **%** |
|---|---|---|
| 1 | Forest | 18.98 |
| 2 | Farmland | 19.60 |
| 3 | Meadow | 34.24 |
| 4 | Water | 2.71 |
| 5 | Urban | 0.09 |
| 6 | Gobi | 10.50 |
| 7 | Firm and Ice | 0.20 |
| 8 | Low-Desertification | 4.47 |
| 9 | Mod-Desertification | 3.14 |
| 10 | High- Desertification | 6.06 |

## 5 CONCLUSION

Remote sensing has been widely used for monitoring and assessing in the present and dynamic situations of desertification and drought at local, regional and global scales. Many countries and institutions have made achievement in this area. Since 1999 the " Asian Thematic Programme Network on Desertification Monitoring & Assessment (TPN1)" has made delightful progress by the joint efforts of all the TPN1 member countries but we still have hard work to do. There are now 20 TPN1 member countries. The desertification Status map of Asia now have been completed the first raw map .The next step aims at conducting ground control by gathering ground truth and provide training to those countries not yet able to be fully involved in image interpretation and monitoring processes. We appeal to sequential and more supports and assists from international, regional and sub-regional organizations, developed countries and all interested countries. All of the efforts and results will undoubtedly contribute to combat desertification, the serious hazard to our planet. Fruitful and successful implementation of TPN1 will assuredly facilitate Asian countries' actions for combating desertification and improve Asian natural environment toward sustainable development.

## ACKNOWLEDGMENTS

This work is supported by UNCCD (secretariat of the convention to combat desertification of U.N. ), Image Processing and mapping by Asian Thematic Programme Network on Desertification Monitoring &Assessment (TPN1). In this case, the authors would like to thank Dr. Wubo, Ms.Liuyan, Prof. Chexuejian and express the appreciation for their plentiful dedication and constructive suggestions.

## REFERENCES

[1] ERDAS IMAGINE Field Guides. ERDAS, Inc. Atlanta,Georgia 1997

[2] HONGLIANG, F., JIANTING, Z., WEIGUO, L., YOULIANG, Q., 1998: ERDAS Image Processing . Institute of Geographical Sciences and Natural Resources Research, CAS

# Estimating regional change of land-use and carbon sink capacity in slash/burn ecosystems in mountainous mainland of Laos based on satellite imagery

Y. Inoue[a], J. Qi[b], T. Horie[c], Y. Kiyono[d], Y. Ochiai[d], K. Saito[c], H. Asa[c], T. Shiraiwa[c], and L. Douangsavanh[e]

[a] National Institute for Agro-Environmental Sciences, Tsukuba, Ibaraki, 305-8604, Japan, email: yinoue@affrc.go.jp
[b] Michigan State Univ., USA
[c] Kyoto Univ., Japan
[d] FFPRI, Japan, [e] NAFRI, Lao PDR

## ABSTRACT

The objective of this study was to assess and predict the land-use and carbon balance in the slash/burn ecosystems in mountainous mainland of Laos. We constructed a comprehensive dataset that includes long-term satellite images, and geospatial information such as digital elevation maps, soil and meteorological maps, and ground-based data such as crop yield, fallow biomass, soil $CO_2$ flux, and soil carbon contents. Geo-spatial simulation based on the dataset suggested a catastrophic spiral of decreasing soil carbon and fertility, and increasing slash/burn area, i.e., biomass burning and $CO_2$ emission unless no effective strategies for alternative ecosystem managements are carried out. Alternative ecosystem management scenarios based on rice-based cropping system were also investigated. The simulation over 20 years suggested that the slash/burn ecosystem was a source of $CO_2$ for the atmosphere under the present situation, but could be switched to a sink under the alternative land-use and ecosystem management strategies.

**Keywords:** $CO_2$, ecosystem, fallow, GHG, land cover, land use, shifting cultivation, remote sensing, rice, cropping.

## 1 INTRODUCTION

The terrestrial food production ecosystems in the Mountain Mainland in Southeast Asia (MMSEA) have been changing under the unprecedented pressures from increasing human population, globalization of market economy, and global climate change [1]. The major agricultural land use in the region is so called “slash and burn agriculture” (“shifting cultivation”), which is an important food production technology in the steep mountainous areas. Although this traditional food production ecosystem used to be sustainable and/or harmonized with natural resources and environment, it could hardly be sustainable due to such human pressures; the slash/burn area has been expanding and the fallow period has been shortened [2].

This drastic change of ecosystems is closely linked with the environmental changes in both global and regional scales, i.e., a number of unfavorable changes such as decreasing soil fertility, food productivity and forest resources as well as the negative impact on atmosphere [3]. Hence, it is strongly required to develop more sustainable and environment-friendly ecosystem management methods from the viewpoints of food, resource and environmental security [4]. Nevertheless, scientific data and assessments on the long-term and wide-area changes of land use and carbon balance for the region are very limited [5].

Thus, the first objective of this study is to understand the long-term change of land use, vegetation, and carbon flow based on geo-spatial data including satellite imagery as well as on-site measurements. The second objective is to predict land use and carbon balance in the near future, and to assess the effects of alternative land-use/ecosystem management scenarios.

## 2 STUDY AREA

As a study area, we selected the central part of northern Laos with the size of 150 km x 150 km (Figure 1), since it is a typical region for slash/burn agriculture, and assumed to be representative of similar ecosystems in MMSEA. The central position of the area is [E102° 03’ 48.9’’, N20° 13’ 12.8’’], and the whole area is covered by a Landsat scene (Row46/Path129). It is often referred that people in the area consists of more than sixty ethnic groups [5].

The elevation ranges from 300 m to 2000 m, and the slope is from 40% to 100%. The most important crop in the area is upland rice, and some other crops such as job's tear, sesame, paper mulberry are grown. Major tree species include *Irvingia malayana* and *Castanopsis echinocarpa*. Teak plantation was started about 10-15 years ago. The mean annual rainfall for the area is about 1300 mm with the annual variability (SD) of 260 mm, but more than 90% of the rainfall is during the wet season from April to October. Within the large study area, we also set an area for intensive field survey (15 km x 15 km) near Luangphabang (Figure 1). The region is also typical for the MMSEA for opium cultivation, which was found to be correlated with deficit in rice production [5].

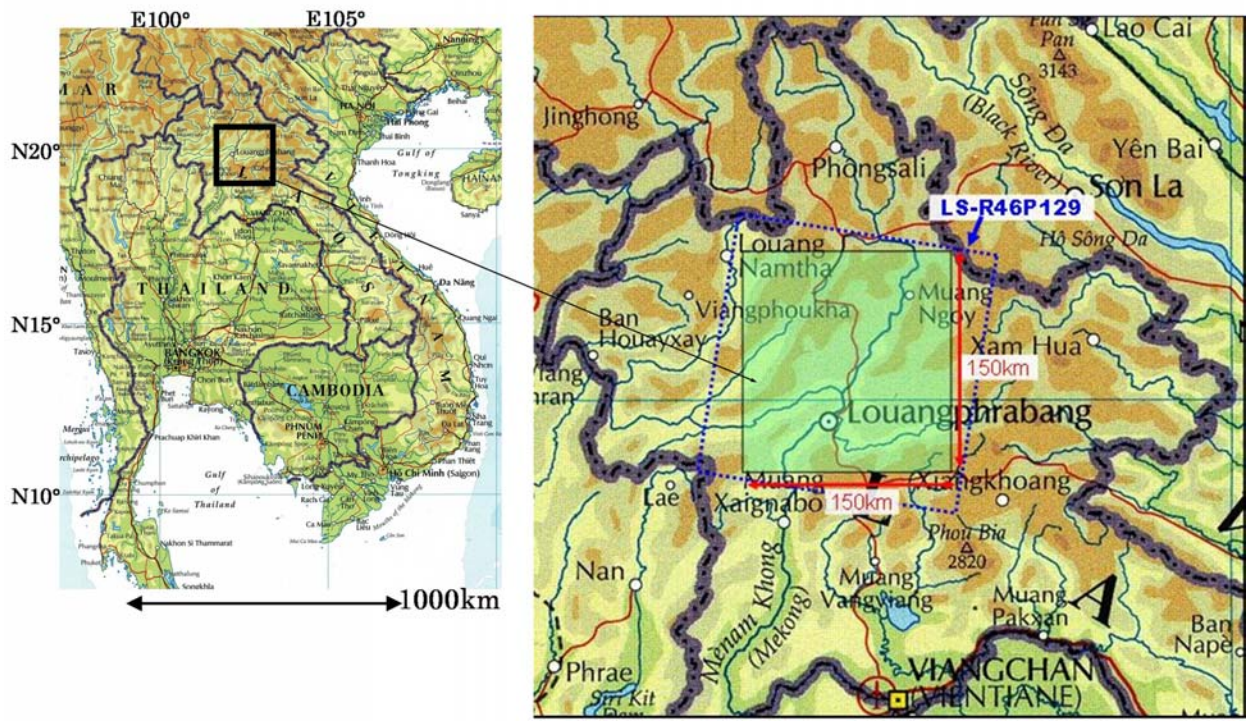


**Figure 1.** The Study area; northern part of Lao P.D.R. The dotted area indicates a full Landsat scene (Row46/Path129).

## 3 DATA AND METHODS

### 3.1 Dataset

We have been constructing a comprehensive dataset for the study area, which includes (1) satellite images over 1970's-2004 periods (Landsat, SPOT, IKONOS, QuickBird, etc.), (2) topographic and digital elevation maps, (3) GMS-derived daily PAR at a resolution of 5 km, (4) soil maps, (5) ground-based hyperspectral measurements, (6) monthly data of air temperatures (max, min, mean) and precipitation at 250 m resolution, (7) crop yield and biomass for various cropping systems, (8) biomass of fallow biome, (9) soil $CO_2$ flux and carbon contents.

Ground-based spectral measurements were made over a wide range of water bodies, bare soils, crops, slash/burn surfaces, and fallow vegetations using a hyperspectral radiometer (ASD, 400-2500 nm). Information on the history of land-use and cropping conditions was obtained through field survey. Biomass, crop yield, soil carbon content, and soil $CO_2$ flux during both cropping and fallow periods were measured based on destructive sampling, chamber method, and chemical analysis in the experimental plots in the intensive study area. Several fallow plots (40m x 40m) at different canopy ages were installed for continuous measurement of biomass of the fallow biome without human disturbance.

We are still continuing the collection of geo-spatial data and on-site measurements to create more thorough dataset in the region.

### 3.2 Approach

We analyzed several sets of satellite imagery to overview the long-term and wide-area change of land-use/land-cover in the study area. For the preliminary assessment of carbon balance at the regional scale, we used a simple

approach (a) based on land-use pattern derived from multi-temporal satellite images and ground-based measurements of carbon balance components. First, high resolution satellite was used to generate polygons of land-use parcels based on segmentation procedures using spectral and morphological information by using eCognition (Definiens). The classification results as well as size and spectral properties were validated with ground-based field survey and measurements. Next, vegetation indices, such as $NDVI_{[830, 660]}$=[ρ830-ρ660]/[ρ830+ρ660] were calculated for all available multi-temporal images, and stacked into an individual file for each index, respectively (the ρ### indicates the spectral reflectance at the wavelength of ### nm). Digital number was simply used for this calculation without any radiometric, atmospheric and topographic corrections after careful geometric corrections. All index values were averaged for each polygon of land-use parcel derived at the first step, and used to determine the year of slash/burn i.e., cropping in the history at the parcel basis. Third, biomass and soil $CO_2$ flux during cropping year were estimated from the on-site measurements. The biomass during fallow period was expressed as a function of canopy age based on periodical biome measurement. Fourth, all information was synthesized to assess the long-term (20 years) carbon balance at the regional scale under present and alternative land-use/ecosystem management scenarios.

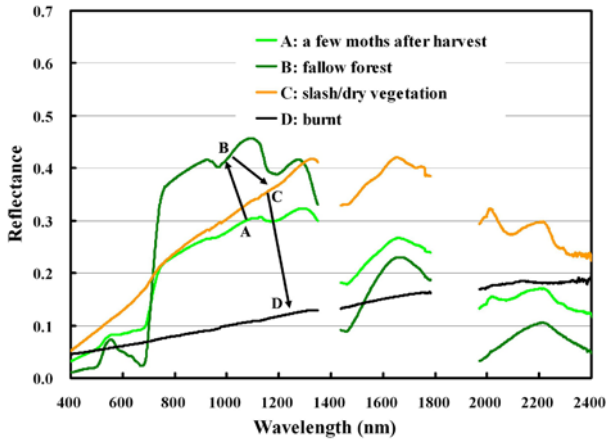


**Figure 2.** Simplified changing process of reflectance spectra after harvesting to slash-and-burning.

The other two approaches, i.e., (b) the linkage of satellite-derived land-use information and process-based biomass model, and (c) the linkage of land-use and biomass information derived from satellite images and process-based models, are also designed in this study. Nevertheless, the approach (b) requires a lot of input data for the process-based model, and the approach (c) further requires tedious tasks for radiometric, atmospheric and topographic (BRDF) corrections to derive physically-consistent spectral signatures. These two approaches are attractive from the methodological point of view, but need a lot more data and information, while it is not yet assured if these approaches would provide more reliable and precise assessment [6]. Hence, at the moment, we focus on the results from the approach (a), which may be simple but allow rough assessment with less data availability. Image analysis was conducted by using Imagine 8.7 (ERDAS) and eCognition.

## 4 RESULTS AND DISCUSSION

It was obvious that the slash/burn agriculture be common throughout the study area irrespective of ethnic group, elevation, and slope, considering from preliminary overview of satellite imagery, geographic information, and ground-based field survey. That is, similar land-use was presumed to be found in the large area over MMSEA, i.e., northern part of Thailand, Laos, Myanmar and Vietnam, as well as southern part of China. A preliminary analysis based on Landsat imagery showed that the forest area in the northern part of Laos (186,000 $km^2$) was more than 90% in both 1973 and 1985, while it decreased down to around 80% in 1992. We selected seven cloud-free areas of 40km x 50km on those images to estimate accurate trends in forest area. The most drastic change was found up to be 20% during the period (from 1973 to 1992). It was also presumed that the deceasing trend might have been accelerated after 1985.

### 4.1 Spectral Characteristics of Major Ecosystem Surfaces

Hyper-reflectance spectra over a wide range of land-surfaces were obtained in the study area. The spectral reflectance at red and near-infrared wavelengths was obviously different between densely vegetated areas and slashed/sparsely vegetated areas. Reflectance at shortwave infrared wavelengths showed clear differences as affected by moisture and burning conditions, respectively. Figure 2 depicts a typical changing process of the reflectance spectra after crop harvesting through re-growth, fallow forest, slashing, to burning.

The response of vegetation indices for different land surfaces are shown in Figure 3. Five vegetation indices, i.e., $NDVI_{[830,660]}$=[ρ830-ρ660]/[ρ830+ρ660], $NDVIm_{[830,1650]}$=[ρ830-ρ1650]/[ρ830+ρ1650], $NDVIb_{[830,2220]}$=[ρ830-ρ2200]/[ρ830+ρ2200], $NDVIx_{[660,2200]}$=[ρ660-ρ2200]/[ρ660+ρ2200], and $NDVIs_{[1650,660]}$=[ρ1650-ρ660]/[ρ1650+ρ660] were calculated for the ground-based hyperspectral data. The subscripts “m”, “b”, and “s” for

$NDVIm_{[830, 1650]}$, $NDVIb_{[830, 2200]}$, and $NDVIs_{[1650, 660]}$ imply the major sensitivity of these spectral indices to "moisture", "burning", and "senescence", respectively [7]. The $NDVIx_{[660,2200]}$ showed little change for the wide range of targets, so that it could not be suitable for change detection. The other four indices had similar information that was useful for distinguishing green vegetation, slashed/dry vegetation, senescent vegetation, burnt surface, and bare soil surfaces, respectively. Nevertheless, the $NDVIb_{[830,2200]}$ seemed to be useful specifically for distinguishing burnt surfaces, while $NDVIm_{[830,1650]}$ may be effective to detect slashed/dry vegetation areas due to higher sensitivity to moisture conditions. Differences of green biomass in different fallow periods may be best inferred from the $NDVI_{[830,660]}$, since it is most sensitive to green biomass. The $NDVIs_{[1650,660]}$ had similar information as $NDVIb_{[830,2200]}$, $NDVI_{[830,660]}$, and $NDVIm_{[830,1650]}$, but the dynamic range was less than the others. Therefore, when

shortwave infrared wavelength is available, it may be efficient to use $NDVIm_{[830,1650]}$ and $NDVIb_{[830,2220]}$, with $NDVI_{[830,660]}$ although $NDVI_{[830,660]}$ can be used for the same purpose when wavelength bands are limited to visible and near-infrared regions as for IKONOS and QuickBird.

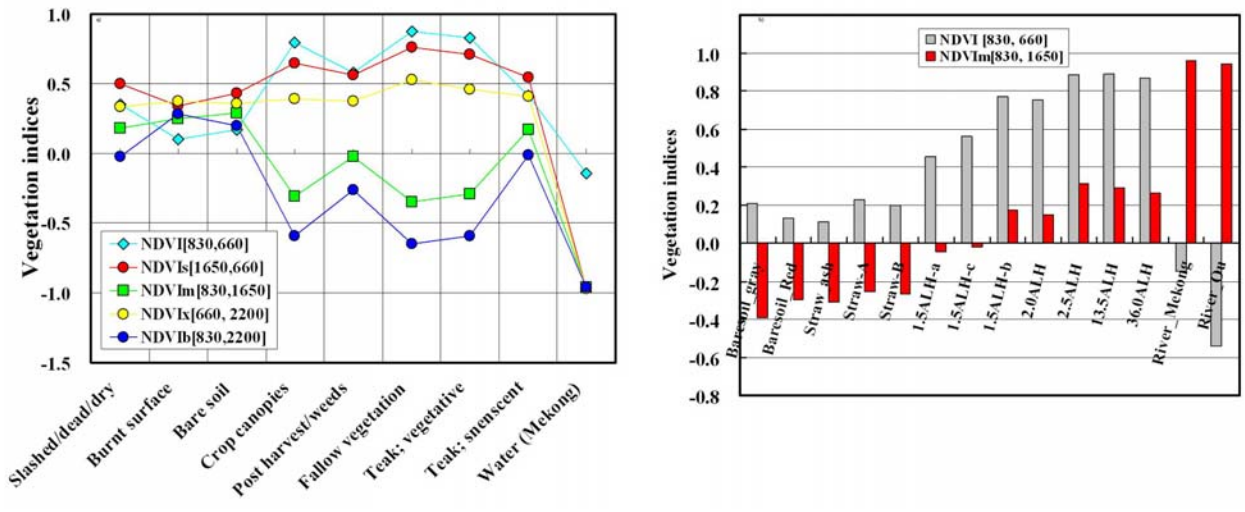


**Figure 3.** Response of vegetation indices to major land-surface targets in the study area. The ###ALH indicates the number of months after last harvesting.

**Table 1.** Change of slashed/sparse vegetation areas.

| Site ID | Feb. 6, 1992 | Feb. 6. 2001 | |
|---|---|---|---|
| **10 km x 10 km** | **a (%)** | **b (%)** | **b/a*100 (%)** |
| **A** | 4.2 | 35.0 | 835 |
| **B** | 10.0 | 23.3 | 233 |
| **C** | 16.6 | 30.3 | 182 |
| **D** | 5.0 | 5.9 | 118 |
| **E** | 2.8 | 6.1 | 217 |
| **F** | 15.3 | 31.0 | 202 |
| **G** | 12.4 | 19.0 | 153 |
| **H** | 18.3 | 17.2 | 94 |
| **Average** | 10.6 | 21.0 | 254.4 |
| 1) The eight sites of 10 km x 10 km area were selected over the 7700 km2 (110km x 70km) area in the central part of northern Laos. 2) The slashed/sparse vegetation areas were extracted | | | |

Spectral reflectance values were derived from some satellite images (Landsat-ETM+) through radiometric, atmospheric and topographic BRDF corrections using digital elevation map (DEM), and compared with the ground-based reflectance values for the similar targets. The reflectance values from satellite imagery showed good agreement with the ground-based values for the test pieces.

## 4.2 Recent Change of Land-use and Land-cover

A pare of Landsat images taken on the same day of year (February 6) in 1992 and 2001 were used to estimate the land-cover change in the region. Eight square areas (10 km x 10 km) were selected randomly from the whole scene (180 km x 180 km). In each subset, "dense/green vegetation" and "slashed/sparse vegetation" areas have been classified based on the unsupervised classification method. A great change was clearly observed between the two images (Table 2). The percentage of "slashed/sparse vegetation" area has greatly increased in all selected areas except for

one (H) where little change occurred. An example image for the site-C is presented in Figure 4 where the percentage of "slashed/sparse vegetation" area has increased by 82% from year 1992 to 2001. There must be some miss-classifications, and some bias in selection of the target areas; however, the eight areas of 100 km$^2$ size (800 km$^2$ in total) may be large enough to assess the representative trend in land-use change in the past ten years.

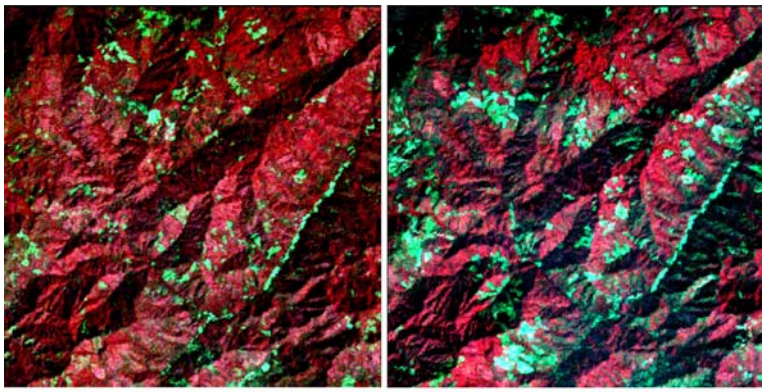


**Figure 4.** Comparison of slashed / sparse-vegetation areas (Bluish green areas) on the same day of year in 1992 and 2001. Notes 1) The size of the area is 10 km x 10 km, respectively, 2) Imagery is from Landsat TM and ETM+. 3) Classification was done using 6 spectral bands at pixel basis.

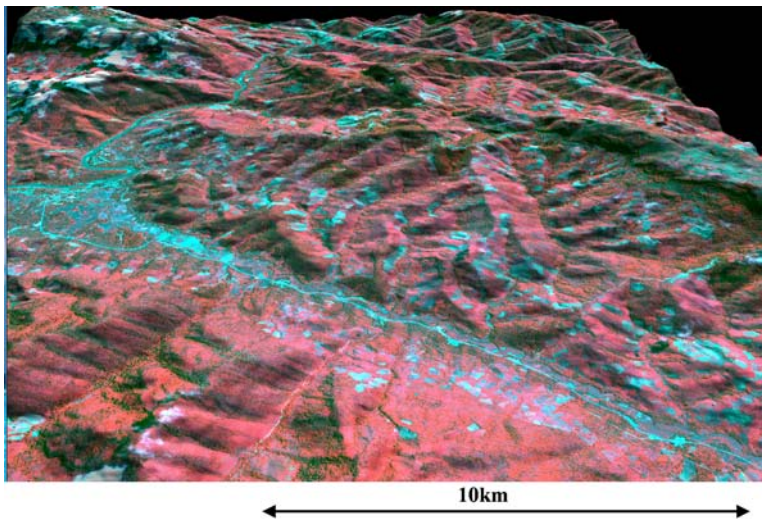


**Figure 5.** A 3D view of the intensive study area near Luangphabang. Notes: The spectral image is from QuickBird on Oct. 18, 2003. The spatial resolution is 2.4 m for spectral images and 10 m for digital elevation map, respectively. The G, R, and NIR bands are assigned to B, G, and R colors, so that the bluish color represents the slash/burn land-use during the year, and reddish color indicates the densely vegetated areas, respectively.

More detailed analysis was conducted for the intensive study area of about 300 km$^2$ (Luangphabang Province) using high-resolution multi-spectral imagery (QuickBird, Oct. 18, 2003; 2.4 m resolution). A 3D view of the intensive study area is shown in Figure 5. The spatial resolution was 2.4 m for the spectral image and 10 m for the digital elevation map, respectively. The land-use, especially the slash/burn areas with different fallow periods were classified by segmentation analysis using the spectral and shape information in the imagery. Segmentation approach was quite useful for generating the polygons for slash/burn land-parcels since the slash/burn fields are shifted by unit of such parcels of a few *ha*. In general, the parcel-based analysis may be more efficient and suitable than conventional pixel-based analysis for change detection of land-use [8], because the averaged spectra and/or indices for each parcel may be more representative of its land-surface condition and because the boundary polygons created for land-use parcels can be used for various spatial analyses. Results showed that the areas for slash/burn fields in the particular year and shot-term fallow parcels (1-3y) were 12.9% and 34.8%, respectively in 2003 (Table 2). The accuracy of the classification was estimated to be 100% from the concurrent ground survey. The ratio of the latter to the former is about 2.7, which implies that the average land-use cycle is approximately 4 years, i.e., 1 year for cultivation and 3 years for fallow period in the region. The potential area for slash/burn land-use was estimated to be 67.4 %, although the potential forest area could be 97.7%. The slash/burn cycle may be shorted by governmental regulation that limits the possible areas for slash/burn land-use. This may lower the crop productivity of the land due to reduced soil fertility [5]. It was also suggested that area of the burnt-parcels has increased by about 10% during last ten years, which suggests that the average rate of annual increase of slash-and-burn area may be 0.96% for the last decade. Unfortunately, there seems no good reason that this increasing trend will be reduced and that the governmental policy to sweep away the slash/burn cropping form the entire region will be realized.

**Table 2.** Land use in the intensive study area (300 km2) estimated from QuickBird image on Oct.18, 2003 based on segmentation procedure and ground-based survey.

| Land use | Parcels | Area (ha) | Area (%) |
|---|---|---|---|
| **Slash/Burn [0 year]** | 4031 | 3952 | 12.9 |
| **Slash/Burn [1-3 years]** | 5348 | 10656 | 34.8 |
| **Slash/Burn [4-20 years]** | 3467 | 6010 | 19.6 |
| **Conservation Forest (CF)** | 4704 | 7759 | 25.4 |
| **Teak** | 824 | 1515 | 5.0 |
| **Road/House/Bare** | 603 | 326 | 1.1 |
| **River/Pond** | 85 | 174 | 0.6 |
| **Paddy/Other crop lands** | 177 | 202 | 0.7 |
| **Total** | 21875 | 30595 | 100 |
| | | | |
| **Sum S/B** | 12846 | 20618 | 67.4 |
| **Sum S/B+CF** | 18374 | 29892 | 97.7 |

Notes:
1) Slash/Burn [0], [1-3], and [4-20] means slash-and-burn areas with follow period of 0, 1-3, and 4-20 years, respectively.
2) Land-use parcels were derived from Quickbird/MSS image (spatial resolution 2.4 m) by segmentation analysis using reflectance and shape. Classification accuracy was estimated to be 100% from the ground survey.
3) "Sum S/B" means the sum of all Slash/Burn areas with different fallow years; "Sum S/B+CF" is the sum of Slash/Burn and Conservation Forest which is the potential forest area.

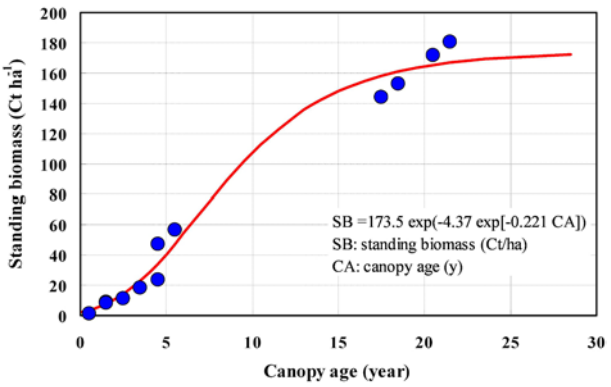


**Figure 6.** Total biomass of fallow biome expressed as a function of canopy age. Data are derived from on-site measurements in the continuous survey plots. This biomass is assumed to be the natural value without human disturbance although, in actual land-use, some biomass is taken out by village people for daily use that may be about 7 tC ha-1 y-1 by rough estimation.

## 4.3 Long-term Simulation of Land-Use and Carbon Balance

We estimated components of carbon balance between the ecosystem and atmosphere such as biomass production during cropping and fallow periods, soil $CO_2$ flux, and regional change of slash/burn land-use based on the on-site measurements. As the first approximation, we simply expressed the total biomass of fallow biome as a function of canopy age (Figure 6), since the canopy age, i.e., the number of years after the last slash/burn cropping can be derived from satellite imagery at the basis of land-use parcel. This biomass is assumed to be the natural value without human disturbance although, in actual land-use, some biomass is taken out by village people for daily use that may be about 7 tC $ha^{-1}$ $y^{-1}$ by rough estimation [9]. Since few quantitative data are available concerning this subject, we continue these on-site measurements for improving the simple approach and for calibration/validation of process-based ecosystem models.

On the basis of the on-site measurements and image analysis, we simulated the long-term change of land-use and carbon balance of the ecosystem under the present and alternative land-use scenarios (Table 3). We are investigating the several cropping systems (Figure 7) as options for alternative land-use management based on on-site agronomic experiments [10]. Considering the possible economic inputs, environmental impact, technological background, and the topographical conditions in the region, it may not be suitable to apply modern agricultural technologies such as advanced machinery and agro-chemicals. In this sense, it is a highly ecological and agronomic challenge to seek higher sustainability, crop productivity, and income without the conventional modernization of agriculture. Hence, the rice-based cropping systems may be most feasible options for the region since rice is most important food in the area. The relay cropping of rice and pigeon pea is most promising for the moment, and was used as a basic cropping system in the alternative land-use and ecosystem management scenario in the simulation of carbon balance.

The simulation was conducted for the whole study area of 22,500 $km^2$ (Figure 1) for the period of next 20 years. In the scenario of present land-use, the value of annual increase rate of slash/burn cropping area was assumed to be the same as in the past decade, i.e., 10 % per 10 years. Average fallow period was assumed to be 3 years based on the above analysis. In the alternative land-use scenario, rice is cropped with legume cash plants once for two years, where the productivity was higher by 1.5 times than the single rice cropping that is supported by experimental results. We also assumed that this cropping system can be continued for 5 years, and some of slash/burn areas could

be excluded from slash/burn use into conservation forest, and consequently the fallow period could be extended to 10 years. The seasonal soil $CO_2$ flux was estimated from the daily soil temperature based on the relationship between measured $CO_2$ flux and soil temperature. No use of any agrochemicals was assumed as in the present condition.

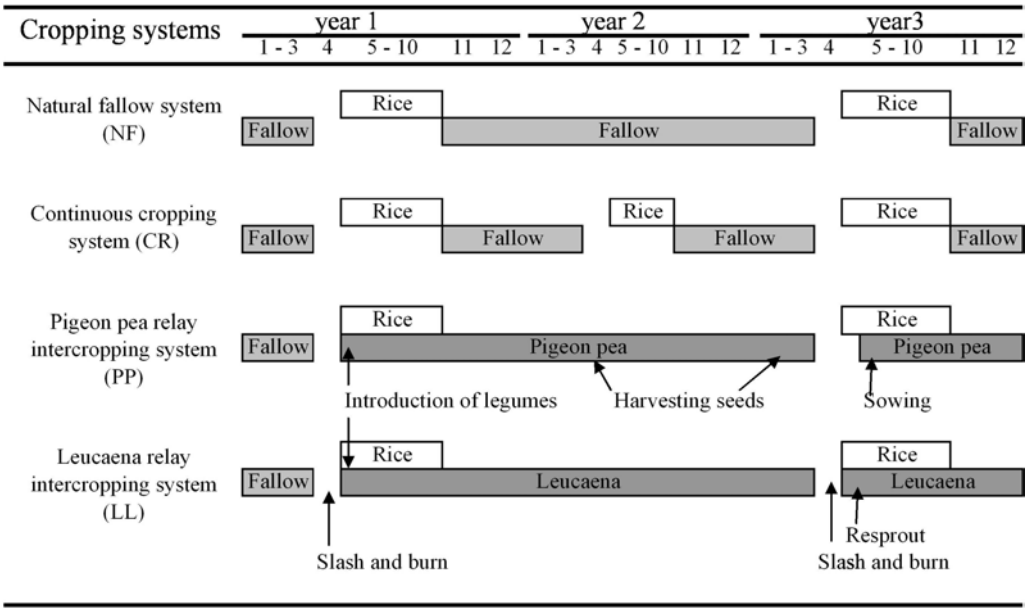


**Figure 7.** Cropping systems are compared for alternative land-use and ecosystem management options.

Results showed that the carbon is transferred from the ecosystem into the atmosphere when the present situation is continued. The long-term fallow area will have to be used for mote intensive slash/burn cropping. It has been pointed out that repetition of short-term slash/burn cropping would have serious negative effects on soil productivity and accelerate the growth of weeds. Weeding is the most tedious management practices in rice cropping in slash/burn cropping [5]. These negative effects were not included in the simulation, but the results will obviously be more serious when such effects are included. In the alternative scenario, on the other hand, the area of long fallow and conservation forest will be increased, and the ecosystem will increase the carbon sink capacity. The simulation results suggest that the slash/burn ecosystem is a source of $CO_2$ for the atmosphere under present situation, but could be switched to a sink by changing the land-use and ecosystem management strategies.

In summary, the simulation based on the remote sensing, GIS and on-site measurements suggests a catastrophic spiral of decreasing soil carbon and fertility, and increasing slash/burn area, i.e., biomass burning and $CO_2$ emission unless no effective strategies for alternative ecosystem managements are carried out. This may cause serious problems in food security as well as issues of environment and resources. The simulation also suggests that alternative land-use scenarios based on inter-cropping may improve the situation by elongating the fallow period and suppressing biomass burning. Enhancement of forest area should benefit village people since they largely depend on water and non-timber products from the conserved forests. The present synthesis of data, knowledge, and analysis is still preliminary, and further studies are needed for more precise and reliable assessment and prediction of the ecosystem dynamics. The evaluation of alternative scenarios from the socio-economic and cultural points of view is important.

## 5 CONCLUSIONS

The present study revealed the real conditions of the land-use in the slash/burn ecosystems in northern part of Laos based on the comprehensive geo-spatial data set. We also made a preliminary simulation of the long-term change of land-use and carbon balance in the region under several land-use/ecosystem management scenarios. Results showed the serious degradation of food productivity and forest resource as well as negative atmospheric impact. Some alternative ecosystem management methods may allow longer fallow period and more robust food and environmental security. Further quantitative research is needed for assessment and prediction of land-use and ecosystem dynamics. The synergistic use of remote sensing, GIS, modeling, and on-site measurements is most promising approach for the ecosystem and environmental issues at the regional scale.

**Table 3.** Long term simulation of land-use and carbon balance between ecosystems and the atmosphere for the whole study area of 22500 km2. Values are indicated in annual averages over 20 years.

| Land-use and ecosystem management scenario : | Present condition | | | | |
|---|---|---|---|---|---|
| Land use | Units | slash/burn cropping | Short fallow | Long fallow & Conservation Forest | Ecosystem scale assessment |
| Aerial ratio | [%] | 14.1 | 38.2 | 15.0 | |
| Aerial change after 20 years | [%] | 2.6 | 6.9 | −9.5 | |
| A. Biomass stock increment | [kg- $CO_2$/ $km^2$/y] | 2.970E+05 | 2.230E+06 | 3.025E+06 | |
| B. Plant litter into soil | [kg- $CO_2$/ $km^2$/y] | 2.732E+05 | 6.712E+05 | 1.721E+06 | |
| C. Microbial flux from soil surface | [kg- $CO_2$/ $km^2$/y] | 2.200E+06 | 2.200E+06 | 2.200E+06 | |
| D. Sum of A, B and C per unit area | [kg- $CO_2$/ $km^2$/y] | −1.630E+06 | 7.014E+05 | 2.546E+06 | |
| E. Value of D for the whole study area | [kg- $CO_2$/ y] | −5.188E+09 | 6.023E+09 | 8.587E+09 | 9.423E+09 |
| F. Biomass burning for the study area | [kg- $CO_2$/ y] | 0 | −1.485E+10 | | −1.485E+10 |
| G. Ecosystem-atmosphere carbon balance for the whole study area | [kg- $CO_2$/ y] | | | | −5.432E+09 |
| H. as above per unit land area | [kg- $CO_2$/ $km^2$/y] | | | | −2.414E+05 |

| Land-use and ecosystem management scenario : | Alternative scenario based on sustainable cropping systems | | | | |
|---|---|---|---|---|---|
| Land use | Units | slash/burn cropping | Short fallow | Long fallow & Conservation Forest | Ecosystem scale assessment |
| Aerial ratio | [%] | 16.8 | 17.2 | 33.3 | |
| Aerial change after 20 years | [%] | 0.0 | −14.2 | 14.2 | |
| A. Biomass stock increment | [kg- $CO_2$/ $km^2$/y] | 1.154E+06 | 3.287E+06 | 3.025E+06 | |
| B. Plant litter into soil | [kg- $CO_2$/ $km^2$/y] | 7.788E+05 | 9.741E+05 | 1.721E+06 | |
| C. Microbial flux from soil surface | [kg- $CO_2$/ $km^2$/y] | 2.200E+06 | 2.200E+06 | 2.200E+06 | |
| D. Sum of A, B and C per unit area | [kg- $CO_2$/ $km^2$/y] | −2.668E+05 | 2.061E+06 | 2.546E+06 | |
| E. Value of D for the whole study area | [kg- $CO_2$/ y] | −1.007E+09 | 7.616E+09 | 1.909E+10 | 2.570E+10 |
| F. Biomass burning for the study area | [kg- $CO_2$/ y] | 0 | −8.804E+08 | −1.809E+10 | −1.897E+10 |
| G. Ecosystem-atmosphere carbon balance for the whole study area | [kg- $CO_2$/ y] | | | | 6.726E+09 |
| H. as above per unit land area | [kg- $CO_2$/ $km^2$/y] | | | | 2.990E+05 |

| | | |
|---|---|---|
| Improvement of carbon balance by the alternative ecosystem management scenario for the whole study area | [kg- $CO_2$/ y] | 1.216E+10 |
| as above per unit land area | [kg- $CO_2$/ $km^2$/y] | 5.404E+05 |

## REFERENCES


[1] RASUL, G. AND THAPA, G.B., 2003: Shifting cultivation in the mountains of south and Southeast Asia: Regional patterns and factors influencing the change. *Land Degradation & Development* 14, pp. 495-508.

[2] PETERS, W. J. AND NEUENSCHWANDER, L.F., 1988: Slash and burn; farming in the third world forest. University of Idaho Press, Moscow, 113p.

[3] COCHRANE, M.A., ALENCAR, A., SCHULZE, M.D., SOUZA JR., C.M., NEPSTAD, D.C., LEFEBVRE, P., AND DAVIDSON, E.A., 1999: Positive feedbacks in the fire dynamic of closed canopy tropical rain forests. *Science* 284, pp.1832-1835.

[4] CZIMCZIK, C.I., MUND, M., SHULZE, E.D., AND WIRTH, C., 2005: Effects of reforestation, deforestation, and afforestation on carbon storage in soils. In: The Carbon Balance of Forest Biomes (Eds. Griffiths, H. and Jarvis P.G.), Taylor & Francis, pp.319-330.

[5] RODER, W., 2001: Slash-and-burn rice systems in the hills of northern Lao PDR: Description, challenges and opportunities. International Rice Research Institute, 201p.

[6] INOUE, Y., 2003: Synergy of remote sensing and modeling for estimating ecophysiological processes in plant production. *Plant Production Science* 6, pp.3-16.

[7] WILSON, E.H. AND SADER, S.A., 2002: Detection of forest harvest type using multiple dates of Landsat TM imagery. *Rem. Sens. Env.* 80, pp.385-396.

[8] HAYES, D.J. AND SADER, S.A., 2001: Comparison of change-detection techniques for monitoring tropical forest clearing and vegetation regrowth in a time series. *PERS* 67, pp.1067-1075.

[9] KIYONO, Y., OCHIAI, Y., CHIBA, Y., ASAI, H., SAITO, K., HORIE, T., SONGNOUKHAI, V., NAVONGXAI, V., AND INOUE, Y., 2005: Studies on improvement of ecosystem management and carbon sink capacity in the shifting cultivation ecosystems – Effect of the use of forest products on the long-term biomass of fallow biome -. Proc. 15th Annual Meeting of Japanese Society of Tropical Ecology.

[10] SAITO, K., LINQUIST, B., ATLIN, G.N., PHANTHABOON, K., SHIRAIWA, T., AND HORIE, T., 2005: Response of traditional and improved upland rice cultivars to N and P fertilizer in northern Laos. Field Crops Research, (in press; available on line).

# Desertification vs. Rehabilitation Processes across the Egyptian-Israeli Borderline

A. Karnieli[a]

[a] The Remote Sensing Laboratory, Jacob Blaustein Institutes for Desert Research, Ben Gurion University of the Negev, Israel, 84990, email: karnieli@bgu.ac.il

## ABSTRACT

Year-to-year fluctuations of rainfall in the northern Negev desert provide an opportunity to characterize and assess the temporal dynamics of desertification, phenology, and drought processes. Such information was retrieved and analyzed by combined use of satellite imageries in the reflectivity and thermal spectral bands.

Data covering four-years of coarse spatial resolution and images from a high revisit time satellite, namely the NOAA-14, were used. The images were processed to produce the Normalized Difference Vegetation Index (NDVI) and the Land Surface Temperature (LST). These measures were applied to the sand field in the northwestern Negev (Israel), which is almost totally covered by biological soil crusts, and to an adjacent region in Sinai (Egypt), consisting mainly of bare dune sands. Various manipulations of the data were applied. Time series presentation of the NDVI and LST reveals that the NDVI values correspond to the reaction of the vegetation to rainfall and that LST values represent seasonal climatic fluctuation. Scatterplot analysis of LST vs. NDVI demonstrates the following: (1) The two different biomes (Sinai and the Negev) exhibit different yearly variation of the phenological patterns: two seasons in Sinai moving along the LST axis, and three seasons in the Negev - where the NDVI axis represents the growing season; (2) The Sinai has an ecosystem similar to that found in the Sahara, while the Negev, only a few kilometers away, has an ecosystem similar to the one found in the Sahel; (3) Drought indicators were derived by using several geometrical expressions based on the two extreme points of the LST – NDVI scatterplot. The later analysis led to a discrimination function that aims to distinguish between the drought years and the wet years in both biomes.

Results from the current study show that a great deal of information on dryland ecosystems can be derived from four, out of five, NOAA/AVHRR spectral bands. The NDVI is derived from the red and the near-infrared bands and the LST from the two thermal bands. Combined use of these two products provides more information than any product alone.

**Keywords:** NOAA/AVHRR; NDVI; Land Surface Temperature; Desertification; Phenology; Drought.

## 1 INTRODUCTION

The severe recurrence of droughts in the Sahel and other regions, as well as an apparent accelerated southward advance of the Sahara Desert, led to extensive international discussions and to the establishment of the United Nations Conference on Desertification (UNCOD). At this meeting, desertification was defined as "land degradation in arid, semi-arid, and dry sub-humid areas resulting mainly from adverse human impact" (UNEP, 1992).

The three basic dryland processes, namely desertification, phenology, and drought, are strongly linked. Drought is part of the cause of desertification and certainly makes the situation worse. Mainguet (1994) states that desertification is "revealed by drought". The phenology of natural plants is changed by either desertification or drought processes. It is expressed, for example, by changes between grasses and shrubs, C3 and C4 species, or palatable to unpalatable species. The objective of the current paper is to characterize and assess the temporal dynamics of these three processes, by jointly analyzing reflective and thermal data acquired by satellite remote sensing means.

The Advanced Very High Resolution Radiometer (AVHRR), operated by the National Oceanic Atmospheric Administration (NOAA), with 1 km spatial resolution and high temporal resolution of about 1 day, plays a significant role in monitoring regional and global processes. The most important AVHRR-derived products for ecological applications are the Normalized Difference Vegetation Index (NDVI) and the Land Surface Temperature (LST).

## 2 STUDY AREA

Perhaps the most spectacular phenomenon connected with desertification vs. rehabilitation can be observed across the Israel-Egypt political border (Figure 1). Although the sand field of the Negev desert (Israel) represents the eastern extension of the Sinai (Egypt) fields from the geomorphological and lithological points of view, the area is artificially divided by the political borderline. The borderline is characterized by a sharp contrast; higher reflectance values (brighter) on the Egyptian side and lower reflectance values (darker) on the Israeli side.

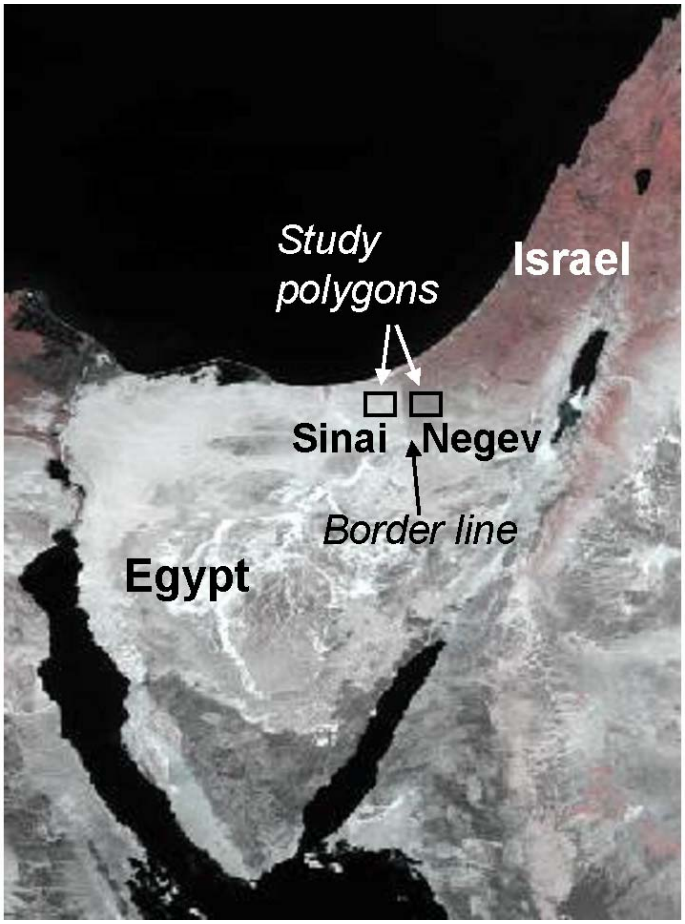


**Figure 1**. Location map based on NOAA-AVHRR image showing the study polygons on both sides of the border between Israel and Egypt. The high contrast across the borderline is due to almost complete cover of biological soil crusts in the Negev and their absence in Sinai.

The traditional and popular explanation asserts that the contrast is mainly due to severe anthropogenic impact of the Sinai Bedouin - especially overgrazing by their black goat and sheep herds, as well as gathering of plants for firewood. The Israeli side of the border has been subject to a conservation of nature policy since the 1950s and especially, under an advanced rehabilitation process since 1982. This interpretation was pioneered by Otterman (1974) and summarized in Otterman (1996). Classification based on satellite and aerial photographs revealed that Sinai is dominated by bare sands (83.5%) while in the Negev, the sands are overlaid by soil biological crusts (71%). Consequently, Sinai is characterized by shifting sand dunes while these dunes have been stabilized in the Negev. As a result, a new theory, recently proposed by Karnieli and Tsoar (1995) and Tsoar and Karnieli (1996), suggests that the contrast is not a direct result of severe overgrazing of higher vegetation but is caused by an almost complete cover of biological soil crusts on the Israeli side, while human and animal activities have prevented the establishment and accumulation of such crusts, as well as trampling and breaking up any existing crusts on the Egyptian side.

Mean annual rainfall in the study area is 90 mm. The current project lasted four years from October 1995 to September 1999. Two of these years were relatively dry (drought) years - 1995/6 and 1998/9, with 32.3 and 31.2 mm rainfall, respectively. The other two years were relatively wet - 1996/7 and 1997/8 with 79.3 and 83.6 mm rainfall, respectively.

## 3 METHODOLOGY

The NOAA-AVHRR data were acquired in High-Resolution Picture Transmission (HPRT) format (~1X1 km) by the ground receiving station located at the Sede Boker Campus (Negev, Israel). NOAA-14 images were obtained for four-years from October 1995 to September 1999 and were processed to produce the Normalized Difference Vegetation Index (NDVI) and the land surface temperature (LST). These measures were applied to two adjacent research polygons at sand field in the northwestern Negev and northeastern Sinai (Figure 1). Various manipulations of the data were applied: (1) time series analysis of the NDVI and LST throughout the 4 years for study; and (2) k-mean analysis with various numbers of clusters.

# 4 ANALYSIS AND RESULTS

## 4.1 Temporal Dynamics of NDVI and LST

The temporal variations of the NDVI and the LST along the four hydrological years of the project are presented in Figure 2. Figure 2a shows that the Negev ecosystem, under an advanced rehabilitation process since 1982, shows higher values of vegetation index (mean NDVI for the whole data set = 0.124 ± 0.039) and high reactivity to rainfall (from 0.116 ± 0.033 during the dry period to 0.143 ± 0.045 in the wet period), especially during wet years (1996/97 and 1997/98). In contrast, the Sinai area, under desertified conditions, presents a very low reaction to rainfall (from 0.086 ± 0.014 during the dry period to 0.096 ± 0.015 in the wet period), maintaining approximately constant NDVI values (mean NDVI for the whole data set = 0.089 ± 0.015). A slight increase in the vegetation index is visible only during the wet years. The differences between the mean NDVI values of Negev and Sinai can be as high as 0.1, following the rainy season of a wet year. Since it is well known that higher NDVI values are caused by a dark soil background, NDVI differences during the dry periods seem to be related to the brightness difference between the two sides of the border, due to the presence of the dark biological soil crusts and, to a lesser extent, the higher vegetation on the Israeli side (Karnieli and Tsoar, 1995).

Figure 2b demonstrates the monthly MVC values of the computed LST in the sampling polygons on both sides of the border. No clear differences in phase are evident. On the contrary, the cyclical temperature trends are similar in the Negev and in Sinai and follow the climatic variations throughout the four years. During the relatively wet winters, evaporation determines large losses of energy from the wet soil surface; low sun irradiance also contributes less significantly than in summer to the soil heat balance. Thus, the minimum LST values are always found in the rainy period during the winter, and can be as low as 20°C. In these seasons, the difference in the amplitude between the polygons is almost negligible. The maximum temperatures are found at the height of summer and can reach values of 58°C. The temperature differences between the two sides of the border can be as high as 7°C.

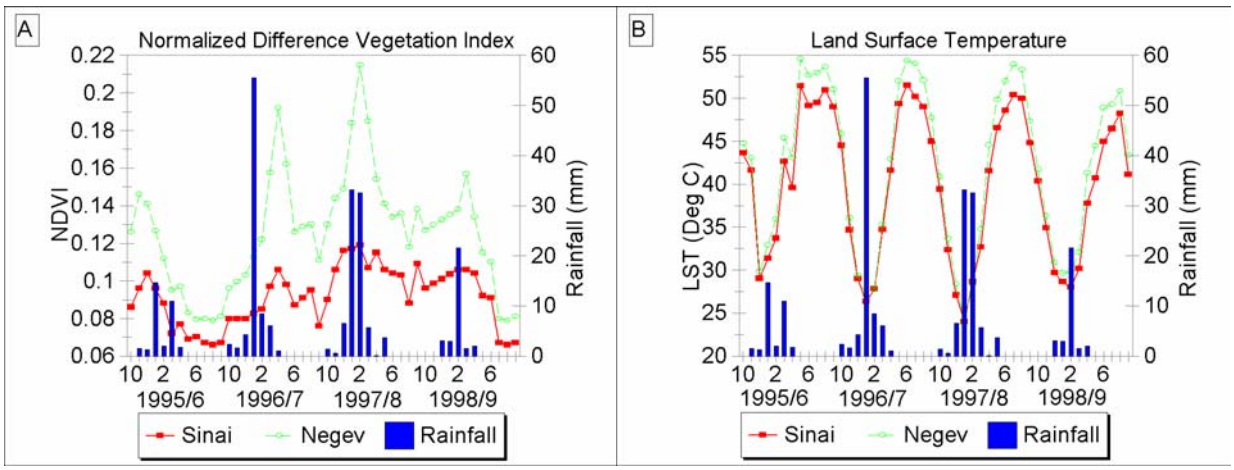


**Figure 2.** Temporal variations of NDVI(A) Tand LS (B) in Sinai and the Negev along the four hydrological years of research. The NDVI values correspond to the reaction of the vegetation to rainfall and that LST values represent seasonal climatic fluctuation.

The explanations for the amplitude differences evident in the dry period are addressed in Qin et al. (2001). Since the sand dunes on the Israeli side are almost completely covered by dark biological soil crusts, they absorb more incident radiation and emit stronger thermal radiation than the bare sand on the Egyptian side. Moreover, although more vegetation is present on the Israeli side, these desert plants, due to their scarcity and dormancy in the hot, dry summer, contribute almost nothing to the regional evapotranspiration that cools the surface. Thus, in the dry season, the Israeli side presents higher values of surface temperatures than in the Sinai.

## 4.2 Desertification Assessment

The combination of reflective and thermal data for determining soil water status or surface water availability has been reported in numerous studies (Lambin and Ehrlich, 1996; 1997). This type of analysis has usually been undertaken by plotting LST against NDVI values (Figure 3a, after Lambin and Ehrlich 1996). Such a method is used in the current research in order to characterize the desertification processes in the study area. A scatterplot of multi-year NDVI vs. LST values was created (Figure 3b). Applying a K-mean analysis of two clusters for the data, it was shown that the combined values of the Negev are significantly different from those of Sinai. Comparing the location of the clusters to the African continental scheme of Lambin and Ehrlich (1996), the current scatterplot demonstrates that the Sinai desertified ecosystem overlaps the area covered by the Sahara biome, while the Negev recovered side of the border, although located only a few kilometers away, exhibits characteristics similar to those of the Sahel biome (although it fits even better to that in the Southern African Hemisphere, discussed in the same paper).

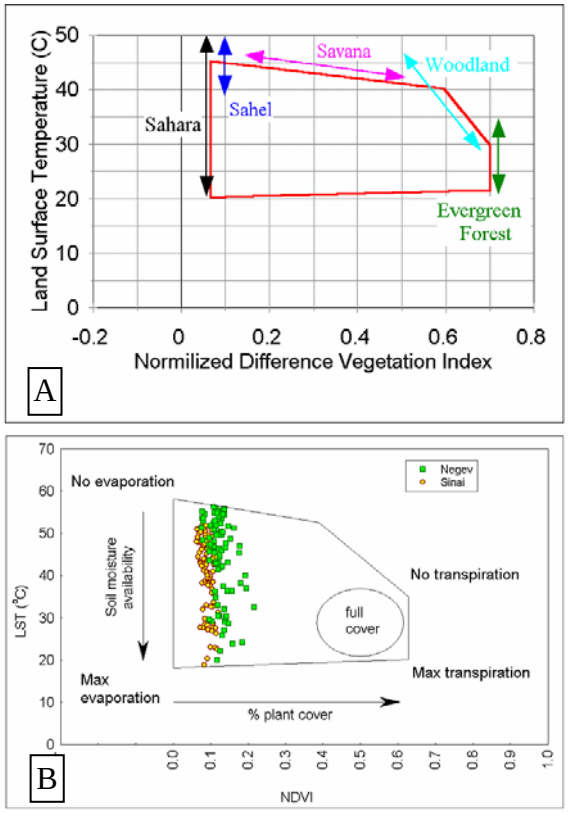


**Figure 3.** (A) Scatter diagram for schematic discriminating of different biomes in Africa as proposed by Lambin and Ehrlich (1996). (B) Data obtained for this study. The Sinai has an ecosystem similar to that found in the Sahara, while the Negev, only a few kilometers away, has an ecosystem similar to the one found in the Sahel.

## 4.3 Phenology

Results of the K-mean analysis reveal that 5 clusters characterize the study area (Figure 4). The Sinai area, under a desertification process, is characterized by just two clusters (1 and 2) corresponding to the dry and wet seasons respectively, and defined by the fluctuations of land surface temperatures throughout the year. In this area, the biological activity is almost non-existent, therefore only the physical meteorological factors are responsible for the movement inside the LST-NDVI space. On the other hand, the recovered ecosystem of the Negev shows relatively intense biological activity and is characterized by movements over three clusters of the LST-NDVI space. In the Negev ecosystem, as in the Sinai, both dry and rainy seasons are evident (clusters 3 and 4) while the third cluster (number 5) represents the growing season, which is evident only on the Israeli side of the border and which includes the highest values of NDVI. Only a few points are presented inside cluster number 5, because it corresponds to the very short period of the year in which the desert reaches its maximum greenness due to the blooming of the annuals.

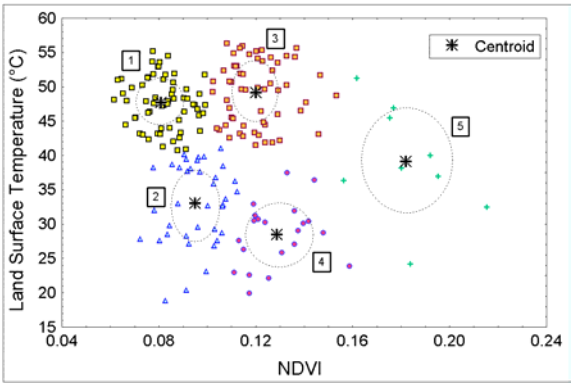


**Figure 4.** btained from the cluster analysis of Groups o NDVI and LST data**.** The numbers refer to the cluster numbers mentioned in the text. The dashed lines represent 1STD from each centroid. The two different biomes (Sinai and the Negev) exhibit different yearly variation of the phenological patterns: two seasons in Sinai (clusters 1-2) moving along the LST axis, and three seasons in the Negev (clusters 3-5) where the NDVI axis represents the growing season.

It is interesting to note that several points belonging to the Negev are located inside cluster 1, which represents the Sinai. Natural arid land systems show a resilient character rather than a resistant one: their stability is not defined by a unique equilibrium state, but according to fluctuations of environmental parameters. Beyond certain limits, they can be associated with multiple-equilibrium states of a domain, inside which the ecosystem does not change its structure. This is the result of adaptation to the harsh, extremely variable desert environment. The overlapping points of cluster 1 are relative to the very dry years (1995/6 and 1998/9). In periods extremely lacking in water, the recovered ecosystem is able to reduce its activity to

the minimum needed for surviving in the area of the LST-NDVI space typical of desertified ecosystems. However, as soon as the precious resource of water is available again, it can immediately react and produce relatively high values of NDVI. On the other hand, the disturbed ecosystem (Sinai) shows the result of a man-made perturbation that has changed its structure: in wet years only an extremely limited response to rainfall is detected.

The multi-year average of the combined NDVI and LST values are presented in Figure 5 in terms of month-by-month trajectories. Phenology starts in October and ends in September of the following year. It is shown that the desertified Sinai ecosystem exhibits the highest variability mostly along the LST axis and is almost unaffected by the NDVI, except for a slight deviation from the straight line between April and July, most likely due to some greenness of perennials. On the other hand, the recovered Negev side of the border exhibits variability on both LST and NDVI axes. Here, the NDVI axis is dominant especially during the wet months (January – July) due to the greening of biological soil crusts, annuals, and perennials. During the summer months, the trajectory moves only along the LST axis.

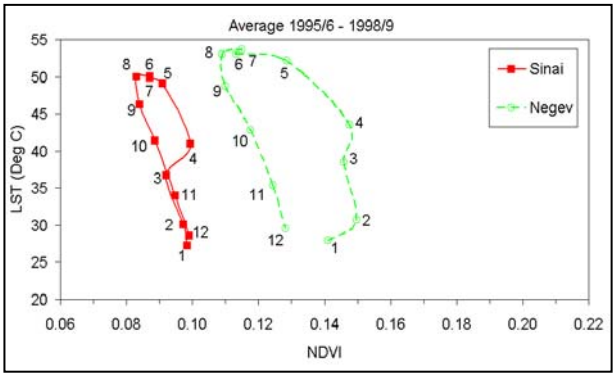


**Figure 5.** Multi-year average of the combined NDVI and LST values in terms of month-by-month trajectories. The desertified Sinai ecosystem exhibits the highest variability mostly along the LST axis and is almost unaffected by the NDVI. On the other hand, the recovered Negev side of the border exhibits variability on both LST and NDVI axes.

## 4.4 Drought Assessment

Breakdown of Figure 5 into the four hydrological years under investigation was performed to demonstrate the annual dynamics. In the Sinai, little difference can be seen between the wet and the dry years, with the same general trajectory shape - long, narrow, and with a vertical pattern along the LST axis. In the Negev, however, there is a considerable difference between the wet and dry years. During the wet years (1996/7 and 1997/8) the shape of the graphs is stretched towards the high NDVI values and the phenological cycle is much more pronounced, whereas during droughts (1995/6 and 1998/9) the NDVI component is much less remarkable and the phenological cycle shrinks significantly.

Figure 6 shows the lines connected between two points defined as (1) the maximum LST – minimum NDVI; and (2) minimum LST – maximum LST, for each of the hydrological years and for the Negev and Sinai ecosystems separately. It may be seen that the Sinai lines are very similar in terms of position and length; however, two groups can be distinguished between the Negev lines. The lines of the wet years are longer and with gentler slopes, whereas the dry-years lines are shorter and steeper. These characteristics can be quantified by three geometrical expressions:

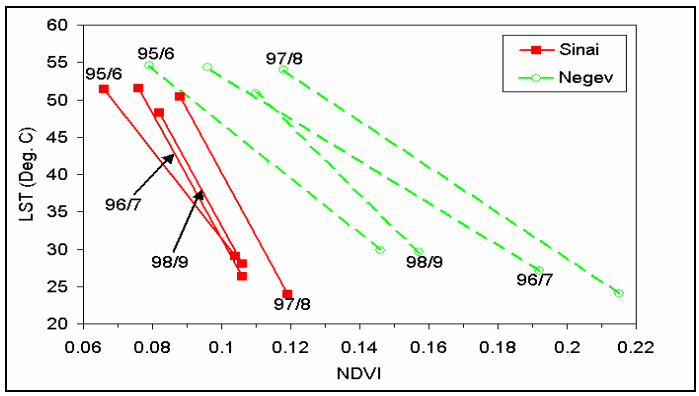


**Figure 6.** Lines connected between maximum LST – minimum MDVI and minimum LST – maximum NDVI for the Sinai and the Negev. Note differences in slope and length of the lines between the two biomes and among years.Note differences in slope and length of the lines between the two biomes and among years.

$$\text{Angle} = \arctan\left(\text{LST}/\text{NDVI}\right) \quad (1)$$

$$\text{Area} = \Delta\text{NDVI} \cdot 0.5\Delta\text{LST} \quad (2)$$

$$\text{Length} = \left(\left(\Delta\text{LST}\right)^2 + \left(\Delta\text{NDVI}\right)^2\right)^{0.5} \quad (3)$$

These three expressions can be used as indicators for quantifying drought years. Evaluation of the three indicators was performed by applying the following Discrimination Function (DF) for each year (i) and for each region (j):

$$DF_{ij} = \left(X_{ij} - X_{mean_j}\right) \Big/ \left(X_{max_j} - X_{min_j}\right) \quad (4)$$

where $X_{ij}$ is the calculated value for each indicator, either in Sinai or in the Negev, in any particular year. $X_{avg}$, $X_{max}$, and $X_{min}$, are the yearly average, maximum and minimum values for each region, respectively. The objective of this function is to discriminate the drought years from the wet years on both sides of the border.

Results of the discrimination function for each of the drought indicators show that for the Negev, each of the indicators successfully separates the two drought years from the wet years, since the $DF_{ij}$ receives either positive or negative values. However, for Sinai, only the "length" indicator is able to show this phenomenon. The other two indicators - slope and angle - produce mixed results. Consequently, the "length" indicator will be used for further analysis.

Using the "length" indicator, Figure 7 presents the $DF_j$ values as a function of the yearly rainfall of each year. Despite the fact that only 8 points are involved in the regression analysis, a clear trend is exhibited between the drought-year cluster (negative values) and the wet-year cluster (positive values). The crossing point between the regression line and the DF=0 line can be used to quantify the threshold between wet and drought years in terms of rainfall amount (54 mm in the current example).

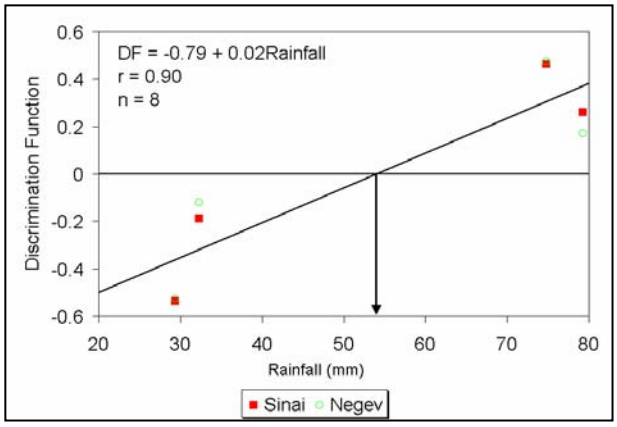


**Figure 7.** Discrimination function values vs. the yearly rainfall amounts of each year. The crossing point between the regression line and the DF=0 line can be used to quantify the threshold between wet and drought years in terms of rainfall amount.

## 5 SUMMARY AND CONCLUSIONS

Desertification, phenology, and droughts processes can be detected and characterized by using four out of five NOAA/AVHRR spectral bands. The NDVI is derived from the red and the NIR bands and the LST from the two thermal bands. Combined use of these two products provides more information than any product alone.

Time series presentation of NDVI and LST reveals that the NDVI values correspond to the reaction of the vegetation to rainfall and that LST values represent seasonal climatic fluctuation. Scatterplot analysis of LST vs. NDVI demonstrates the following:

1. The two different biomes (Sinai and the Negev) exhibit different yearly variations of the phenological patterns: two seasons in Sinai moving along the LST axis, and three seasons in the Negev, where the NDVI axis represents the growing season;

2. The Sinai has an ecosystem similar to that found in the Sahara while the Negev, only a few kilometers away, has an ecosystem similar to that of the Sahel;

3. Drought indicators were derived in terms of three geometrical expressions based on the two extreme points of the NDVI - LST scatterplots. Evaluation of the suggested indicator shows only one that can successfully separate between the drought and the wet years. It is concluded that the AVHRR imagery can provide valuable information for drought monitoring and characterization.

## REFERENCES

[1] DALL'OLMO, G. AND KARNIELI, A, 2002: Following phenological cycles of desert ecosystems using NDVI and LST data derived from the Advanced Very High Resolution Radiometer. *Int. J. Remote Sens. 23*, 4055-4071.
[2] LAMBIN, E.F. AND EHRLICH, D., 1996: The surface temperature-vegetation index space for land cover and land-cover change analysis. *Int. J. Remote Sens. 17*, pp. 463-487.
[3] KARNIELI, A. AND TSOAR, H., 1995: Spectral reflectance of biogenic crust developed on desert dune sand along the Israel-Egypt border. *Int. J. Remote Sens. 16*, pp. 369-374.

[4] LAMBIN, E.F. AND EHRLICH, D., 1997: Land-cover changes in Sub-Saharan Africa (1982-1991): application of a change index based on remotely sensed surface temperature and vegetation indices at a continental scale. *Remote Sens. Environ. 61*, pp. 181-200.
[5] LAMBIN, E.F. AND STRAHLER, A.H., 1994: Change-vector analysis in multitemporal space: A tool to detect and categorize land-cover change processes using high temporal-resolution satellite data. *Remote Sens. Environ. 48*, pp. 231-244.
[6] LIETH, H., 1974: Phenology and Seasonality Modeling. Springer-Verlag, New York.
[7] MAINGUET M., 1994: Desertification – Natural Background and Human Mismanagement. Springer Study Edition, vol.1, 2e ed., Springer, Heidelberg.
[8] OTTERMAN, J., 1974: Baring high-albedo soils by overgrazing: a hypothesized desertification mechanism. *Science 186*, pp. 531-533.
[9] OTTERMAN, J., 1996: Desert-scrub as the cause of reduced reflectances in protected versus impacted sandy arid areas. *Int. J. Remote Sens. 17*, pp. 615-619.
[10] QIN, Z., DALL'OLMO, G., KARNIELI, A. AND BERLINER, P., 2001: Derivation of split window algorithm and its sensitivity analysis for retrieving land surface temperature from NOAA-AVHRR data.. *J. Geophys. Res.106*, pp. 22,655-22,670.
[11] TSOAR, H., AND KARNIELI, A., 1996: What determines the spectral reflectance of the Negev-Sinai sand dunes? *Int. J. Remote Sens. 17*, pp. 513-525.
[12] UNEP 1992: World Atlas of Desertification. Edward Arnold Publishers, Sevenoaks.

# Monitoring and Evaluation of Vegetation Cover Changes in Semi-Arid Areas by Means of Remote Sensing and GIS A Case Study of Khartoum Forest Sub-Sector, Sudan

M. A. Khiry[a] and E. Csaplovics[b]

[a] Department of Forestry, University of Khartoum, Sudan; presently Department of Geosciences, University of Dresden, email: nadakheiry@hotmail.com
[b] Department of Geosciences, University of Dresden, email: csaplovi@rcs.urz.tu-dresden.de

## ABSTRACT

Monitoring vegetation cover changes in arid and semi-arid regions is of high interest for both natural scientists and resource management experts. Vegetation cover change has been considered to be the most important task of land degradation studies. Assessing the status of vegetation cover by remote sensing techniques using various vegetation indices has been successfully applied to semi-arid and arid regions. The presented paper intends to develop monitoring methods for assessing land cover/land use changes by using Landsat satellite imagery in order to analyze the progress of vegetation cover changes and its impact on desertification process in Khartoum State. Vegetation cover changes during a period of 11 years are evaluated using Landsat TM data of 10 Dec 1989 and Landsat ETM+ of 24 Dec 2000. Visual interpretation supported by the analysis of aerial photography and by field observations was applied. Digital image analysis by supervised classification integrating NDVI bands determined the changes of vegetation cover during the period of 1989 and 2000. The process of vegetation cover change was detected by comparative analysis of bi-temporal land use and land cover classifications. Results of investigations proved that the process of degradation in vegetation is highly complex and developing very fast especially in the study area in the western part of Khartoum State. However, the climatic fluctuations and human interference have been the main actors in the process. The findings of the paper are useful for better understanding of the dynamics of vegetation cover changes in the study area. The results are also very important for supporting decision makers to initiate efficient planning and management of forests and to reduce or stop further degradation in vegetation in these arid and semi-arid areas characterized by a fragile ecosystem and limited conditions of vegetation growth. Multi-temporal remote sensing data (TM and ETM) of the study area demonstrate that it is possible to detect and to map the vegetation cover at relatively low cost. Application of remote sensing techniques in monitoring vegetation cover changes and desertification process is well adopted and recommended in such large areas like Khartoum state.

**Key words:** dry lands, vegetation cover changes, remote sensing

## 1 INTRODUCTION

Arid and semi arid lands cover approximately 30-40 percent of the land surface (FAO, 1999). Because of the vast area covered, these lands play a major role in energy balance and hydrologic, carbon and nutrient cycles. The dry land areas are characterized by irregularity and shortage of rainfall, prolonged dry seasons, high temperature and high evaporation. Such variation in climatic factors makes dry lands more fragile and prone to desertification (Elfadul, 1997). The development of vegetation cover in these regions typically undergoes wide seasonal and annual fluctuation, largely regulated by the availability of water. It may be readily impacted by both climatic shifts and human activities such as over- grazing, over-stocking, wood gathering and urbanization.

Combined pressure by man and changes in climatic conditions in these regions resulted in high and serious degradation in natural vegetation, especially in the tropics. In tropical arid and semi arid regions loss of plant cover seems to be related to poor soils and aridity, which prevailed throughout short, as well as, long periods of drought and thus permitted very limited recovery of natural vegetation. According to Rauschkolb (1971), serious degradation in tropical arid and semi- arid land refers to various indicators of desertification, such as dramatic decrease of plant cover, and replacement of existing vegetation by an undesired one. Generally, vegetation cover change has been considered to be the most important task of land degradation in most of environmental studies. Over the past 45 years, approximately 11% of the semi-arid lands have become degraded to the point where their original biotic functions have been damaged, with subsequent reclamation being costly or in some cases impossible. The processes leading to degradation and the extent of the problem worldwide are only being understood recently. The continually increasing global population intensifies pressure on marginal lands, particularly in developing

countries, where population growth and poverty subvert efforts to introduce sustainable agricultural practices, leading to environmental problems such as soil erosion and desertification. Thus, monitoring the vegetation vigor of these lands is of a highly interest for both scientists and resource management specialists. Assessment of the degree to which desertification is increasing is essential to decision-makers and others who are concerned with land degradation. Therefore, continuous monitoring of vegetation is absolutely indispensable and would certainly add much to our knowledge in understanding our living environment and its interactions with climate, as well as, in predicting the future of our planet. According to Tueller (1982 and 1983), remote sensing is considered as a powerful tool that allows inventory monitoring and management for collection of spatial information of semi-arid lands at relatively low costs. Sudan, the largest country in Africa, covers an area of approximately 2.5 million square kilometers. It located between the latitudes 3.2° N to 23.0° N and the longitudes 21.75° E to 38.5° E .Sudan is characterized by a wide range of rain fall zones from nil rain fall in the north to 1500 mm in the south, associated with different ecological regions from the desert in the north to high rainfall woodland savannas in the south. The dry lands (arid average annual rainfall less than 75mm; semi-arid with annual rainfall from 75mm to 300mm), cover approximately 60% of the country (1.5 million square kilometers), thus, constituting the largest area of dry lands in Africa. The dry land is faced with serious environmental and socio- economic problems such as drought, deforestation, desertification, poverty, famine and migration. Such problems, resulted from natural factors and human activities, lead to desertification, (Elfadul, 1997).

Desertification and drought are more than any phenomenon inducing lasting impacts on the natural habitats. Desertification is a term that always reveals or indicates land degradation which is defined by Convention for Combating Desertification (1994) as follows: “land degradation in arid and semi – arid and dry sub-humid areas resulting from various factors, including climatic variation and human activities” The region affected by drought and desertification in Sudan lies between the latitudes 12° N and 18° N and covers the country from the east to west. With severe desertification along the Nile north of Khartoum stretching to the Egyptian border between latitudes 17° N to 20° N. One of the characteristics of this region is that its unstable, fragile and high resilient landscape prone by human and animal disturbance. Andrew (1944) states that “arid regions were areas of high instability, where nature’s balance was so delicate that might be tipped to wards destruction by a slight disturbance whether natural or by human”. Destruction by man (e.g. cutting down woody vegetation) and clear harmful effects of over-grazing, especially during the successive drought years, have led to extended damage of natural vegetation.

During the last decades, Khartoum State has been experiencing a rapid degradation of tree coverage. The destruction of vegetation cover induced by removal of soil layers (wind and water erosion) contributed actively to the extension of the desert southwards. Due to the misuse of the natural resources such desert creeping is confined to the study area and extended to cover large areas. The situation is very serious and inadequate information and poor education of local people which should highlight the socio- ecological value of trees in rural and urban environments is one of the reasons for uncontrolled clearing of trees. Accordingly, this paper explores and assesses the extent to which the decrease of the vegetation cover and its impact on desertification affected the study area during the two addressed periods of 1989 and 2000. The main objectives of this paper are:

- To monitor and evaluate the changes of vegetation cover in the study area within the two addressed periods of 1989 and 2000.
- To produce a land cover change map (1989 to 2000) for the study area by means of remote sensing, GIS and topographic maps.
- To assess the efficiency of remote sensing as a tool for detecting and monitoring vegetation changes at low cost.
- The hypotheses are:
- Changes of vegetation cover in the Khartoum State are usually caused by the fluctuation in annual rainfall and the variation in soil type.
- Desert encroachment in the study area is positively influenced by the loss of vegetation cover, especially in the western part of the study area than the eastern one.
- Measurement of vegetation cover change over time is important for analysis of land degradation processes.

## 2 THE STUDY AREA

Khartoum State lies between latitudes 15°.15′- 16° N and longitudes 32°, 15′ 32°, 45′ E. It located in the center of Sudan at the junction of the Blue and White Nile and occupies an area of about 2611 sq km. It is the smallest

province in the Sudan, extending from the margins of the desert in its northern extremity to wet humid regions southwards. The Nile River divides the area into two parts, one to the west and the other to the east (Figure 1). Khartoum State is located in the semi-arid eco-climatic zone dominated with arid climate, with annual rainfall ranges from 75mm to 160mm falling mainly in July and August. The occurrence of dust storms occurrence almost all the year indicates the presence of more and huge amount of decertified or bare land within and around Khartoum State. The vegetation is dominated by *Acacia tortilis, Acacia nilotica, Faidherbia albida* and *Acacia seyal*. The shrub layer includes *Calotropis procera*, *Ziziphus spina-christi*, *Ricinus communis,* and *Tamarix nilotica*.(Appendixes 1)

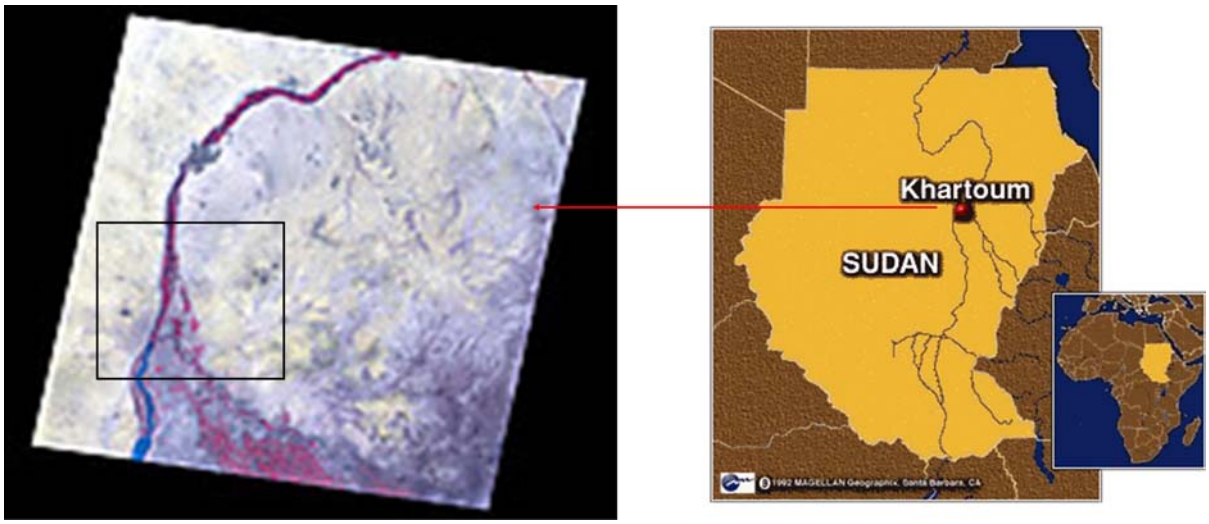


**Figure 1.** The location of the study area ETM+ Landsat7 24 Dec 2000 of Khartoum State, path 173, row 49 (Source: http/www.sudan.net/government/afmap.hty).

## 3 METHODOLOGY

### 3.1 Selection of satellite imagery and image processing

Two clouds -free Landsat TM and ETM scenes reprocessing were selected for the analysis. The two images were acquired in December 1989 and 2000. The TM and ETM data have been acquired simultaneously in seven and nine spectral bands, respectively. The characteristics of TM and ETM bands are suitable for detecting and monitoring the biotic as well as non-biotic types of natural resources. According to Lillesand and Kiefer (2004), as well as Campbell (2002), TM band 1 is useful for soil and vegetation differentiation .TM band 2 detects green reflectance for healthy vegetation and band 3 is designed for detecting chorophly11 absorption in vegetation. The two digital images were geometrically corrected using ground control points provided by the topographic sheets at scale of 1:250000. Spectral enhancement has been performed during the classification and interpretation steps of the both images of 1989 and 2000. The computation of NDVI was applied using the formula:

$$\text{NDVI} = (\text{near IR} - \text{visible red}) / (\text{near IR} + \text{visible red}) \quad (1)$$

The NDVI is highly correlated with green biomass, leaf area index and other vegetation parameters (Tucker, 1976). Time series of band ratios like NDVI imagery may be used by subtraction providing difference imagery. Supervised classifications with combination of the NDVI channel were applied. The classification was based on the field verification and the selection of the training samples respectively. It is important to mention that the study area consists of diverse mixed vegetation and soil types. Thus, vegetation samples have been selected according to different soil types. The two images have been classified into nine classes, and the results were drawn from the analysis of these classes. Accordingly, the final results come out as a bi-temporal land cover and land use of the study area.

### 3.2 Results

Monitoring the natural vegetation cover condition in 1989 and 2000 included all types of vegetation which, have been found in *wadis* and in different soil types. They have been categorized into four different units that are; sparse

vegetation in *wadis,* vegetation on clay soils, vegetation on mixed soils and vegetation on sandy soils. Difference between the western and eastern parts of the study area led to a considerable variation in of vegetation cover. In the part east of the River Nile the vegetation cover seems to be more diverse than in the western one .The detailed classification of the image of the year 2000 presents a clear evidence of quantitative and qualitative changes in the study area. It was found that the green vegetation cover was far better than in 1989 than that of 2000. There was a considerable shifting in the green vegetation cover in 2000, almost in the western part of the study area (Figure 2&3).

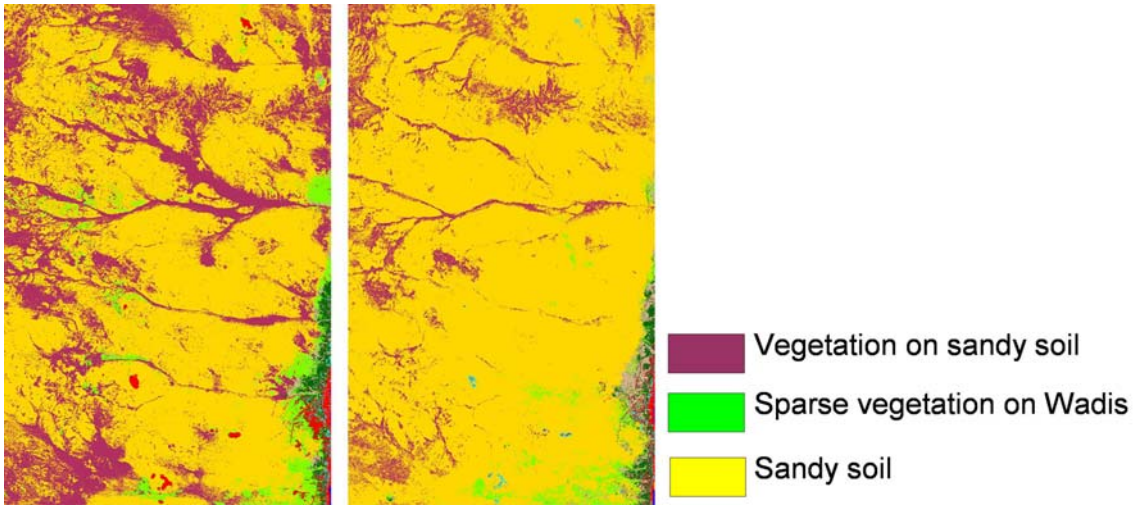


**Figure 2.** The difference in vegetation cover within the Western parts of the study area for the years 1989(left) and 2000 (right).

Vegetation on sandy soil covered about 9.4% of the study area in 1989 and only about 1.3% in 2000. Accordingly, it was clearly proved that the desert creeping was more vigorous in 2000 than 1989. (Table 3).

The dynamic change in vegetation cover was increasing rapidly in 2000. In 1989 vegetation cover showed high percentage of the total area, while in 2000 soil cover the large part of the region. The processes of vegetation cover changes in the study area led to an increase of bare land cover during the addressed 11 years. (Figure 4 &5).

The comparison of vegetation cover in 1989 and 2000 indicates that the western part of the study area shows a significant decrease in green vegetation cover in 2000. In 1989 the total area covered by natural vegetation was about 44.0 % and this value decreased to 27.4% in 2000(Table 1 & 2). It explores clearly that sparse vegetation in *wadis* and vegetation on sandy soils were more affected than other types of vegetation cover. In 1989 sparse vegetation in *wadis* covered 16.5 % of the total area, while in 2000 it was only about 8.4%. This indicates that the degradation of vegetation cover increased rapidly till 2000 and thus supported the encroached of desert areas

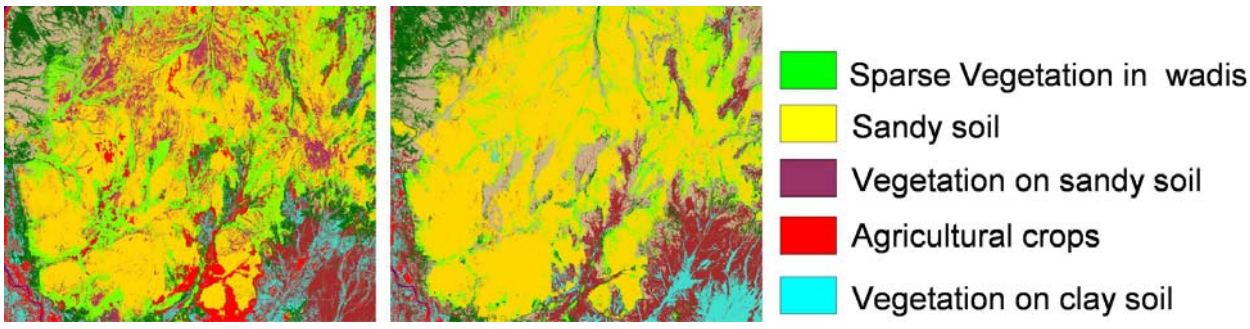


**Figure 3.** The differences within vegetation cover in eastern part of the study area for the years 1989 (a) and 2000(b).

**Table 1.** Distribution of vegetation cover in 1989**.**

| Class name | Area (ha) | (%) |
|---|---|---|
| **Sparse vegetation in Wadis** | 266911.11 | 16.48 |
| **Vegetation on clay soils** | 151790.72 | 9.38 |
| **Vegetation on mixed soils** | 137440.82 | 8.49 |
| **Vegetation on sandy soils** | 155778.91 | 9.62 |
| **Total** | 711921.56 | 43.98 |

**Table 2.** Distribution of vegetation cover in 2000

| Class name | Area (ha) | (%) |
|---|---|---|
| **Sparse vegetation in wadis** | 135360.08 | 8.36 |
| **Vegetation on clay soils** | 167010.78 | 10.31 |
| **Vegetation on mixed soils** | 120178.39 | 7.42 |
| **Vegetation on sandy soils** | 20678.82 | 1.27 |
| **Total** | 443228.07 | 27.38 |

**Table 3.** Comparison between land cover types in 1989 and 2000 of the study area.

| Year | 1989 | | 2000 | |
|---|---|---|---|---|
| **Land cover type** | **Area (ha)** | **(%)** | **Area (ha)** | **( % )** |
| **Agricultural crops** | 215745.2 | 13.33 | 91793.2 | 5.67 |
| **Sparse vegetation in Wadis** | 266911.1 | 16.48 | 135360.0 | 8.36 |
| **Vegetation on clay soils** | 151790.7 | 9.38 | 167910.8 | 10.31 |
| **Vegetation on mixed soils** | 137440.8 | 8.49 | 120178.4 | 7.42 |
| **Vegetation on sandy soils** | 155778.9 | 9.62 | 20678.8 | 1.27 |
| **Clay soil** | 105138.1 | 6.50 | 202676.3 | 12.52 |
| **Mixed soil** | 73530.1 | 4.54 | 186085.3 | 11.49 |
| **Sandy soil** | 501857.9 | 31.00 | 683731.8 | 42.23 |
| **River Nile** | 10525.2 | 0.65 | 11211.8 | 0.69 |

Khartoum State has obviously experienced a considerable change in vegetation covers. The degradation of vegetation cover in the study area comprises quantitative and qualitative changes. The study area is completely located in semi-arid eco-climatic zone with very harsh conditions and diversity needs for human activities. No doubt under such conditions man plays the most powerful and persistent role causing or contributing to land cover changes. During the last decade, the study area has been subjected to successive drought, desertification and famine which influence negatively the natural vegetation cover. Accordingly, it commonly emphasized that while drought causes a quantitative decrease in vegetation cover, man forces intensively using the environment and resources, and thus contributing positively to land degradation. Another principle reason for vegetation change is the annual and perennial fluctuations of climatic factors especially rainfall. The study area is a part of the eco-climatic zone, which is ecologically classified as the dry tropics, characterized by warm dry winters and hot rainy summers.

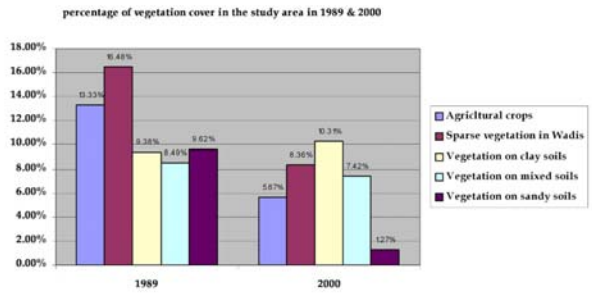


**Figure 4.** Distribution of vegetation cover change in the study area

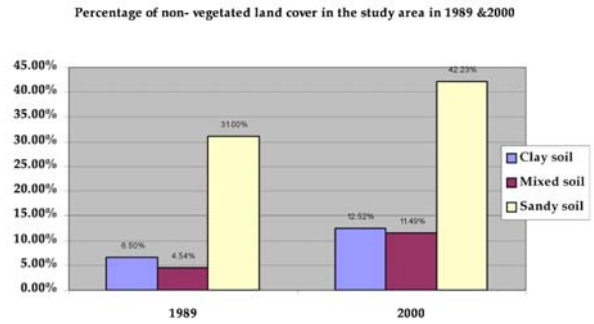


**Figure 5.** Distribution of vegetation cover change in the study area 1989& 2000

Vegetation cover is strangely influenced by variation of rainfall. The growth of vegetation in this region depends on the availability of water in seasonal streams. The inconsistency and unreliability in rainfalls are prominent characteristics of the arid and semi-arid climate in the study area. (Table 4 & Figure 6).

**Table 4.** The total annual rainfall records at Khartoum station from 1989-2000 (Sources: Meteorological Department, Khartoum, 2002).

| **Year** | 1989 | 1990 | 1991 | 1992 | 1993 | 1994 | 1995 | 1996 | 1997 | 1998 | 1999 | 2000 |
|---|---|---|---|---|---|---|---|---|---|---|---|---|
| **Rainfall (mm)** | 79.8 | 40.4 | 44.8 | 67.9 | 39.8 | 231.6 | 194.4 | 199.0 | 155.4 | 110.6 | 130.6 | 60.0 |

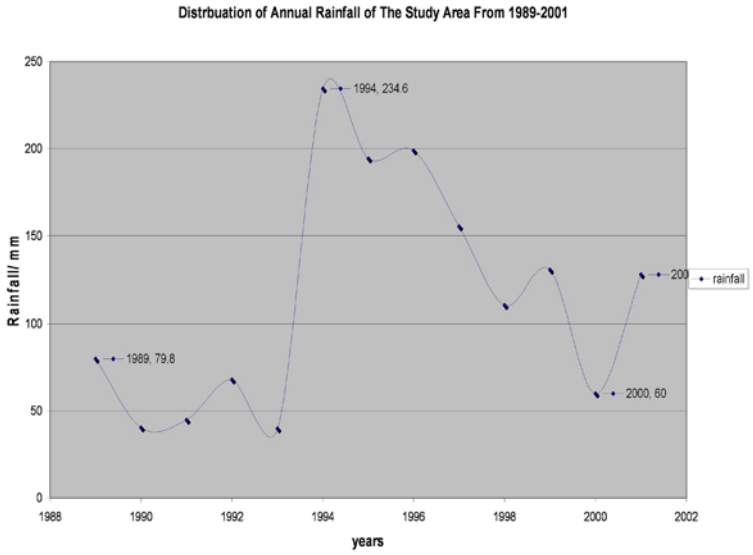


**Figure 6.** Distribution of annual rainfall in the study area from 1989-2001 (Sources: Khartoum meteorological station 2002).

## 4 CONCLUSIONS

The development of satellite technology and remote sensing offers the opportunity for monitoring vegetation cover changes, due to the advantage in allowing sufficient synoptic records of vegetation cover conditions. The paper shows that complete vegetation cover destruction are attributed to climatic fluctuations and human activities (over-grazing & over – cultivation). This can be easily detected and monitored using earth observation satellite data e.g. TM Thematic Mapper ETM. Applications of multi-temporal remote sensing data (TM &ETM) of the study area demonstrate that it is possible to detect and to map vegetation cover at relatively low cost. The paper proves that vegetation cover in Khartoum State is severely affected. Finding of this paper, indicate that the deterioration of vegetation has induced wide-spread degradation phenomena in Khartoum State. This paper shows that decreasing of vegetation cover is severely subjected to the variations in climatic factors such as rainfall and ecological factors during the addressed periods. It evident that inventory and management of arid and semi arid region affected by degradation and desertification needs integrated of earth observation and appropriate methods of satellite image analysis. The results are also very important for supporting decision makers to initiate efficient planning and management of forests and to reduce or stop further degradation in vegetation in these arid and semi-arid areas characterized by a fragile ecosystem and limited conditions of vegetation growth.

## REFERENCES

[1] ANDREW, G (1944): Memorandum and Mapping on Desert creep. Report of Soil Conservation Committee, Sudan Government.
[2] CAMPBELL, B.J. (2002): Introduction to Remote Sensing 3th edition. Taylor and Francis, London. third edition
[3] ELFADL, M.A. (1997): Management of *Prosopis juliflora* for Use in Agro-Forestry System in Sudan, ph.DThesis, University of Helsinki.
[4] FAO, (1999): Forest Inventory Manual Draft Concept Paper FAO,Rome
[5] LILLESAND THOMAS, M. RALPH, W. KIEFER (2004): Remote Sensing and Image Interpretation, 5th edition, John Wiley and Sons. New York.
[6] RAUSCHKOLB, R.S. (1971): Land Degradation , Rome , Soil Bulletin No 13.FAO.
[7] TUELLER, P.T. (1982): Remote Sensing for Rangeland Management. p. 125-140.
[8] TUELLER, P.T. (1983): Rangeland Remote Sensing an Approaches, Proceedings of the RNRF Symposium on the Application of Remote Sensing to Resources Management, Seattle WA, 22-27 May, pp.24.54.
[9] TUCKER, C.J. (1976): Sensors Design for Monitoring Vegetation Canopies. *Photogrammetic Engineering and Remote Sensing* 42 (11)1399-1410.

**Appendices 1** : Vegetation covers types in Khartoum State

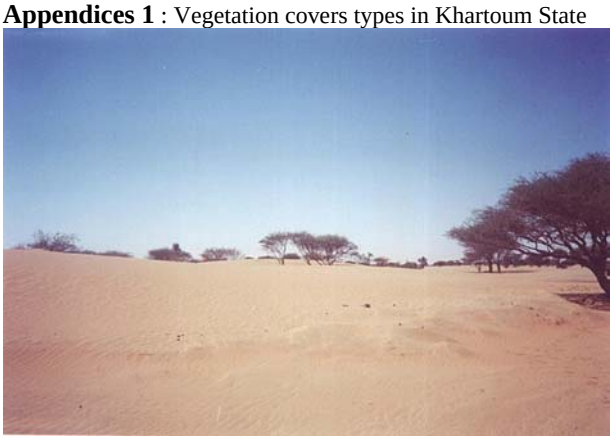

The desert encroachment in western part of Khartoum State

*Acacia tortilis* the dominating tree specie in Khartoum state

*Panicum furgidum* the dominating shrub species in Khartoum state

*Acacia tortilis* & *Panicum furgidum* the dominating tree & shrub species in Khartoum state(degraded areas)

# Detection of sensitive areas for degradation risk by analyzing of seasonal vegetation density along climatic gradient

Z. Makhamreh[a] and J. Hill[a]

[a] Remote Sensing Department, Faculty of Geography/Geosciences, University of Trier, D-54290 Trier, Germany. zeyadmak@yahoo.com

## ABSTRACT

An integrated approach based on remote sensing input was suggested and tested in order to evaluate the sensitive areas for land degradation risk. Quantitative evaluation assessment using SMA applied on multi-seasonal satellite images that incorporate the advantages of vegetation dynamics and temporal spectral curve was used for this purpose.

A multi-seasonal Landsat Thematic Mapper (TM) and (ETM+) data set consisting of two successive years was used to characterize vegetation cover dynamics and soil types. Image registration was accomplished with half pixel accuracy. A combined method for the correction of radiometric and topographic effects was performed using the 5S transfer model. Endmembers for the SMA were derived image-based and selected for representative vegetation types and soil orders. Spectral mixture modelling was used in order to identify and characterize seasonal vegetation dynamics and environmentally sensitive areas in northern Jordan.

Analysis of the spatial distribution and dynamics of vegetation conditions emerge different classes of vegetation communities. The high vegetation abundance class is covered by natural forest and fruit tree mainly olives, while the moderate vegetation cover class is determined mainly by the annual vegetation with wheat and barley as dominant land use. On the other hand, the vegetation density decreases substantially in the summer season. The most important derived class is the low vegetation abundance and high soil fractions, which explains the dynamics of vegetation-soil. Perennial vegetation is dominant in the areas receiving more than 450 mm rainfall, while annual vegetation is dominant in the 250-350 mm rainfall zone. The vegetation abundance in the 200 mm zone is very low.

The seasonal vegetation dynamics illustrates the importance of soil components as an independent component in the land degradation assessment. In this context, the sensitive areas for land degradation have been evaluated based on seasonal vegetation dynamics, vegetation abundance, and soil fraction. It is noticeable that 30 % of the total study area, which represents dense vegetation cover and bare soil, show almost constant fraction throughout the year with less than 10 % of variation. This means that the seasonal ecosystem dynamics in the rainfall zones above 500 mm and less than 200 mm are very negligible. The highest changes in vegetation ratio and respectively highest degradation risk were registered in the cultivated land use systems, especially the annual crops. Accordingly, the active landscape processes and potential sensitive areas for degradation were derived.

This approach takes into account the reflectance spectra at two significant times in the growing season and hence, allows for identification of major landscape processes and components. Quantitative temporal analysis of vegetation and soil communities under rainfed agriculture condition gives important information on the active landscape processes, dynamic of the land conditions and their possible degradation risk.

**Keywords:** Seasonal vegetation dynamics, sensitive areas, rainfed agriculture, SMA, vegetation ratio, Northern Jordan, Mediterranean regions.

## 1 INTRODUCTION

Land cover types and vegetation canopy information is vital to many environmental applications including land suitability assessments and degradation studies [1], [2]. In the Mediterranean regions, the dynamic interactions of ecosystem's components are very variable and highly influenced by the climatic conditions [3], [4]. The dynamic interactions of vegetation communities are very important in the characterization of vegetation under semi-arid conditions. In this context, the seasonal vegetation patterns and areal proportions of the perennial vegetation, annual vegetation, and soil components are crucial elements for the temporal analyses of vegetation communities under rainfed agriculture in Jordan [5].

Accordingly, it can be hypothesized that risk of land degradation will be reflected on the vegetation characteristics as well as soil properties. Therefore, reliable assessment of land degradation risk could be obtained

by considering both the seasonal dynamics of vegetation conditions and soil characteristics. This hypothesis has been tested and evaluated through a quantitative approach for assessment of sensitive areas for land degradation.

Plant phenology has been of interest to remote sensing scientists for many applications including vegetation production [6], land cover classification [7], and vegetation dynamics [8]. Since vegetation communities and agricultural crops are dynamic, observing and monitoring their development, for instance vegetation dynamics over time, could provide better information on the state and quality of landscape components.

Quantitative parameterization of seasonal vegetation cover properties and bare soil showed their importance in understanding and characterizing the dynamics of land use and related ecosystem processes in Jordan [5]. However, single-date image analysis is not able to represent the dynamic variability in landscape features. In this context, the application of multi-temporal image data has been recommended to study the landscape characteristics, since the maximum discrimination between different crop types occurs at different stages in the growth cycle [9], [10].

Derivation and extraction of vegetation and soil related indicators have been performed benefiting from the high spectral contrast of vegetation relative to soils. The concern is for observing vegetation communities and estimation of green vegetation cover [11]. The traditional land cover classification has been widely performed in different ecological regions for monitoring land cover changes [12]. Moreover, the analysis of spectral vegetation indices mainly the NDVI was widely used in the vegetation studies [13], [14].

An efficient approach for land cover classification and vegetation abundance estimation is spectral mixture analysis (SMA) [15]. It is a physically based approach that relates the image reflectance to the real surface features and efficient to detect sub pixel components [16]. Moreover, it is able to provide quantitative indicators for assessing many environmental phenomena [17], [18]. SMA has become an essential tool for remote sensing vegetation analysis and was utilized for calculating land cover fractions within a pixel [19], land cover change [20], and seasonal dynamics of vegetation [21], [22]. The SMA was used in this study in order to provide a quantitative assessment of vegetation and soil fractions and analyze the seasonal vegetation dynamics.

## 2 STUDY AREA CHARACTERISTICS

The study area occupies the eastern part of the Mediterranean region in northern Jordan as shown in figure (1). It is located between Latitudes 32° 15´ and 32° 30´ North and Longitudes 35° 45´ and 36° 15´ East and covers an area of 1000 km $^2$. The southern boundary is about 30 km north of Amman; the northern boundary is a few kilometres south of the Syrian borders.

Land cover types vary between natural, semi-natural, and cultivated areas. The dominant natural vegetation types are forest and shrubs [23], while the dominant Oak forest species is Quercus coccifera covering the largest area of the forestland. The dominant shrubs are Artemesia herba-alba covering mainly the 300-400 mm rainfall zone.

Cultivated lands are characterized by rainfed agriculture, which depends on the rainfall amounts and distribution. The main subdivisions of rainfed agriculture are fruit trees and field crops. The dominant fruit trees are olives, grapes and orchards, while the dominant field crops are wheat, barley and legumes.


**Figure 1.** Study area location

The prevailing climate is of arid Mediterranean type and characterized by dry hot summers and mild wet winters. Most of the precipitation occurs during the winter months November to April. Annual and seasonal rainfall variability is very high both in space and time. The general pattern of precipitation for representative meteorological regions within the study area is shown in figure (2).

This diversity ranges from semi-arid conditions where average rainfall amounts are about 200 mm, to semi-humid conditions where the average rainfall is about 600 mm.

Soil types in the studied area show wide variations in their characteristics, covering different soil orders according to the soil taxonomy classification [25]. The major soil orders found in the region are Inceptisols, Entisols, and Aridisols [23]. These soils are almost exclusively in the xeric moisture regime and exhibit a thermic temperature regime, while the eastern part lies in the transitional xeric-Aridic moisture regime and has thermic temperature regime.

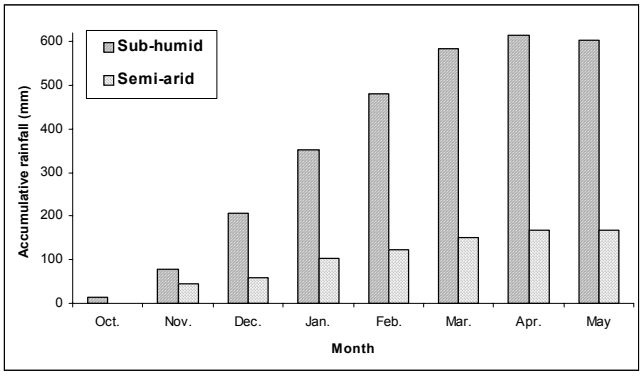


**Figure 2.** Show the long-term average rainfall distribution for representative Meteorological regions in the study area [24].

## 3 METHODOLOGY

The imagery data set for this study consists of one Landsat TM image acquired at first of May 1998 and one Landsat ETM+ image acquired at seventh of August 1999. Selection of image combinations was based on the crop calendar and growth pattern of the vegetation types in the study area. The spring scene of May 1998 provides good conditions for evaluation of the total vegetation abundance, while the summer scene of August 1999 is optimal for determination the permanent vegetation and soil types. It is assumed that the inter-annual variability of phenology measurements between the two years is relatively low, because photosynthetic activity is highly dependent on the photoperiod and temperature, both of which are relatively stable [26], and therefore it is assumed that there are no differences in the permanent vegetation growth between the two years.

In order to identify the fraction of vegetation types, the two images were combined together (spring-summer) to form one layer stack. This approach has been used and proved its advantages in multi-temporal vegetation analysis and land cover classification in the Mediterranean regions [5], [27].

Geometric correction was performed using ground control points to establish the transformation between the image and map coordinates based on a Digital Elevation Model (DEM) created from 1:50000 scale topographic maps with 20 m isohyets interval. The control points were taken from topographic maps and fieldwork using GPS. The radiometric value assigned to each pixel was calculated using the cubic convolution method. The accuracy of geometric correction was ranged within a half pixel. Atmospheric correction was based on the modelling procedure developed by Hill and Mehl [28], which incorporates the topographic correction module into a radiative transfer code to correct the atmospheric and terrain-induced illumination effect. This method is originally based on the radiative transfer model as developed by Tanré [29]. The radiometric correction and the Ångström-relation were calculated iteratively according to $\tau_a = 0.2 * \lambda^{-1.4}$.

SMA has been widely used for quantitative vegetation assessment. It classified into linear and nonlinear according to the complexity of scattering processes. If each photon interacts with a single land cover type within the field of view, then the mixing can be considered linear and the modelled spectra is the linear summation of the spectrum of each land cover type multiplied by its surface fraction [15], [21], [30]. However, those studies have been used the linear un-mixing approach due to its simplicity compared to the non-linear approach. Therefore, the linear un-mixing approach was applied in this study. Hence, mathematically, for every image pixel in any band, the spectral reflectance R can be modelled as follows:

$$R_i = \sum_{j=1}^{n} F_j \cdot RE_{ij} + \varepsilon_i \qquad (1)$$

where $R_i$ is the reflectance of the mixed spectrum in band i, $RE_{ij}$ is the reflectance of the endmember spectrum j in band i, $F_j$ denotes the fraction of endmember j, and $\varepsilon_i$ the residual error in band i. Equation (1) can be solved by matrix-inversion in order to determine the proportions of REi. The proportions should be sum to unity, expressed mathematically as:

$$\sum_{j=1}^{n} F_j = 1 \qquad (2)$$

Selection of appropriate endmembers for the unmixing model is very important to represent the thematic objectives and to have an accurate result [17]. Improvements in the standard image processing techniques allowed using image-derived endmembers with high accuracy [15]. In this study, the endmembers were derived using the pixel purity index method [31]. At the same manner, the endmembers for the summer 1999 were selected and analyzed, and then a final model was selected. The best-performing model consists of Quercus Cocifera spectrum representing green vegetation, limestone spectrum, soil, and shade spectrum. The derived endmembers for composite image are illustrated in figure (3).

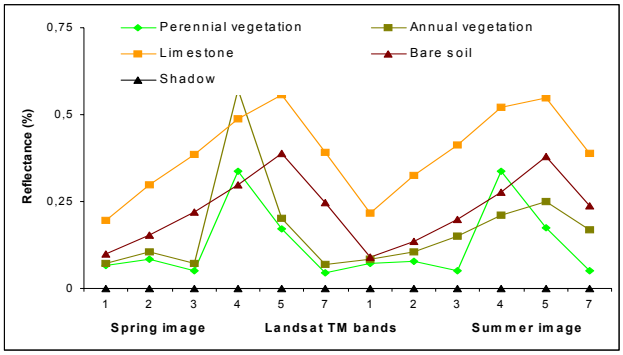


**Figure 3.** The derived endmembers for the composite image of Landsat TM 1998 and Landsat ETM+ 1999.

Figure (3) show the derived endmembers for the composite image of Landsat TM 1998 and Landsat ETM+ 1999. The perennial vegetation reflectance is almost constant over the year. Both the spring and summer spectra are almost identical for perennial vegetation. Spectra of the annual vegetation present typical green vegetation spectra in the spring season, while during the dry season, their spectra are similar to different soil spectra in the region.

Evaluation of the mixing model was performed by examining the root mean squared error (RMSE) and the residual image for both datasets. Application of the model on the multi-date images considerably improves the overall performance and decreases the residual error. The analysis of the residuals revealed that the imagery do not contain significant spatial or spectral anomalies, which indicates that the soil and vegetation components have been addressed reasonably well for all image pixels.

Distribution of residual error is consistent with the settlements, the highway structure, and the mining activities. However, as the interest is in the interpretation of vegetation and soil features, the urban areas were not included as separate endmember in the unmixing model, which explain the high error encountered in the urban areas in the image. Comparison of this image fraction with the geological map of the region indicates that those errors are related to the presence of limestone rock type, which forms the core element used in building materials in this region [32].

The next step is the normalization of the shade fractions, which was done by apportioning the shade fraction to the other endmember components, according to the following equation

$$F = 1/(1 - F_{\text{shade}}) \tag{3}$$

In this way, the shade fraction is portioned to the remaining endmembers according to their fractional abundances in the pixel [33].

## 4 SEASONAL-DYNAMICS OF LANDSCAPE COMPONENTS

Dynamics of vegetation cover and land use types over the growing seasons provides useful information on the nature of dominant processes that govern the landscape development. Investigation of the abundance distributions show there are two main vegetation communities dominating in the region, based on growth cycle pattern, namely the annual and perennial vegetation. The spatial distribution of vegetation abundance for the composite image can be examined in figure (4).

The spring image contains a higher level of green vegetation than the summer season, mainly due to the presence of annual vegetation crops. This pattern of land use is more dominant in the 250-400 rainfall zones. Most of the annual vegetation consists mainly of wheat in the high rainfall areas, and barley in the low rainfall areas. This is mainly due to the effect of seasonal rainfall pattern, which explains the distribution of vegetation community and abundance in the study area. The densities of perennial vegetation are high in the western part, where sub-humid rainfall conditions exist. Most of the perennial vegetation consists mainly of forest and fruit trees such as olives and orchards. On the other hand, the summer image consists mainly of perennial vegetation and soils. The dominant vegetation types in the summer season are forest in the western area, irrigated farms in the eastern part and olives in the other parts. The distribution of the soil fractions in the summer season is a displacement of the annual vegetation abundance in the spring season.

Seasonal vegetation characteristics can be explained by the investigation of vegetation fraction images with the rainfall distribution patterns. Vegetation abundances increase with the raising of rainfall amounts to reach a maximum value in the 550-650 mm rainfall zones. The permanent vegetation reaches a minimum contribution below the 350 mm rainfall due to the variability of rainfall amounts and high evapotranspiration demands. Annual vegetation is dominant under this condition with a maximum 40 % abundance, which explains the low agricultural productivity of field crops under rainfed conditions without supplemental irrigation.

However, the total perennial vegetation abundances below than 250 mm rainfall amounts do not reach more than 10%, while the dominating vegetation type consists mainly of irrigated vegetable farms. In contrary, the distribution of soil fractions has adverse relationship with vegetation abundance and rainfall amounts.

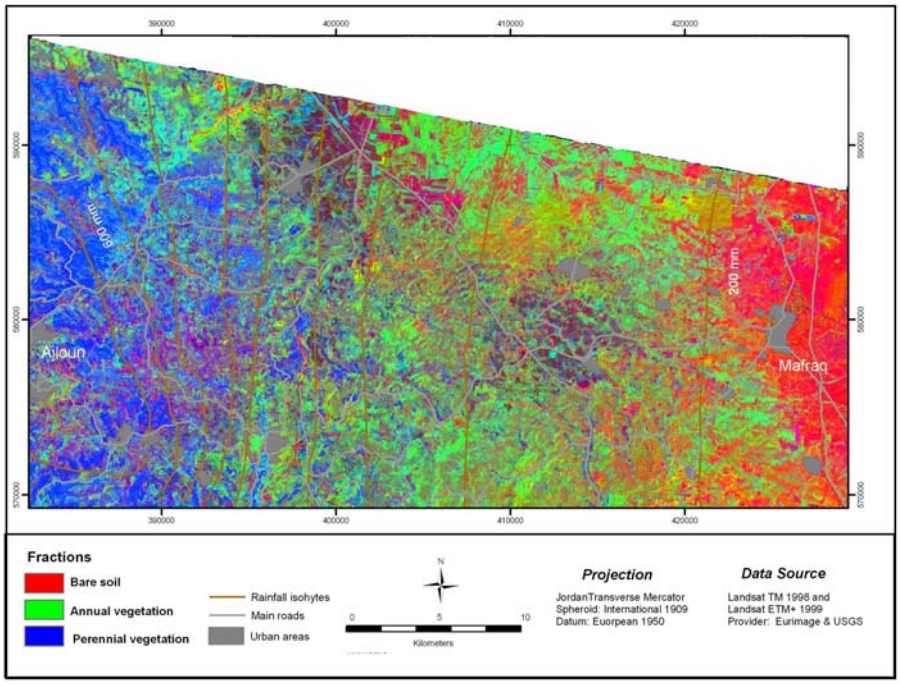


**Figure 4.** Distribution of the perennial vegetation, annual vegetation, and soil fractions in 1998/1999

## 5 DERIVATION OF SENSITIVE AREA FOR DEGRADATION PROCESSES

Analyzing the seasonal dynamics of vegetation cover and soil fractions in an integrated manner could produce reliable estimation for the landscape conditions. In order to prove this proposition, the vegetation conditions were evaluated on a seasonal basis including the maximum and minimum value. Detecting the active landscape processes and rate of seasonal vegetation dynamic were derived by introducing the vegetation ratio concept, which is expressed as the maximum to the minimum vegetation fraction in the growing season.

The minimum vegetation ratio value represents no changes, while the maximum one represents maximum changes in the vegetation. The sensitive areas for land degradation were derived synoptically utilizing the rate of vegetation dynamics, vegetation abundance, and soil fractions layers.

Figure (5) shows the spatial distribution of proposed degradation risk classes derived based on the seasonal rate of vegetation dynamics, vegetation abundances, and fractions of soil types. It is noticeable that 32.3 % of the total study area has almost constant fraction throughout the year with less than 10 % of changes. The dominant land cover is the natural forest and tree crops in the western parts of the study area, while the soil fraction is dominant in the eastern parts, mainly the Aridisols. Accordingly, it can be concluded that the seasonal ecosystem dynamics in the rainfall zones above 500 mm and less than 200 mm precipitation are very negligible.

The second class represents the slight change of vegetation ratio, the spatial distribution of this class is not restricted to a certain rainfall zone, and it comprises mainly rangeland, shrubs, and tree crops with 29.7 %. The third class with a moderate ratio of changes is the cultivated land with 28 %. The highly variable vegetation class represents the field crops; this class covers 10 % of the study area.

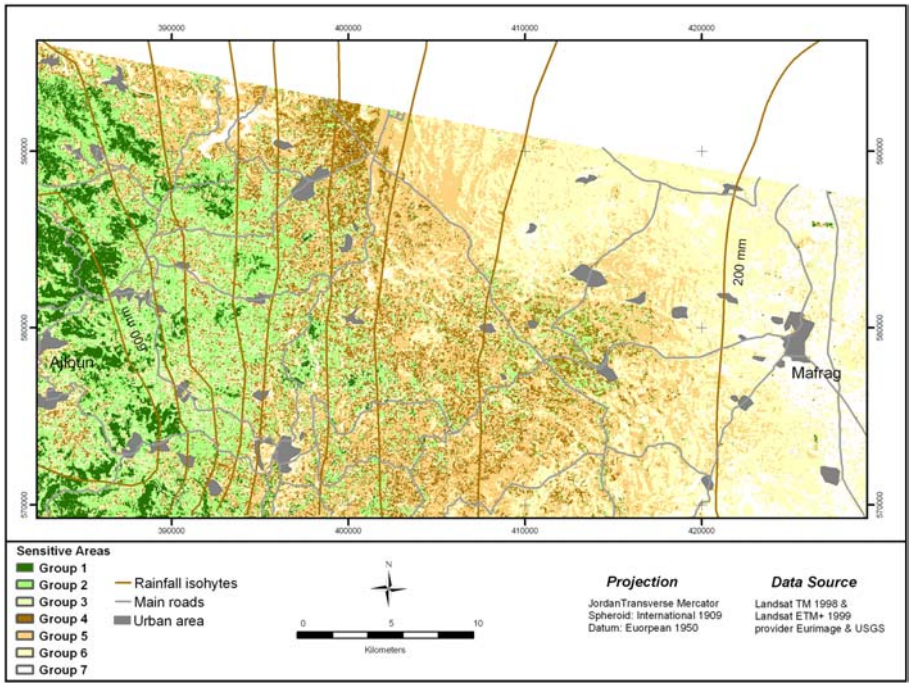


**Figure 5.** Spatial distribution of proposed degradation risk classes derived based on seasonal rate of vegetation dynamics, vegetation abundance and fractions of soil types.

Summary of the major classes are given in table (1), which describe the state of land condition in relation to their vegetation and soil properties.

**Table 1:** Characteristics of the main degradation risk classes based on seasonal rate of vegetation dynamics and fractions of soil types.

| Degradation Risk | Vegetation abundance | Rate of dynamics | Dominant condition |
|---|---|---|---|
| **(G1)** | >= 0.60 | Low | Forest |
| **(G2)** | < 0.60- 0.40 | Slight | Tree crops |
| **(G3)** | < 0.40- 0.20 | Slight | Tree crops |
| **(G5)** | 0.20 – 0.3 | Low/high | Soil-Field crops |
| **(G6)** | < 0.20 | Low/high | Soil-Field crops |
| **(G4)** | < 0.20 | Slight | Soil- Inceptisols |
| **(G7)** | < 0.10 | Low | Soil-Aridisols |

Generally, there are three categories of possible degradation risk that are dominated by vegetation (G1, G2, and G3), soil (G4 and G7) and rate of changes (G5 and G6). Group one (G1) characterized by more than 60 % ground vegetation cover and dominant in the sub-humid rainfall regions and in the western parts of the studied area. The same conditions are applicable also to the Group two (G2), in which the vegetation cover dominates the land condition with different levels depending on the influence of ground vegetation cover. The percentage of vegetation cover in this class ranges between 40-60 %. At the same manner Group three (G3) has ground vegetation cover ranges between 20-40 %. Spatially this class is adjacent to the G2 and dominant in the high rainfall zones.

Group four (G4) is characterized by low vegetation cover and high fractions of Inceptisols. The areal distribution of this group is dominant in the sub-humid rainfall zones. However, the presence of low vegetation cover is explained by the prevailing land use pattern and the farming system in the region. On the other hand, Group seven (G7) characterized by high fractions of Aridisols, this class consists of about 7.6 % and exist mainly under Calcic soils and bed rocks under 200 mm rainfall amounts. The existing of bare soils provides minimum protection for the soil surface against the impact of soil and wind erosion.

Group five (G5) is characterized by vegetation cover range between 20-40 %, the spatial distribution of this class is dominant under the medium 300-400 mm rainfall zone with 22.3 % of the study area and exists mainly under field crops. Group six (G6) is characterized by less than 30 % vegetation cover and high Calcic soil fractions, the spatial distribution of this group consists of 25.6 %; it is dominant in the low rainfall zone below 300 mm and

exists mainly under rainfed field crops and low rangeland density. The existing land use system under groups 5 and 6 provides minimum protection for the soil surface against the impact of soil and wind erosion. The tillage practice at the soil surface is one of the agricultural activities that contribute to the deteriorations of soil physical properties and increase the risk of soil erosion.

## 6 CONCLUSIONS

Total rainfall amounts and variability plays the main role in the distribution of vegetation types and the active landscape processes in the study area. Most of the landscape processes takes place in the rainfall zones between 200 and 500 mm with different rates of dynamics depending on the available soil moisture, soil types, and other factors. Perennial vegetation is dominant in the 450-650 mm rainfall zone, while annual vegetation is dominant in the 250-350 mm rainfall zone. The vegetation abundance in the zone below 200 mm is very low. Quantitative estimation of the vegetation and soil abundance derived from the unmixing approach gives a representative evaluation for the seasonal vegetation conditions and environmentally sensitive areas. Assessment of the land conditions show a general trend of decreasing vegetation quality levels with decreasing rainfall amounts, which is reflected in decreasing percentage of vegetation cover and increasing percentage of Aridisols fractions.

The constant and relatively low dynamic rates are represented by G1, G2, and G3 for vegetation and by G4 and G7 for soils. The vegetation cover decreased gradually from G1 to G3, it consists mainly of perennial natural vegetation and tree crops. However, the main difference between these groups is the seasonal rate of vegetation dynamics, which is constant in G1 and changes slightly in G2 and G3. At the same manner G4 and G7 show constant to slight rate of changes during the growing season and therefore the soil characteristics determine the land conditions level. However, the main seasonal vegetation dynamics occurs under G5 and G6. Different rates of vegetation dynamics exist under those groups, which give an indication for the dominant-limiting factors that affect the vegetation growth and dynamics. These groups represent the highest seasonal dynamics and consequently the most sensitive areas for degradation risk subjected to different anthropogenic factors.

## ACKNOWLEDGMENTS

The Catholic Academic Exchange Service (KAAD) financially supported this work, this is gratefully acknowledged. Special thanks for Prof. Taimeh, University of Jordan, and Dr. Geerken, Yale University, for kindly providing the satellite images.

## REFERENCES

[1] TRIPATHY, G. K., GHOSH, T. K. and SHAH, S. D., 1996: Monitoring of desertification process in Karnataka state of India using multi-temporal remote sensing and ancillary information using GIS. *Int. J. Remote Sens.* 17, pp. 2243-2257.

[2] DWIVEDI, R. S., KUMAR, A. B. AND TEWARI, K. N., 1997: The utility of multi-sensor data for mapping eroded lands. *Int. J. Remote Sens.* 18, pp. 2303-2318.

[3] SCHMIDT, H. AND KARNIELI, A., 2002: Analysis of temporal and spatial patterns in a semi-arid environment observed by NOAA AVHRR imagery and spectral ground measurements. *Int. J. Remote Sens.* 23, pp. 3971-3990.

[4] AL-BAKRI, J. T. AND SULIMAN, A. S., 2004: NDVI response to rainfall in different ecological zones in Jordan. *Int. J. Remote Sens*, 25, pp. 1-17.

[5] MAKHAMREH, Z. AND HILL, J., 2005: Spectral mixture analysis for characterization and of seasonal vegetation dynamics in northern Jordan. I$^{st}$ Göttingen GIS & Remote Sensing Days, Environmental Studies, 7-8 October, Göttingen, Germany, (Göttinger Geographische Abhandlungen, Heft 113).

[6] TUCKER, C. J. AND SELLERS, P. H., 1986: Satellite remote sensing of primary production. *Int. J. Remote Sens,* 7, pp. 1395-1416.

[7] LLOYD, D., 1990: A phenological classification of terrestrial vegetation covers using shortwave vegetation index imagery. *Int. J. Remote Sens.* 11, pp. 2269-2279.

[8] LÜDEKE, M. K. B., KANECEK, A. AND KOHLMAIER, G. H., 199: Modelling the seasonal $CO_2$ uptake by land vegetation using the global vegetation index. Tellus 43B, pp. 188-196.

[9] HLAVAKA, C. A., HARALICK, R. M., CARLYLE, S. M. AND YOKOMA, R., 1980: The discrimination of winter wheat using a growth state signature. *Remote Sensing of Environment.* 9, pp. 277-294.

[10] HILL, J., 1993: High precision land cover mapping and inventory with multi-temporal earth observation satellite data, The Ardèche experiment. PhD Thesis, University of Trier, Germany, EUR 15271 EN, Office for Official Publications of the European Communities, Luxembourg.

[11] PINTY, B. AND VERSTRAETE, M. M., 1992: GEMI: a non-linear index to monitor global vegetation from satellites. *Vegetation*, 101, 15-20.
[12] MÜCHER, A. C., 2000: Land cover characterisation and change detection for environmental monitoring of pan-Europe. . *Int. J. Remote Sens*, 21, 1159-1181.
[13] FUNG, T. AND SIU, W., 2000: Environmental quality and its changes, an analysis using NDVI. *Int. J. Remote Sens*, 21, 1011-1024.
[14] SOBRINO, J.A. AND RAISSOUNI, N., 2000: Toward remote sensing methods for land cover dynamic monitoring: application to Morocco. *Int. J. Remote Sens*, 21, pp. 3535-366.
[15] ADAMS, J.B., SABOL, D.E., KAPOS, V., ALMEIDA, R., FILHO, R., ROBERTS, D.A., SMITH, M.O. AND GILLESPIE, A.R., 1995: Classification of multispectral images based on fractions of endmembers:
[16] SMITH, M.O., USTIN, S.L., ADAMS, J.B. AND GILLESPIE, A.R., 1990: Vegetation in deserts: I. A regional measure of abundance from multispectral images. *Remote Sensing of Environment*. 31, pp. 1-26.
[17] TOMPKINS, S., MUSTARD, J. F., PIETERS, C. M. AND FORSYTH, D. W., 1997: Optimization of endmembers for spectral mixture analysis. *Remote Sensing of Environment*, 59, pp. 472-489.
[18] HILL, J., HOSTERT, P. AND RÖDER, A., 2003: Observation and long-term monitoring of Mediterranean ecosystems with satellite remote sensing and GIS,. *Management of Environmental Quality*, 14, pp. 51-68.
[19] CROSS, A. M., SETTLE, J. J., DRAKE, N. A., PAIVINEN, R. T. M., 1991, Sub-pixel measurement of tropical forest covers using AVHRR data. *Int. J. Remote Sens*, 12, 1119-1129.
[20] ELMORE, A. J., MUSTARD, J. F., MANNING, S. J. AND LOBELL, D. B., 2000: Quantifying vegetation change in semi-arid environments: Precision and accuracy of spectral mixture analysis and the NDVI. *Remote Sensing of Environment*, 73, pp.87-102.
[21] ROBERTS, D. A., GREEN, R. O. AND ADAMS, J. B., 1997: Temporal and spatial patterns in vegetation and atmospheric properties from AVIRIS. *Remote Sensing of Environment*, 62, pp.223-240.
[22] GARCIA, M. AND USTIN, S. L., 2001: Detection of interannual vegetation responses to climatic variability using AVIRIS data in a coastal savannas in California, *IEEE Transactions on Geoscience & Remote Sensing,* 39, pp.1480-1490.
[23] MOA, Ministry of Agriculture, Jordan, 1995: The Soils of Jordan, Report of the National Soil Map and Land Use Project, Undertaken by Ministry of Agriculture, Huntings Technical Services Ltd., and European Commission. Level One, Level Two, Level Three, and JOSCIS Manual.
[24] DOM, Department of Metrology, Jordan, 2000: Statistical Reports of the Rainfall Distribution in Jordan.
[25] USDA (United States Department of Agriculture), 1998: Soil Survey Division Staff: Keys to soil taxonomy, 8th Edition.
[26] REED, B.C., BROWN, J.F., VANDERZEE, D., LOVELAND, T.R., MERCHANT, J.W. AND OHLEN, D.O.,1994: Measuring phenological variability from satellite imagery. *Journal of Vegetation Science.* 5, pp. 703-714.
[27] GRIGNETTI, A., SALVATORI, R., CASACCHIA, R AND MANES, F., 1997: Mediterranean vegetation analysis by multi-temporal satellite sensor data. *Int. J. Remote Sens.* 18, 1307-1318.
[28] HILL, J. AND MEHL, W., 2003: Geo und radiometrische Aufbereitung multi und hyperspektraler Daten zur Erzeugung langjähriger kalibrierter Zeitreihen. *Photogrammetrie Fernerkundung Geoinformation.*1*,* pp. 7-14.
[29] TANRÉ, D., DEROO, C., DUHAUT, P., HERMAN, J. J., PERBOS, J. AND DESCHAMPS, P. Y., 1990: Description of a computer code to simulate the signal in the solar spectrum – the 5S code. *Int. J. Remote Sens. 11,* pp. 659-668.
[30] SETTLE, J.J. AND DRAKE, N.A., 1993: Linear mixing and the estimation of ground cover proportions. *Int. J. Remote Sens.. 14,* pp. 1159-1177.
[31] BOARDMAN, J.W., KRUSE, F.A. AND GREEN, R.O., 1995: Mapping target signatures via partial unmixing of AVIRIS data. *Proc. of the 5th Annual JPL Airborne Earth Sciences Workshop, Pasadena,* 1, pp. 23-26.
[32] ABDELHAMID, G., 1995: Geology of Jarash and Mafraq area, 1:50,000 Geological Map. National Resources Authority, Geology Directorate, Amman, Jordan.
[33] ADAMS, J.B., SMITH, M.O. AND GILLESPIE, A.R., 1993: Imaging Spectroscopy: Interpretation Based on Spectral Mixture Analysis, In: Pieters, C.M. and Englert, P. (eds.): Remote Geochemical Analysis: Elemental and Mineralogical Composition Cambridge University Press.

# Application of Remote Sensing and Geographical Information Systems to Monitoring and management of Maâmora Forest in North West, Morocco

M. Mansour[a] and H. Hafdaoui[a]

[a] Institut National d'Aménagement et d'Urbanisme. Av. Allal Fassi. Rabat-Instituts. Rabat. Morocco. Tel +212 37 77 16 24 / Fax: +212 37 77 50 09. email:majidmansour@hotmail.com

## ABSTRACT

The main object of this study is to develop reliable method for integration of remote sensing system and the GIS for investigating and monitoring of Maâmora forest. Covering about 150000 Ha, lies along the Atlantic coast in the west, between Rabat and Kénitra, contains holm oak, cork oaks, eucalyptus, acacia, pines, pear trees, etc. The multi-dates study of Maâmora Forest from SPOT images and additional data (plot plan, existing documents) were collated and fed into a GIS. The changing forest situation as degradation, felling and reforestation was mapped by applying the supervised classification of the SPOT multispectral images of 1991 and 2001.

**Keywords:** monitoring, deforestation, drought, cork oak, GIS, satellite images

## 1 INTRODUCTION

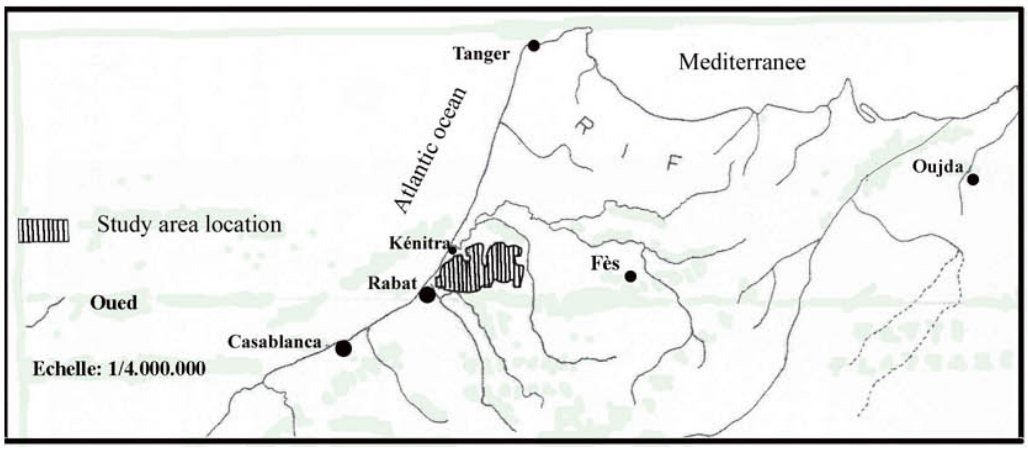


**Figure 1.** Study area location.

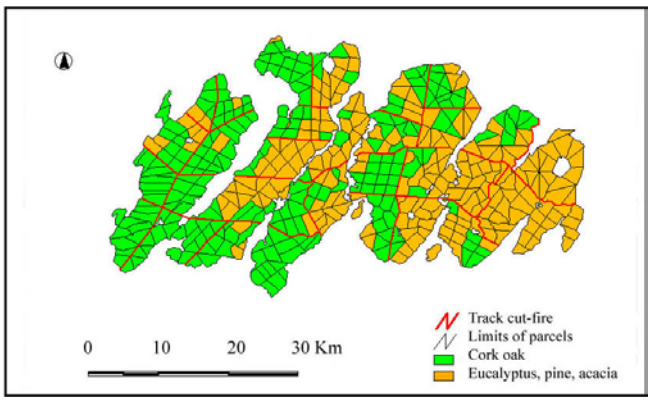


**Figure 2.** Native species (cork oak) and introduced species (Eucalyptus, Pine, Accacia).

Maâmora forest, situated along the Atlantic coast to the North West of Morocco (Fig. 1), lies between 6° and 6° 45 ' of west longitude, 34° and 34° 20 ' of North latitude. Delimited in 1917-1919. The total area is, about 134.000 Ha. It is made up of a native species, cork oak and introduced species, eucalyptus, pine, acacia (Fig. 2). The forest is divided into five cantons, 33 groups and 460 forest plots (Fig. 3). A study was conducted on the changing state of Maâmora Forest, using remote sensing techniques and GIS, to supplement the static data and improve its management. Maâmora forest constitutes one of the biggest cork oak plain in the world. In spite of this important reserve, it's surface knew during these last four decades a reduction of 40%, covering about 102.000Ha in 1951 and

only 60.000Ha in 1992 [1]. Various factors contribute to widespread natural resource degradation in areas of Maâmora [2]: climatic variation, increasing population density, economic pressures and overexploitation of forests. The law of 1976 on the local collectivities, had assigned in communes the forest product merchandising. Only, they have the obligation in counterpart to reinvest 20% of these returns to the safeguard and surveillance of forests. The crossing of township limits with the forest space of the Maâmora, (Fig. 4 and Table 2) demonstrates the part of each township in forest resources.

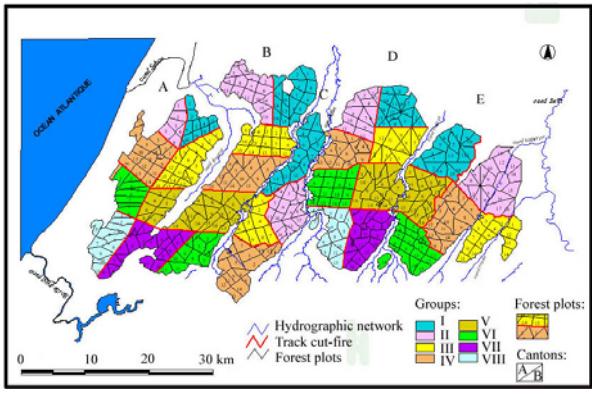


**Figure 3.** Maamora forest is divided into 4 cantons (A, B, C, D), 33 groups and 460 forest plots.

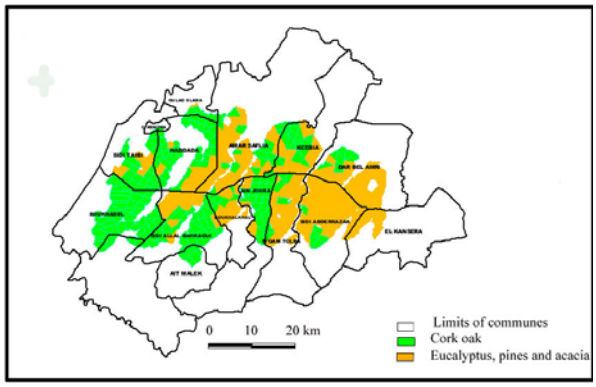


**Figure 4.** The crossing of communes limits and the forest space of the Maamora**.**

**Table 2.** Maamora communes and forest resources.

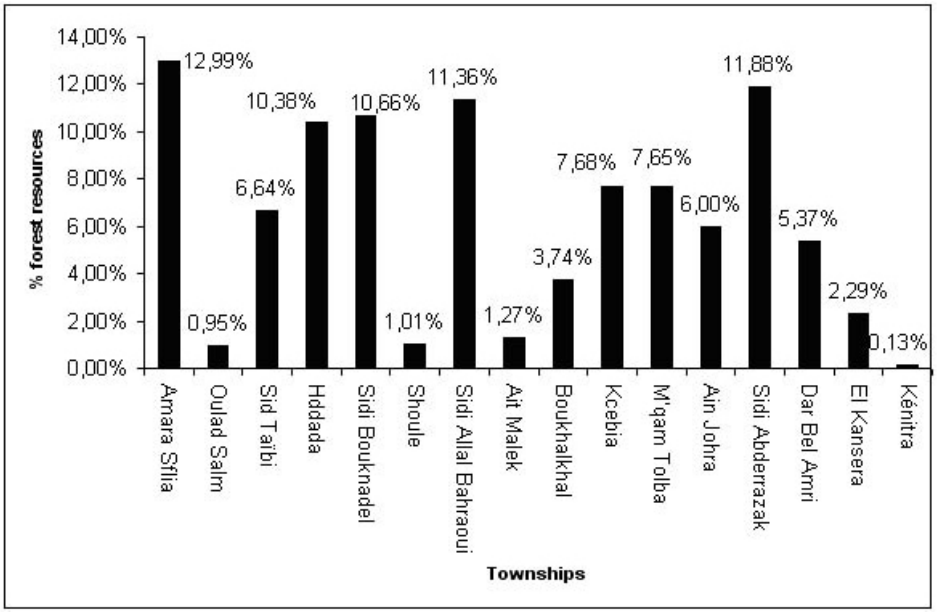


## 2 MATERIALS AND METHODS

**Table 2**. Images specifications

| Image | Date of acquisition | Wavelength | Spatial resolution |
|---|---|---|---|
| **SPOT-XS** | 27-07-1991<br>12-06-2001 | 1) 0.50-0.59 m<br>2) 0.61-0.68 m<br>3) 0.79-0.89 m | 20 m |

### 2.1 Remote sensing data

Data acquired by optic remote sensing systems were used in the study. The specifications are summarized in Table 2.

### 2.2 Method

The methodology developed has led to the implementation of a GIS-based forest monitoring system that will be entirely

operational once all the conventional data have been digitized and integrated (plot plan, topographic map, map of types of stand, management operations). The database can be updated on a regular basis depending on the scale and frequency of change in the forestry environment (Fig 5).

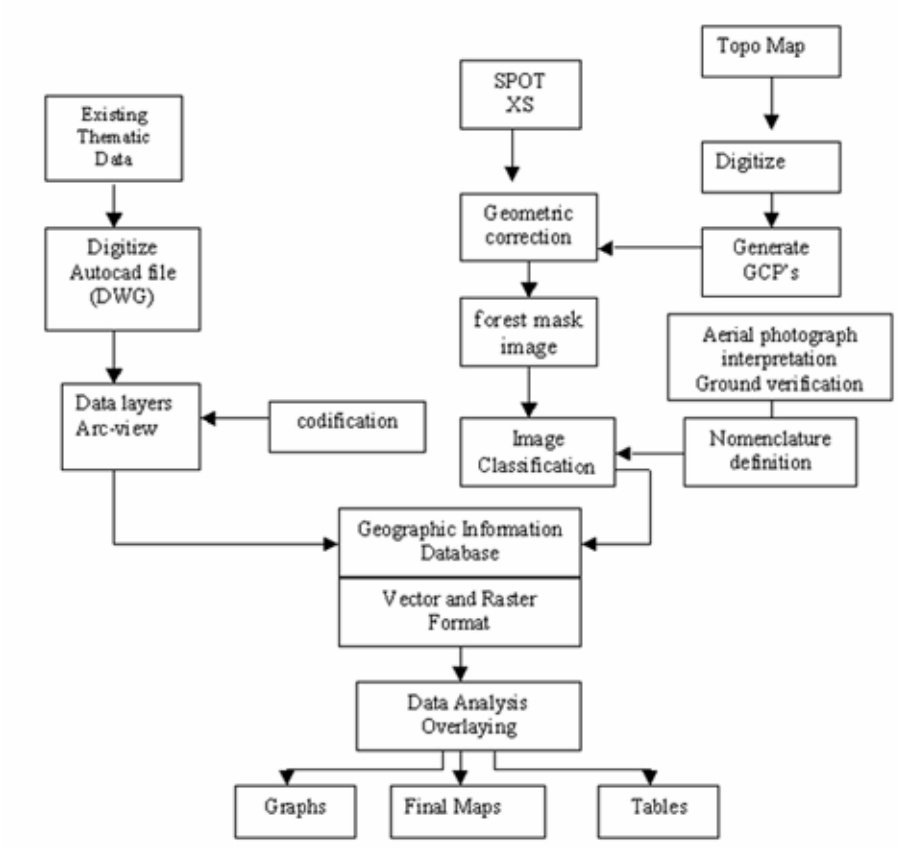


**Figure 5.** Schematic flowchart of the applied method in this study.

## 3 RESULTS AND DISCUSSIONS

Results of this research show that it possible to monitor Maâmora forest with a reasonable accuracy using optical satellite images. The spectral information can be connected with precision to change in the physiology of the forest vegetation. We have tested this approach, with some limited success when classifying eucalyptus species and the dense cork oak. These values vary for the same unit according to their density.

The changing forest situation was mapped by applying the differences method and by supervised classification of the SPOT multispectral images of 1991 and 2001 (Fig 6 and 7). The results of this multi-dates study and existing data (plot plan, topography, etc.) were collated and fed into a GIS. The degradation of the cork oak has been appraised to 0,8%, corresponding to a loss of 234 Ha / year (Table 3). During period of 1991 to 2001, about 2220 Ha of pines and acacia forest disappeared and changed to another land uses. Areas forested in eucalyptus increased during de same period about 3460 Ha. This increase is a detriment of a native species, cork oak.

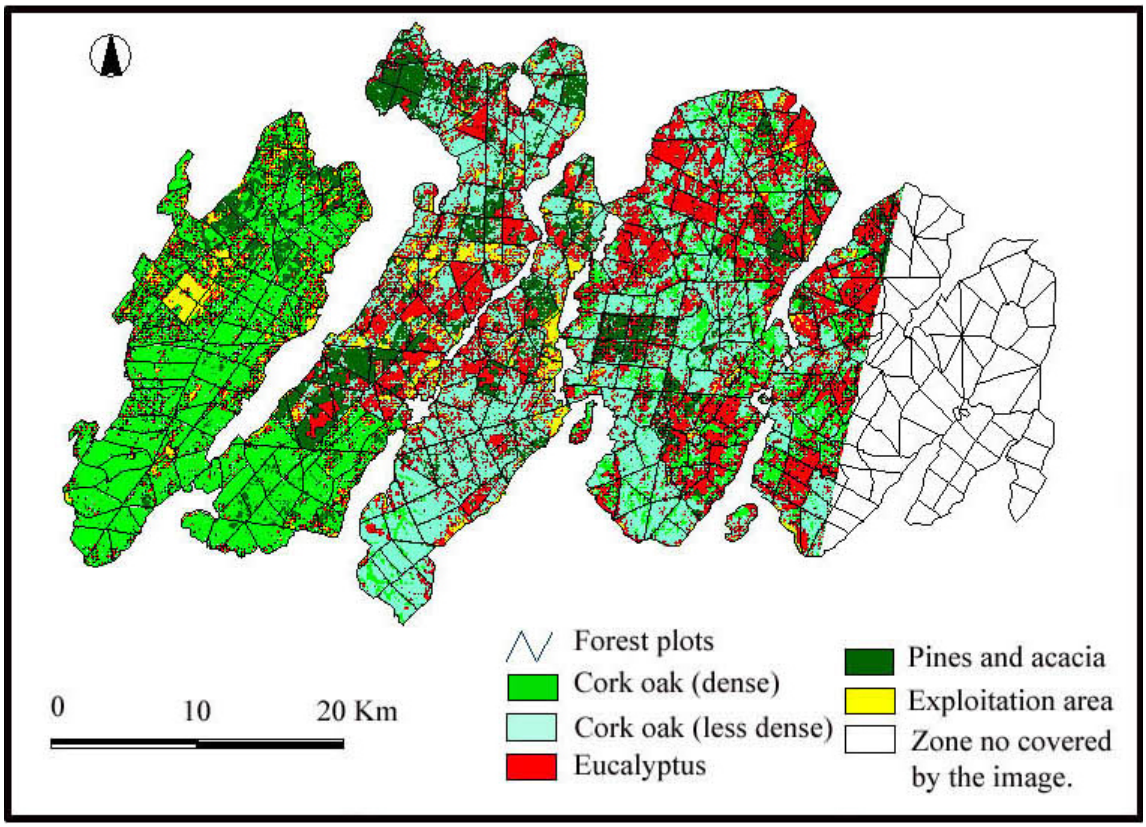


**Figure 6.** Classification of image 1991.

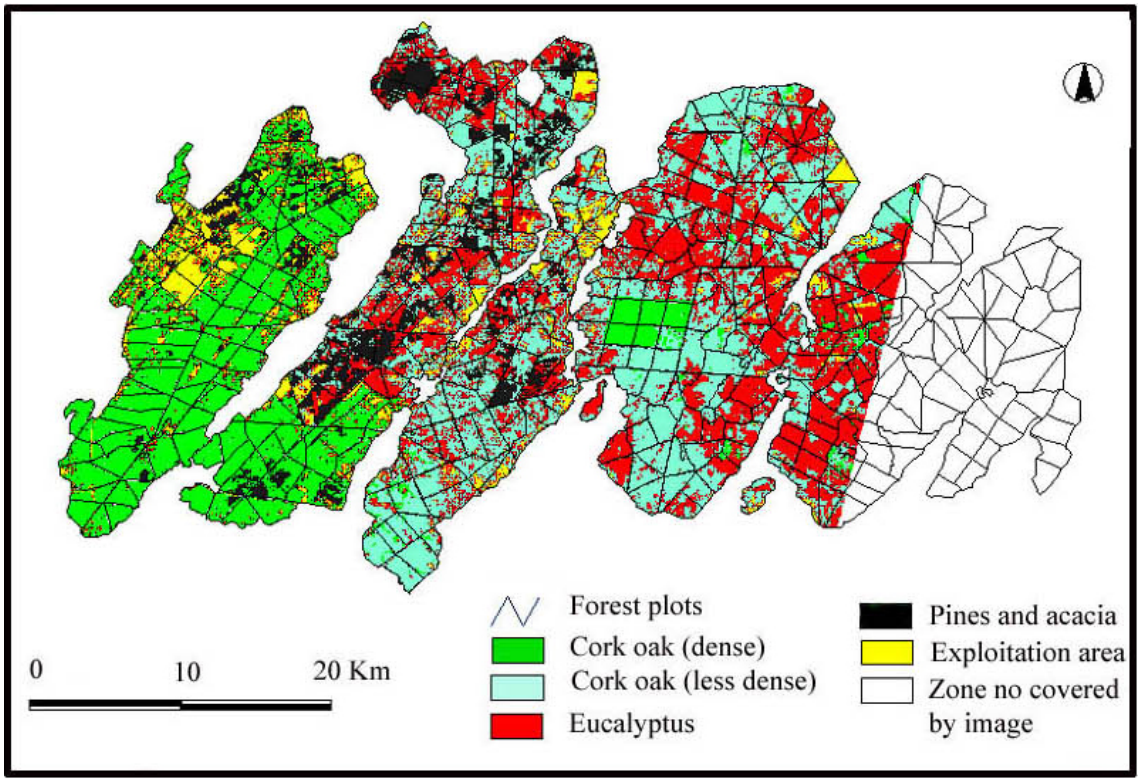


**Figure 7.** Classification of image 2001.

The difference of multispectral images, 1991 and 2001, demonstrates the main changes occurred on 10 years (Fig. 8).

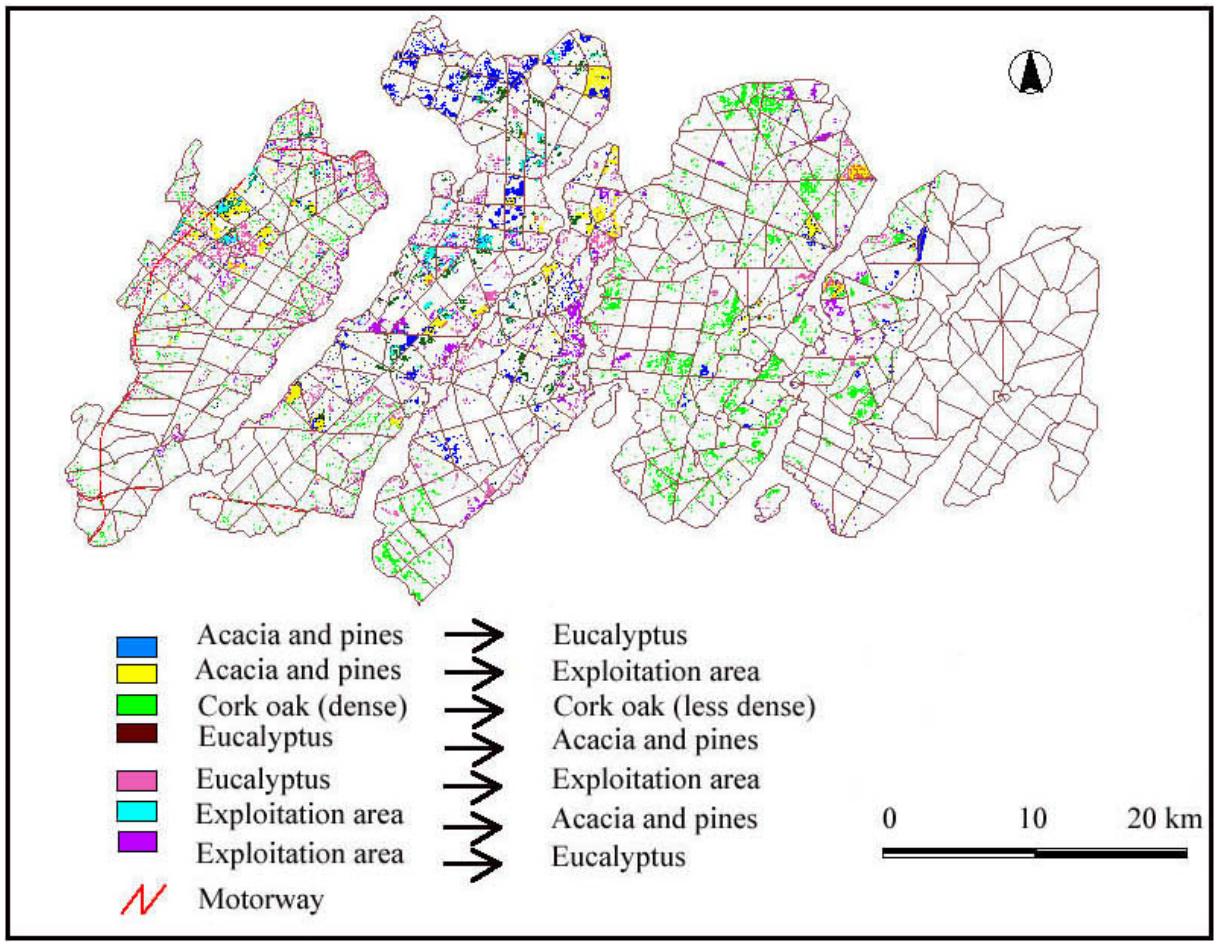


**Figure 8.** The difference of multispectral images, 1991 and 2001, illustrates the changes occurred during 10 years.

This regression of cork oak is essentially owed to a mortality following the conjugated action of the prolonged drought, human induced events, and absent of natural regeneration. In fact, it's necessary to participate the local population while permitting them to benefit, under control, of the exploitation of forest products.

**Table 3.** Changes in Maâmora forest from 1991 to 2001

| Class | Classification Image 1991 | Classification Image 2001 | Variation % | Variation Ha |
|---|---|---|---|---|
| **Cork oak (dense)** | 25 962 Ha | 24 093 Ha | -7,20 | -1870 |
| **Cork oak (less dense)** | 40 329 Ha | 39 857 Ha | -1,17 | -470 |
| **Eucalyptus** | 25 501 Ha | 28 960 Ha | +13,56 | +3460 |
| **Pines and acacia** | 12 657 Ha | 10 437 Ha | -17,54 | -2220 |
| **Exploitation area** | 5831 Ha | 7355 Ha | +26,14 | +1520 |

## 4 CONCLUSION

The use and management of forest resources need to be based on the mapping and inventory of forestry environment. Remote sensing and geographic information systems provide for the continuous monitoring of forest developments by detecting changes and for the integration of the results into existing databases. The operational availability of high-resolution satellite imagery opens up large possibilities for investigating and monitoring forest

resources. Compared with information acquired by traditional methods. The study was conducted on the changing state of Maâmora Forest; using Remote sensing technique and GIS improve its management. The changing forest situation (degradation, reforestation) was mapped by applying the difference method and by supervised classification of the SPOT multispectral images of 1991 and 2001 during a ten years interval. The multidates use of satellite imagery has provided access to synoptic and up to date information for mapping, illustration and modelling of natural and human-induced events, such as degradation, reforestation and exploitation. This technique helps decision making for the enhanced management and development of forest resources. The database can be updated on a regular basis depending on the scale and frequency of change in the forestry environment.

## ACKNOWLEDGMENTS

We would like to thank the mixed commission UNESCO/ ISESCO in Rabat for their financial support to this research.

## REFERENCES

[1] DIAGANA, M. (1997):Contribution to the survey of sensitivity and impacts of factors anthropic and forest management on the deterioration and the desertification of the forest of Maâmora. Memory of master, ENFI. Salé, 122p.

[2] HARRACHI, K. (2000): Investigating on reasons of deperissement of the cork oak (*Quercus L. suber*) in the forest of the Maâmora. Thesis of University George August, Götting, Germany. 130P.

# Application of Remote Sensing and GIS to Assess Continuous Land Cover Changes in Forestlands of the Southwest Ethiopia

B. S. Muzein[a] and E. Csaplovics[a]

[a]Technische Universität Dresden,
email: bedru.sherefa-muzein@mailbox.tu-dresden.de, csaplovi@rcs.urz.tu-dresden.de

## ABSTRACT

Footprints of forest degradation and deforestation that are induced by activities of human being are investigated via spatio-temporal land cover change analysis. Policy and decision makers need to be provided with accurate, timely and simple information that shows the rate, extent and trend of major land cover change processes. This is especially urgent for countries where desertification is encroaching and land degradation is making the livelihood of local farmers hard, because such detrimental processes are usually stimulated by the very economic policy it was meant to alleviate poverty. Through classification of three period satellite images and simple overlay analysis that made use of expert contextual pixel editing, the detrimental effect of policy on the forest base of southwest Ethiopia is shown. In order to generate proper legends that are meaningful and easily distinguishable, a variety of raster variables like DEM, Percent Vegetation Cover (PVC), temperature, rainfall, and soils were used in addition to the satellite images. Classified maps of each year were superimposed with each other. The pixels of combinations of three-period classified maps were expert edited to generate series of change process maps. Up to 20% of the total land was found to suffer permanent deforestation or degradation, while only 1 in 40 cases exhibited a successful rehabilitation, natural succession or restoration in the 28 years period.

**Keywords: Ethiopia**, deforestation, degradation, land cover, change process.

## 1 INTRODUCTION

### 1.1 Background

The change of states from one form to another is a natural phenomenon to both biotic and abiotic components of our planet. The duration of the episode is, however, quite relative and varies from one entity to another. In the absence of excessive human interference, natural forest of tropical region exhibit little conspicuous change in short period of time, if they do at all in spatial terms. As a quick fix to recurring food shortage in the highlands of Ethiopia, a huge government sponsored resettlement programme was introduced in the 1980s around the forestlands of southwest Ethiopia. The same area had been the subject of large-scale state coffee plantations establishment. Such national economic policy driven interventions altered the ages old agricultural practices in the area and detrimental land cover changes have taken form. The changes themselves are dynamic in nature that begs a close scrutiny.

### 1.2 Remote sensing of degradation process

In order to mitigate the degradation of natural resources and harness expansion of desertification, the presence of timely and reliable information on the change dynamics of the natural features is indispensable. There exists a demand for such information probably since human being has started worrying about natural resources. The type of information required and the supplying technique, accordingly evolved through time to present days. The ever-growing availability of satellite driven data provides ample opportunities to properly assess and understand the continuous change process. However, our current technical and institutional capacity to make use of most of the available remote sensing information is not only very limited [12], [15] but also fall short of the requirement for proper analysis and presentation of long term continuous processes [11], [14]. Illustration of land cover dynamics is usually limited to animation in electronic medias, virtual reality or reduced to comparing two period data without indicating what is going on in between. A method of expert contextual editing of land cover change attributes to come with simple and comprehendible output is suggested in this paper in order to make such information available and easily understandable to decision makers who may be lay persons to the GIS world.

### 1.3 History of forest cover change assessment in Ethiopia

Even though arguments run around its reliability [13], it is widely believed that by the turn of the last century, 40% of the country had been covered by high forest formations before it dwindled to the current 2-3% coverage [1], [3] and [5]. The present remnant climax high forest trees in the compounds of churches and cemeteries, where they are

usually kept growing, probably signifies that such a high forest indeed covered a substantial portion of the nation. Even in terribly degraded and highly rugged landscapes of the northern highland, where desertification is on the verge of taking over, one can find such living evidences. Reliable and accurate information about the forestland condition of Ethiopia are scarce and usually very hard to find. Forest Resources Assessment 2000 [8] estimated that the 1997 forest cover of Ethiopia was 4.2%. A decade ago, in the same series of the study, Forest Resources Assessment 1990, [7] presented a tabulated output that indicated the 1989 forest cover to be around 12.9%! There is again a huge disparity in the estimation of the available forest cover as well as the rate of deforestation between national and international studies. According to [6] and the Conservation Strategy of Ethiopia [9] estimates the annual rate of deforestation in the range of 150000 and 200000 hectares. The regional forest action program of the Southern Nations and Nationalities People Regional State [16] broadens the range to be 80000 to 200000 hectares. Such an estimate may entertain a certain amount of exaggeration to alert the public or in order to get attention from the government. Something that cannot be ruled out, though, is the inability to clearly estimate the change due to technical difficulties or organizational inconveniency. The decadal studies of forest assessment by the FAO [7] and [8] put the estimate of deforestation to be 38600 and 40000 hectares of natural forest per year respectively.

### 1.4 The Study Area

The study region is situated in th southwest of Ethiopia, in the Bench-Maji and the Sheka Zones, around the border with the Sudan. The specific study area is located within the distance range of 550-600 km from the capital Addis Ababa covering an area of nearly 4900 km². The geographic coordinates of the center of the study area is 35°19'39"E, 7°07'46" with an elevation range of 600-2700 m.a.s.l, mean annual average T° range of 14 to 28°C and an average rainfall of 900-2650 mm/year.

The area is part of the only known wild coffee gene pool in the world.

## 2 OBJECTIVE

The main objectives are:

- Mapping deforestation and forest degradation processes in time and space.
- Identifying the many responsible factors in degradation processes and quantifying the impact of each agent across time.
- Providing clues pertaining the restoration potential of degraded and deforested lands by showing the permanency or temporal nature of degradation footprints.

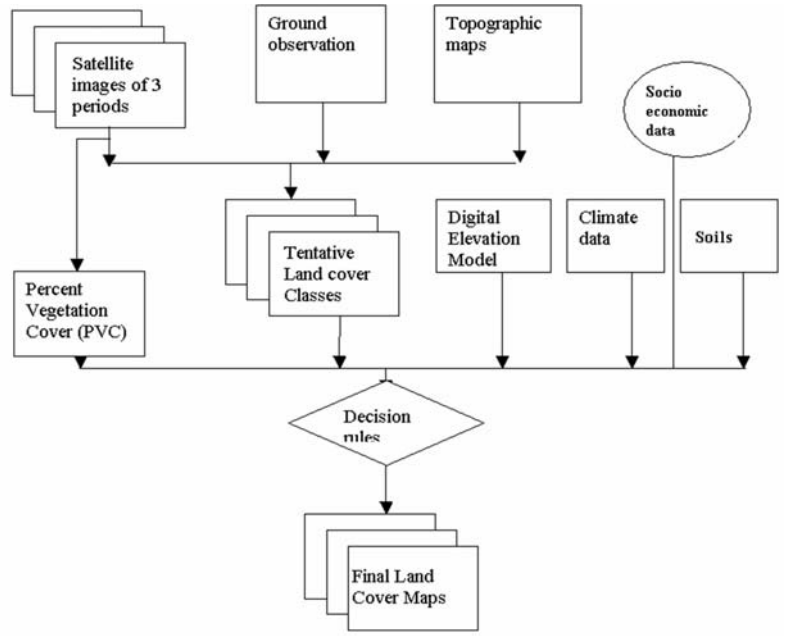


**Figure 1.** Flow chart of single period land cover classification.

## 3 MATERIALS AND METHODS

### 3.1 Land cover classification

The study period ranges from 1973 to 2001. In addition to these 'Start and End' periods, satellite image of a third intermediate period, namely 1987, were procured for this study. It would be impossible to see the change dynamics by using only the two period images.

After routine geometric correction and radiometric enhancement tasks, the recent image was thematically classified in order to generate a sampling guide map [4]. Using this map, sufficient number of ground verification points was randomly distributed. Around Two hundred forty six samples plots, each with size of 3 pixels by 3 pixel ETM+ images, were actually accessed and necessary data for signature generation were collected. A land cover class was

assigned to each set of spectral signature under the Maximum Likelihood image classification algorithm in ERDAS IMAGEN. This supervised classification resulted in land cover classes that were categorized solely on spectral information of the image. In fact the essence of remote sensing seldom transcends beyond such results. However, this result was considered only as tentative land cover class in our case because additional further discrimination of classes based on non-spectral information was found out to be crucial to capture all heterogeneity in the landscape. To this end, a Rule Based Decision Tree Classification scheme was employed to further separate the tentative land cover classes. First a Knowledge base was built upon the interrelationships of raster variables like: Shuttle Radar Topographic Mission (SRTM) generated Digital Elevation Model; fraction of Pixel Vegetation Cover [2], soils, Inverse Distance Weight interpolated rainfall and temperature. Decision rules that had been built based on observations; interviews and literatures were given to the classifier. For example, the classifier determined a 'coffee' forest class by identifying forest areas that fulfilled the edaphic and climatic requirements for coffee plant occurrence [17]. Sets of final land cover classes were developed for each period as final result.

## 3.2 Definition of land cover classes

Land cover classes were categorized according to the material the land was covered with during the time of image capturing. Some land use elements that reflects the economic use of the land were used to make further thematic separation that was deemed useful for this study.

### 3.2.1 Forests:

a. Evergreen monatne forest: Evergreen forests situated above 2000 m.a.s.l and not suitable for coffee growth.

b. Evergreen forest with coffee understory (coffee forest): Evergreen forests situated below 000 m.a.s.l and within area suitable for coffee growth.

c. Semi-deciduous lowland forest: Evergreen and deciduous forests situated below 2000 m.a.s.l and not suitable for coffee growth.

d. Combretum Terminalia woodland: Lowland forest dominated by combretum and terminalia species.

### 3.2.2 Agriculture

a. Cultivated land and human settlement: area identified as cultivation lands with no or very little inclusion of tree patches and human settlement areas.

b. Agroforestry oriented household farms: predominantly agriculture area with significant amount of tree patches. The tree patches are mostly leftovers of forest fragmentation rather than deliberate planting of trees as the term agroforestry literally means.

c. Agropastoral dominated household farms: agriculture areas with vast pasture areas.

### 3.2.3 Others

a. Large scale coffee plantations: spatially contagious vast areas assigned solely for coffee plantation.

b. Wooded savannah: savannah land with noticeable tree inclusions.

c. Lowland grassland: grasslands in lower areas where pastoralism is not practiced because of cattle diseases.

d. Intermittent highland bogs: impassable marshes and bogs at high altitudes.

e. Water bodies: lakes and dams.

## 3.3 The change dynamics

Land cover changes from 1973 to 1987, 1987 to 2001 and finally 1973 to 2001 were determined based on previous and contemporary land classes values and separate 'change' maps were produces. Then change dynamics was further evaluated by combining the change value of the 'change' map 1973-1987 and 1987-2001. When trying to depict long-term change processes in a single snapshot, each analysis or visualising unit (pixel, grid cell or vector polygon) represents the value of a function of one of the combination of land cover classes over time. Usually the numbers of combinations are very high when data from several period of time are used. The amount of possible combinations or alternatives are given as:

$$C = \prod_{1}^{p} Np,$$

where C is the possible number of Land cover class combinations, Π is multiplication and

N is number of land cover classes in a given Period (p).

If N is the same in all periods then,

$$C = N^p \quad .$$

With an increase in p, N grows exponentially. A subjective contextual editing based on actual ground information and expert knowledge brings C into manageable number of classes that can be reasonably visualized and interpreted.

There were 1728 combinations of classes in the first output of the change dynamics analysis. However, they were summarized and only 15 meaningful legends were derived from all these combinations. The legends represent the change dynamics classes that show not only the process involved but also the nature of permanency of those classes.

Average annual rates of change in land cover extent or areas affected by a certain land cover change process are calculate as

$$r = \frac{\ln\left(\frac{p1}{p2}\right)}{t},$$

where ***r*** is the average annual rate, ***p1*** and ***p2*** are land cover magnitudes in period 1 and 2 respectively and ***t*** is the time span in number of years.

## 4. RESULTS AND DISCUSSION

### 4.1 Area, proportion of land cover classes and rate of changes through time

The first straightforward results of the image classification were extent and location of each land use class. Differences in spatial coverage of the classes were determined through overlay analysis of two thematic maps at a time. Annual average rate of change is calculated for each pair of images; see table 1. Negative values represent a decreasing trend in size while the positive ones are an increase trend.

Expansion of cultivation agriculture and settlement, which often go together, was found out to be the fastest growing trend in the first period as settlement programs were vigorously implemented in mid 80 after the notorious

**Table 1.** Size of land cover classes and their annual average rate of changes.

| | Area (hectares) | | | Annual Average Change Rate (%) | | |
|---|---|---|---|---|---|---|
| | **Y1973** | **Y1987** | **Y2001** | **1973-1987** | **1987-2001** | **1973-2001** |
| **Cultivated land and Human Settlement** | 14316.31 | 66329.23 | 72420.42 | 10.95 | 0.63 | 5.79 |
| **Intermittent Highland Bogs** | 1020.27 | 1765.75 | 2566.63 | 3.92 | 2.67 | 3.29 |
| **Wooded Savannah** | 18544.40 | 23578.81 | 34882.24 | 1.72 | 2.80 | 2.26 |
| **Large Scale Coffee Plantations** | 0.00 | 9921.96 | 18163.62 | 0.00 | 4.32 | |
| **Agroforestry Oriented Household Farms** | 85757.44 | 85508.73 | 71646.78 | -0.02 | -1.26 | -0.64 |
| **Evergreen Montane Forest** | 56533.49 | 50959.10 | 44235.30 | -0.74 | -1.01 | -0.88 |
| **Semi-Deciduous Lowland Forest** | 83086.60 | 74511.67 | 69806.06 | -0.78 | -0.47 | -0.62 |
| **Evergreen Forest with Coffee Understory** | 192214.74 | 161091.19 | 142875.18 | -1.26 | -0.86 | -1.06 |
| **Water Bodies** | 178.37 | 147.42 | 188.20 | -1.36 | 1.74 | 0.19 |
| **Combretum Terminalia Woodland** | 23889.41 | 11721.82 | 11512.58 | -5.09 | -0.13 | -2.61 |
| **Agropastoral Dominant Household Farms** | 13533.87 | 3539.22 | 20777.76 | -9.58 | 12.64 | 1.53 |

drought that took the lives hundreds of thousands of people in the country. In the second period, this trend decreased dramatically, since there were continuous abandonments of such areas. Perhaps the increase in agropastoral-dominated household farming in the second period has a direct connotation to it. However, it was still the cultivation agriculture, which was the result of an abrupt influx of people that was found to show a high overall growing rate. Forests that harbor coffee and the terminalia combretum wood area had experienced a remarkable

decline in the first period before the montane evergreen forest took that role due to degradation that was induced by selective logging of high value trees.

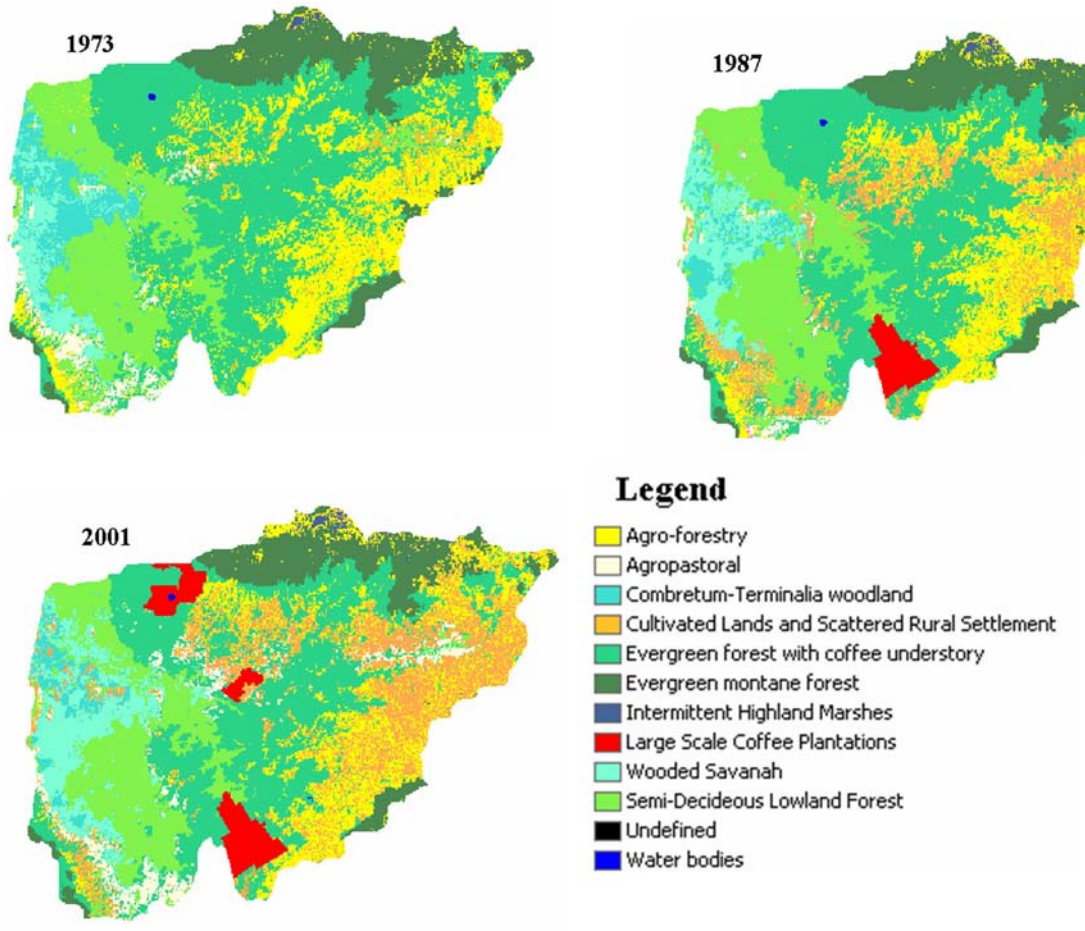


**Figure 2.** Spatial location of land cover classes.

## 4.2 Spatial coverage and temporal rate of land cover change processes

The terms 'amelioration' and 'rehabilitation' are used to express the improvement of forest classes through restoration and healing of forest classes respectively. Spatially distinct areas for each designated change process were measured after attributes of the output of the overlay analysis were contextually summarized. This task requires good understanding of the ground situation and history of the area in order to assign a change process value to each combination of land cover classes. For example, if part of a grassland class is converted to combretum woodland, this changed part of the polygon or aggregate of pixels would be assigned restoration or amelioration. The same reasoning goes for deforestation and forest degradation based on severity of the negative impact. The modification of an agroforestry like field into agriculture is considered degradation. Table 2 shows the size of the area affected by each land cover change process, while Figure 3 illustrates the spatial

**Table 2**. Major land cover change processes and the impacted area.

| | 1973-1987 | 1987-01 | 1973-2001 |
|---|---|---|---|
| **Amelioration** | 13157.23 | 19723.4 | 9560 |
| **Deforestation** | 34661.39 | 20386.3 | 55770 |
| **Degradation** | 68004.49 | 62574.8 | 86891 |
| **Rehabilitation** | 15953 | 18987.6 | 18912 |
| **Undefined/Unexplained** | 828.495 | 1015.9 | 1620 |
| **Modification/minimum change** | 12525.06 | 17666.7 | 9401 |
| **No detectable process** | 343945.2 | 348666.2 | 306942.9 |

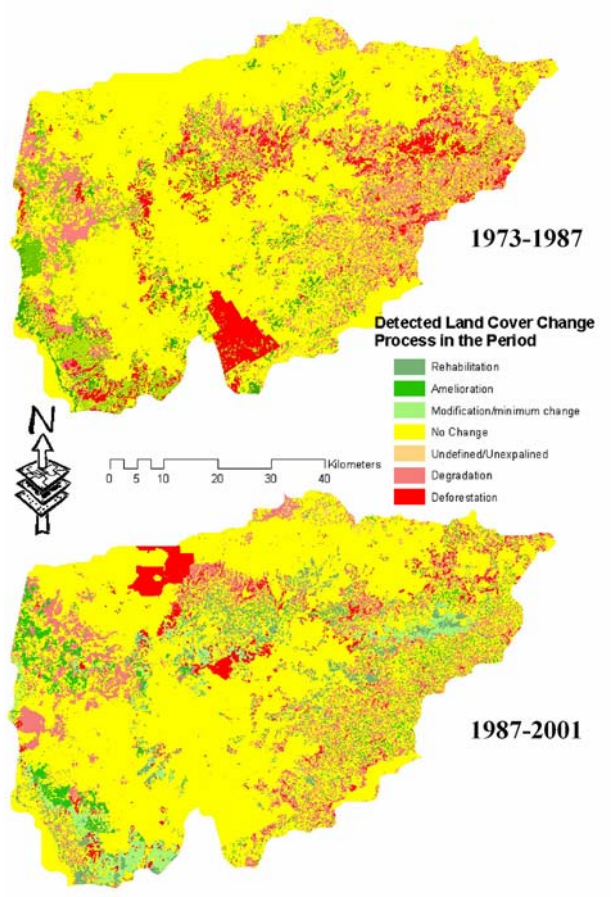


**Figure 3.** Spatial location of land cover change processes.

location where each process had taken place.

Table 2 depicts the complexity of change processes in the study area. The figure shown as the amount of land that went through a certain change process through the whole period of time has little direct correspondence with values of the first period and second period. A rehabilitating area in the first period might have experienced a complete degradation or other process. In the other section of this paper the permanency of this processes is shown. The improvement, both amelioration and rehabilitation, in natural resources condition appears to be in good shape when one looks the short term trend. A natural succession of open field into forest classes was also included in this category. However, degradation was found to be affecting a lion's share of the total area in the long term time span.

### 4.3 Major agents of deforestation and forest resources degradation process

Human related activities are known to play the greatest role in the conversion and modification of forest related resources [10]. As demonstrated elsewhere in this paper, the same had been found to be true in the study area. Government sponsored settlement programme was immediately followed by spontaneous settlement. The latter was also driven by the establishment of large-scale coffee plantations, which themselves are responsible for up to 32% of the permanent deforestation or for 1/5 of the total permanent negative consequences.

**Table 3.** Cause of deforestation and degradation (from forest classes of higher class to lower forest class or non forest classes) in Hectares.

| | **1973-1987** | **1987-2001** |
|---|---|---|
| **Agroforestry Oriented Household Farm expansion** | 30122.7 | 18679.2 |
| **Agropastoral Dominant Household Farm expansion** | 1435 | 4571.1 |
| **Degradation of semi-deciduous forests to sparse Combretum Terminalia Woodland** | 132 | 1034 |
| **Expansion of Cultivation land and Human Settlement** | 48791.5 | 35917 |
| **Large Scale Coffee Plantations establishment** | 9165.3 | 7676.6 |
| **Grassland expansion** | 13015.7 | 15081.9 |

### 4.4 Visualising time-stamped land cover change map

Little would have been observed if only the 'Start and End' period image were analysed. The used of additional intermediate images is technically feasible. The challenge comes during an attempt to visualise the result of all. As has been described elsewhere in this paper, a series of contextual editing was performed to summarize the long list of combinations and bring them to manageable size for visualization. Processes that persist in both periods, i.e for the whole 28 years, were tagged as permanent activities. Other activities were grouped together according to their

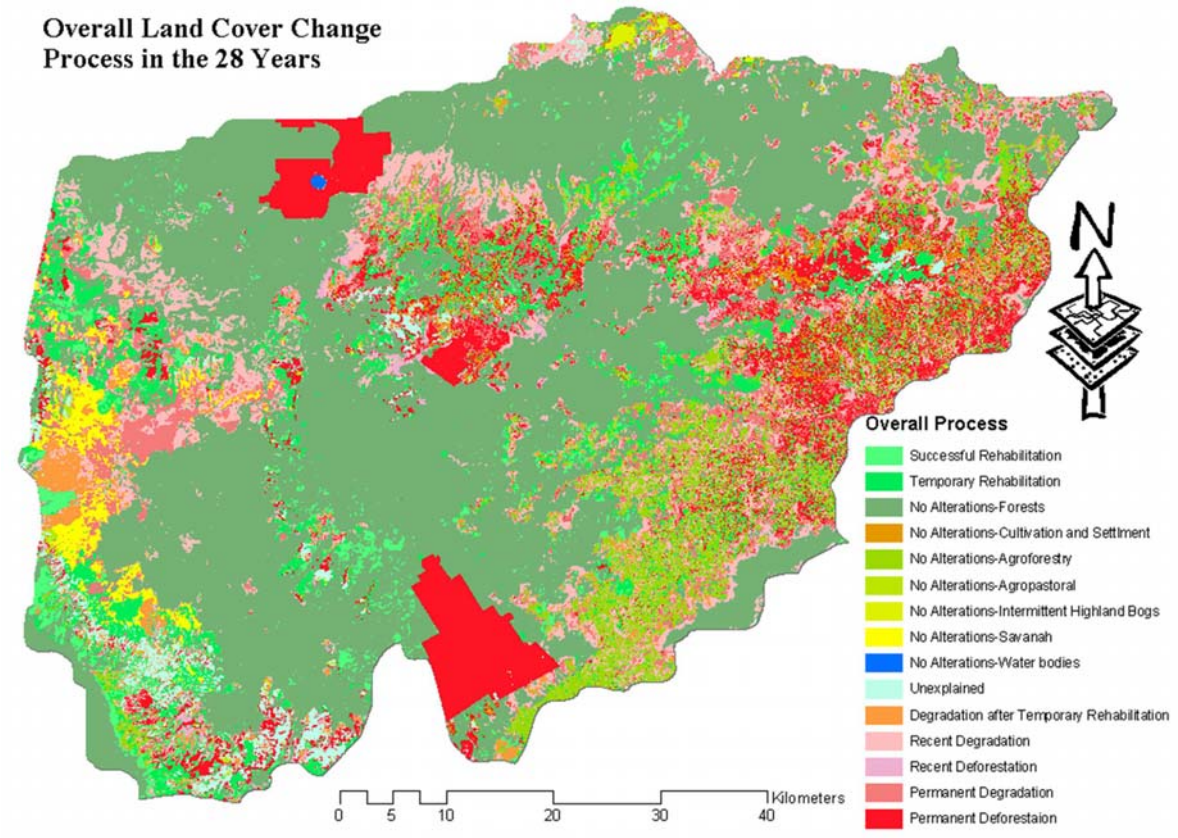


**Figure 4.** Temporal nature of land cover change processes and spatial extent of time tagged land cover change processes.

**Table 4.** Size and proportion of impacted area

| Overall Change Process | Area in Hectars | % of Total |
|---|---|---|
| **No Alterations-Forest** | 230497.43 | 47.13 |
| **Permanent Deforestaion** | 52633.30 | 10.76 |
| **Recent Degradation** | 49749.05 | 10.17 |
| **Temporary Rehabilitation** | 36912.29 | 7.55 |
| **Permanent Degradation** | 34892.23 | 7.13 |
| **No Alterations-Agroforestry** | 27736.19 | 5.67 |
| **Successful Rehabilitation** | 13162.28 | 2.69 |
| **Degradation after Temporary Rehabilitation** | 12226.96 | 2.50 |
| **Unexplained** | 11111.31 | 2.27 |
| **No Alterations-Savannah** | 7255.20 | 1.48 |
| **No Alterations-Cultivation and Settlement** | 6327.44 | 1.29 |
| **Recent Deforestation** | 4659.69 | 0.95 |
| **No Alterations-Intermittent Highland Bogs** | 983.95 | 0.20 |
| **No Alterations-Agropastoral** | 785.83 | 0.16 |
| **No Alterations-Water bodies** | 142.55 | 0.03 |

type of impact and duration of the processes. As high as 1/5 of the total land mass suffered permanent form of negative changes as far as forestry resources are concerned. However, the successful come back and healing

amounted only to statistically dwarf 2.69% of the land surface. When we look at each land cover class separately, only 400 ha of land have been detected to rehabilitate from non-forest class in to evergreen montane forest. The previous land cover of this rehabilitated land was largely grass, which may not have been put to agropastoral use as the suitability of the area for animal husbandry suffers several limiting factors.

## 5 CONCLUSIONS AND RECOMMENDATIONS

Application of remote and sensing GIS provides the opportunity not only to depict the static nature of a land resource, but also the dynamic nature of these entities. Remote sensing products provide information about the time of data capture. Addition of expert knowledge to combination of pixel information makes presentation of continuous remote sensing end products to politicians, decision makers and non-GIS experts in a simple map easier.

The case study demonstrated the different pace of deforestation and degradation processes. National policy matters and international market situations sometime governed the pace. For example, the encroachment of agricultural land on forest areas was very dramatic only in the 70s and 80s. Later, it has shown tremendous decrease in expansion to a point where it is now even lower than the rate of population growth. The reasons are manifold. However, coffee markets seem to play a greater role. Despite dramatic decrease in coffee price globally, local benefit of coffee production is still relatively better than the years of former communist era. In areas of high agricultural potential that are more remote from markets, like this study area, comparative advantage is greater in production of high-value non-perishable cash crops such as coffee than cereals. However, the coffee value is very much influenced by the international price. That means the sources of dynamics of change for this small area are not only local but also global. The coffee forest is ecologically and economically speaking not a forest anymore. Trees that are not suitable for coffee shade are systematically killed. Since the ground needs to be clean for easy coffee gathering, almost every kind of seedling is frequently wiped out from the ground. The coffee oriented management system is atrocious for tree biodiversity and future regeneration of the forest. However, complete clearance of forests slowed down because of the coffee they are providing shade for.

## ACKNOWLEDGEMENT

The Deutsches Akademisches Austausch Dienst provided financial assistance during the fieldwork for the first author.

## REFERENCES

[1] BREITENBAH, F.V., 1962.:Natural forestry planning: A feasibility and priority study on the example of Ethiopia. *Ethiopian Forestry Review*, 3/4: pp. 41-68.
[2] CARLSON, T., RIPLEY, D., 1997: On the relation between NDVI, fractional vegetation cover, and leaf area index. *Remote Sensing of Environment* 62, pp. 241-252.´
[3] CHAFFEY, D.R., 1980. Southwest Ethiopia Forest Inventory Project. Ministry of Overseas Development, Land Resources Division, Surrey, England.
[4] CONGALTON, R.G. 1988: A comparison of sampling schemes used in generating error matrices for assessing the accuracy of maps generated from remotely sensed data. *Photogrammetric Engineering and Remote Sensing*, 54. pp. 593-600.
[5] ETHIOPIAN FORESTRY ACTION PROGRAM., 1994: The challenge for development . EFAP secretariat. Addis Ababa.
[6] ETHIOPIAN HIGHLANDS RECLAMATION STUDY., 1985: Development Strategy. Part III, Addis Ababa
[7] FAO., 1993: FOREST RESOURCES ASSESSMENT 1990: Tropical Countries. Forestry Paper 112, Rome, Italy
[8] FAO., 2001: FOREST RESOURCES ASSESSMENT 2000. Internet Edition: http://www.fao.org/forestry/fo/country
[9] FEDERAL DEMOCRATIC REPUBLIC OF ETHIOPIA, 1997: The Conservation Strategy of Ethiopia. The Resources Base, Its Utilization and Planning for Sustainability. Addis Ababa, Ethiopia.
[10] GEIST, H., 2000: Setting the stage for examining key drivers of land-use/cover change processes. *LUCC Newsletter* Number 5 p. 9. Louvain-la Neuve.
[11 HAY, G., BLASCHKE, T., MARCEAU, D., BOUCHARD, A., 2003: A comparison of three image-object methods for the multiscale analysis of landscape structure. *Journal of Photogrammetry and Remote Sensing* 57, pp. 327-345.
[12] HOFFER, R. M., 1986: Digital analysis technique for Forestry Applications, in The Use of LANDSAT Data in Forestry, hardwood academic publishers, Chur pp 61-110.
[13] Forest Resources and MoA Forestry development and legislation, In NCSCD Volume 3, Ethiopia's Experience in Conservation and Development. ONCCP, Addis Ababa.
[14] LANGREN, G., 1992: Time in Geographic Information systems. Taylor and Francis, London.
[15] McCloy, R. K., 1995: Resource Management Information Systems. Process and practice. Taylor & Francis. London.
[16] SNNPRS. 1999. Southern Nations Nationalities and Peoples State Forestry Action Program, Main Document. Awassa, Ethiopia.
[17] TEKETAY, D., 1999: History, Botany and Ecological Requirements of Coffee. *Journal of the Ethiopian Wildlife and Natural History*.20. pp 28-50

# Modeling of settlement-dynamics by change detection analysis of remotely sensed and socioeconomic data on Tenerife

S. Naumann[a] and A. Siegmund[a]

[a] University of Education, Department of Geography, Im Neuenheimer Feld 561, 69120 Heidelberg, email: naumann@ph-heidelberg.de, siegmund@ph-heidelberg.de

## ABSTRACT

Since the 1960s the island Tenerife is characterized by a change of the socioeconomic situation, mainly caused by mass-tourism. On account of the increasing tourism – about 4.9 million accommodated tourists in 2003 – as the most important issue in the economy of the island, the socioeconomic situation and land use and land cover changed in the same time. Fallow land, land wasting, land degradation and increasing settlements are some of the main consequences. This leads to a growing necessity of geoecological analysis and to an increasing demand for an adequate monitoring database.

The aim of the study is a regional analysis of environmental risks, especially to develop a model with which scenarios for development of settlements in the future under different boundary conditions will be computed. This scenario based on the data of the preceding development of changes of settlements and non-built up areas and of changes in socioeconomic conditions. These hypothetical driving forces and their variabilities in time and space contain data of population, tourist infrastructure and the amount of employees per sector. On the assumption that the driving forces have a constant trend, the model shows a potential development of the extension of cities and villages in 25 years. The estimation and knowledge of the on-going-trend seems to be very important not only for the ecological aspects but also for the regional planning system of the island.

**Keywords:** Change detection, socioeconomy, land cover/land use modeling, settlement-dynamics, land degradation

## 1 INTRODUCTION

The research area for modeling settlement-dynamics and its effects on the ecological environment is Tenerife, which belongs to the Canary Islands in the mid-Atlantic. Due to the enormous horizontal and vertical extent (2.052 $km^2$ area, up to 3.718 m altitude) the island is characterized by a variation of geological, climatological and vegetational factors leading to a heterogeneous landscape [1] (Fig. 1).

These physical geographical characteristics are one of the reasons for being such a popular destination for tourists to spend their holidays, especially from European countries like United Kingdom, mainland Spain, Germany, and others. Being in its infancy in the 60s, the mass tourism increased from 1978 to 2002 by 269 % to about 4.8 million tourists a year. This development involved a social and economic change from an agrarian to a service society. In fact in 2002 more than 75 % of the number of persons employed on Tenerife worked in the tourism sector, whereas in 1978 it comprised only 56 %. Due to these socioeconomic changes conditional on tourism the changes in land use and land cover has increased at the same time. The trend leads to a spatial concentration of the working and living area near to the coasts (only 19 % of the total area can be used for settlements because of topographical reasons) and increasing fallow land in undeveloped area with the consequences of raised erosion- and land degradation-risk. Even more because of the trend of decreasing precipitation in the canary region, there is a big risk for desertification, especially in the semiarid region in the south of the island.

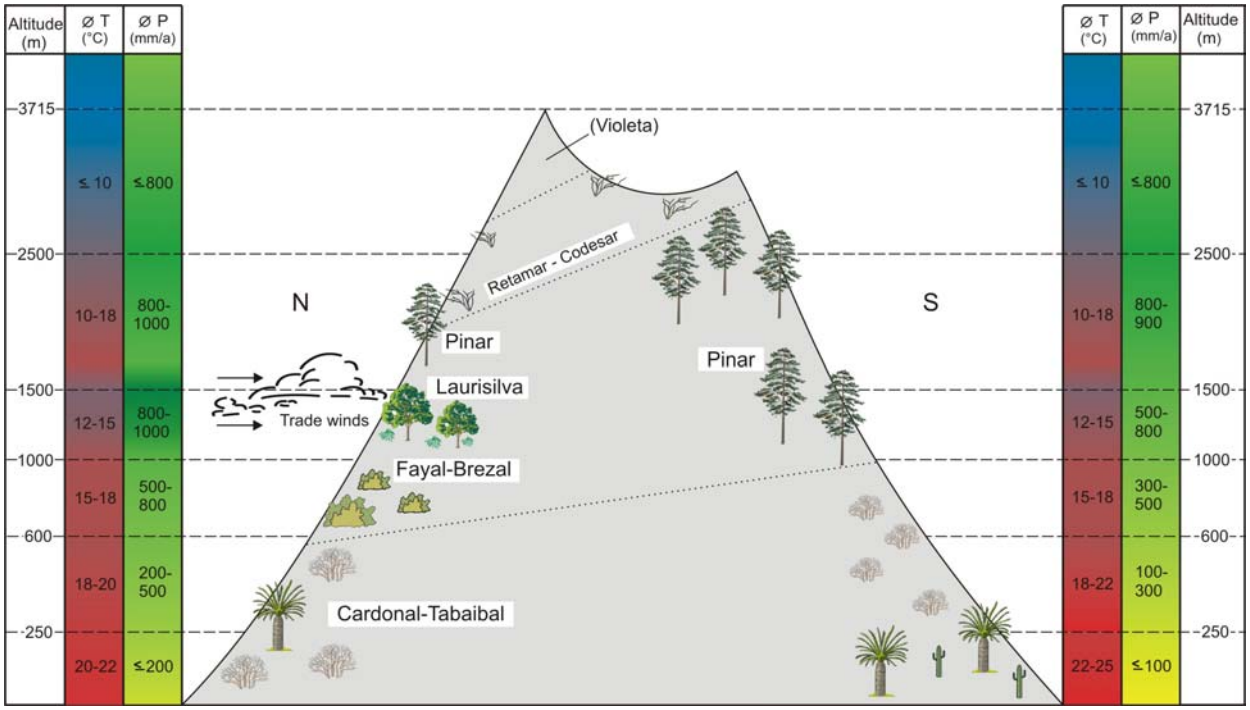


**Figure 1.** The vertical and horizontal arranged zones of distinguish climate parameters entail different vegetation structures lead to a heterogeneous landscape, based on [2].

Different technologies of remote sensing and geographical information systems were used to analyze the changes in land cover and land use and to detect the social and economic driving forces on this development for an appropriate period of 25 years. The first aim was to classify different temporal remotely sensed data and to analyze the spatial pattern and its spatial temporal changes of land cover and land use. Based on the two-period LANDSAT-scenes of Tenerife and on some high resoluted orthophotos of special areas on the island, an object-oriented algorithm for the classifications was used leading in a post-classification method to detect the changes. The extracted spatial pattern and its spatial temporal changes of land cover and land use can be regarded as basic information, describing the composition and the configuration of the area, which is related to geoecological conditions and reflected the social, cultural and economic development. To derive the interface between natural conditions and human influence, different socioeconomic data types have been clipped and correlated with the results of the land cover land use changes.

Especially the increasing settlements which have been calculated, comparing the years 1978 and 1996/2002 and the consequences for the regional planning system leads to the construction of a model showing a scenario for the development of the cities and villages in 25 years by constant trend of driving forces in different classes of probability [3].

## 2 DATA

The basis for modeling settlement-dynamics on Tenerife includes classifications and change detection analysis, which have been done with data of LANDSAT 3 MSS taken on the 13$^{th}$ of November 1978 and LANDSAT 7 ETM+ taken on the 11$^{th}$ of February 2002.

For the knowledge-based classification of the remote sensed data it was necessary to collect training areas with the help of GPS (Global Positioning System). Altogether there have been collected 311 ground truth data, approximately 5,4 % of the area of Tenerife [4], some of them have been used as ground check data for the accuracy assessment. The parameters of the randomly allocated training areas recorded were: geographical position, altitude, slope, aspect, size, type of land cover or land use class, species, covering rage and height of vegetation population.

As previous studies showed unsatisfactory results concerning the few number of land cover and land use classes, as well as the accuracy of the classification, several collateral data were elevated for increasing the classification results. The use of further natural parameters to classify the remote sensed data is based on the heterogeneous landscape of the island and of the dependence of the land cover classes as well as of some land

cover/land use classes on these factors. This dependence is conditional essentially on the altitude ranging up to 3.718 m above sea level, further on the aspect due to the trade winds, as well as on slope and geological circumstances. Because of that it seemed to be helpful to create a Digital Elevation Model (DEM) by digitizing the contour lines of topographical maps in a scale of 1:50,000 and evaluate altitude, aspect and slope. Additionally, the geological map 1:100,000 had converted into digital form.

The statistical data based either on municipality or in zones derived from ISTAC (Instituto Canario de Estadistica) and from Servicio Tecnico de Desarollo Económico en Tenerife. These data have been edited and embed in a (GIS). Regarding the purpose of detecting land cover and land use changes, data of the past (1978) and the present (2002) have been integrated. Finally, data of inhabitants, employees per sector and number of tourists could be integrated in the model.

## 3 METHODOLOGY

Modeling the dynamics of settlement on Tenerife is based on three major procedures: object-oriented classification with remotely sensed data, change detection analysis and the final index-method with the different driving forces (see Fig. 2).

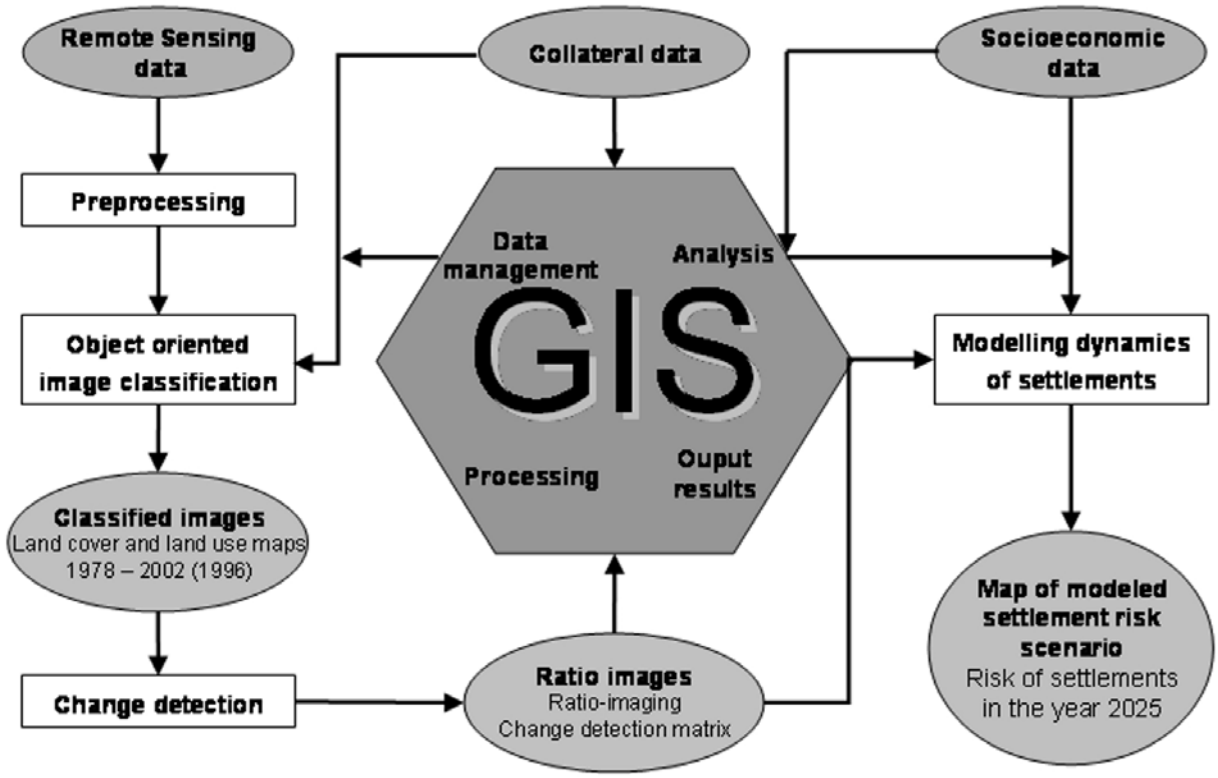


**Figure 2.** Flowchart of the applied procedure for modeling settlement dynamics.

### 3.1 Object-oriented classification

The decision using an object-oriented classification algorithm for the dataset is based on experiences with the traditional pixel-based classifications of the same area with insufficient results. Analysis with non-contextual methods like maximum likelihood classification, support vector machines and iterated conditional modes showed only coarse results with salt and pepper effects and insufficient accuracy [4].

The classifications based on a Fractal Net Evolution Approach [5], which is incorporated in the software eCognition and include multiresolution segmentation and object-oriented framework. With the help of the segmentation the picture elements with similar spectral or textural values can be united in homogeneous objects (spectral information and shape) by minimizing the heterogeneity in the image. Summarized the segmentation leads to generating the image in meaningful objects, which represent shapes of real-world-objects and includes the knowledge of the neighboring objects in horizontal and vertical direction. The segmentation proceeding which was applied has been a multiresolution segmentation, with the possibility to classify in different levels of scale, which

are related with the help of a semantic net. On account of the segmentations as a heuristic optimization procedure, low, middle and high resoluted levels have been created to get the best classification basis for each class in form of details.

The knowledge based classification algorithm is done by fuzzy logic and assumes a hierarchy where the classes are implemented. The feature extraction is based on rules defining membership functions or nearest neighbor functions [6]. The fuzzy algebra is used to define the membership functions of each class, translating feature values into fuzzy values between 0 and 1 [7]. The class descriptions can contain spectral, geometrical and statistical information of the objects, as well as relations between the objects.

The classification based on a multiresolution segmentation approach with which different scales of segments can be classified into separate levels. Furthermore not only the spectral information of the remote sensed data have been used for the classification but also non-spectral information, like altitude, slope and aspect, as well as a geological map. The image classification bases on a class hierarchy with different levels, build by the segmentation.

### 3.2 Change detection

A post-classification method has been applied as the change detection method, based on classified bi-date images of the island Tenerife. The advantage of using this method, compared to image enhancement or image regression based ones´ is the contained information about the area where the change has occurred (spatial information) but also about the "from-to-class" (subject information). The accuracy of this procedure depends on the accuracy of each of the independent classifications, since every error in the individual classified map will be presented in the change detection result [8]. Concerning this fact all classified image data have been tested with the help of an accuracy assessment based on ground check areas, which have been taken on several field trips. Likewise using object-oriented classification method the accuracy seemed to be better than using a pixel-based approach.

### 3.3 Index-method for modeling settlement dynamics

The model for detecting settlement dynamics based on an index-method where the driving forces will be recorded separately and their importance will be weighted [9]. As a first step homogeneous areas of each factor were defined with constant parameters. Based on pixel with the spatial resolution of 15 m three groups were build: group land cover and land use, group topography and group socioeconomic, which based again on individual levels (see Fig. 3).

Weighting the levels and groups is mainly based on correlation analysis, derived from change detection between 1978 and 2002. First of all the individual factors in the levels have been assessed to the probability to get settlement areas (I1). Afterwards the levels have been assessed after their weight inside the group (I2), where the sum of the indices of each group has to get 1. Finally the groups one below the other have been weighted (I3) and up to the final risk (meant as probability) to get settlement areas in the future. With the help of the past changes these results have been controlled and adapted iterative to get the optimal correspondence to the real situation. The susceptibility of each homogeny area resulted of the addition of each factor levels.

The level land cover and land use based on the classification and change detection of the satellite images 1978 and 2002. Concerning on the total area the following relative decline of classes to the favour of settlements has been calculated: agriculture acreage (13.8%), cardonal (9.5%), coastal zone (13.1%) and tabaibal (9.9%). Buffering the areas of settlements of 2002 and comparing them with the areas of 1978 it shows, that the new build up areas are mainly lying within a radius of 3 km. Therefore the level proximity to settlements has been separated in three graduated factors with 3, 2 and 1 km distance. The data showing the changes in amount of tourists are divided in four zones, whereas the changes data of the population belongs to municipality level. The levels have been separated in four factors (tourist zones) and six factors (population) incipient with regression, stagnation and four graduate factors of progression. The level altitude and slope represent the natural limited factors of the expansion of settlements and have been entered in the model with six factors in the first case and eight in the last case (see Table 1).

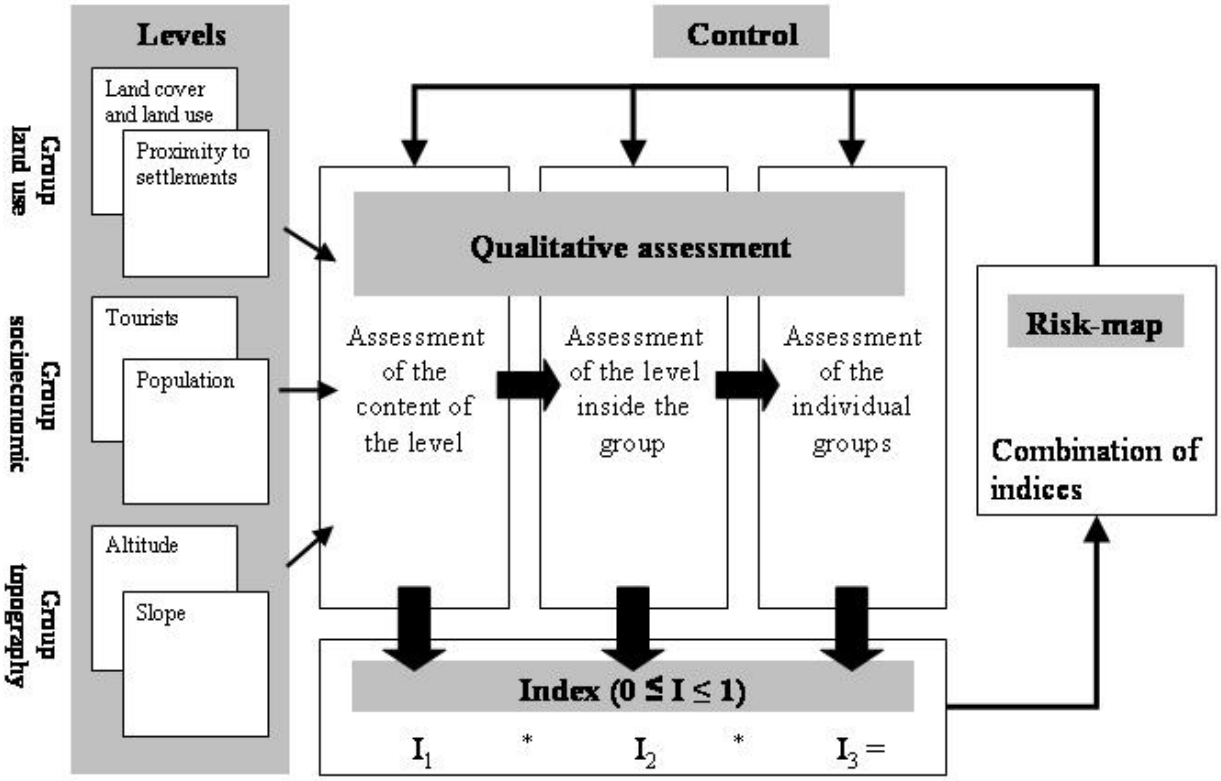


**Figure 3.** Flowchart for modeling the expansion of settlements with the help of the index-method.

After preparing, weighting and adding all indices which determine the process of expansion the settlements a result could be calculated within a GIS with five-scale probability categories. At last the potential new settlements which are situated in nature reserves have been eliminated. The validation of the model is still in process by applying the indicators and methods on another period of time using the already existing classified LANDSAT 3 MSS-scene and a LANDSAT 5-TM scene of 1986 as the starting point so that the results of the model can be validate by already existing data.

**Table 1.** Overview of the used indices and their weighting for calculating the driving forces.

| Level | Assessment level ($I_2$) | Group | Assessment group ($I_3$) | Total index $I_T=I_2*I_3$ |
|---|---|---|---|---|
| **Land cover/land use** | 0.6 | Land use | 0.5 | 0.3 |
| **Proximity to settlements** | 0.4 | | | 0.2 |
| **Tourists** | 0.6 | Socioeconomic | 0.4 | 0.24 |
| **Population** | 0.4 | | | 0.16 |
| **Altitude** | 0.4 | Topography | 0.1 | 0.06 |
| **Slope** | 0.6 | | | 0.06 |
| | | *Per group Σ = 1* | *Σ = 1* | *Σ = 1* |

## 4 RESULTS

### 4.1 Object-oriented image classification

The classification, based on an object-oriented method, additional geographical data and "a-priori"-knowledge, includes 20 land cover and land use classes. The result is shown in Fig. 4. An accuracy assessment based on ground truth data comes to an overall accuracy of 98.9 % and a Kappa-Index of 97.9. Checking the omission and

commission error for each class of the image also gives optimal results, especially compared to a former pixel-based classification of the area with considerably fewer classes, where overall accuracy only reached 90.2 % [4].

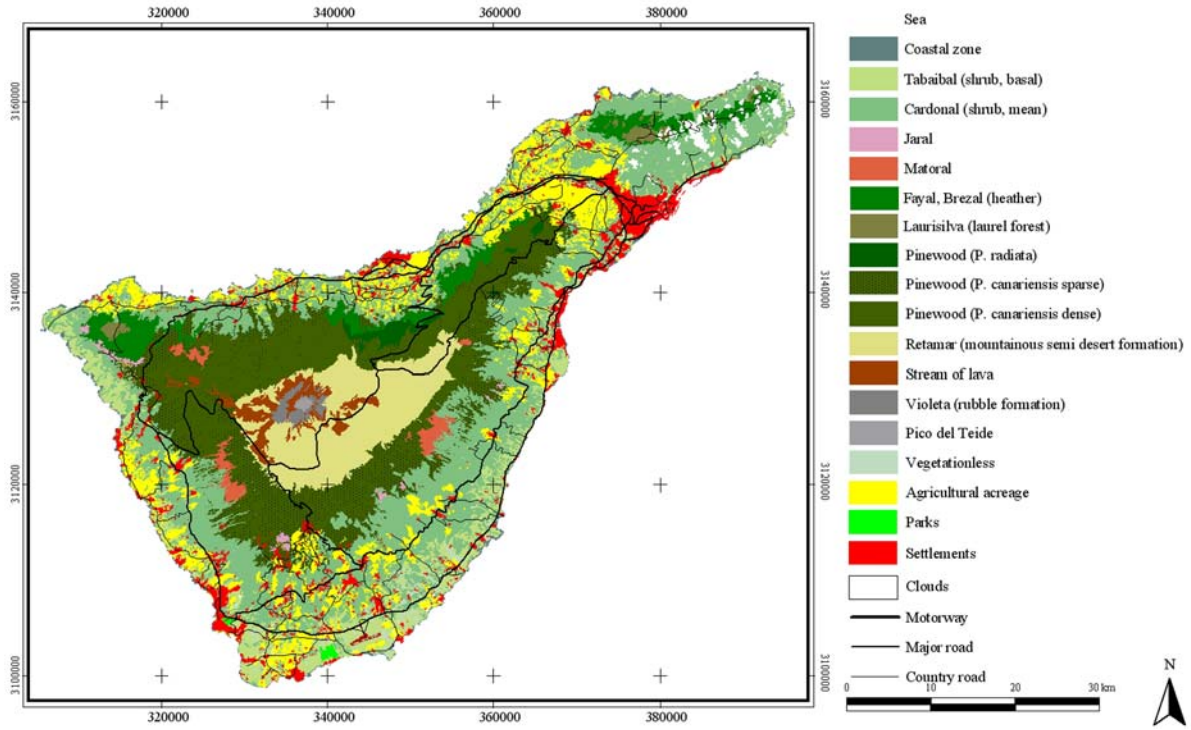


**Figure 4.** Land cover / land use map of Tenerife, based on object-oriented image classification of LANDSAT 7 ETM+ (2002).

## 4.2 Change detection

The method for detecting changes in land cover and land use from 1978 to 2002 on Tenerife was based on a matrix, showing the from-to class in that time. An extract of the matrix is shown in Fig. 5, concerning the classes *cardonal* (shrub, sparse vegetation, euphorbia), *agricultural acreage* and *settlement*. In this connection the classes *cardonal* and *agricultural acreage* lost area from 1978 to 2002, whereas *settlements* increased. Areas of *cardonal* in 2002 belonged to nearly 14 % *agricultural acreage*, whereas about 83 % had been to *cardonal* before. Concerning the area under cultivation in 2002 the change detection shows an opposite trend, but one has to take into consideration that the total area of *agricultural acreage* decreased from 1978 to 2002 by 20 %. The *settlements* gained 269 % area, which initially belonged to the classes *tabaibal*, *cardonal* and *agricultural acreage*.

This analysis shows the enormous expansion of settlements during the last 24 years at expense of other natural vegetation formations and agricultural acreage. Especially vegetation formations like pine forest, tabaibal and cardonal play an important part for the ecosystem of Tenerife. But on account of the increasing mass tourism on the island since the 60s of the last century, the increasing population and the socio-economic changes, there have been a big demand for more development area for housing estates and especially tourist infrastructure, like hotels apartments etc. To get information how these areas which are covered by settlements will grow if the trend goes on like before and to get information about further analysis about degradation and desertification of the concerning land, a scenario for the dynamics of the settlements was developed.

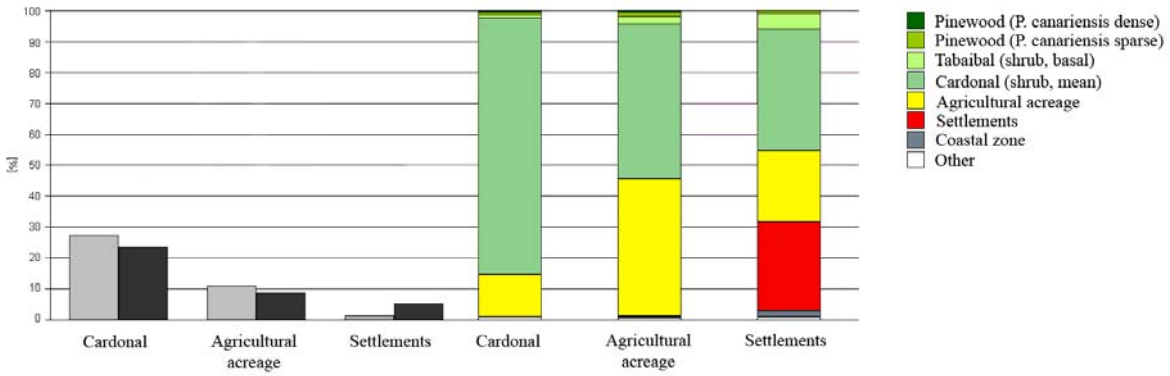


**Figure 5**. Changes of individual classes between 1978 (grey) and 2002 (black) and composition of these classes in 2002.

## 4.3 Index-method for modeling settlement dynamics

The index-method for modeling the dynamics of settlements for Tenerife is based on spatial land cover and land use data, their changes over space and time and the changes in the socioeconomic data. The results are figured in a scenario including the actual road network and the situation of settlements in the year 2002 (Fig. 6).

The five classes describe the probability with which the respective area will be built up. In particular the south part of the island, next to the already existing big tourist cities Playas de las Americas and Los Cristianos holds a very high probability. Just as the Orotava-valley in the north holds a great potential to be built up completely, like analysis showed that since 1982 every year 68 ha of the valley fall victim to development area [10]. The built-up areas in the northern part will gain too, but the dimension is not so high, as it is in the south, due to the topographical limiting factors and the less tourists. Due to the proximity of the capital Santa Cruz de Tenerife and the university-city La Laguna the area in the north eastern part shows a high probability. Summarized, areas near to the coast are more endangered to be built up in the next time than areas in the more upper highlands, which shows the important role of tourism in this context. But just these coastal areas are of big ecological interest, especially for vegetation aspects, what leads to a higher risk of land degradation. Above all these risks are situated in the south, concerning to the increasing tourist centers which lead the local population to migrate to these social and economic better developed areas.

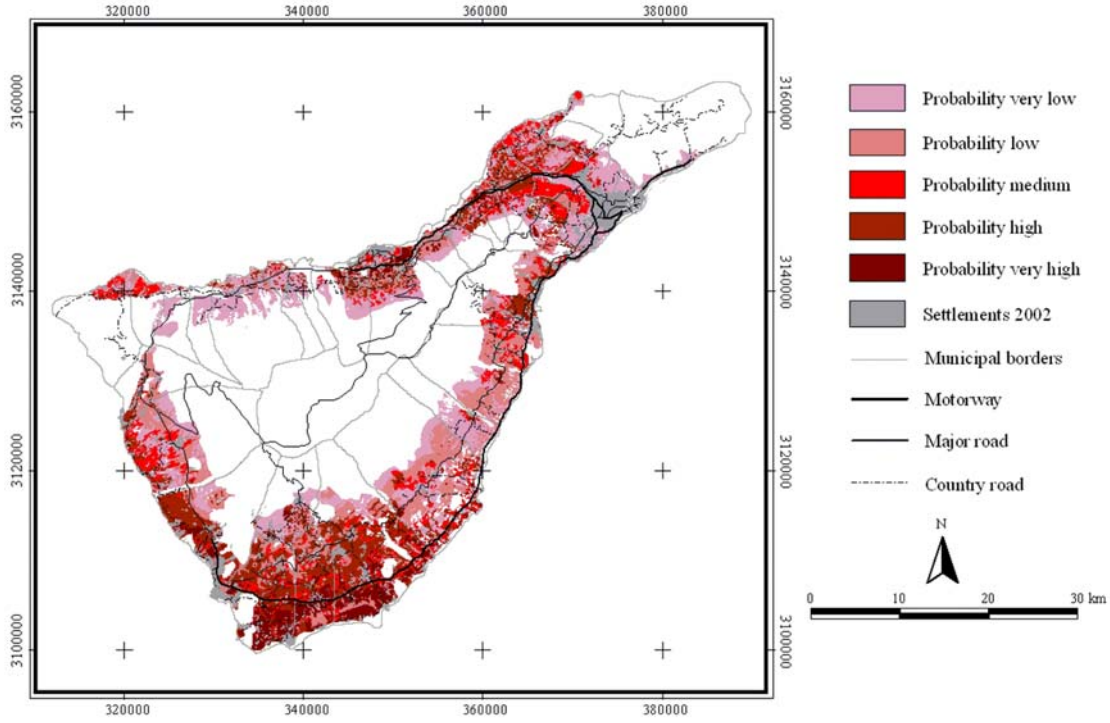


**Figure 6.** Modeled scenario of different probability classes for the dynamics of settlements on Tenerife.

## 5 CONCLUSIONS

Caused by the heterogeneous landscape of Tenerife the used object-oriented classification method showed in its results better accuracy to detect different land cover / land use classes than traditional pixel-based methods. This is mainly based on the "a-priori"-knowledge which can be inserted in the classification process by fuzzy-logic based membership functions. Another advantage is given through the integration of additional layers, like altitude, aspect, slope etc. which show a high dependence on the distinguished vegetation formations.

The model for dynamics of settlement by probability classes, derived by an index-method based on weighting the driving factors in a three step process with the help of qualitative indices seemed to achieve optimal results. The procedure of modeling areas for the development of settlements will be furthermore validated by using a satellite image of 1986.

The increasing tourism on Tenerife show lasting effects to the ecosystem – among others the expansion of settlements and fallow land which leads in land degradation and – especially in parts of the south of the island - to the risk of desertification. The results of the developed model showed to be transferred to different tourism regions in the semiarid subtropics (e.g. Mediterranean region), where extreme relieves like in the example of the canary islands are also given.

## REFERENCES

[1] SIEGMUND, A. AND NAUMANN, S., 2001: Der Einsatz satellitenbildgestützter Klassifikationsverfahren zur Analyse von Landnutzungsstrukturen auf Teneriffa. *Geoöko*, 22, pp. 103-116.

[2] HÖLLERMANN, P., 1982: Studien zur Morphodynamik und Geoökologie der Kanareninseln Teneriffa und Fuerteventura, Göttingen.

[3] NAUMANN, S. AND SIEGMUND, A., 2004: Object-oriented image analysis and change detection of land-use on Tenerife related to socio-economic conditions. *Proceedings of SPIE*, 5574, pp. 172-183

[4] KEUCHEL, J. ET AL., 2003: Automatic land cover analysis for Tenerife by supervised classification using remotely sensed data. *Remote Sensing of Environment*, *86*, pp. 530-541.

[5] BAATZ, M. AND SCHÄPE, A., 1999: Object-oriented and multi scale image analysis in semantic networks. Proc. of the 2nd International Symposium on Operationalisation of Remote Sensing Conference and Exhibition August 16th–20th 1999, Enschede.

[4] NIEMEYER, I. AND CANTY, M. J., 2001: Knowledge-Based Analysis of Change Images by Object-Oriented Post-Classification. *Remote Sensing of Urban Areas*, *Regensburger Geographische Schriften, 35*, pp. 232-240.

[5] BAUER, TH. AND STEINNOCHER, K., 2001: Per-parcel land use classification in urban areas applying a rule-based technique. *GIS*, *6***,** pp. 24-27.

[6] LILLESAND, TH. M. AND KIEFER, R. W., 2000: *Remote sensing and image interpretation*, New York.

[7] JUANG, C. H. ET AL. 1992: Mapping slope failure potential using fuzzy sets. *Journal of Geotechnical Engineering, 118,* pp. 475-493.

[8] POTT, R. ET AL., 2003: Die Kanarischen Inseln - Natur- und Kulturlandschaften, Stuttgart.

# Automatic detection of foggaras using remote sensing

G. Pace[a], M. Quartulli[a], L. Compagnone[a], P. Laureano[b] and M. Burgi[b]

[a] Advanced Computer Systems, Via della Bufalotta 389, 00139 Roma, Italy
[b] Ipogea, Vico Conservatorio, 75100 Matera, Italy

## ABSTRACT

Foggara (karez or qanat) irrigation systems consist of underground tunnels placed in correspondence to an aquifer with the aim of bringing water out to the surface within European and Maghrebian countries. The tunnels are usually straight and with a slope sufficient to allow the water to drain out into an overground irrigation system.

We investigate the feasibility of automatically mapping such man-made scene elements from remote-sensing data. In particular, the respective characteristics of optical and Synthetic Aperture Radar (SAR) systems are introduced and analyzed by considering a new class of probabilistic hierarchical geometrical for the extraction and characterization of such man-made scene elements from remote-sensing data. The hierarchical nature of the model implies that it can be adapted to work with both optical and SAR data with limited modifications and that the reconstruction problem is decomposed in terms of a series of simpler tasks. Examples are given both on optical airborne and C-band ERS data.

**Keywords:** foggara mapping, object-level structural information extraction, hierarchical modeling

## 1 INTRODUCTION

The need for automatic methods for the characterization of the content of Earth Observation (EO) data in terms of parametrically described scene objects is growing with the increasing data volumes delivered by existing and forthcoming sensors. Computationally efficient statistical models for the scene elements of interest and for the associated data phenomenologies are developed and applied in an increasing number of application scenarios to this end.

The foggara mapping problem is an example of such an application scenario: foggara irrigation systems consist of underground tunnels placed in correspondence to an aquifer with the aim of bringing water out to the surface within European and Maghrebian countries. The tunnels are usually straight and with a slope sufficient to allow the water to drain out into an overground irrigation system. They have typical widths of a few meters and lengths of several kilometers. Although they play the essential role of collecting water resources that serve desert oases, they are only mapped to a very limited extent, in the sense that only about 2000 of the estimated 6500 kilometers of existing canalizations are reported in maps up to date.

From the application point of view, although a number of significant projects are carried out on desertification monitoring with support from international organizations such as UNESCO, yet desert mapping applications only seldom appear at the focus of remote sensing research and operation.

Both optical and radar systems are considered for this mapping purpose. The sensitivity of side looking Synthetic Aperture Radar (SAR) configurations to the geometry of the imaged scene as well as to its radiometry makes it an interesting tool in the mapping of scene elements that can be described in terms of structural information. Nevertheless, optical images are currently available with higher coverage at metric resolutions, hence they constitute the main focus of the demonstration in this paper.

While meters-deep canalizations are observable only with difficulty, wells are used to allow access to their inner parts for cleaning and mantainance. It is this wells that are usually observable in high resolution data. The characteristics of the corresponding galleries can be identified based on the alignment of these pixel-based items.

Examples of subsurface canalization mapping in the Sahara environment are presented from optical and C-band ERS SAR data.

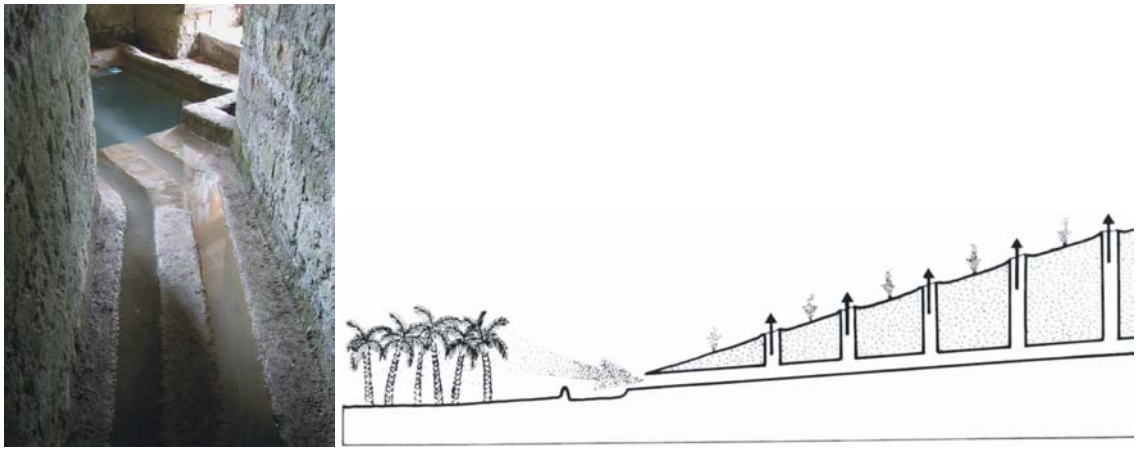

**Figure 1.** Typical foggara internal view and structure: tunnels are straight and horizontal with a slope to allow the water to drain out into an oasis or irrigation system.

## 2 THE FOGGARA MAPPING PROBLEM

Foggaras [1] are traditional systems of water catchment and distribution typical of arid and semiarid areas.

Water resources are collected by means of an extraordinary technique, which exploits the underground drainage tunnels locally called *foggara*. This method dates back thousands of years and is adopted over a very large area stretching from China to Spain, throughout Persia and as far as Latin America (Goblot, 1979). The foggara of the Sahara desert are very similar to the *qanat* or *kariz* of Persia, the *falaj* of Arabia, the *khottara* of Morocco and the *madjirat* of Andalusia, although they have different characteristics. Very similar water systems have been found in Peru and in Mexico within pre-Columbian farm units called *hoyas* (Soldi, 1982).

These ancient methods of water production and the complex management procedures are still used in the regions of Gourara and of Touat in the Algerian Sahara desert. These systems are made up of about one thousand foggara half of which are still working. They extend for 3,000 km to 6,000 km. underground. The several wells on the surface, which can be recognized by their characteristic raised edge resulting from the excavation wastes, help to identify the tunnel. The wells are dug about 8 to 10 meters apart in order to guarantee proper ventilation during the underground digging; they are also used for maintenance work but they are not used for extracting water. The tunnels are straight and horizontal with a slope to allow the water to drain out into an oasis or irrigation system.

The structure of the oasis can be described as being made up of a 4 to 8 kilometre-long foggara which starts from the edge of the depression and goes upstream towards the highland, of a fortification situated along a rocky edge and of a strip of palm-grove extending downstream into the sebkha, as deep as the foggara's water capacity allows. The amount of the ploughing land that can be obtained from the desert depends on the water resources of the drainage tunnel. However, the possibility of extension towards the bottom of the sebkha encounters an insurmountable limit because here the salt concentration of the soil is higher. Therefore, the palm-grove is extended along the borders of the sebhka by excavating new foggara and building new villages.

The technique of foggara is in competition with the technique of the artesian wells which dry water of the foggara by pumping it mechanically deep in the soil. The quantity of water drawn up by using the system of wells is major than the capacity of the ground water table which, as a result, exhausts over time.

On the contrary, a foggara enables water catchment fitting the processes of ground water table replenishment and, as a result, a long lasting sustainability.

To investigate the problem of foggara mapping from remote sensing data, we concentrate on the Timimoun and on the Touat areas in Algeria, both in the area reported in Figure 2.

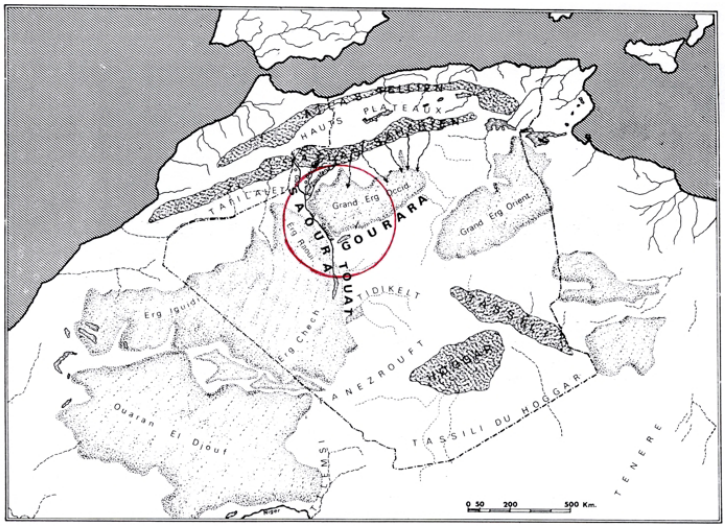


**Figure 2.** The test area of interest, in Algeria.

## 3 REMOTE SENSING OPTICAL AND SAR FOGGARA PHENOMENOLOGY

As is evident from Figure 3, while the underground canalizations tend not to be visible at all in optical data, the wells that are used to allow access to their inner parts for cleaning and mantainance are usually well observable in high resolution optical data. The characteristics of the corresponding galleries can be identified based on the alignment of these pixel-based items.

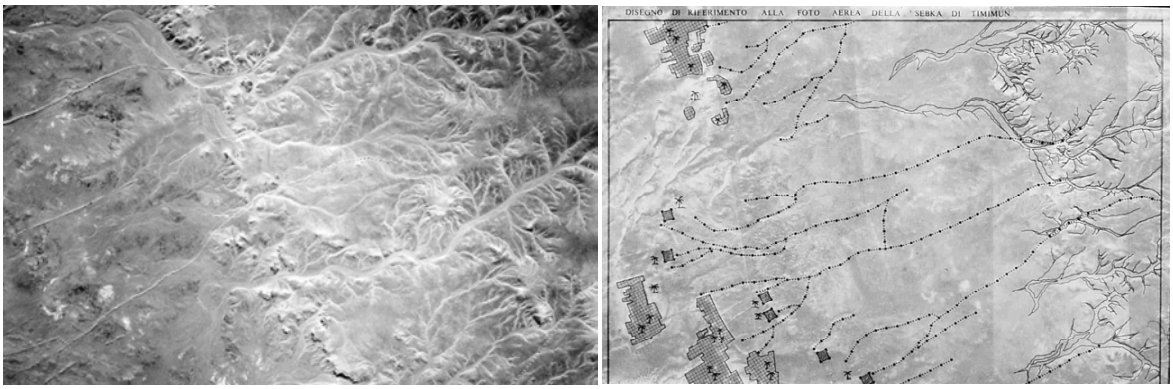


**Figure 3.** A high-resolution optical image of the Timimoun test area, in Algeria, together with a ground truth sketch depicting the foggara structure visible in the image.

SAR sensors are operated in side-looking configurations, that is pointing off at about 35 degrees to the side. The combination of the activce illumination system and of the side-looking configuration makes SAR systems very sensitive to the scene geometry and radiometry [2]: geomorphological structures tend to be evident in SAR imagery together with soil characteristics such as its humidity, which tends to impact in a very direct way the local radiometric reflectivity of the scene: surface variations near the size of the radar's wavelength cause strong backscattering and a rough surface will backscatter more brightly when it is wet. Hills and other large-scale surface variations will tend to appear bright on one side and dim on the other.

Furthermore, in very dry sand environment conditions, the penetration depth of microwave systems has been shown to extend to a few meters. These characteristics make the SAR a unique tool for the investigation and mapping of desert environments.

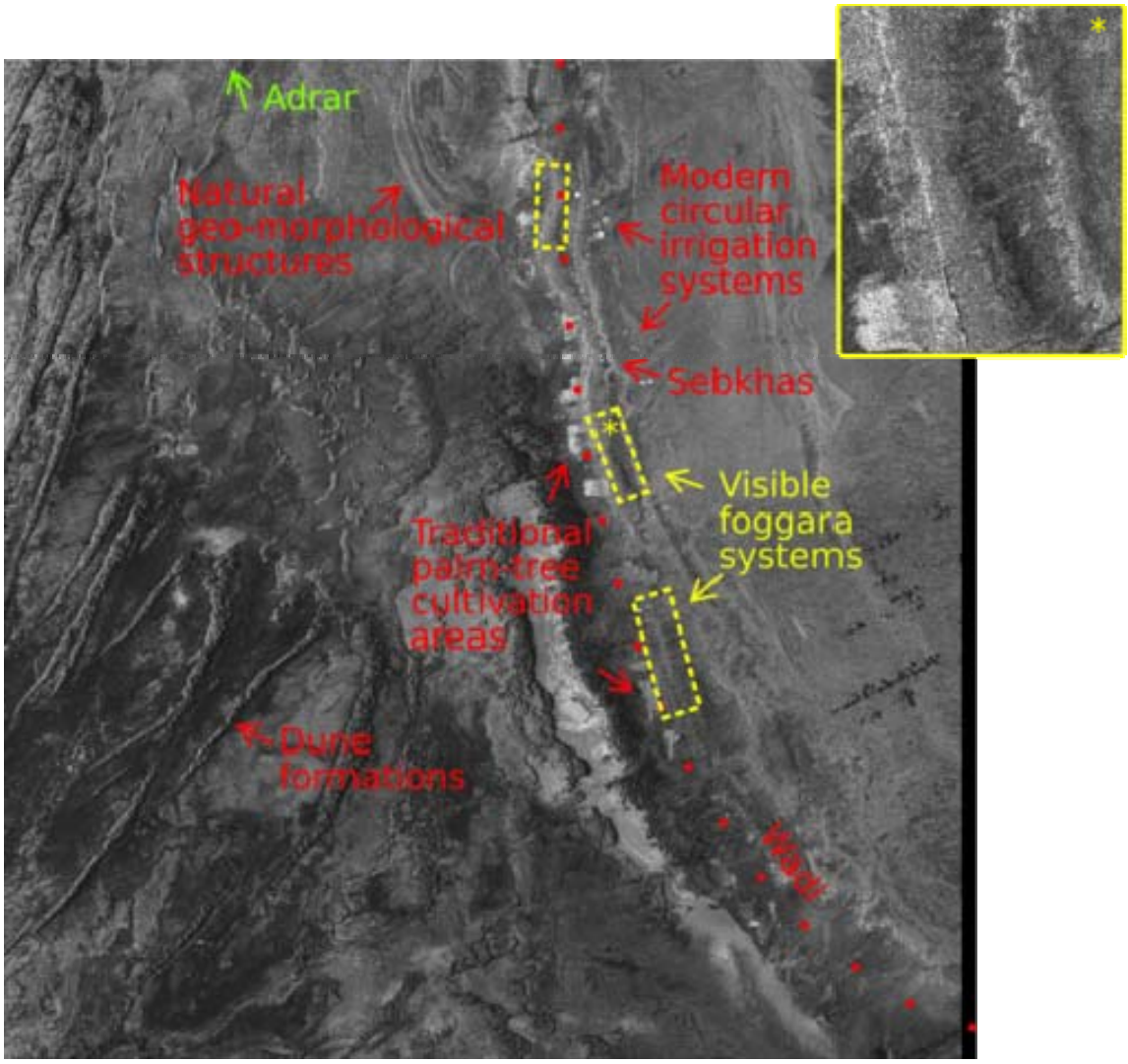


**Figure 4.** C-band ERS SAR PRI dataset of the Touat area with superimposed scene description annotations. The zoom rectangle in the upper left corner shows a full resolution clip of the dataset. Details are shown in Figure 5.

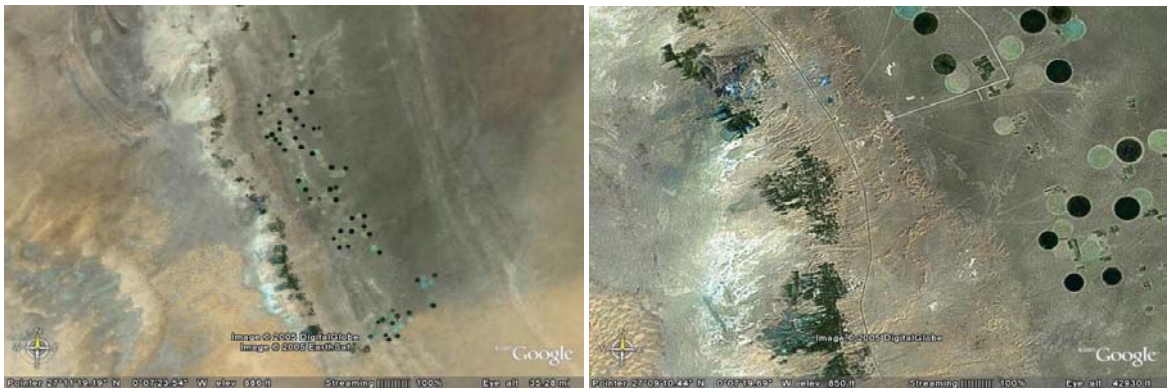

**Figure 5.** Detail corresponding to modern circular irrigation systems of scene in Figure 4 at different resolutions from optical sensors.

In decametric resolution SAR datasets, the peculiar sensitivity of SAR systems to the combination of scene geometry and humidity allows a very clear understanding of both the scene geomorphology, (as in Figure 4, with the central wadi extending vertically across the image) and the presence of geometrically structured elements

introduced by human activity. Even at C-band, the full resolution clip shows how the canalizations extending from the wadi to the palm tree areas on the left of the clip are visible as linear structures with different reflectivity.

At higher resolutions and even longer wavelengths as those of the L-band systems currently in the planning stage, the wells that are used to allow access to their inner parts for cleaning and mantainance should be even more easily observable than in high resolution optical data as cavity-like scene elements in tendentially linear geometrical configurations over an unstructured natural background. The characteristics of the corresponding galleries might then be identified based on the alignment of these pixel-based items.

Nevertheless, optical images constitute the main focus of the demonstration in this paper since they are currently available with higher coverage at metric resolutions.

## 4 MODELING AND ESTIMATION ALGORITHM DESCRIPTION

The proposed model and the related inference algorithm (Figure 6) are essentially hierarchical in nature [3]. The different layers in the model are described by probabilistic descriptions and are linked with each others by conditional probabilities. The associated inference algorithm considers each couple of modeling layers trying to infer the most probable status of each layer in terms of the preceding one before progressing with the estimation.

The analysis proceeds from lower dimensionality elements (the extracted bright point set T=t) to higher dimensionality ones (the reconstructed graph G=g): a hierarchy of models is composed as in

$$D \rightarrow T \rightarrow S \rightarrow G \qquad \text{scene model hierarchy}$$

where D=d is the original data, T is a process whose samples t describe target sets, S=s expresses the set of segments and G=g the resulting reconstructed canalization graph forest, with prior probabilities $p_T(T=t)$, $p_S(S=s)$, $p_G(G=g)$ describing models for the elements and likelihoods $p_{T,D}(T=t|D=d)$, $p_{S,T}(S=s|T=t)$, $p_{G,S}(G=g|S=s)$ linking them. The estimation algorithm proceeds as follows: targets that cannot be statistically explained in terms of their image neighborhood are extracted from the data.

The extracted estimated target set $t_0$ is the input for the next estimation level: the complete space of segments generated by the points is generated and explored in order to generate a sub-space of most probable segments which is maximized by enumeration of the space of configurations S=s of segment sets keeping $t=t_0$ fixed.

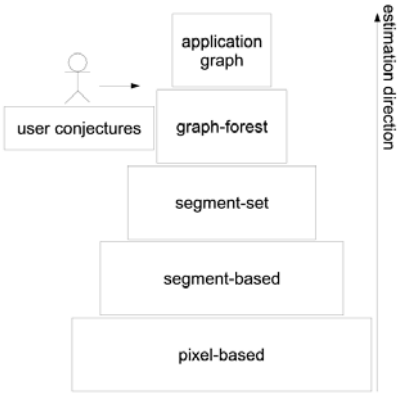


**Figure 6**. Hierarchical estimation direction description.

In the case of segment sets, for the probability of a configuration only objects already in the configuration are considered to compute the probability of the new composed configuration. A simple sampling scheme is considered: most probable object sets are generated as if by sampling, but the complete space of configurations is available for the optimization [4]. A candidate point is connected to the nearest one only if the probabilistic distance between them is similar to the one characteristic of the existing segment set. A series of disconnected segment sets is obtained at this level. The segment sets are then connected with each other.

Once again, the extracted set of segments $s_0$ is used as an input to the graph estimation stage that estimates the most probabile graph $g_0$ by maximizing a Bayesian probabilistic measure of belief $p_{G,S}(G=g|S=s)$ that can be factorized into a multiplication extended to segment sets.

The last layer of the estimation considers user input in terms of training in order to define a further measure of belief in the scene reconstruction result based on both the existing broader reconstruction and user conjectures.

An notable point is that each modeling layer has higher dimensionality and usually a smaller number of estimated objects than the preceding ones: a large number of image pixels, in the order of millions, is reduced to a few tens of thousand targets, which in turn are mapped to thousands of segments, that are in turn combined to tens of graph elements that build up a forestof graphs with typically only a few of elements.

The system operates than what can be seen as a bottom-up construction of a scene description that is more and more summarized.

It must be noted that the obtained A-Posteriori probabilistic description of the scene is non-analytic. Nevertheless the system operates on probabilistic spaces with finite and well-known dimensionality with a limited number of elements. It therefore follows that enumeration-based, brute-force algorithms can be used for the estimation of maximimally probable configurations instead of more complex and computationally expensive stochastic optimization algorithms.

## 5 EXAMPLES

An example of the results of the application of the described algorithm to an optical image with sub-metric resolution acquired from an airborne platform are presented in Figures 7 and 8.

We start from the identification of isolated points in an aerial image (7a) of Timimoun, in Algeria. The isolated points (8a) map wells that bring air to the underground canalizations.

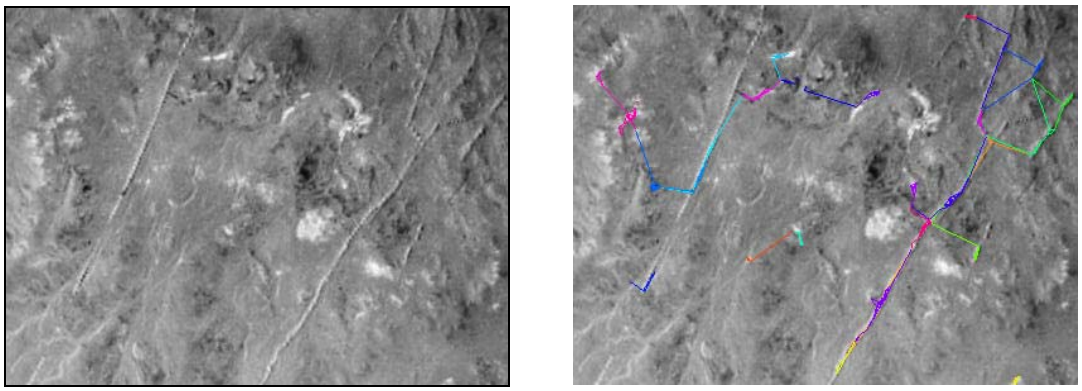

(a) (b)

**Figure 7**: Algorithm input and result. We start from the identification of isolated points in an aerial image (7a) of Timimoun, in Algeria. A set of connected cluster groups is inferred (7b) that tends to reproduce the linear aspect of the original foggara.

Figure 8 reports a more detailed view of the intermediate estimation layers of the algorithm. The extracted points are fused into a set of most probable segments (8b). The probability measure linking the point set to the segment set space essentially considers the length of the segments favouring the shortest ones. The segment set configuration is the basis for the estimation of a segment cluster space (8c), which is populated by aggregations of segments with similar geometrical properties in terms of slope, intercept and geometrical location. Based on the most probable configuration in this space (8d), a further set of better connected cluster groups is inferred that tends to reproduce the linear aspect of the original foggara.

The obtained results tend to indicate the possibility of employing the described algorithm to map subsurface canalization in Maghrebian countries. The subsurface penetration capabilities of L-band SAR in very dry conditions might provide better discrimination capabilities.

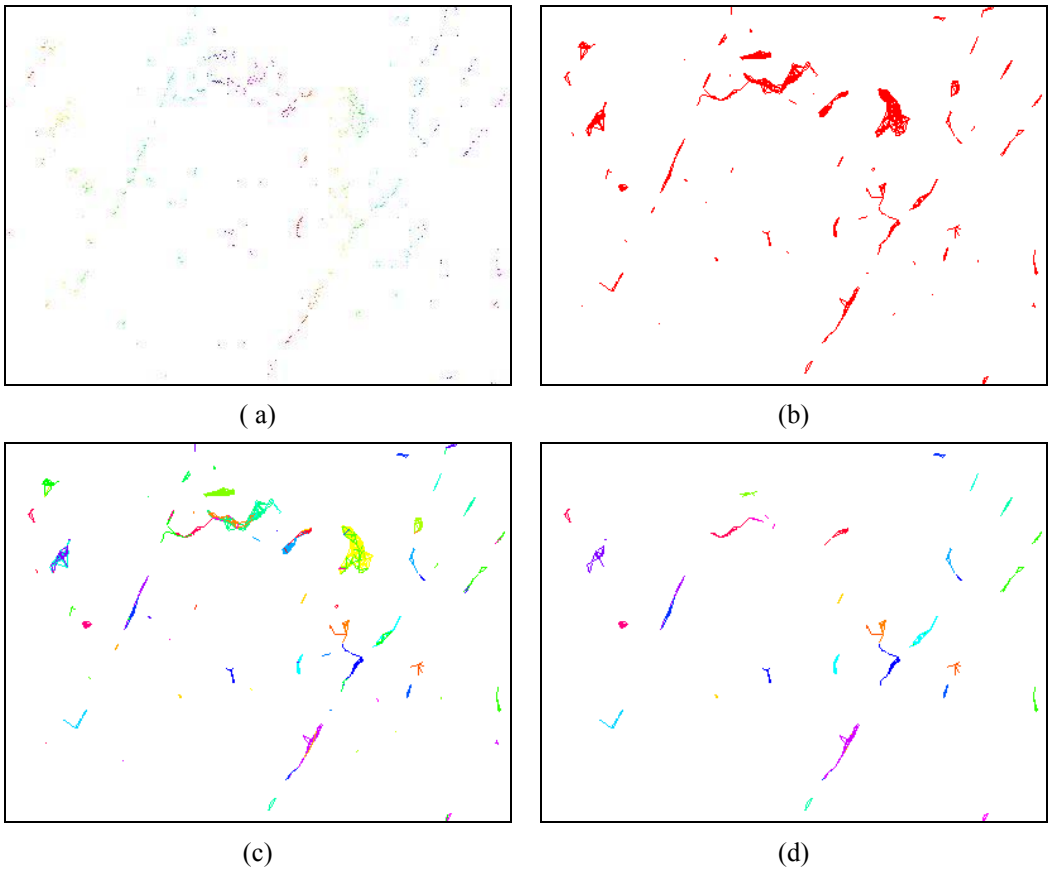


**Figure 8**: Algorithm intermediate estimation levels. The isolated points (8a) map wells that bring air to the underground canalizations. The extracted points are fused into a set of most probable segments (8b). The probability measure linking the point set to the segment set space essentially considers the length of the segments favouring the shortest ones. The segment set configuration is the basis for the estimation of a segment cluster space (8c), which is populated by aggregations of segments with similar geometrical properties in terms of slope, intercept and geometrical location. Based on it, a most probable configuration in this space (8d) is generated.

## 6 CONCLUSIONS

Foggara irrigation systems consist of underground tunnels placed in correspondence to an aquifer with the aim of bringing water out to the surface within European and Maghrebian countries. The tunnels are usually straight and with a slope sufficient to allow the water to drain out into an overground irrigation system.

The feasibility of automatically mapping such man-made scene elements from remote-sensing data was investigated in this paper.

In particular, the respective characteristics of optical and Synthetic Aperture Radar (SAR) systems were introduced and analyzed by considering a new class of probabilistic hierarchical geometrical for the extraction and characterization of such man-made scene elements from remote-sensing data.

The hierarchical nature of the model implies that it can be adapted to work with both optical and SAR data with limited modifications and that the reconstruction problem is decomposed in terms of a series of simpler tasks. The algorithms for the extraction and characterization associated to these models are expressed in terms of Maximum-A-Posteriori estimation: Bayesian probability is considered as a measure of belief in the reconstructed scene, given the data and related user-expressed knowledge. Such measure need to be maximized in order to obtain the scene description that best matches the input signals and conjectures.

Examples were given both on optical airborne and C-band ERS data.

A novel class of probabilistic hierarchical geometrical models was introduced that aims at the characterization of linear man-made scene elements in remote-sensing data.

## ACKNOWLEDGMENTS

The authors would like to thank Cosimo Marzo of the Italian Space Agency for providing the data used.

## REFERENCES

[1] LAUREANO, P., 2001: Atlante d'acqua, conoscenze tradizionali per la lotta alla desertificazione, *Bollati Boringhieri, Torino*

[2] CURLANDER, J.C. AND MCDONOUGH, R.N., 1992: Synthetic Aperture Radar: Systems and Signal Processing, *Wiley-Interscience*

[3] MACKAY, D.J.C., 1991: Maximum Entropy and Bayesian Methods in Inverse Problems, *in Bayesian Interpolation, Kluwer Academic Publisher, pages 39-66*

[4] CRESSIE, N.A.C., 1991: Statistics for Spatial Data, *Wiley-Interscience*

# Applicability and Limitations of Land Use / Land Cover Classification Using High Resolution Satellite Imagery in Arid and Semi-Arid Areas of the Northern Kordofan State (Sudan)

M. Salih Dafalla[a] and E. Csaplovics[b]

[a] University of Khartoum, Department of Soil Science and Environmental Studies, presently at Department of Geosciences, University of Dresden
[b] Department of Geosciences, University of Dresden

## ABSTRACT

Sudan as the largest African country extends over a variety of eco-climatic zones, ranging from desert at north to the savanna zone in the south. Being one of the Sahelian countries it faced numerous drought periods. Semi-arid regions of the Sudan are thus heavily attacked by severe desertification, which is driven by climatic as well as human impacts.
Spatial data on dynamics of land use and land cover is poor and thus insufficient. Nevertheless extended knowledge on state and changes of land use and land cover is needed in order to support the implementation of sustainable strategies of regional (re)development. The main objective of this study is to discuss the applicability of sources and methods of remote sensing for reliable classification of land use / land cover (LUC) in terms of the specifications set up by FAO, UNCCD and others. The area of the case study is located in the Sahelian eco-climatic zone in Northern Kordofan State, Sudan. A geometrically and radiometrically corrected sub-scene of Landsat ETM+ imagery (174/51) of Nov.27$^{th}$ 1999 was used in this study. Moreover, ancillary data and interviews recorded during field work were used to support image classification. Applying image analysis and statistical software allowed for producing colour composites used for on-screen and in-situ mapping as well as for calculating vegetation indices and other band ratios and finally for classifying imagery by means of clustering algorithms. The study area was divided into five regions; unsupervised classification was carried out for these regions to produce 11 classes for each region, only 9 signatures were selected. These signatures were labeled to their corresponding land use / land cover types. This study supports the increasing activities in integrating systematical and periodical monitoring of regional dynamics of land use and land cover by means of operationalised low-cost and easy-to-handle tools of remote sensing and geoinformation analysis on national and regional levels in the Sudan.

**Keywords:** Sudan, Sahelian zone, Northern Kordofan State, Land use / land cover, Unsupervised / supervised classification**.**

## 1 INTRODUCTION

Sudan is the largest African country covering an area of approximately 2.6 million km2 and inhabited by a population of about 29.4 millions. The country extends over a variety of eco-climatic zones, ranging from desert at north with nil annual rainfall to the savanna zone in the south with up to 1200 mm annual rainfall [2]. Being one of the Sahelian countries it faced numerous drought periods, especially during the 1960s and 1980s. Severe famine and large immigration movements occurred. Semi-arid regions of the Sudan are thus heavily attacked by severe desertification, which is driven by climatic as well as human impacts (UNSO, 1992).

Sudan is considered one of the poorest countries in world [4]. Besides all kinds of data supply, especially spatial data on dynamics of land use and land cover is poor and thus insufficient. Nevertheless extended knowledge on state and changes of land use and land cover is needed in order to support the implementation of sustainable strategies of regional (re)development [3, 5].

The difficulties concerning land use / land cover classification in semi-arid regions by means of remote sensing are well known. Since vegetation-soil-patterns in arid and semi-arid zones respectively are characterized by a sparse distribution of often non-photo-synthesising vegetation (NPV) its spectral behaviour often interferes with spectral signatures of bare soil patterns [7]. Moreover, the spatial heterogeneity at pixel level is strongly affecting systematic separation between dominant land uses. Therefore, there are many studies recommending subpixel unmixing analysis as suitable method to overcome such constrains [1], but still there are many difficulties to be overcome such as unavailability of spectral libraries for dominant plant species and soil types.

## 2 OBJECTIVES

The main objective of this study is to discuss the applicability of sources and methods of remote sensing for reliable classification of land use / land cover (LUC) in terms of the specifications set up by FAO, UNCCD and others.

## 3 METHODOLOGY

The area of the case study is located in the Sahelian eco-climatic zone in Northern Kordofan State, Sudan. These regions generally provide reasonable harvests of rainfed crops as sesame, millet and hibiscus, of gum arabic (*Acacia Senegal*) and plenty of livestock such as sheep and camels. Severe constraints for the development of medium- to long-term strategies of sustainable land management are raised by temporal variations of impacts of drought and desertification during the last decennia[3].

A geometrically and radiometrically corrected sub-scene of Landsat ETM+ imagery (174/51) of Nov.27th 1999 was used in this study (Fig. 1). Moreover, ancillary data of the relevant topographic map sheets 1:250000, a land use map, a vegetation map and interviews recorded during field work were used to support image classification.

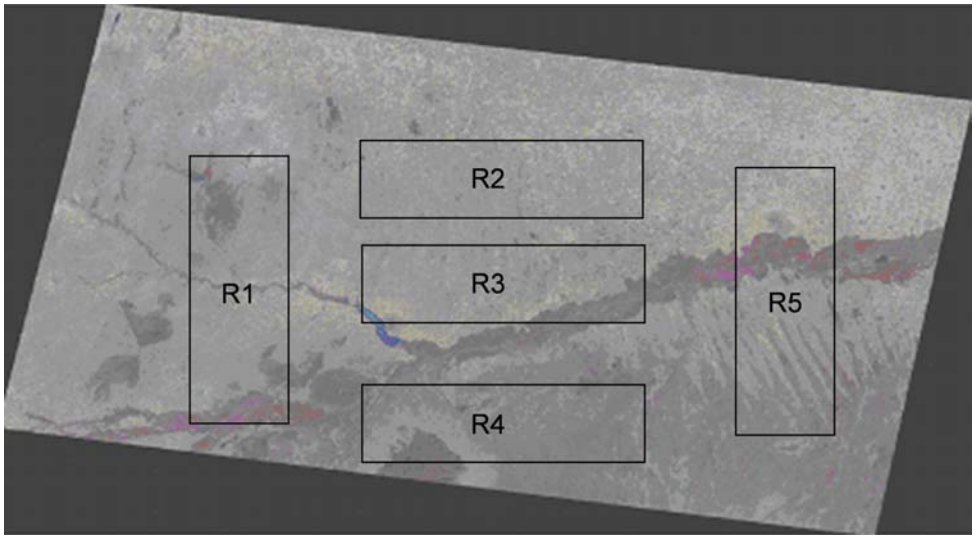


**Figure 1.** ETM+ Subscene of the study area.

Applying image analysis and statistical software allowed for producing colour composites used for on-screen and in-situ mapping as well as for calculating vegetation indices and other band ratios and finally for classifying imagery by means of clustering algorithms.

The study area was divided into five regions (R) (Fig. 1); unsupervised classification was carried out for these regions to produce 11 classes based on previous study have been carried out by the Northern Kordofan Rangeland Development Programme (NKRDP) (Personal communication) for each region using visible bands 1, 2, 3 in addition to NIR and SWIR bands 4, 5, and 7. As result of thematic similarity among these 5x11 spectral classes, only 9 signatures were selected after evaluation of the produced spectral classes selected by visual interpretation and by analysis of spectral signatures and scatter plots (Appendices A, B, C, D, F). These 9 signatures were labeled to their corresponding land use / land cover types. Finally a supervised classification using Mahalanobis Distance Classifier was applied to produce the classified image. This classification approach was adopted since it allowed for the detection of a variety of additional spectral classes within the subset, thus for a better representation of its heterogeneity.

## 4 RESULT

Despite the above mentioned limitations the overall classification accuracy meets values of around 75%. The dominating land use / land cover classes in the region of interest are small-scale traditional agriculture on sand (23.08), open shrubland (19.27%), fallow land (14.75%), grassland (12.47%), open forest (11.61%), shrubland on clay (10.25%), closed shrubland (4.15%), mixed forest and shrubland (3.99%) and natural water surfaces (0.39%) (Table 1, Fig. 2 and Fig. 3). Apart statistical uncertainties full-area coverage of reliable classified data was mainly limited by the structural heterogeneity of the areas, due to typical vegetation continua in grasslands of varying

densities as well as by the building materials in rural settlements, which comprise wood and grasses cut in the local environment. However, the preliminary results of the study are promising as they evidently provide more detailed spatial information on regional patterns of land use and land cover than up to now.

**Table 1.** Main dominant LULC classes.

| Class Name | Area (Ha) | % |
|---|---|---|
| **Traditional Agriculture on Sand** | 285240 | 23.0883 |
| **Open Shrubland** | 238090.5 | 19.27186 |
| **FallowLand** | 182292.8 | 14.7554 |
| **Grassland** | 154052.8 | 12.46956 |
| **Open Forest** | 143441.2 | 11.61062 |
| **Shrubland on Clay** | 126691.2 | 10.25482 |
| **Closed Shrubland** | 51329.33 | 4.154771 |
| **Mixed Forest and Shrubland** | 49351.9 | 3.994712 |
| **Natural Water Bodies** | 4941.242 | 0.399961 |

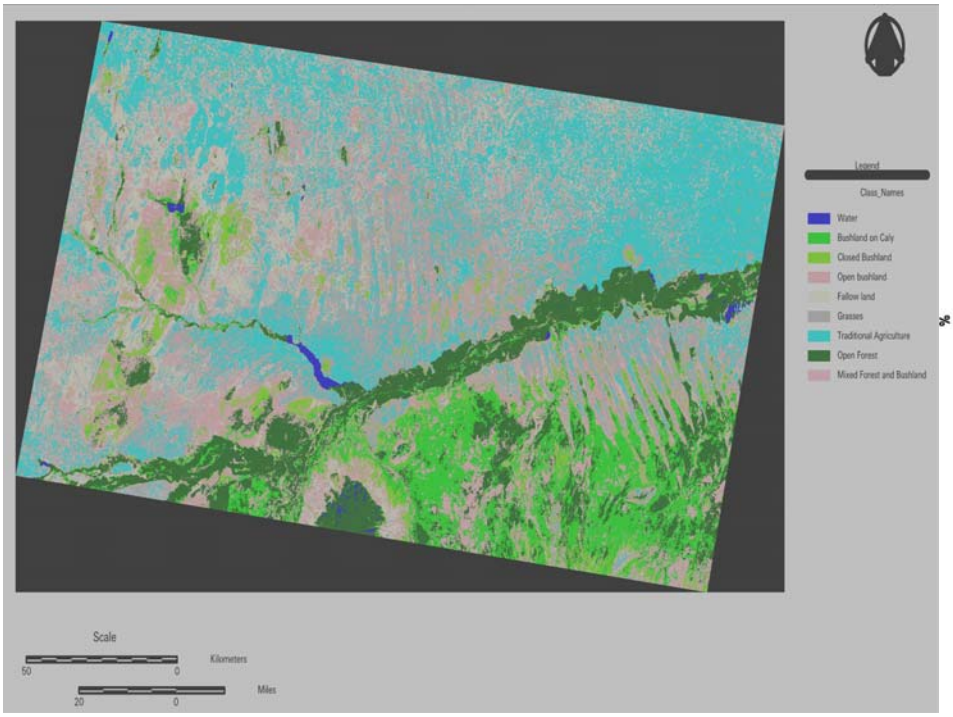


**Figure 2.** Main dominant LULC classes.

**Figure 3:** Main dominant LULC classes areas and percentages.

## 5 CONCLUSION

This study, as part of comprehensive LULC change research in Northern Kordofan State, supports the increasing activities in integrating systematical and periodical monitoring of regional dynamics of land use and land cover by means of operationalised low-cost and easy-to-handle tools of remote sensing and geoinformation analysis on national and regional levels in the Sudan.

## REFERENCE

[1] ELMORE, A.J., MUSTARD, J.F., MANNING, S. AND LOBELL, D., 2000: Quantifying percent live cover in multitemporal data of a semi-arid region: Comparison between spectral mixture analysis and NDVI. Remote Sensing of Environment 73, 87-102.
[2] DANIDA, 1989: Enivronmental Profile: Sudan. Danida, Ministry of Foreign Affairs. Sect1: National Overview, 8-15.
[3] HIELKEMA, J.U., PRINCE, S.D. AND ASTLE, W.L., 1986: Rainfall and vegetation monitoring in the savanna zone of the Democratic Republic of Sudan using the NOAA Advanced Very High Resolution Radiometer. Int. J. Reomte Sensing, 1986, Vol. 7, No. 11, 1499-1513.
[4] HINDERSON, T. 2004: Analysing Environmental Change in Semi-arid Areas in Kordofan, Sudan. Seminar Series nr 109. Geobiosphere Science Centre, Physical Geography and Ecosystem Analysis, Lund University.
[5] INTERNATIONAL FUND FOR AGRICULTURAL DEVELOPMENT (IFAD), 2004: Environmental Assessment Study. Main Report. Republic of Sudan, Western Sudan Resource
[6] NORTHERN KORDOFAN RANGELAND DEVELOPMENT PROGRAMME (NKRDP). 2004: Unpublished Report. Personal communication, Mr. Abdelrahman Ahmed Khatir. Agricultural Research Corportation, Elobeid, Sudan.
[7] SCHMIDT, H. AND KARNIELI, A., 2000: Remote sensing of the seasonal variability of vegetation in a semi-arid environment. *Journal of Arid Environments* (2000) 45**:** 43–59. Available online at http://www.idealibrary.com
[8] MANAGEMENT PROGRAMME. PART 1: Greater Kordofan. Near East and North Africa Division Project Management Department.
[9] UNITED NATIONS SUDANO-SAHELIAN OFFICE (UNSO), 1992: Assessment of Desertification and Drought in the Sudan-Sahelian Region 1985-1991.

## Appendices

**Appendix A**: Descriptive statistics of six bands

| | Mean | Std. Deviation | N |
|---|---|---|---|
| MEAN1 | 60.2541 | 3.9586 | 55 |
| MEAN2 | 59.4310 | 7.7080 | 55 |
| MEAN3 | 80.3925 | 18.9569 | 55 |
| MEAN4 | 76.8581 | 17.7228 | 55 |
| MEAN5 | 100.6771 | 29.4468 | 55 |
| MEAN6 | 76.8979 | 25.4968 | 55 |

**Appendix B**: Pearson correlation coefficients between means of six bands for 55 spectral classes

| | MEAN1 | MEAN2 | MEAN3 | MEAN4 | MEAN5 | MEAN6 |
|---|---|---|---|---|---|---|
| MEAN1 | 1.000 | 0.911 | 0.768 | 0.586 | 0.623 | 0.612 |
| MEAN2 | 0.911 | 1.000 | 0.926 | 0.714 | 0.714 | 0.745 |
| MEAN3 | 0.768 | 0.926 | 1.000 | 0.906 | 0.899 | 0.930 |
| MEAN4 | 0.586 | 0.714 | 0.906 | 1.000 | 0.986 | 0.976 |
| MEAN5 | 0.623 | 0.714 | 0.899 | 0.986 | 1.000 | 0.985 |
| MEAN6 | 0.612 | 0.745 | 0.930 | 0.976 | 0.985 | 1.000 |

**Appendix C**: Scatter diagram for bands 1, 3 and 4 for 55 spectral classes

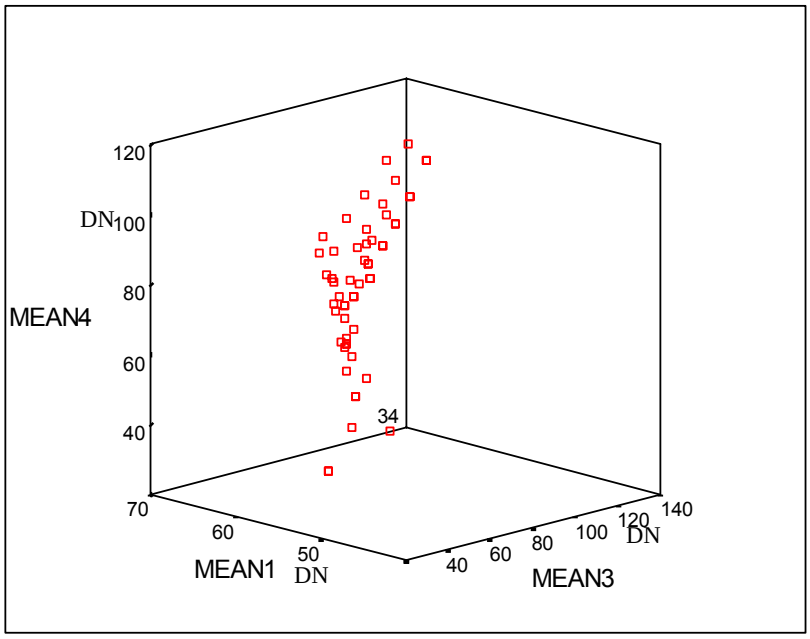


**Appendix D**: Scatter diagram for bands 1, 3 and 6 for 55 spectral classes

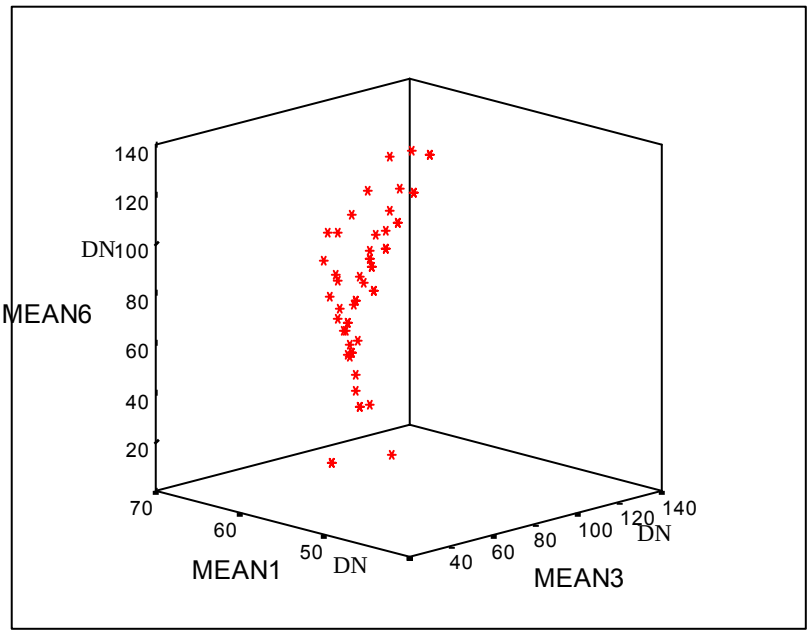

**Appendix E**: Frequency distribution of mean DN values of all bands for 55 classes.

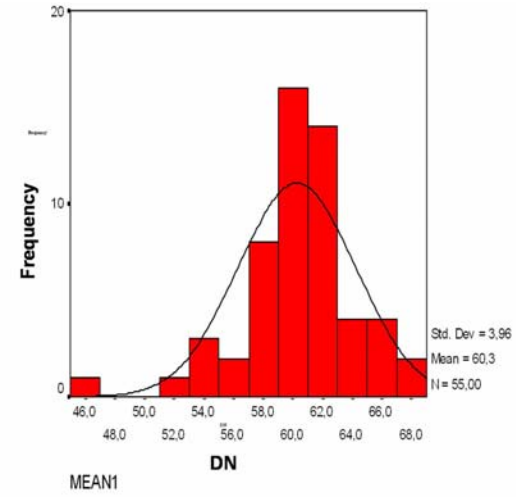


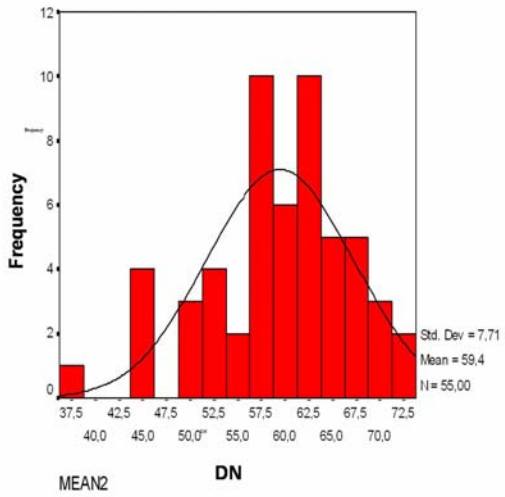


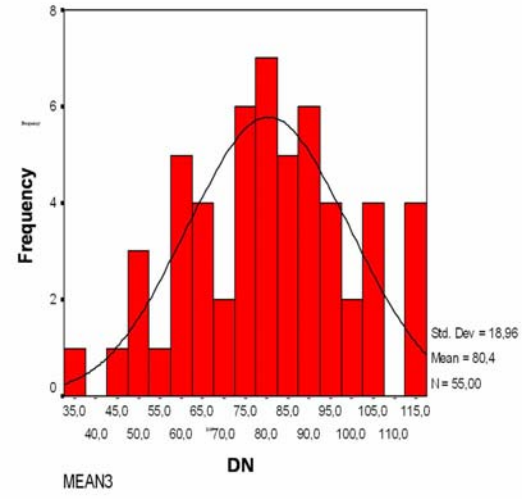


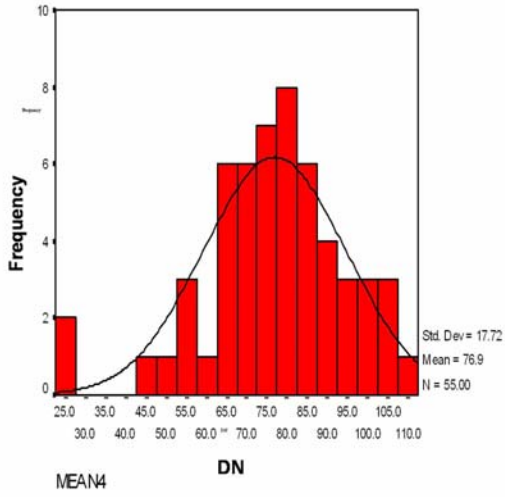


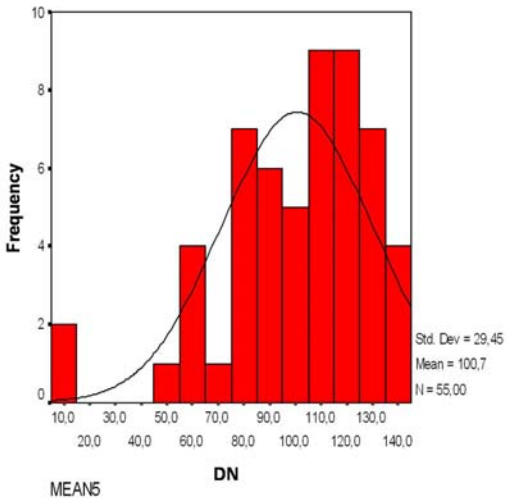


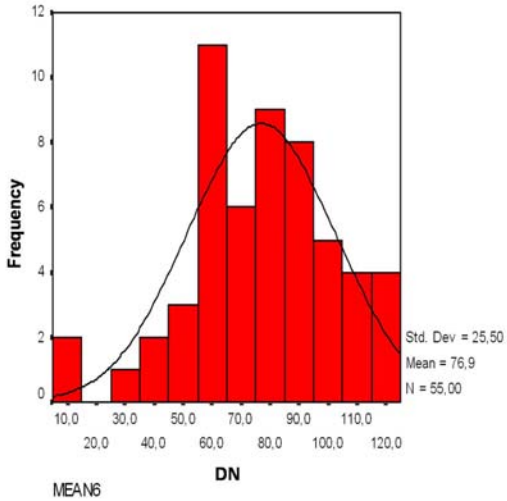

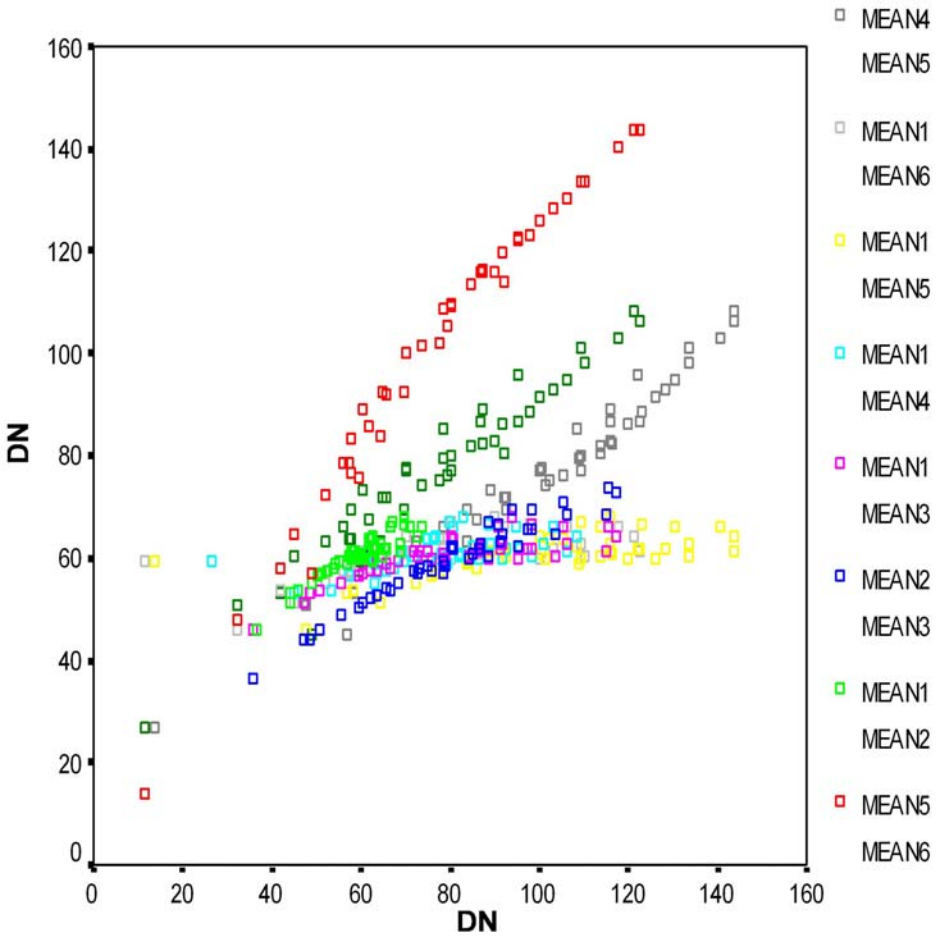
DN
DN
0
20
40
60
80
100
120
140
160
MEAN4
MEAN5
MEAN1
MEAN6
MEAN1
MEAN5
MEAN1
MEAN4
MEAN1
MEAN3
MEAN2
MEAN3
MEAN1
MEAN2
MEAN5
MEAN6

# Monitoring Dynamics of Landcover in Semiarid Wetlands , A Case Study for the Niger Inland Delta (Mali)

R. Seiler[a] and E. Csaplovics[a]

[a] Departement of Geosciences, Technische Universität Dresden, Helmholtzstrasse 10, D-01062 Dresden, email: rseiler@rcs.urz.tu-dresden.de, csaplovi@mailbox.tu-dresden.de

## ABSTRACT

The Sahel, the semi-arid fringe south of the Saharan deserts, is one of the most endangered zones worldwide, as are the sensible semi arid regions in Sub-Saharan Africa in general. The extent of annual flooding of the vast plains during September to December depends on water levels of the main rivers Niger and Bani. The interaction among pre-flood, flood and post-flood conditions strongly affect land use patterns in and around the delta. Human impact is mainly driven by irrigated rice cropping, rainfed agriculture, grazing and browsing of herds and flocks as well as by fuelwood consumption. Assessing and mapping dynamics of land use are made possible by the systematic application of remote sensing and image analysis. Operational missions of earth observation contribute to the establishment of multi-seasonal and multi-annual monitoring schemes. This paper presents results of an application of Medium Resolution Imaging Spectrometer (MERIS) for monitoring spatio-temporal patterns of land cover and land cover change in Sub Saharan wetlands. The MERIS instrument operates with a 15 band setting in the visible and near infrared part of EMS. It acquires data with spatial resolution of 300 m (full resolution mode), allowing for analyses at regional to global scale. Main focus of this paper is laid upon the vegetation cover dynamics at the Niger Inland Delta and the neighbouring Plateau du Bandiagara with the help of MGV Index.

**Keywords:** ENVISAT MERIS, land cover change, MGVI.

## 1 GEOGRAPHIC SITUATION

The ecoclimatic zones of Sahelian Africa are characterised by a three months rainy season from July to September and a nine months dry season respectively. In contrast to its semi-arid environment, the Niger Inland Delta's ecology can be described by a mosaic of permanently, periodically and not-periodically flooded areas. Their extent varies both in scale and in time due to irregularities of amount and seasonal distribution of annual rainfall in the catchment areas and the resulting water supply contributed by the river system. While the Inland Delta is dominantly covered by irrigated fields or grasslands during flood and post-flood months (late July til October to January), most of the photosynthetically active vegetation withers during the rest of a year. The fact that water is available throughout the year or at least during certain periods of the dry season forces increasing human impact on vegetation and soils. The ecological balance of semi-arid Sub-Saharan regions in general and of the Niger Inland Delta in particular is out of equilibrium due to specific varieties of destabilizing input factors.

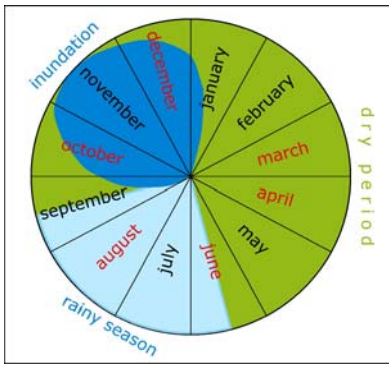


**Figure 1**: Niger Inland Delta - seasonal dynamics, red months denote acquisition dates within a year.

From the above mentioned water regime result 2 seasonal variation cycles, a rainy – dry cycle and a flooding-drainage fluctuation, as illustrated in Fig. 1. These 2 cycles appear with a temporal delay of about 3 to 4 months and are superimposed by a 3rd variation that counts for several years (fluctuation between dry years and years with sufficient precipitation). This latter cycle is dominantly affected by the 2 seasonal ones, but high spatial variability of precipitation does not permit a causal linkage. In particular, low amount of rainfall in the delta may profit from extended rainfall in the headwaters, thus inducing reasonable extent of flooding.

Availability of water represents the main restricting factor for vegetation growth in the Sahel. Vegetation follows the above described water cycles with a temporal delay, which may vary from few days (germination of grasses) up to several months (death of trees caused by lack of water). Development of (annual) grasslands with sparsely distributed patches of shrubby vegetation dominantly composed of Combretaceae sp. is characteristic for the Sahelian landscape, [1], [2] and can according to [3] and [4] be categorised into three layers:

(a) grass layer with annual grasses and herbs (height 40 cm – 80 cm)

(b) shrub layer (height 50 cm –300 cm)

(c) tree layer, sparsely distributed single trees (height 3 m to 6 m).

Ligneous layers of shrubs and trees cover only small parts (up to 25%), while grassy layers extend over up to 80% of the surface, [5]. Annual grasses are withering during dry season. Thus grassy layers are affected and/or destructed by bush fires and strong winds. Patterns of bare soil appear and extend during the mid- and late dry season.

Beside semi-natural vegetation cover, large areas of the delta are used for rainfed (sorghum) and irrigated (rice) agriculture. Annual and perennial grasses prevail within the banks of the mare and along the mayo. These areas serve in the late dry season as pasture for nomadic or transhumant cattle breeders. They are especially valuable, as mares outside the delta are parched during mid-dry season at latest. See Fig.2 for a landscape profile of the Inland Delta.

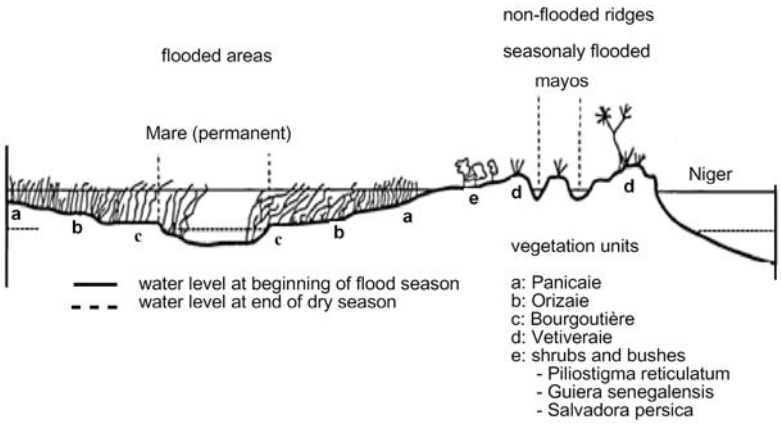


**Figure 2.** Subsection of Niger Inland Delta – landscape profile. Adapted from [6].


**Figure 3.** Area of Interest.

Current research focuses on the central Inland Delta itself and the adjacent Plateau du Bandiagara, which is strongly related to the delta both in terms of socio-economic as well as socio-ecological aspects. The region of interest lies in between 15°48'N, 5°12'W / 13°24'N, 2°54'W and is indicated in Fig. 3 by the red rectangle.

Seasonal changes were analysed with a time serie of 5 MERIS Level 1B datasets from 2002/03. August displays the situation at end of rainy season. October coincide with beginning of flood period. Imagery of December provides information about the extension of the flood. April data document the situation at mid-dry season and June imagery shows late dry season.

## 2 MERIS DATA CHARACTERISTICS

Medium Resolution Imaging Spectrometer (MERIS) as a payload of European environmental Satellite ENVISAT was launched into space in March 2002. The optical sensor collects data at full mode with a spatial resolution of 300 m or at reduced mode with 1200 m resp., thus allowing for landcover analysis at regional to global scale. The instrument measures reflected Top Of Atmosphere radiances in 15 bands in the spectral range 408 - 905 nm. Coverage of the entire earth surface within an interval of 3 days is possible due to a swath width of 1150 km. [7]

MERIS offer great potential for detection of absorption characteristics related to seasonal and annual variations in the photosynthetic activity of leaf pigments (chlorophyll a and b, antocyanine or carotenoids), thanks to its narrow bandwiths of mostly 10 nm. Ratios of near-infrared and red bands allow for computation of vegetation indices. The analysis of water colour provides information on the condition of open water surfaces, thus allowing for the detection of variations in sediment concentration indicating occurrence and extent of current. As water reflectance or absorption features occur in very small bandwidths of the electromagnetic spectrum (EMS), MERIS will allow for new applications in this field.

Limiting factor is the geometric resolution of MERIS data. As each MERIS pixel covers 90.000 m², monitoring at regional to global scale is possible. Investigation at local level is restricted to areas with homogenous landcover situation. While this restriction may sound rather deplorable, one have to keep in mind that MERIS offers improved spatial resolution anyway compared to longliving NOAA-AVHRR and even in relation to MODIS.

## 3 PREPROCESSING

While the MERIS sensor measures reflected sun radiation with the help of CCD technique, all spectral measurements are made by individual sets of sensors (of the CCD) for each pixel along an image line. This causes small variations of the spectral wavelength of each pixel along the image line and is known as "smile effect". For the MERIS instrument the variations per pixel are in order of 1 nm between adjacent cameras, while they are in order of 0.1 nm within one camera. To avoid disturbances in further processing steps, we corrected all images for the smile effect with ESA's Level 2 smile correction algorithm as it is implemented in BEAM 3. 2 software [8]. After performing this preprocessing step we obtain MERIS data with normalised wavelengths within one spectral band with respect to the relevant reference wavelengths. All future analyses were performed with these smile-corrected data.

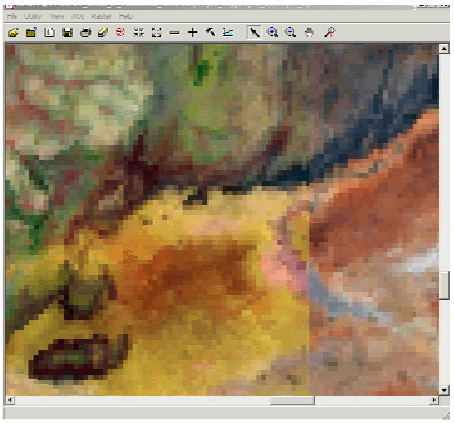

**Figure 5.** Superimposed Orthoimages April (left) and June (right) 2003.

MERIS data are, as all remote sensing data in the optical range of the EMS, affected by atmospheric influences and the variable solar irradiance. To enable a sophisticated comparison it's necessary to convert the sensors TOA radiance values into surface reflectance values (SR). For this atmospheric correction we used the *S*implified *M*ethod for *A*tmospheric *C*orrection (SMAC), described in [9]. We excluded pixels that are affected by clouds during the correction process with the help of the quality-flags that ESA provides within the MERIS Level 1B data. This exclusion worked only suboptimal, as pixels at the very edges of clouds or those that are hazy, could not be detected with this method. Therefore, we had to create mosaics from datasets that have similar acquisition dates (only a few days delay) and are at least partly cloud free.

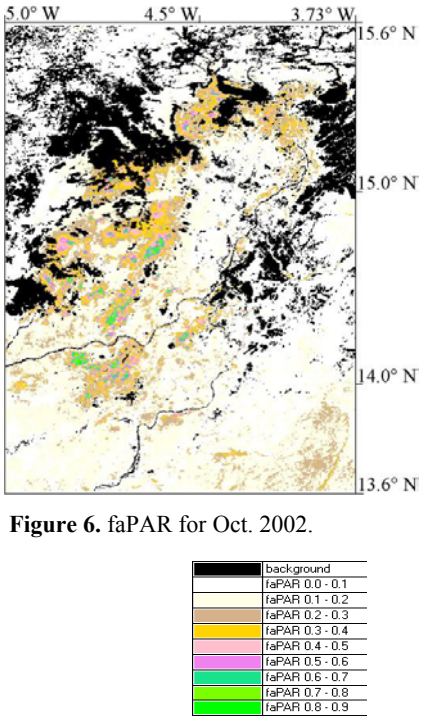


**Figure 6.** faPAR for Oct. 2002.

For change detection purposes it's necessary that all considered images refer to a unique projection. To assure this and to remove parallaxes, resulting from varying acquisition conditions, we orthorectified all images. As source for elevation information we used the GETASSE30 DEM and got Orthoimages with respect to the WGS84 ellipsoid. All these steps were performed with the software package BEAM version 3.2 [8].

Without precise GCPs available, it is hardly possible to validate the absolute accuracy of the orthorectification. Compared with topographic maps at scale 1 : 200.000 all Orthoimages showed good correspondence, no displacement of features were observed. The relative accuracy between Orthoimages is below ½ pixel and is illustrated for a part of the central Falaise du Bandiagara at Fig. 5.

## 4 VEGETATION COVER ANALYSIS

Investigation about the state and/or the amount of vegetation is one of the main objective in the field of land surface related remote sensing applications. Many methods and in particular various vegetation indizes have been introduced, to quantify certain vegetation parameters. All of them take into account that vivid green vegetation shows a specific reflection signal in the red and near infrared part of the electromagnetic spectrum. Among others, the Normalised Difference Vegetation Index (NDVI) has a long and far reaching history in serving as index for quantifying green vegetation cover. Its simple calculation may be one reason for the common usage, although various problems are also commonly known, when it comes to the evaluation of the index values.

A specific problem for vegetation analysis in semi-arid environments is the low vegetation cover. Thus the at the sensor received backscattering is likely a combination of soil related and vegetation related signal. Pixel values represent therefore mixed information. This rises the question of 'how to separate the soil signal (or more general spoken the background signal) from the vegetation related signal part?'. To overcome this issue [10] proposed a replacement of the red channel at NDVI by a polynomial combination of the red and blue channels of the used sensor. The same principle but in an extended manner follows the MERIS Global Vegetation Index (MGVI), that was introduced by [11]. This index combines the red channel as well as the near infrared channel with the blue one by separate polynoms that consider varying illumination and viewing geometry within the image. In addition to an index value that represents the faPAR, a MGVI calculation provides several flags that can be used to evaluate pixel with invalid index values. With the help of these flags a separation of bare soil and water bodies from vegetated areas seems to be promising. Fig. 6. illustrates the faPAR values in October 2002 for the Central Inland Delta. The background in this image consists of areas with bare soil, water bodies and cloud affected pixel.

## 5 STATISTICAL ANALYSIS

### 5.1. Water Bodies

Using the flags that are provided as sideeffect of the MGVI processing, we analysed the temporal behaviour of water bodies in the Central Inland Delta. Therefore we superimposed the relevant water masks for all 5 acquisition dates and classified this multitemporal image. Numerous small patches of temporary flooded Mare appear around the major lakes in the Northern section of the Inland Delta (Lac Débo and Lac Kourientze), as can be seen in Fig. 7. Their time of flooding depends on the arrival of the high water of river Niger. Therefore the northern sections are inundated later (during december, indicated by cyan) than the central und southern parts of the Inland Delta (indicated by red and magenta). Irrigated agriculture near the city of Mopti during flood period is well illustrated by the large areas in magenta.

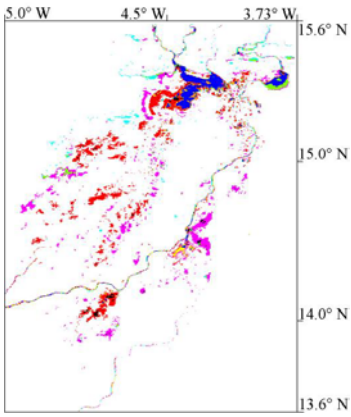


**Figure 7.** Water bodies, according to MGVI flag.

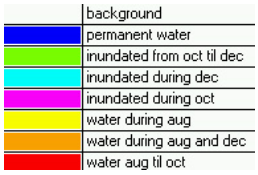


### 5.1. Temporal Behaviour of Vegetation Types

As MGVI provides an estimation of faPAR and faPAR follows the specific vegetation cycles during a growth season, it is possible to classify the different types of vegetation – those that are induced by the rainy season and the other(s) that is/are induced by inundation – by using MGVI.

**Table 1.** Scattering between ISODATA with 4 classes and 8 classes (relative count of pixel).

| | inundation, marginal | rainy, marginal | rainy, strong | inundation, strong |
|---|---|---|---|---|
| rainy | 15 | 18 | | |
| rainy, mean | | 16 | | |
| inun, early | 5 | 19 | 13 | |
| rainy, strong | | | 17 | |
| inun, cont. | 7 | 10 | 12 | 8 |
| inun, early - strong | 3 | 4 | 6 | 11 |
| inun, late - strong | | | 2 | 14 |

To test how many groups of vegetation can be distinguished by their temporal patterns, we applied the ISODATA algorithm with varying numbers of initial classes. At the beginning, we used 4 classes, that were increased later to 8 and finally to 12 initial classes. While semi-arid and wetland vegetation can be distinguished already in the 4 classes case, a separation of vegetation groups within these two supercategories becomes even with 12 initial classes not very reliable, as can be seen at the temporal signatures given in Fig. 8. Only the discrimination of wetland vegetation in early and late growing once seem to be reasonable. As shown in Tab. 1, significant interference exist between vegetation groups that have their origin in the rainy season and in early flood. The 2 classes that represent semi-arid vegetation in the 4 classes case were splitted into 3 new classes each, although one of the initial equally distributed 8 classes becomes empty during the iterative ISODATA processing with 8 classes. This indicates, that the temporal behaviour of the vegetation, and therefore the different groups of vegetation, can't be described sufficiently with 4 classes and that the changes in faPAR values occur with more than one period. The later conclusion yields to the need of data in a high repetition rate, especially for the time slot from the end of rainy season to the first half of the flooding phase. While during the end of the rainy season and early flood period the

changes in faPAR occur rapidly and with great amplitude, the changes from end of inundation towards rainy season take place with less speed.

The transition from 8 classes towards 12 classes show a similar situation for only one class. The fast changing situation between end of rainy season and inundation was not sufficiently described with the 8 classes case. But all other vegetation groups were reasonable classified within the 8 classes case already. A mapping of the temporal course of faPAR values based on the ISODATA classification with 12 initial classes is given in Fig. 9, while Tab. 2 provides the scattering of classes for the ISODATA 8 classes and 12 classes instance.

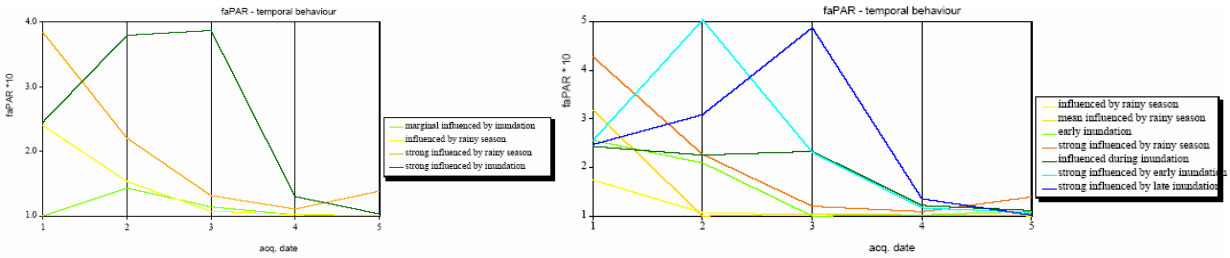


**Figure 8.** Temporal signatures of faPAR values for ISODATA classification with 4 classes (above right), 8 classes (above left) and 12 classes (below).
The acquisition dates are 1 – Aug. 2002, 2 – Oct. 2002, 3 – Dec. 2002, 4 – Apr. 2003, 5 – June 2003.

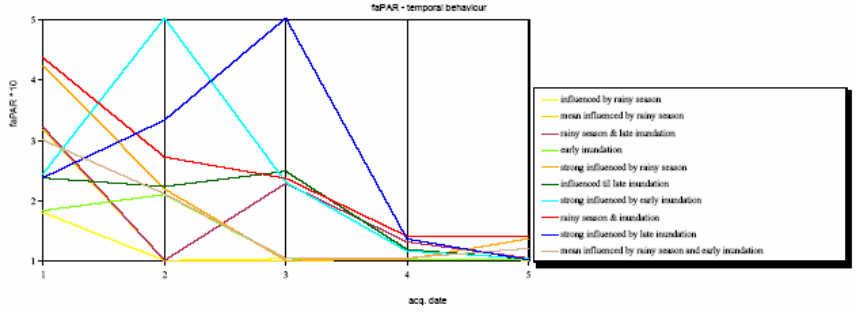


**Table 2.** Scattering between ISODATA with 8 and 12 classes (relative count of pixel).

| | rainy | rainy, mean | inun, early | rainy, strong | inun, cont. | inun, early - strong | inun, late – strong |
|---|---|---|---|---|---|---|---|
| rainy | 27 | | | | | | |
| rainy, mean | | 24 | | | 9 | | 3 |
| rainy & late inun. | 2 | 14 | | 4 | 13 | 7 | |
| inun., early | 17 | | 25 | | | | |
| rainy, strong | | | 26 | 23 | | | |
| inun., late | | 1 | 19 | 8 | 16 | 5 | |
| inun., early - strong | | | | | 22 | | 15 |
| rainy & inun. | | | | | | 20 | |
| inun., late - strong | | | | 18 | 12 | 10 | 11 |
| rainy, mean & inun, early | | | | | | 6 | 21 |

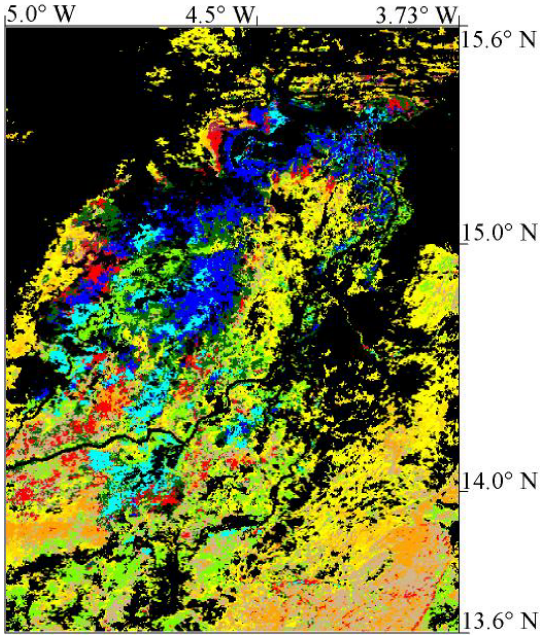


**Figure 9.** Temporal behaviour of faPAR, ISODATA classification, 12 initial classes.

## 6 ASSESSMENT OF THE CLASSIFICATION RESULTS

As the vegetation types that are influenced by inundation rely on the water that comes along the flooded rivers, those types should be found at lower altitudes only, but vegetation that rely on precipitation should be possible to find at all altitude levels. To assess these dependency we used the digital elevation model SRTM-DEM as it is described by [12]. After filling the gaps in the original data with interpolated values, we grouped elevation values into equidistant groups at an 40 m intervall.

A mean elevation group (< 260 m = 1, 260 < 280 m = 2, …, 560 < 600 m = 11) and the standard deviation was then calculated for each vegetation type within the last 2 rows. This statistic illustrates the separability of vegetation types along the elevation – the more a vegetation is influenced by precipitation the more it is distributed over all altitudes and the more it is influenced by inundation, the more it is concentrated at the lower altitudes. The later case is characterised by lower mean and a smaller standard values. But the statistical analysis shows also very clearly the problem to discriminate vegetation that is influenced by precipitation and/or early inundation. In these cases (columns 4, 8 and 9) the mean altitude as well as the std. dev. doesn't seem to be very reliable.

The 3 right columns contain the percentage of pixel for each elevation intervall that have been classified as rainy, inundated or rainy & inundated vegetation respectively. This calculation show a significant decrease for inundated vegetation for the higher altitudes. Although it remains to conclude that the classification performs not realy satisfactory as pixel that are classified as "inundated vegetation" at elevations above 320 m are not realiable detected.

**Table 3.** Distribution of vegetation classes over elevation intervals.

| | rainy | rainy, mean | rainy & late inun. | inun., early | rainy strong | inun., late | inun., early - strong | rainy & inun. | inun., late - strong | rainy, mean & inun., early | % class. as rainy | % class. as inun. | % class. as rainy & inun. |
|---|---|---|---|---|---|---|---|---|---|---|---|---|---|
| 560 m < 600 m | 2 | | | | | | | | | | 100% | | |
| 520 m < 560 m | 24 | 15 | | 7 | 13 | | | 2 | | 2 | 82,5% | 11,1% | 6,3% |
| 480 m < 520 m | 44 | 35 | | 40 | 58 | 6 | 9 | 34 | | 43 | 50,9% | 20,4% | 28,6% |
| 440 m < 480 m | 59 | 52 | | 49 | 77 | 16 | 19 | 48 | | 67 | 48,6% | 21,7% | 29,7% |
| 400 m < 440 m | 85 | 72 | 5 | 54 | 73 | 11 | 14 | 41 | | 55 | 56,1% | 19,3% | 24,6% |
| 360 m < 400 m | 87 | 83 | 2 | 60 | 62 | 20 | 18 | 36 | | 54 | 55,0% | 23,2% | 21,8% |
| 320 m < 360 m | 88 | 82 | 4 | 68 | 67 | 17 | 10 | 31 | | 41 | 58,1% | 23,3% | 18,6% |
| 300 m < 320 m | 75 | 69 | 8 | 55 | 64 | 30 | 27 | 42 | | 69 | 47,4% | 25,5% | 27,1% |
| 280 m < 300 m | 81 | 70 | 26 | 61 | 63 | 45 | 38 | 50 | 3 | 88 | 40,8% | 28,0% | 31,2% |
| 260 m <280 m | 97 | 91 | 84 | 96 | 89 | 95 | 92 | 90 | 93 | 182 | 27,5% | 37,3% | 35,3% |
| < 260 m | 43 | 32 | 25 | 28 | 23 | 46 | 37 | 29 | 47 | 66 | 26,1% | 42,0% | 31,9% |

## 7 CONCLUSIONS AND FUTURE PROSPECTS

The MGV index is suitable for vegetation cover analyses on semi-arid environments. It provides an equivalent to the faPAR, that can be used as classificator for different vegetation types. The quality flags that come with the MGVI value, can serve as mask for water bodies and bare soil. Thus enabling a separation of the three main object categories with the help of only one index. To prove the suitability of MGVI for long time analysis, an extention of the time serie until 2005 is currently prepared. In this context it would be nice to have MGVI values on a regular 10 to 16 day basis for investigation on biomass production during a growth season and for interannual comparisons. The currently used dataset with its rather episodic distributed 5 acquisition dates per year does not permit sophisticated conclusions for an interannual time frame, as the arrival of the high tide varies as well as the temporal distribution of the flood. Therefore more data per time intervall are needed, especially between the end of rainy season and the early flood.

Research on soil types will be carried out in near future with additional information from ISRIC soil data base.

## ACKNOWLEDGMENTS

The authors like to thank ESA for providing ENVISAT-MERIS data in the frame of ESA-ENVISAT AO-776. K. Adenauer Foundation funded PhD work of Ralf Seiler. The authors like to thank also Ms. Elisabeth Vollmer and Ms. Jana Schmidt for fruitful cooperation during their Diploma thesis.

## REFERENCES

[1] BREMAN, H., AND DERIDDER, N., 1991 : Manuel sur les pâturages des pays sahéliens. Karthala, Paris.
[2] CSAPLOVICS, E., 1992: Methoden der regionalen Fernerkundung – Anwendungen im Sahel Afrikas. Springer, Berlin - New York.
[3] LEHOUÉROU, H.N., 1989: The grazing land ecosystem of the African Sahel. Springer, Berlin New York.
[4] CSAPLOVICS, E.; 1998: Integrative Methoden der Dokumentation und Analyse lokaler Desertifikationsprozesse im Sahel Afrikas – zur Bedeutung von Fernerkundung und geographischem Informationssystem, Die Erde 129, pp. 195-210.
[5] KUßEROW, H., 1995: Einsatz von Fernerkundungsdaten zur Vegetationsklassifizierung im Südsahel Malis. Verlag Dr. Köster, Berlin.
[6] DIALLO, O. A., 2000 : Contribution à l'étude de la dynamique des écosystèmes des mares dans le Delta Central du Niger, au Mali. Thèse, Université Paris I.
[7] MERIS HANDBOOK, http://envisat.esa.int
[8] BEAM HANDBOOK, http://scipc3.scicon.gkss.de/beam/documentation.html
[9] RHAMAN, H., DEDIEU, G., 1994: SMAC: a simplified method for the atmospheric correction of satellite measurements in the solar spectrum. Int. J. Remote Sensing, Vol. 15, Nr.1, pp. 123 – 143.
[10] ESCADAFAL, R., ALBINET, F., 2005: Remote Sensing of low vegetation cover for desertification monitoring in arid regions. presented at Remote Sensing and Geoinformation Processing in the Assessment and Monitoring of Land Degradation and Desertification - RGLDD, Trier, Sept. 2005.
[11] GOBRON, N., MÉLIN, F., PINTY, B., TABERNER, M. AND VERSTRAETE, M. M., 2003: MERIS Global Vegetation Index: Evaluation and Performance. IN: Proc of the MERIS User Workshop, Frascati, Italy, 10-14 November, European Space Agency SP 549.
[12] CHARACTERISTIC OF SRTM-DEM, http://www.jpl.nasa.gov/srtm/

# Integrated environmental and socio-economic modeling using LIES for desertification monitoring and assessment in the observatory of Menzel Habib (South Tunisia)

M. Sghaier[a], M. Ouessar[a], E. De Laitre[b], D. Leibovici[b], M. Loireau[b], L. Bennour[a], M.A. Ben Abed[a], M. Fetoui[a], A. Ouled Belgacem[a], A. Tbib[a], H. Taamallah[a], R. Boukhchina[a], D. Ouerchefani[a] and H. Dhaou[a]

[a] Institut des Régions Arides (IRA), Médenine, Tunisia, email: S.Mongi@ira.rnrt.tn
[b] Centre IRD, Montpellier, France

## ABSTRACT

In the frame of the implementation of the national action plan (NAP) as part of the UNCCD, a network of observatories for the assessment and monitoring of desertification has been set covering the main agro-ecological zones of Tunisia. Menzel Habib represents one of the main observatories in a typical arid zone threatened by desertification. It was chosen and certified as ROSELT/OSS site. This site is part also of the arid zones observatory implemented by IRA in the frame of the national monitoring system of desertification coordinated by the national focal point of the UNCCD. It is in this framework that the GIS based model LEIS (Local Environmental Information System) (in French known as SIEL) developed by the ROSELT team in Montpellier [1] was applied to this observatory. The used data was issued from achieved and on going multidisciplinary monitoring of the observatory covering the biophysical (soil, water, climate, vegetation) as well as the agro-socio-economic (population, agriculture and pasture practices, land uses, etc.) aspects. Three types of information were used: remotely sensed data (satellite images), field measurements (vegetation biomass, yields, GPS, etc.), and socio-economic surveys (households, income, activities, etc.). All these information have been integrated in a GIS environment (ArcGIS) and the model was run to produce spatial ecological and agricultural balances at the level of the observatory. Then, multiple scenarios have been conducted to assess the impacts of changing one or many parameters (population, drought recurrence, livestock, wood consumption, etc.). In fact, the final output of the model is to make at the disposal of the various actors of development, researchers and technicians, a Spatial Decision Support System (SDSS) for planning and monitoring of combating desertification plans and natural resources management in the dry areas.

**Keys words:** Desertification, monitoring, evaluation, local, modelling, LEIS, observatory, Tunisia.

## 1 INTRODUCTION

Desertification threatens around 52 % of the land area of Tunisia suitable for agriculture, forestry and pasture farming [2]. The loss of land productivity has been triggered by incompatible forms of land use that result in soil degradation and salinisation, water and wind erosion.

Tunisia has an ancient tradition of combating land degradation and desertification. In fact, the country has been seeking solutions to these problems with own means and international support for a long time ago. However, the investments and organization of the efforts of combating desertification started right after the independence within the framework of the various strategies for the protection and management of natural resources, and lastly within the implementation of the national action programme to combat desertification (NAP-CD) ratified in 1998 as part of the UNCCD [2]. The CCD urged that combating desertification cannot be limited to only technical measurements but must, on the contrary, be considered like as complex unit of coherent actions by taking into account its socio-economic dimensions as well as the biophysical and environmental aspects. In fact, chap. 12 of Agenda 21 and Art. 16 of the CCD recommend developing of desertification control dashboards to enable a better understanding, by decision-makers and stakeholders, of the phenomenon and efficient joint action to curb its unfavorable effects.

It is for that reason that the CCD signatories admitted the importance to control the monitoring/evaluation of combating desertification programs and that the national focal point (NFP) would have a global vision of the process of implementation of these programs.

The decentralized implementation of NAP, by giving more importance of the role of the local actors, strongly challenges the national decision makers to take up the challenge of decentralization, dialogue and the coordination of the actions between the various actors at different levels: national, sub-national, and local.

The OSS developed an environmental monitoring program which aims at supporting the setting up, by the countries, of dashboards of combating desertification to serve the implementation of national policies for environment protection and sustainable management of natural resources. This program includes projects and initiatives for environmental monitoring at various levels and by various means, from the field study to the low and high-resolution satellite images. It focuses on supporting the setting up, by the concerned countries, of environmental monitoring mechanisms to support decision to serve the development. Its components: NAP monitoring-evaluation Indicators , Climatic change in the context of drought and desertification, ROSELT (long-term ecological observatories monitoring network), IMAGES (satellite images for meteorology, agrometeorology and environment management in the Sahel-Saharan zone and information system on desertification (SID) contribute, on the regional level, in a better understanding of the desertification process thus enabling African and European scientific institutions to develop methodologies for co-observation of environmental inter-observatory measurements either on the ground or using satellite images [3].

With the development of GIS and spatial information technologies, huge successes have been gained at the large scale levels. Nevertheless, still some difficulties remained at the local scale due mainly to the related high costs relates to the setting up of heavy monitoring networks, the integration of the various ecosystem components (biophysical, socio-economic, etc.), the specificities of local sites, and the difficulties related to the management and handling of the databases (RS, surveys, biophysical, etc).

It is in this framework that Tunisia has set up a bunch of observatories scattered throughout the country based on the agro-ecological and socio-economic zoning [4]. Menzel Habib, the study site of this paper, is one of the eight observatories of the arid zones of the country and it is also certified by the ROSELT network [5]. Therefore this paper aims to:

- Test, at the local level of the ROSELT/OSS and NAP observatory of Menzel Habib, of the LIES model developed by the Roselt team,
- Set up of an integrated environmental and socio-economic desertification monitoring network,
- Explore the possibilities of developing a spatial decision support system (SDSS) to be used by the local development agencies and decision makers.

## 2 MATERIALS AND METHODS

### 2.1 Study Site

The observatory of Menzel Habib is located between the parallels 34° and 34° 20° north, and meridian 9° 15' and 9° 58 ' east (figure 1). It forms part of the natural area of the low southern plains of Tunisia. With annual precipitations of about 150 mm/an, it is localised in the lower arid Mediterranean stage bioclimatic with mild winter. The water resources constitute the most constraining in this region. The soil potentialities are diversified but present various constraints related to texture sensitive to erosion and poor fertility. The principal vegetation formations are represented by the steppe with *Rhanterium suaveolens* on sandy soils. On the sandy loam soils, the steppe is based on *Arthrophytum scoparium* and of the post-farming formations based on *Artemisia campestris* or of *Haplophyllum vermiculare* substituting steppe with *Artemisia herba-alba*. On soils with crusts, the dominant vegetation formations are characterized by *Gymnocarpos decander* and *Atractylis serratuloides*. Under the effect of the extension of cropped areas, clearing and pastoral overexploitation, the steppe formations regress rapidly and even with an alarming speed in some cases [6].

Menzel Habib is a rural county occupying the north-western part of the province Gabès. Created in 1982, it covers an area of about 100,000 ha. The censuses of 1994 indicate that the local population is of 11,700 inhabitants forming 1818 households. The social and economic changes, which happened during the last four decades, have seriously affected the traditional ways of life and the forms of adaptation to the climatic aridity. Demographic rise, the sedentarisation of herderss, the privatization of the land, the liberalization of the economy, modernization of the agriculture and the changes of the modes of use and of exploitation of grazing space constitute active elements of ecological and socio-economic dynamics of the area. Many actions and programs for combating desertification have been undertaken in the region. However, the impacts on the livelihood of the local population are far below the sought objectives in spite of the full engagement of the various research and development structures [7].

The area is strongly marked by an anthropisation related to a pastoral operating system which induced important ecological and socio-economic disturbances. The extension of the rainfed cropped areas has been done at the

expense of the rangelands in the plateaux and the plains. The irrigated agriculture starts also in certain sectors to mark the agrarian landscape. Nowadays, the anthropisation of the medium has reached a level which arises seriously questions on the ecological future of the area and the sustainability of the undertaken social and economic development actions [8].

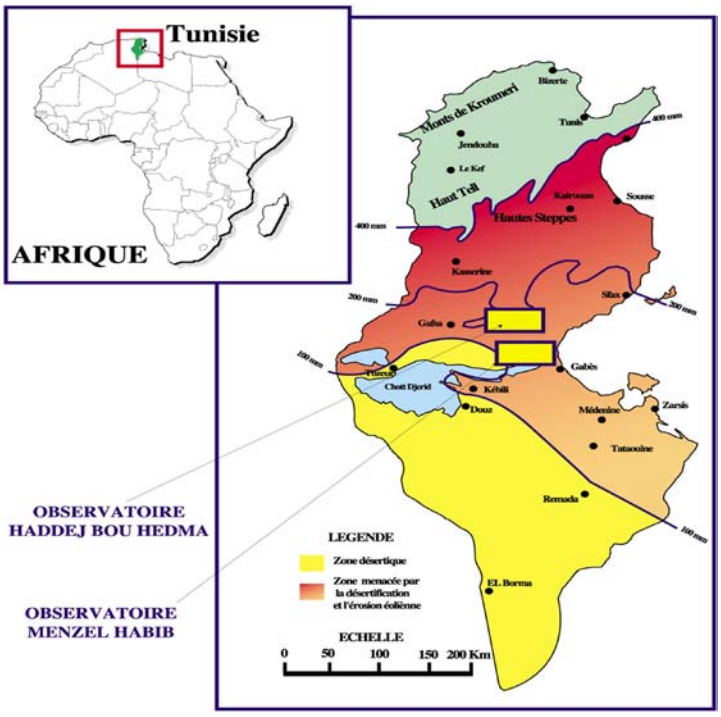


**Figure 1.** Location map of the observatory of Menzel Habib (South Tunisia).

## 2.2 LEIS Model

LEIS (Local Environment and Information System) model was developed by the ROSELT team [1]. It is a conceptual and IT based tool which is to be developed for every observatory in the network. The objective of LEIS-ROSELT is to integrate variable data, such as bio-physical and socio-economic data, and to facilitate the processing of this data into products for the interpretation of the causes, consequences and mechanisms of desertification, for the monitoring of environmental change at local level.

The LEIS implemented within the ROSELT/OSS observatories, are focused on the spatial integration of the dynamic interactions between populations and the environment, in particular through their expression in rural space in terms of uses and resources. Further details are found in [1].

## 2.3 Methodology

The methodology applied is stepwise made of 5 main stages until reaching the final results as shown by figure 2.

### 2.3.1 Step 1: Exploitation Territories (ET) construction

The delineation of the Exploitation Territories (ET) is the first step of modelling. It was based on the selection of 22 activity centres according to the structuring activity (agricultural territories) of the observatory. The exploitation territories are modelled by a centred model, based on the weighted Thiessen algorithm [1]. Classically, the standard formula is : $\sqrt{weight / dis\tan ce}$

Several criteria are combined by the algorithm are linked to a different weight:

The Population criterion makes reference to the population that exploits the territory resources according to the structuring activity, linked to the Activity Centres (AC) and to the Strategic Groups (SG).

The age criterion makes reference to the AC, the age minimum and age maximum take into account the evolution history of the population in the observatory. Values of age min and age max were estimated to 20-50 years and 23-60 years, respectively, during the modelling period (2001-2004).

The threshold distance of access to resources indicates the travelling distance to be crossed by the population resident in each AC in order to have access to resources in the observatory. It was estimated for the whole AC between 4 and 35 km .

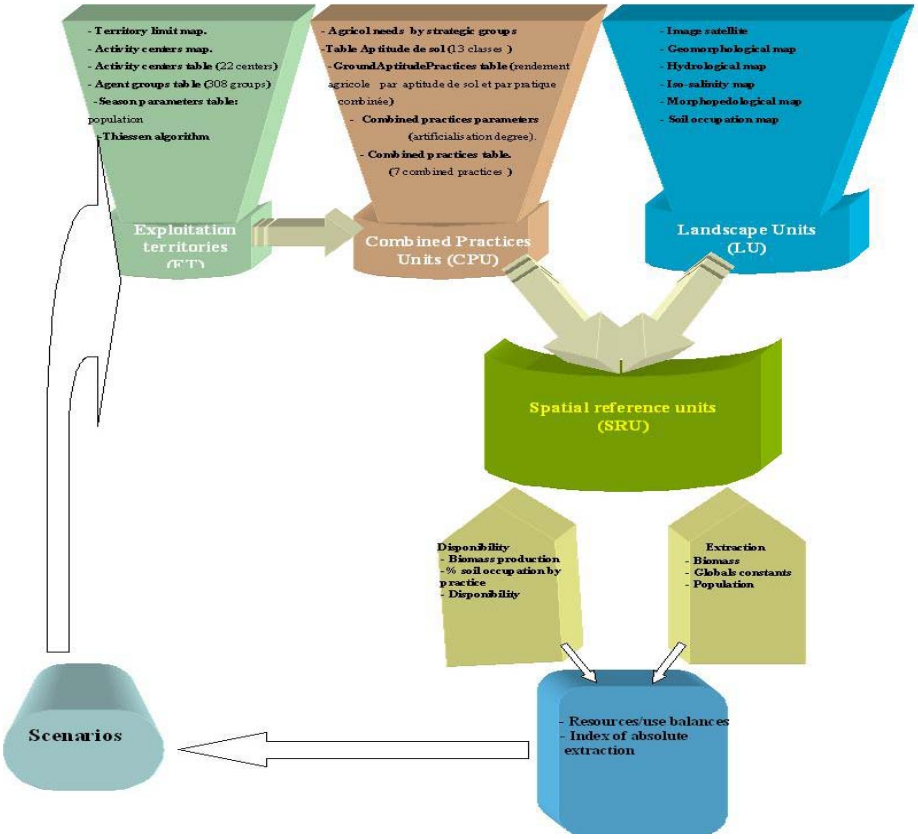


**Figure 2**. LIES modelling phases as applied to the observatory of Menzel Habib.

The selected modelling period spreads over 4 and corresponds to the period 2001-2004, considered to be representative of the climatic and physical characteristics of the observatory of Menzel Habib.

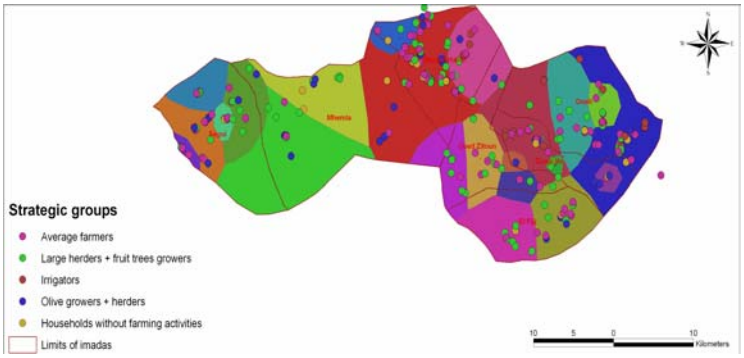


**Figure 3.** Spatial distribution of the strategic groups.

Two agent groups were identified, a Human Agent Group (HAG) and an Animal Agent Group (AAG) for each AC. For the HAG, one typology of the Strategic Groups (SG) was elaborated according to the resources exploitation strategies in the observatory. The multidimensional methods (factorial correspondence analysis method and ascending hierarchical clustering method) were used on the basis of data collected from field surveys (305 households interviewed in 2004). The human strategic groups (HSG) are:

- Large herders + fruit trees growers (106 households, 35 %),
- Olive growers + herders (41 households, 13.5 %),
- Households without farming activities (23 households, 7.5 %),
- Average farmers (114 households, 37 %),
- Irrigators (21 households, 7 %).

Figure 3 shows the spatial distribution of the identified strategic groups.

The animal strategic groups are defined according to a typology based on the mode of control and the mobility of the animal herds:

- Non transhumant herds.

- Transhumant herds in the observatory of Menzel Habib.
- Herds transhumant outside the observatory of Menzel Habib.

### 2.3.2 Step 2: The Combined Practices Units (CPU) construction

This stage consists in building the map of CPU which requires the determination of the combined practices characterizing the observatory. 7 combined practices were identified: PC0: No practice, PC1: Olive trees behind jessour, PC2: rainfed olives, PC3: Cereals, PC4: Olive behind tabias, PC5: Irrigated system, PC6: Pastoral practices.

The needs are defined as the exploitation necessary for life for groups of individuals on the exploitation territory. They are calculated based on the bio physical and socio economic data collected by the monitoring set up in the observatory. The percentages of land use per practice combined were also estimated.

Finally, the combined practices were spatially distributed based on the estimate of the degree of artificialization, which expresses the degree of the man made efforts in term of investments brought to the environment, on one hand, and the soil characteristics, on the other hand.

### 2.3.3 Step 3: The Spatial References Units (SRU)

The Spatial References Units (SRU) are polygons, of which the whole set covers the observatory territory; they make use of the notion of localised resources in the landscape, and the notion of usage and application on a given space by a combination of exploitation practices (agricultural, pastoral, forestry) defined below by combined practices [1]

The SRUs are obtained by crossing two types of geographical information: Landscape Units (LU) and Combined Practices Units (CPU) obtained in step 2.

The landscape is defined by the layer of LU, polygons whose characterisation is defined by [1]. Once this structuring into SRUs is modelled, it is possible to proceed to the calculation of resource/usage balances and to the calculation of indicators of resource degradation risks or desertification risks.

### 2.3.4. Step 4: The resource/usage balances and calculation of indicators

To create spatial resource/usage balances and to calculate indicators, the needs of the population and the resources available are estimated and modelled by LEIS. The balances and indicators are calculated per year, though the resource extractions can be calculated per season and accumulated to evaluate the annual resource extraction.

From the calculations of resource extractions, available resources and balances, it is possible to calculate indicators. The main indicator is the Absolute Resource Extraction Index (AREI) for a usage. It corresponds to the relationship between the resource extractions (P) and the available resources (D) for the current SRU [1]: AREI =P/D. It is therefore possible to produce balance maps or desertification risk index maps.

The data are obtained from the field biophysical system of surveillance (several local and meteorological stations are implemented in the observatory to observe the biophysical parameters as land cover, biodiversity, soil characteristics) and from the socioeconomic surveys carried out in 2004 and 2005.

### 2.3.4 Step 5. Scenarios

To create a scenario, some specific LEIS parameters have to be changed. The scenarios are presented according to the numeric and/or cartographic parameters from three general LEIS aspects: Usages aspect and resources aspect for which the parameters directly influence the first two aspects (there may be an accumulation of evolution scenarios). For this application, four scenarios have been tested:

Scenario 1 corresponds to a uniform double increase in all AC of the human and animal populations. It aims thus to assess the increase of pressure on resources.

Scenario 2 considers a human population increase by AC similar to that of the period 1994-2004. In this case, the rate of population increase varies from -14 % to + 244 %. The animal population was kept constant.

Scenario 3 differs from the last scenario by doubling the animal population in all the AC.

Scenario 4 aims to assess the potential extension of irrigation based on the availability of water resources (quantity and quality (salinity)). Then, the landscape units and soil suitability maps were modified.

## 3 RESULTS

As indicated in the methodology, the results of the model LEIS evolves from one stage to another until the development of the scenarios. In this part, we will present the main results of the model related to the reference situation as well as the scenarios.

The first stage allowed the development of the ET map corresponding to the 22 AC in the observatory of Menzel Habib (figure 4). It shows the relative importance of the territories of exploitations and the centres of activities of Menzel Habib, Sefia, Ouali and Zougrata with 14394 ha (15 %), 12558 ha (13 %), 8630 ha (9 %) and 7687 ha (8 %), respectively. The other territories of exploitation such as Ouled Souissi, Essoud, remain very reduced.

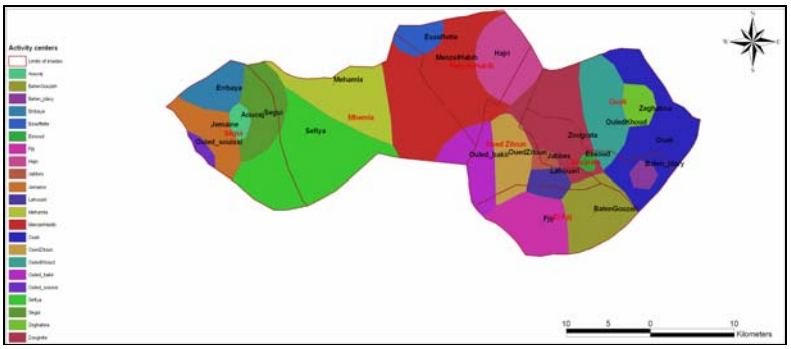

**Figure 4.** Map of the exploitation territories.

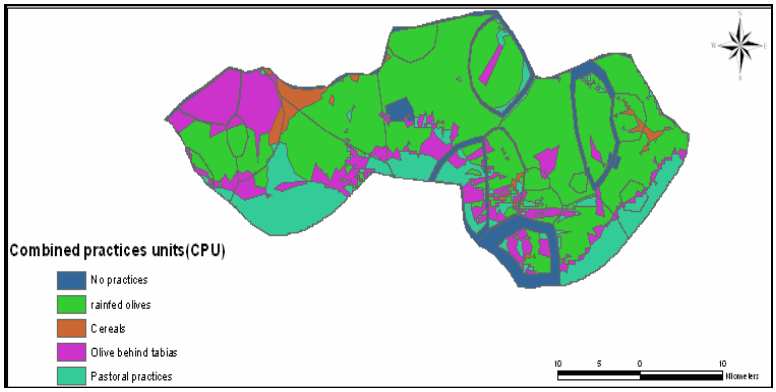


**Figure 5.** Map of combined practices units.

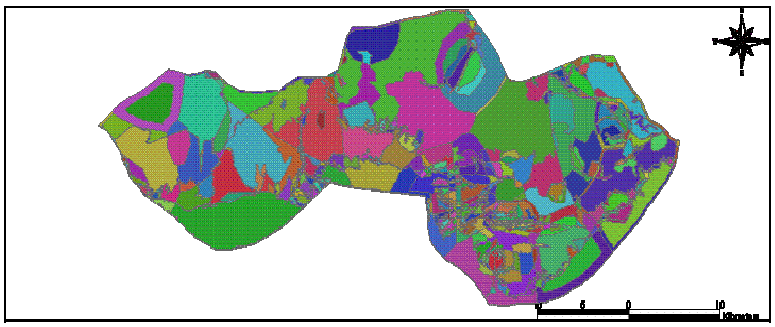

**Figure 6.** Map of the spatial reference units.

The CPU map CPU (figure 5) shows only five practices out of the initially considered seven CPU. It shows the prevalence of rainfed olives, olives behind tabias, and grazing (pasture) covering 48246 ha (50 %), 12107 ha (13 %) et 11815 (12 %) respectively. It seems that the map of the soil suitability and the adaptation of these practices to the biophysical and socio-economic conditions of the observatory explain these results. The non occupied area (21783 ha (23 %) is relatively large too.

The two CP of olives behind jessour and irrigation seem to be heavily constrained by the importance of the effort (equipment, input) and the artificialization degree required for their implementation.

The combination of the two maps of CPU and the PU produced the map of SRU (figure 6) which represents the basis for calculating the balance and the indicators. 1716 units RSU were identified.

The results of the spatial agricultural (case of olive trees) balance of resources/usage shows that the majority of the observatory (95319 ha (98.9%)) is in deficit. In fact, the maximum of risk (< 5000 kg) are recorded in 57020 ha, that is 59% of the observatory. Zones at average risk represent that 1.1 % of territory of the observatory (either 1069 ha). They are found mainly in the area of Sefia which receives additional runoff water from wadi Segui in the west.

The situation is improved in the case of the agricultural use based on cereals. Indeed, the balance resources/usage shows areas with low risk ( 20335 ha that is 21 %). The areas with maximum risk are absent whereas the areas with very high to high risk remain important (54854 ha that is 57%). This reveals that this observatory, pastoral vocation, is very vulnerable to the

agricultural activity and presents a high risk at all anthropic disturbances. These results are confirmed by the field observations and previous studies conducted in the same site [8, 9 10, 11, 12].

The results of the forest resource/usage balance reveal only one zone of maximum of risk located in the south west of the observatory. The areas where the with no extraction (zero risk) are dominant and cover 34573 ha (36%). This confirms the non forest vocation of the site because of the absence of forest ecosystem.

The pastoral resource/usage balance indicates that the area with maximum risk and very high risk cover 37254 ha that is 38.6 % of the observatory.

The results of estimate of the AREI confirm the tendencies revealed by the balance. In fact, the agricultural use "olive-tree" the area with maximum risk is important and reached 37511 ha that is 40% of territory (figure 7). For the cereals, the risk is less important. High to maximum risk are absent. The area at average risk (fulfilment by the resources of 45 to 62.5 % of the demands) are also reduced (3985ha that is 4 %) (figure 8).

For the pastoral use (figure 9), except a zone covering approximately 32128 ha (33 %) where forest extraction are null, the majority of the observatory present an indicator ranging between 0 and 45 % (cover rate of the extraction by the resources available). These results confirm the pastoral vocation of the observatory.

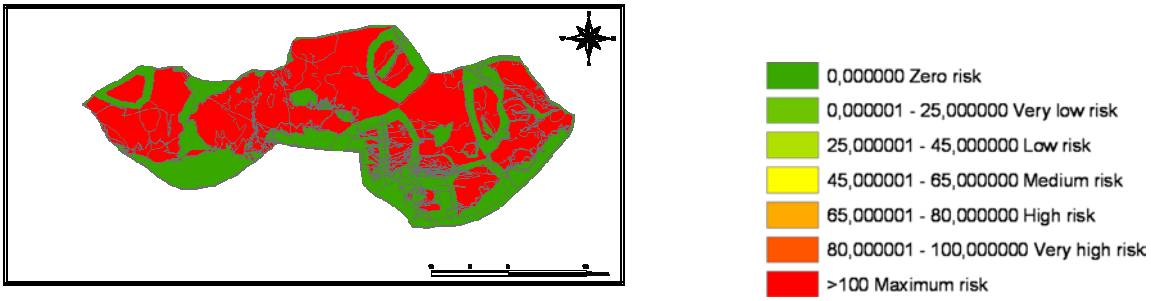


**Figure 7.** AREI (Olive-trees).

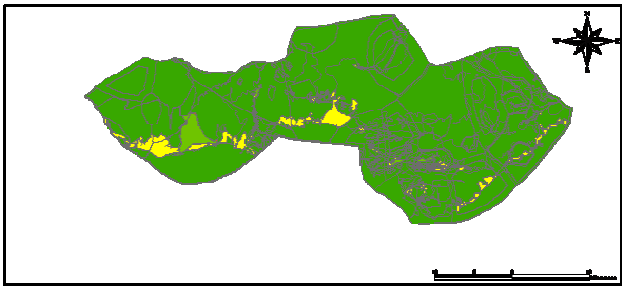

**Figure 8.** AREI (Cereal).

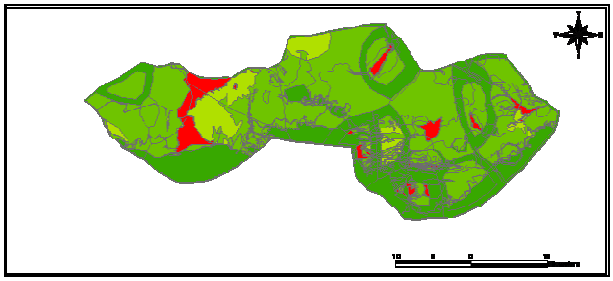

**Figure 9. Pastoral** extraction index.

The results of the 4 scenarios tested are summarized in the table 1 to table 5.

Scenario 1, which envisage doubling the human and animal population at the AC of the observatory, started to have effect only from the stage 2 (CPU). In this case, the ET map remains unchanged whereas the UPC and SRU maps as well as the results of the balance and the indicators may vary too.

For the UPC map, the unit "none practice" is reduced by 8528 ha, that is a reduction of 61 %, whereas the two CP "rainfed olives" and "olives behind tabias" recorded a significant extension by 14% 26%, respectively (table 1).

**Table 1.** Distribution of CPU by scenario.

| CPU | Reference modelling | Scenario 1 | Scenario 2 | Scenario 3 |
|---|---|---|---|---|
| **No practice** | 21783 | 8528 | 18635 | 21802 |
| **Olive trees behind jessour** | 0 | 0 | 0 | 0 |
| **Rainfed olive** | 48246 | 54913 | 49661 | 48429 |
| **Olive behind tabias** | 11815 | 14899 | 12568 | 11832 |
| **Cereals** | 2438 | 2536 | 2519 | 2441 |
| **Irrigated system** | 0 | 0 | 0 | 0 |
| **Pastoral practices** | 12107 | 15512 | 13004 | 11988 |
| **Total** | 96 388 | 96388 | 96388 | 96388 |

**Table 2.** Estimation of the pastoral Absolute Resource Extraction index (AREI) by scenario.

| Classes of desertification risk | Reference modeling (ha) | Scenario 1 (ha) | Scenario 2 (ha) | Scenario 3 (ha) |
|---|---|---|---|---|
| **Risk zero** | 32 128 | 22 363 | 21 308 | 32125 |
| **Very low risk** | 52 232 | 48 661 | 49 355 | 52235 |
| **Low risk** | 7 159 | 12 167 | 12 340 | 7159 |
| **Medium risk** | 96 | 2 576 | 2 612 | 96 |
| **High risk** | 10 | 2 257 | 2 289 | 10 |
| **Very high risk** | 15 | 3 053 | 3 097 | 15 |
| **maximum risk** | 4 749 | 5 312 | 5 387 | 4749 |
| **Total area** | 96 388 | 96 388 | 96 388 | 96 388 |

The results of the indicators show the aggravation of the situation for the agricultural use (olive-tree and cereals) and the pastoral and forest use. In fact, the areas of high risk and maximum risk evolved from 4774 to 10662 ha and from 2841 to 4623 ha, respectively. It confirms the assumption that the risk increases as a function of the effect of anthropic actions in this observatory.

Scenario 2 envisages a differential increase in population in the AC and a doubling of the animal population. Changes were recorded on the level of the results. In fact, the exploitation territories knew important variations (figure 10). For example, the are of the AC of Mehamla Ouled Khoud, Lahouarai and Sefiya, were extended by 44 % (9398 ha), 40 % (7256 ha), 36 % (17107 ha) and 28,5 % (1885 ha), respectively, whereas it was reduced in other such as Segui (-72.6 %) and Baten Jedary (-62.6 %) because of the negative growth of the populations. The maps of CPU and SRU did not know major changes compared to the reference situation.

The (ARI) relating to the agricultural activity (olive-tree) reveals a degradation of the situation. In fact, the maximum zone of risks increased by 17 % and reached an area of 68957 ha, that is around 70 % of the territory of the observatory. It indicates the extreme vulnerability of the natural environment to this type of activity and confirms the pastoral vacation of the observatory.

**Table 3.** Estimation of the Forest Absolute Resource Extraction index (AREI) by scenario.

| Classes of desertification risk | Reference modeling (ha) | Scenario 1 (ha) | Scenario 2 (ha) | Scenario 3 (ha) |
|---|---|---|---|---|
| **Risk zero** | 33 335 | 21 616 | 30 978 | 33 332 |
| **Very low risk** | 58 930 | 69 693 | 60 741 | 58 642 |
| **Low risk** | 1 135 | 403 | 333 | 271 |
| **Medium risk** | 146 | 53 | 99 | 42 |
| **High risk** | 152 | 46 | 33 | 45 |
| **Very high risk** | 438 | 1 086 | 167 | 1 069 |
| **maximum risk** | 2 251 | 3 491 | 4 036 | 2 986 |
| **Total area** | 96 388 | 96 388 | 96388 | 96 388 |

**Table 4.** Estimation of the agricultural (Olive tree) Absolute Resource Extraction index (AREI) by scenario.

| Classes of desertification risk | Reference modeling (ha) | Scenario 1 (ha) | Scenario 2 (ha) | Scenario 3 (ha) |
|---|---|---|---|---|
| **Risk zero** | 37511 | 89966 | 27431 | 37506 |
| **Very low risk** | 0 | 1730 | 0 | 0 |
| **Low risk** | 0 | 0 | 0 | 0 |
| **Medium risk** | 0 | 4629 | 0 | 0 |
| **High risk** | 0 | 0 | 0 | 0 |
| **Very high risk** | 0 | 60 | 0 | 0 |
| **maximum risk** | 58877 | 3 | 68957 | 58882 |
| **Total area** | 96 388 | 96 388 | 96388 | 96388 |

**Table 5.** Estimation of the Agricultural (Absolute Resource Extraction index (AREI) by scenario.

| Classes of desertification risk | Reference modeling (ha) | Scenario 1 (ha) | Scenario 2 (ha) | Scenario 3 (ha) |
|---|---|---|---|---|
| **Risk zero** | 90732 | 89966 | 89966 | 37503 |
| **Very low risk** | 1615 | 1730 | 1730 | 0 |
| **Low risk** | 0 | 0 | 0 | 0 |
| **Medium risk** | 3985 | 4629 | 4629 | 0 |
| **High risk** | 0 | 0 | 0 | 0 |
| **Very high risk** | 52 | 60 | 60 | 0 |
| **maximum risk** | 3 | 3 | 3 | 58885 |
| **Total area** | 96388 | 96388 | 96388 | 96388 |

Concerning the index of pastoral absolute removal, the risk of desertification increased significantly. In fact, the zones of average risk to very extremely risk passed from 821 ha to 7886 ha (9 times).

Scenario 3 is of physical nature and considers the taking into account of potentialities of the water resources in the observatory. The simulation results shows no major changes in the CPU maps.

The calculation of the indicators of removal absolute revealed a degradation of situation concerning the forest activity. In fact, the zones at the risk very extremely risk to maximum risk passed from 2689 ha to 4055 ha. The situation remained virtually identical for the pastoral activity. The situation remains identical for the agricultural activity (olive-tree and cereals).

## 4 CONCLUSIONS

Desertification is a major problem in Tunisia and needs monitoring and evaluation through setting up of local observatories. Since desertification is a multidimensional problem, recourse to modelling is inevitable. The application of an integrated GIS based model LEIS in the PAN-LCD and Roselt observatory of Menzel Habib shows promising results. In fact, the simulation results confirm the pastoral vocation of the observatory and the high risks to be embedded following the intensification and extension of the all forms of farming. Therefore, the LEIS shows high potential of use as a spatial decision support systems. The simulation through scenarios revealed the high vulnerability of the natural ecosystem to the anthropic actions. Therefore, LEIS model could be used as useful tool for integrated and interdisciplinary approaches. However,

several difficulties and issues need to be solved, such as the integration of the LEIS, applied at local scale, in the national and regional of monitoring and evaluation system of desertification.

## ACKNOWLEDGMENTS

This paper is part of the ROSELT/OSS project *'Renforcement des observatoires au nord du Sahara'* funded by the Swiss Cooperation (SDD) and the Tunisian Ministry of Scientific Research, Technology and Development of Competencies. The contribution and the assistance of the other members of the project research team are highly appreciated.

## REFERENCES

[1] ROSELT/OSS, DS3, 2004 : Concepts, méthodes et mise en oeuvre pour l'évaluation des risques de désertification : Système d'Information sur l'Environnement à l'échelle locale (SIEL) du programme ROSELT/OSS. Collection ROSELT/OSS, Document scientifique n°3, Montpellier.

[2] MEAT (MINISTERE DE L'ENVIRONNEMENT ET DE L'AMENAGEMENT DU TERRITOIRE), 1998B : Atlas du gouvernorat de Médenine. BERA, MEAT, Tunis.

[3] OSS (OBSERVATOIRE DU SAHARA ET DU SAHEL), 2004 : Stratégie 2010 de l'OSS. OSS, Tunis.

[4] SGHAIER M., 2002 : Etude sur le cadre d'organisation institutionnelle du «SE/PAN-LCD Tunisie, Projet de mise en place du suivi-évaluation du PAN-LCD en Tunisie, 12 p.

[5] IRA, 2005: Mise en place d'un Observatoire des Zones Aides pour le Développement Durable (OZADD), 6 p.

[6] OULED BELGACEM, A., 2005: Dynamique de la végétation et resources pastorals de l'observatoire de Menzl Habib. Rapport Roselt/OSS.

[7] IRA AND ROSELT/OSS, 2003: Programme de travail général pour la période 2003-2005 de la grappe d'observatoires ROSELT/OSS Haddej Bou Hedma / Menzel Habib en Tunisie, Annexe Technique de Convention de financement n°597, 11p.

[8] TBIB A., 1998 : Conséquences de l'utilisation des ressources naturelles sur l'équilibre écologique en milieu aride tunisien: "Cas de Menzel Habib". D.E.A. d'Ecologie Générale. Faculté des Sciences Sfax: 89 p.

[9] FLORET CH. AND PONTANIER R., 1982 : L'aridité en Tunisie présaharienne: Climat, sol, végétation et aménagement. Trav. Docum. ORSTOM, n° 150: 544 p.

[10] KHATTELI H., 1995: Erosion éolienne en Tunisie aride et désertique. Analyse des processus et recherches des moyens de lutte. Thèse Doct. Sci. Biol. Appli. Aménag. terrs et Forêts (Ph.D.). Univ. Gent, 180 p.

[11] JAUFRET S., 2002 : Validation et comparaison des divers indicateurs des changements à long terme dans les écosystèmes méditerranéens arides. Application au suivi de la désertification dans le sud Tunisien, Thèse de doctorat.

[12] SGHAIER M. AND JRAD, H., 2002 : Elaboration d'indicateurs synthétiques et d'interface dans l'observatoire de Menzel Habib, Atelier de réflexion sur l'observation environnementale et socio-économique et dispositif de suivi évaluation à Menzel Habib, Gabès 10 -12 avril 2003, 14p.

# Spatio-temporal Eco-geomorphic changes along climatic gradients in the Eastern Mediterranean: the synergy of remote sensing and field studies

M. Shoshany[a], T. Svoray[a] and M. Sternberg[c]

[a] Geo-Information Engineering, Faculty of Civil & Environmental Engineering, Technion, IIT, Haifa, 32000, Israel, email: maximsh@tx.technion.ac.il

[b] Department of Geography and Environmental Development, Ben-Gurion University of the Negev, Beer-Sheva 84105, Israel; email: tsvoray@bgumail.bgu.ac.il.

[c] Department of Plant Sciences, Faculty of Life Sciences, Tel Aviv University, Tel Aviv, 69978, Israel; email: MarceloS@tauex.tau.ac.il;

## ABSTRACT

Modes of bio-physical transition between the shrub dominated and the dwarf shrubs areas, and between the dwarf shrubs and desert fringe communities were revealed for a North to South climatic transect in Israel. This was achieved by combining data derived from the application of adaptive unmixing on seasonal Landsat TM imagery, with field data of bio-physical properties of representative species. In this way there is obtained a synergy between the representation of the spatio-temporal patterns of life-form communities with characteristic biomass and volume information derived for these life-forms. High rates of bio-physical changes were detected in the two transition areas, whereby the spatially average biomass and volume had decreased (twice) at the magnitude of 50- 60% within a distance of less than 3 km. These modes of change do not correspond to the generalized linear rainfall gradient sought for this climatic gradient. Assessment of the resulting patterns with comparison to exiting phytogeograpnical map indicated the added value of such synergy in terms of both the eco-geomorphic and the climatic potential implications.

**Keywords:** Remote Sensing, adaptive unmixing, climatic gradients, biophysical properties, woody plants.

## 1. INTRODUCTION

Relationships between soil and vegetation patterns are primary representations of eco-geomorphic systems. While these systems evolve over long time scales with cumulative effect of processes occurring at wide range of spatial scales, observed soil and vegetation patterns are just snapshots. The idea behind studying these relationships along climatic gradients is then that the catena of soil and vegetation patterns may describe sequences of long-term eco-geomorphic evolution. Identifying threshold zones between characteristic spatial patterns would then infer regarding boundaries between resilient eco-geomorphic sub-systems. These boundaries will shift presumably with the expected global warming (IPCC, 2001) especially in Mediterranean regions where areas adjacent to the sea are expected to get warmer at a lower magnitude than inland areas. Characterizing change in vegetation-soil relationships along climatic gradients and identifying threshold zones consist important aims for remote sensing. However, this is a very challenging task due to the inherent heterogeneity of Mediterranean areas (see [20] for example discussion of soil heterogeneity and [8] regarding the remote sensing aspect), their temporal variability (both seasonal and inter-annual), the frequent changes in land-use mosaics, and the superimposition of past climatic and land-use conditions. The principle generalized paradigm for explaining vegetation and soil patterns' change hypothesize that these patterns are dependent on mainly the variation in the average annual precipitation along the climatic gradient. Questions concerning what is the real spatial correspondence between patterns of vegetation formations and precipitation decrease? and, what are the vegetation characteristic which best represent the vegetation response to climate conditions? are among the questions needed to be answered in order to improve our understanding of the expected eco-geomorphic changes which might follow global warming.

This paper represents a part of ongoing integrated research which was carried out during the last decade, addressing the various problems of environmental remote sensing along the climatic gradients of Israel. These different studies were conducted along different climatic transects along the North to South and West to East Mediterranean to arid gradients of Israel (Figure 1). Landsat MSS, Landsat TM, Spot, JERS, and ERS-2 images

were acquired for these transects. Various interpretation methods were developed ranging from simple empirical modeling of vegetation cover- reflectance relationships ([5]. [6] & [7]); through biophysical modeling of radar backscattering ([9], [16] & [17]) to development of Knowledge Based Systems for crops mapping and identifying the boundary zone between agricultural and natural areas (see [1] & [2]). This article is focused on the combination of field and remote sensing studies which facilitated better understanding of the humid - semi-arid transition along the gradient between Avisur Highland (450 mm average rainfall) to the northern outskirts of Beer-Sheva in the south (~ 200 mm average rainfall). In sections 2 and 3 there will be described the remote sensing and field data collection. In section 4 there will be provided a generalized description of the results obtained by combining the two studies.

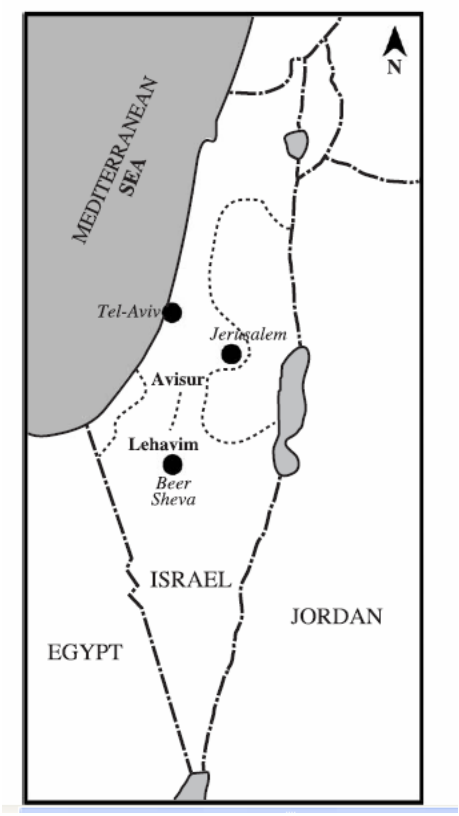


**Figure 1.** Location of the main study area.

## 2 MAPPING RELATIVE COVER OF THREE VEGETATION LIFE FORMS

In 1996 there was initiated a new study along the gradient extending from the Judean Hills in the North (Avisur Highland) and the Northern Negev Hills in the south (Lehavim). In this study there was introduced the adaptive unmixing method which overcomes the limitation set on the number of end-members by using Landsat TM images (see [15]). Optimizating endmembers' selection was gained by a preceding stage of classifying the region into areas representing characteristic vegetation and soil combinations. For each of these regions there were defined soil, rock and vegetation image endmembers. Application of the unmixing on three images representing important phonological stages in the natural vegetation growth yielded three raster information layers describing the spatial distribution of vegetation fractional cover. Based on phenological logic, there were defined the relative fractions of three life-forms: Herbaceous growth, Dwarf Shrubs and Shrubs. Figure 2 describes the fractions' distribution of these life-forms The new data was analyzed with reference to a phytogeographical map of the region which was prepared by Sapir [4]. Patterns of shrubs, dwarf shrubs and herbaceous vegetation could be inferred and it was possible to detect cover changes between the 1970s and the late 1990s ( in general terms due to the generalized nature of the phytogeographical map). The data provided also an indication to the wide distribution of Sarcopoterium Spinosum which consists one of the dominant Dwarf shrubs species known to spread extensively over the Mediterranean Basin. Cover percentage data for each of the different life-forms was found instrumental for improving the SAR capabilities in retrieving volumetric information (see [17]). Here, this information was combined with data from the field surveys in order to improve our understanding of the different transitions occurring along the transect.

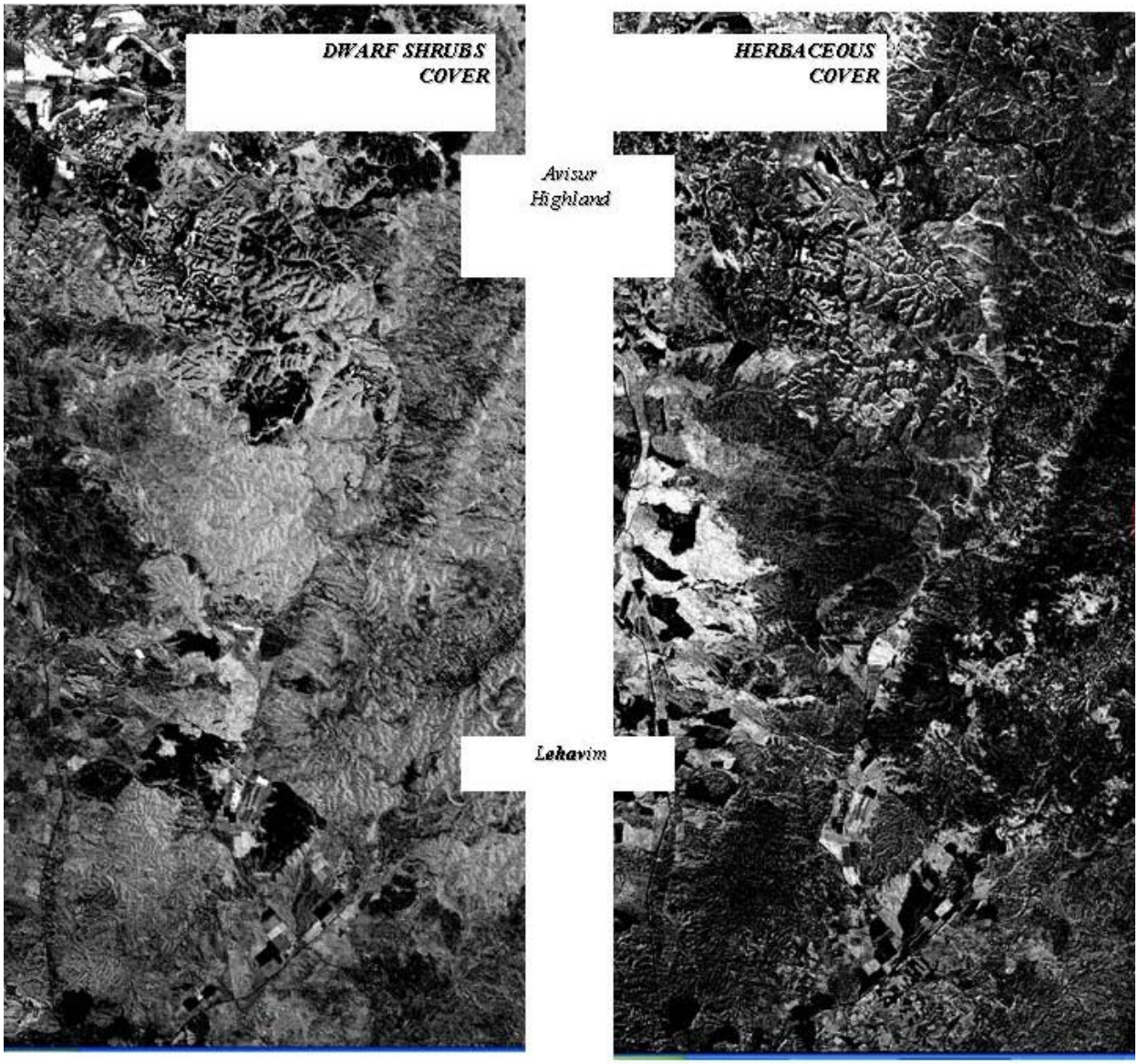


**Figure 2.** Relative fractions of Herbaceous growth and Dwarf shrubs along the climatic gradient (White: full cover; Black: no cover).

## 3 FIELD STUDIES

Two field studies facilitated the development of our understanding of the biophysical vegetation changes: one involved with a detailed survey of the biomass characteristic of different shrub species in the extreme two sites of this transect; and the second, involved with detailed survey of herbaceous vegetation biomass variation inbetween these two sites. In a parallel study there were assessed the volumetric soil content properties along the same transect. The data collection methods utilized in these three studies will be described in the following sections.

### 3.1 Biophysical properties of woody vegetation

In the first, 16 quadrats of 10 m X 10 m (eight south-facing and eight north-facing slopes) were established and the vegetation was recorded. Dominant 10 shrub species were measured using allometric parameters of area and volume, and representative branches were cut and weighed (see [4]). The slope aspect influence on the biomass characteristics was found to yield some unexpected results, however, generally speaking there was found that the woody vegetation biomass in Avisur Highland site was 3 times higher than that of Lehavim site ( 15 vs 5 $kgm^{-2}$), while that the vegetation volume in Avisur Highland site was 5 times higher than that of Lehavim site (1,500 vs 7,500 $m^3$/ha ). Then, with reference to the need to understand the structural volumetric characteristics of the

vegetation there were weighted the dry and wet biomass of the leaves and woody parts in 20 cm sections from the vegetation top inward (See [13]). Results indicated the most of the leaf biomass is concentrated in the most outer 20 cm layer of the upper canopy.

### 3.2 Biophysical properties of Herbaceous vegetation

A field survey of dominant homogenous herbaceous vegetation in the study area included overall 57 plots (of which 33 were of natural herbaceous vegetation and 24 of wheat and barley), 0.3 ha in size, were used to estimate aboveground biomass with the 'harvest and assessment' method of Tadmor [20]. Aerial Aboveground Biomass (AAB) was estimated visually at 100 quadrants of $0.625m^2$, located within each of the 57 plots. These estimates were regressed against direct aboveground biomass harvests from 10 random samples of the 100 quadrates. DGPS (differential global positioning system) readings of each plot's centre were conducted in order to allow assessment with reference to the satellite image data. The results of the field campaigns yield a wide distribution of AAB levels: natural herbaceous vegetation varied between 0.05 $kgm^{-2}$ and 0.3 $kgm^{-2}$ while the herbaceous crops had extended the upper range to a value of 0.6 $kgm^{-2}$.

### 3.3 Soil moisture content

During field surveys in February, April and May 1997 and in April and June 1999, soil moisture content was measured in 16 plots (8 at the semi-humid Avisur site and 8 at the semi-arid Lehavim site) to determine the validity of the remote sensing soil moisture model. Another 57 plots distributed randomly in the study area were sampled only during April and June 1999. Soil moisture content in all of these plots was measured from bare terrain. The location of each plot was measured by differential Global Positioning Systems (GPS) to link the field measurements with the ERS-2 SAR pixels. The procedure was implemented as follows: For each plot, samples of soil were taken from ten randomly distributed sites. Each soil sample weighted about 200 g and was taken from the 0–5 cm depth and sealed in thermal-resistant plastic bags. The bags were weighed before and after 24 h drying at $105^oC$ in a standard oven. Gravimetric soil moisture was calculated using the well-known ''double weight'' method. Previous studies have shown empirically that the radar backscatter is more sensitive to volume scattering than to changes in mass. To correspond to the linear soil moisture model, the gravimetric soil moisture measurements were converted into volumetric measures, based on bulk density measurements for the specific soils of the study area.

## 4 ASSESSMENT OF BIO-PHYSICAL TRANSITIONS ALONG THE CLIMATIC GRADIANT

Figure 3 provides a schematic representation of the North to South profiles of the different gradient properties. According to rainfall data collected at 4 sites, annual average precipitation decreases almost linearly between Avisur Highland and Beer Sheva. The generalized trend of soil moisture content determined from the soil samples indicated a similar linear trend as well, although with significant variance. As could be inferred from figure 2, vegetation cover of the three life-forms exhibits high spatial variation with high representation of human induced patterns : Pine Plantations, crop fields, houses and roads. Two stripes of less affected areas were detected , one between Amatzia and Dvira and one between Lehavim and Beer Sheva. For these two stripes there were calculated average north to south profiles, with their bio-physical properties estimated by combining the different information sources. The resulting patterns are described as follows:

- Total vegetation cover was found to be characterized by two transition areas : a gradual change near Lehavim and a sharp change north of Beer Sheva. These two transition are mainly explained by rates of decrease in the relative coverage of Dwarf shrubs on one hand and the increase in the bare soil/ rock cover on the other,
- Total biomass : this was determined by deriving characteristic biomass values for each of the three life-forms from the field studies, and by applying them at each pixel' according to the cover proportions determined earlier. Two 'steps' (four transitions) were detected, whereby the northern 'step' south of Amazia represents the transition from shrub dominated communities to dwarf shrubs domination, and in the southern 'step' between Lehavim and Beer Sheva the dwarf shrub domination is replaced by bare soil/rock cover domination. The biomass change in these two 'steps' is high : a decrease by almost 50% .
- Total volume: in similar way to the total biomass there were utilized characteristic values from the field studies and then again applying them according to the relative life-form proportions. Obviously, there were detected again two 'steps' however, the magnitude of reduction at the northern step was

even higher than for the biomass : vegetation volume of the dwarf shrub area was approximately 35% of the characteristic values determined for the shrub areas. The volume reduction between Lehavim and Beer Sheva was by 'only' 50%.

The phytogeographical map of [4] is inferring regarding the generalized pattern of vegetation transitions along the climatic gradient. However, the inclusion of the bio-physical parameterizations added significant insights regarding the rates of transitions which are highly influenced by the spatial heterogeneity of the life-form compositions. An important addition from our data concern the mode of change from the Batah to the desert fringe vegetation: there is a significance presence of transition zone between these two phyto-geographical regions. This could be just representing differences between the mapping methods (see discussion on that in [7]), or representation of spread of dwarf shrubs into the desert fringe areas. The later option can be assessed by using historical air photographs (see [3]. [10]. & [14]).

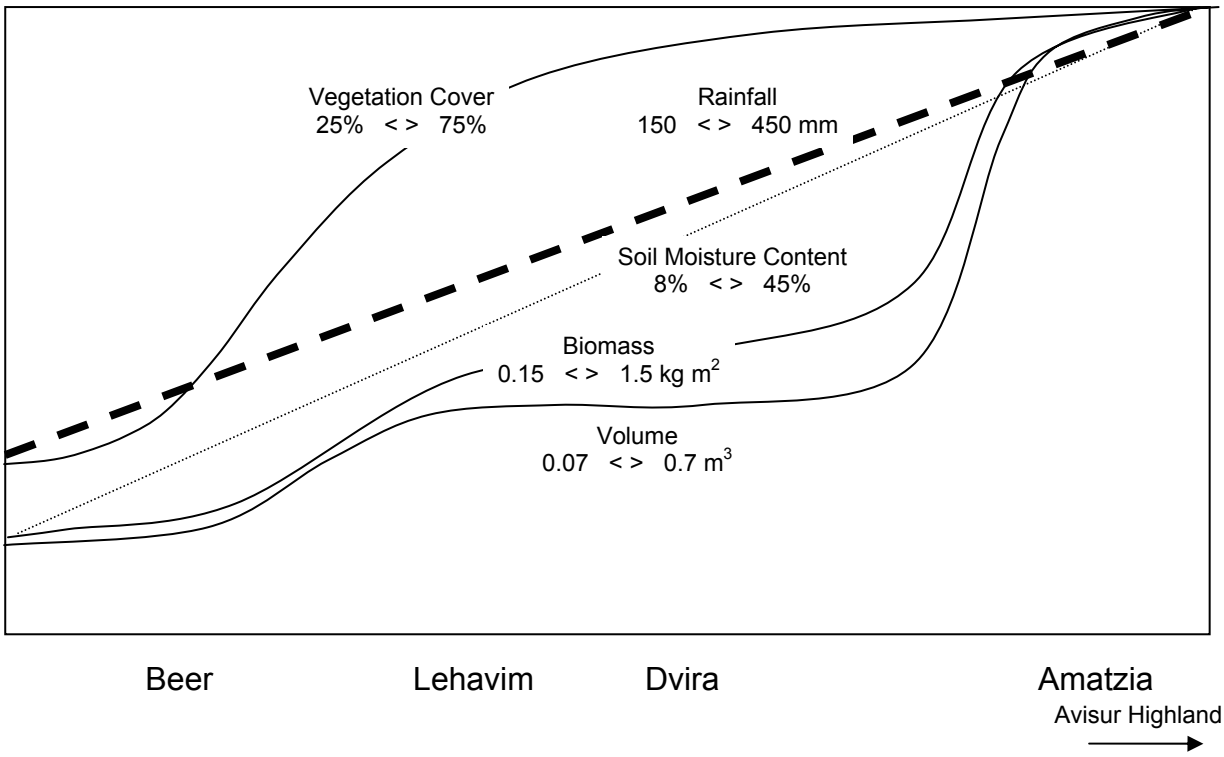


**Figure 3.** Generalized schematic representation of North – South variation of rainfall, soil misture, vegetation cover, biomass and vegetation volume along the climatic gradient.

## 5 DISCUSSION AND CONCLUSIONS

For most of the country, existing soil and vegetation maps are outdated (except for a forest survey conducted recently by the Forestry Branch of the JNF – Jewish National Fund). For example, the most detailed regional phytogeographical mapping of the Avisur Highland – Lehavim area was conducted during the 1970s [4] and had not been revised since. Furthermore, the existing information refers to the generalized and visually interpreted phytogeographical units rather than to parametric and systematic mapping of vegetation properties. The methodologies developed in the above mentioned studies facilitated the production of a most spatially detailed data bases of soil and vegetation properties. Using this information, an insight was gained into the eco-geomorphic structure of the climatic gradient. In this part of the study we discussed the benefits from combining spatially detailed vegetation fraction cover using the adaptive unmixing with characteristic field derived biomass and volume data for the different life-forms. Modes of bio-physical transition between the shrub dominated and the dwarf shrubs areas, and between the dwarf shrubs and desert fringe communities were not documented before in such spatial detail and geographical extent. The new data is of primary importance in eco-geomorphic and climatic research in view of the expected global warming. Of significance is the preliminary indication for southward spread of the dwarf shrubs. Such spread, if proven, reduces the surface albedo and might be followed by atmospheric cooling in the transition zones which might counteract the expected global warming in this area. Soil recovery due to this spread may in the long run increase the primary productivity of these regions and the further southward spread of Mediterranean shrubs.

## REFERENCES

[1] COHEN, Y. AND SHOSHANY, M., 2002: Integration of remote sensing, GIS and expert knowledge in national knowledge-based crop recognition in Mediterranean environment. *Int. J. of Applied Earth Observation and*
[2] COHEN, Y. AND SHOSHANY, M., 2005: Analysis of convergent evidence in an evidential reasoning knowledge-based classification. *Remote Sensing of Environment, 96(3-4),* pp. 518-528.
*[3]* KELMAN, E. AND SHOSHANY, M., 2005: Implicit Reconstruction of Patch dynamics from single date aerial photographs : mutuality and complementarity in Pattern Change. *Int. J. of Remote Sensing*, 26(9), pp. 2021-2028.
[4] SAPIR, G., 1977: Joudean Lowland vegetation and the affinity between vegetation distribution to habitat conditions. MSc thesis, Department of Botany, Hebrew University, Jerusalem, in Hebrew, English abstract.
[5] SHOSHANY, M., KUTIEL, P. AND LAVEE, H., 1994: Remote Sensing of vegetation cover along a climatological gradient. *ISPRS Journal of Photogrammetry and Remote Sensing.* 49, pp. 1-8.
[6] SHOSHANY, M., KUTIEL, P. AND LAVEE, H., 1995: Seasonal vegetation cover changes as indicators of soil types along a climatological gradient: a mutual study of environmental patterns and controls using remote sensing. *Int. J. of Remote sensing,* 16, pp. 2137 - 2151.
[7] SHOSHANY M. KUTIEL P.AND LAVEE H. ,1996: Monitoring temporal vegetation cover changes in Mediterreanean and arid ecosystem using a remote sensing technique: case study of the Judean mountain and the Judean desert. *Journal of Arid Environment* 32, pp. 1-13.
[8] SHOSHANY, M., 2000: Satellite Remote Sensing of Mediterranean Vegetation: A review within an Ecological Research. *Progress in Physical Geography* , 24(2), pp. 153-178.
[9] SHOSHANY, M., SVORAY, T., CURRAN, P., FOODY, G. AND PEREVOLOTSKY, A., 2000: The relationships between ERS-2 SAR backscatter and soil moisture: generalization from a humid to semi-arid transect. *Int. Journal of Remote Sensing, 21(11)*,pp. 2337-2343.
[10] SHOSHANY, M., 2000: Detection and analysis of soil erodibility patterns using multi-date airphotographs : the case study of Avisur Highland, Israel. In: Hassan, M., Slymaker, O., and Berkowicz, S.M. (ed.): The Hydrology-Geomorphology Interface : Rainfall, Floods, Sedimentation, Landuse, IAHS Publ. No. 261, pp. 127-138.
[11] STERNBERG, M. AND SHOSHANY, M., 2001: Bio-physical slope related differences in Mediterranean woody formations: a comparison of a semiarid and an arid sites in Israel. *J. of Ecological Research, 16, 335-345* .
[12] SVORAY, T , SHOSHANY, M., CURRAN, P., FOODY, G. AND PEREVOLOTSKY, A., 2001: Relationship between bio-physical parameters of four life-forms and ERS-2 backscatter in the semi-arid zone of Israel. *International Journal of Remote sensing.* 22(8), pp. 1601-1607.
[13] STERNBERG, M. AND SHOSHANY, M., 2002: Aboveground biomass allocation and water content relationships in Mediterranean trees and shrubs at two climatological regions in Israel. *Plant Ecology, 157,* pp. 171-179.
[14] SHOSHANY, M., 2002: Landscape fragmentation and Soil erodibility in south and north facing slopes during ecosystems recovery : an analysis from multi-date airphotographs. *Geomorphology*, 45, pp. 3-20.
[15] SHOSHANY, M. AND SVORAY, T., 2002: Multi-date adaptive spectral unmixing and its application for the analysis of Ecosystems' transition along a climatic gradient. *Remote Sensing of the Environment*. 81, pp. 1-16
*[16]* SVORAY, T. AND SHOSHANY, M., 2002: SAR based estimation of Aerial Above ground Biomass (AAB) of Herbaceous vegetation in the Semi Arid zone of Israel : A Modification to the Water Cloud Model. *International Journal of Remote sensing, 23,* pp. 4089-4100.
*[17]* SVORAY, T. AND SHOSHANY, M., 2003: Herbaceous Biomass Retrieval in Habitats of complex composition: A Model Merging SAR images with Unmixed Landsat TM data. *IEEE Transactions on Geosciences and Remote Sensing, 41(7),* pp. 1592-1601.
*[18]* SVORAY, T., SHOSHANY, M. AND PERVOLOTZKI, A., 2003: Mediterranean rangeland response to human intervention: a Remote Sensing and GIS study, *J. of Mediterranean Ecology, 4,* pp. 3-11.
*[19]* SVORAY, T. AND SHOSHANY, M., 2004: SAR-based mapping of soils by Multi-Scale analysis of drying – rates. *Remote Sensing of Environment 92(2),* pp. 233-246.
[20] TADMOR, N. H., BRIEGHET, A., NOY-MEIR, I., BENJAMIN, R. W. AND EYAL, E., 1975: An evaluation of the calibrated weight-estimate method for measuring production in annual vegetation. *Journal of Range Management*, 28, pp. 65–69.
[21] YAALON, D. H., 1997. Soil in the Mediterranean region: What makes them different? *Catena*, 28, pp. 157–169.

# A Geo-statc Satellite Based Monitoring System-CEWBMS Applied for Climate and Soil Drought Monitoring in China

S. Siheng[a] and A. Rosema[b]

[a] Academy of Forest Inventory & Planning /China National Desertification Monitoring Center, State Forestry Administration, No 18 Hepingli Dongjie, Beijing, China
ssheng2002@yahoo.com
[b] Environmental Analysis and Remote Sensing (EARS), 2600 AK, Delft, Netherlands
andries.rosema@ears.nl

## ABSTRACT

China is seriously affected by desertification. Although China's government has paid great attention and taken effective efforts in large scale to combat desertification nevertheless, under the dual pressure of population growth and economical development, the general tendency of desertification is still accelerating!

The China National Desertification Monitoring Center at the Academy of Forest Inventory and Planning , the State Forestry Administration has organized the national desertification survey and monitoring once in every 5 years. A large amount of Landsat TM image as well as men power, money had been consumed in this effort.

The Dutch company EARS has developed a unique technology to use geo-stationary weather satellite for measuring and monitoring the energy and water balance. The technology provides synoptic information on actual evapo-transpiration and the net radiation on a day by day basis.. All animal and plant live depends on the availability of water and the radiation conditions. Therefore the information provided by this technology is highly relevant to desertification and plant production.

Through a co-project the aforementioned units has developed the Chinese Energy and Water Balance Monitoring System (CEWBMS) using geo-stationary satellite data for desertification monitoring application. The system has been running for 5 years. The Climatic Moisture Index (CMI) Distribution Map and The Soil Moisture Index (SMI) Distribution Map of nationwide China have been produced in decade of days, monthly and yearly by the system. It will benefit the aided decision making of various authorities for drought and desertification combating.

The CEWBMS has also a large potential application in environment, hydrology, meteorology, climatology, as well as the forecasting of agricultural and grassland production.

**Keywords:** Desertification Monitoring, CEWBMS, CMI, SMI

## 1 THE DROUGHT , DESERTIFICATION PROBLEM AND MONITORING IN CHINA

### 1.1 Desertification and Climatic Zones of Desertification

In 1994 the United Nations Convention to Combat Drought and Desertification has defined the desertification concept as various forms of land degradation in arid, semiarid and sub-humid arid climatic regions resulting from various factors, including climatic variations and human activities. It includes soil erosion caused by wind and/or water; deterioration of the physical and biological or economical properties of soil; long term loss of natural vegetation etc..

The climatic moisture index applied by UNCCD in order to classify climatic zones. Climatic Moisture Index defined as:

**CMI** = **P** / **APE**. ( **P**:Annual Precipitation;**APE**:Annual Potential Evapotranspiration). Five climatic zones are classified in accordance with moisture index, namely:

**Table 1.** Climatic zones and related moisture index.

| Climatic zone | Climatic moisture index |
|---|---|
| extreme arid area | <0.05 |
| arid area | 0.05-0.20 |
| semi-arid area | 0.21-0.50 |
| dry sub-humid area | 0.51-0.65 |
| humid area | >0.65 |

### 1.2 Drought , Desertification Problem in China

China is seriously affected by drought and desertification with big area, wide distribution and serious adverse impact. In the north and north-west of China the ecology is fragile and the climatic conditions variable. There are big annual economic loss in China from desertification. However, the land area encroached by only sandy desertification every year reaches 2460 $km^2$.

### 1.3 Urgent Needs for Desertification Monitoring

The socio-economic development in the desertification area as well as in other parts of China is closely related to the base status, dynamic changes and future development of desertification affected land. Also for properly management of desertification combating activities, overview information is required at the levels where decisions are taken from local to national scale. It is of extremely important and urgent to undertake desertification monitoring in China.

### 1.4 Spatial Scales and Cycles of Monitoring Desertification

Three spatial scales for China national desertification monitoring framework is classified: national scale, provincial scale and typical localities of desertification. The former two levels adapt spatial data source mainly from remote sensing with some field checking of sampling plots while the typical and representative localities uses more detailed monitoring and evaluation methods. The provincial monitoring and the national monitoring which adds up results from the former are undertaken every five years, mainly focusing on specific dynamic monitoring and analysis of different land desertification types and degrees. This kind of monitoring requires somewhat high or middle resolution satellite remote sensing data.

### 1.5 Problem in Macro Desertification Monitoring

According to the definition of desertification to determine the climatic zones is a key task for desertification monitoring and combating. In a first try a large amount of weather station meteorological data (1981-1990) through out China had been used for calculating CMI and made a China Desertification Climatic Distribution Map. However the desertification monitoring and combating activities should be within the desertification climatic zones drew in the map. Because climate change and climatic situation would be various so that the CMI for the same places so the desertified climatic areas would be changing year by year. Consideration of dryer or wetter year should be taken into account for the macro desertification monitoring.

However because of the dynamic nature of the problem and the affecting climatic factors this information has to become available at relatively short intervals. There is an increasing needs for general or macro nationwide and timely monitoring information. This should require the uses of low resolution remote sensing data and would be more flexible, lower costs and has shorter cycle. Commonly meteorological satellite data were adopted for drought monitoring. Drought include air drought, soil drought and crop drought etc.. Scientists use polar satellite data to get the highest temperature and the lowest temperature, then derive the water content of soil. To apply this method there would be some constraints such as clouds cover, satellite pass over the same area at noon and middle night, soil not covered by vegetation. Another alternative method for the higher vegetation coverage area is to use NDVI (normal vegetation index) and the temperature of leaves surface (Ts) which also got through polar satellite. Then use NDVI and Ts to derive the vegetation supply water index of (VSWI). This method has limitation of only could be used for the season of higher transpiration and for vegetation covered area. The another weak point of the above mentioned methods applied for desertification combating is that all their products are not related to the definition of desertification by UNCCD.

## 2. NEW METHODOLOGY AND THE COOPERATING THE CEWBMS

### 2.1 Related developments in the Netherlands

The Dutch company EARS has developed a unique technology to use geostationary weather satellites for measuring and monitoring the energy and water balance. The technology provides synoptic information on the actual evapotranspiration and the net radiation on a day by day basis.

All animal and plant live depends on the availability of water and the radiation conditions. Therefore the information provided by this technology is highly relevant for applications related to desertification and plant production. In Europe and Africa applications have been developed in the field of desertification monitoring, regional water balance studies and crop yield forecasting.

EARS ,CNDMC and other Dutch,Chinese partners have developed the CEWBMS project since 1998. The CEWBMS has been pilot operated for one and half years and have some initial products.

## 2.2 Advantages and Objectives of the CEWBMS

### 2.2.1 Benefits and advantages of the CEWBMS are:

1) The CEWBMS receives the geo-stationary satellite data and derives a lot of useful information closely relevant to specific drought and desertification situation, biomass estimation etc. such as net radiation, sensible heat, evapotraspiration, precipitation, air temperature etc.;

2) The information is timely. Usually it takes several to many months before the information coming from different parts of the country arrives, is processed and integrated and finally analysed. The present satellite technology can provide nation wide results within a few days.

3) The CEWBMS could provide daily, monthly and yearly timely monitoring map products of climatic moisture index (CMI) which has the same definition determined by UNCCD as mentioned before. The system also could produce daily, monthly and yearly timely monitoring maps of soil moisture index (SMI) which are directly related to soil drought and vegetation water supply;

4) The information is synoptic. The exist information systems are of statistical nature and rely on field sampling plots etc. The satellite based results are spatially continuous and cover the whole country. The products of the CEWBMS are not only to give specific CMI and SMI values for some interesting location points or to draw some zoning lines but give a overall distribution map of them. In the producting maps any spatial point has its value of CMI and SMI;

5) The information is objective. Earlier information systems involve a lot of manpower. Results from the field will therefore depend on the personal judgment of the people involved. Yield figures may even be manipulated for political reasons. The satellite technology provides objective and therefore compatible information all over the country.

6) Although the development of the CEWBMS has been taken a lot of efforts the CEWBMS itself is very simple equipped, easier to take care and cheaper to run;

7) The CEWBMS will work at all-weather and surface cover conditions. So the products of the system will not be influenced by clouds, vegetation coverage or bare soil etc..

### 2.2.2 Objectives of the CEWBMS

1) Develop the CEWBMS and install, test running the system in CNDMC. It will complete and improve the nationwide desrertfication monitoring system;

2) The CEWBMS method and products should play a impotent role in overall national desertification monitoring system and be a necessary supplement of normal macro desertification monitoring method which employed many resource satellite data of higher resolution and take longer time;

3) To submit the application reports of drought and desertification monitoring to the State Forestry Administration and the UNCCD;

4) The CEWBMS- a nationwide drought and desertified environment monitoring system is expected to allow for better decision making resulting in improved combat by better planning and timely rescue operations. The possible contribution of the System to the reduction of the yearly economic losses caused by drought and desertification.

## 3 METHODOLOGY DESCRIPTION OF CEWBMS

Geostationary meteorological satellites provide thermal infrared and visible data at 5 km resolution, covering the whole hemisphere. These may be used for drought and desertification monitoring. Data are to be received hourly. After data capture clouds are identified and cloud top levels classified. Subsequently cloud top level frequencies or "cloud durations" are determined. From the hourly full satellite data, composite images are prepared which everywhere represent local noon and local midnight. The extracted data are then processed to image maps of rainfall, radiation, sensible heat flux and actual evapotranspiration. Daily results are first obtained, which are then processed to dekadely, monthly and yearly products.

*Rainfall monitoring*

The most widely used approach to automatic satellite rainfall mapping is based on statistical regression between "cold cloud duration" and rainfall measurements. The technique is not based on cloud information only, but rather

uses the cloud frequency information to interpolate rainfall between the rainfall stations reporting on the WMO Global Tele-communications System (GTS).

*Evapotranspiration monitoring*

The determination of actual evapotranspiration on the basis of meteorological satellite data is carried out in several steps: calibration, atmospheric correction, calculation of net radiation, calculation of the sensible heat flux, determination of the actual evapotranspiration.

*Drought and desertification indices*

Monitoring of the energy fluxes at the earth surface is the key to desertification monitoring. Budyko [5] made a climate classification based on the yearly course of net radiation, sensible heat flux and latent heat flux. Already in 1958 Budyko introduced the *aridity index*, which is defined as the ration of net radiation ($I_n$) and the energy required to evaporate the precipitation (R)

$$AI = In / (L*R) \quad (1)$$

where L is the heat of evaporation. At the United Nations Desertification Conference in Nairobi 1977, a "Climate Aridity Index Map" of the world was presented. In the background document "Climate and Desertification" Hare (1977) discussed its use.

In 1994 the United Nations Convention to Combat Desertification (UNCCD) has defined a slightly different characterisation, using the climatic moisture index (CMI), which is defined as:

$$CMI = L^* R / LEp \quad (2)$$

$LE_p$ is the potential evapotranspiration in energy units. This quantity is closely related to the net radiation $I_n$ and can be estimated with

$$LEp \approx 0.8 * In \quad (3)$$

It is clear that the climatic moisture index (CMI) gives the same information as the aridity index of Budyko (AI). Their relation is

$$CMI \approx 1.25 / AI \quad (4)$$

The UNCCD defined climate types of desertification which can be characterized by the climatic moisture index (CMI) or the aridity index (AI). These indices only indicate a climatic condition, but give no information on the actual desertification state of the ground. In analogy with the climatic moisture index (CMI), EARS has therefore introduced the "Soil Moisture Index" (SMI) in which the rainfall is replaced by the actual evapotranspiration.

$$SMI = LE / LEm \approx 1.25\ LE/In \quad (5)$$

The advantage of the soil moisture index is, that its represents the actual state of the ground surface and includes information on the presence of vegetation, cattle grazing etc. For this reason only the SMI does actually reflect the state of desertification. This index has earlier been indicated as the ideal one for classifying desertification. The reason is that for a long time it was never possible to obtain information on the actual evapotranspiration distribution. The present satellite remote sensing technology developed by our company has changed the situation.

## 4 THE FRAMEWORK AND DEVELOPMENT OF THE CEWBMS

### 4.1 The Framework of the CEWBMS

The operational running CEWBMS consists hardware of a CMAPPS – satellite data receiving and pre-processing system which including a disk antenna and a PC computer for data storage and pre-processing; a PC computer of running the CEWBMS. For calibration and validation of the system products WMO Global Tele-communications System (GTS) meteorological precipitation data and LAS (Large Aperture Scintillometer) measurement data has to be used. The system has been validated by installing five large LAS instruments (which can measure sensible heat flux) in various parts of China, as well as by a large amount of nationwide very solid survey data like rainfall, air-temperature, radiation data. The system generates energy and water balance data/products in time periods of a day, ten days, a month and a year, which were used to conduct experiments in drought and desertification monitoring. Extensive validation illustrated that the data/products generated automatically by this system are trustworthy. The Framework of the CEWBMS is showed as following:

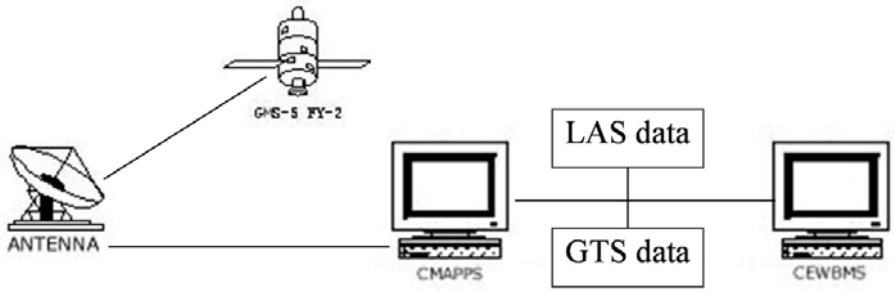


**Figure 1.** CEWBMS framework.

Climatic moisture index (CMI)= Rainfall / Potential evapotranspiration (6)

Soil moisture index (SMI) = Actual evapotranspiration / Potential evapotranspiration. (7)

The maps are base on the integrated results of one year monitoring of rainfall, net radiation and evapotranspiration. These maps prepared for the year corresponding to the testing period and for the preceding year of GMS data reception.

## 5 OPERATIONAL RESULTS OF CEWBMS AND ANALYSIS

### 5.1 Yearly Products Analysis of CMI

The yearly composite maps (from 2000 to 2004) of CMI and SMI compare with existing maps of the (climatic) moisture index which have been prepared earlier in the framework of the United Nations Convention to Combat Desertification, using extensive meteorological ground station data collection methods. To evaluate the utility of the present approach compared to normal methods that we will find the CEWBMS generated map seems very nature and could give specific value for each interesting location. We also could find the boundary of the sub-humid dry region in CEWBMS CMI maps is more towards south than the one of 1981-1990.

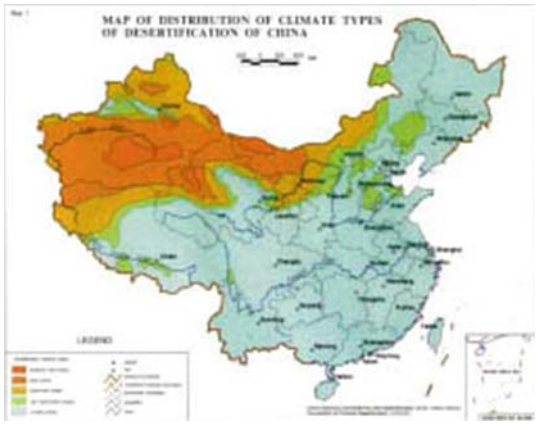


**Figure 2.** China Distribution Maps by Climatic Moisture Index (CMI) generated by Meteorological Data of 1981-1999.

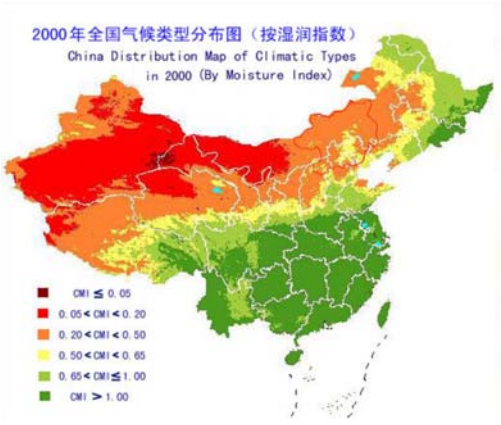


**Figure 3.** 2000 yearly composite map of CMI created by CEWBMS.

## 5.2 Monthly or Season Products Analysis in Different Years

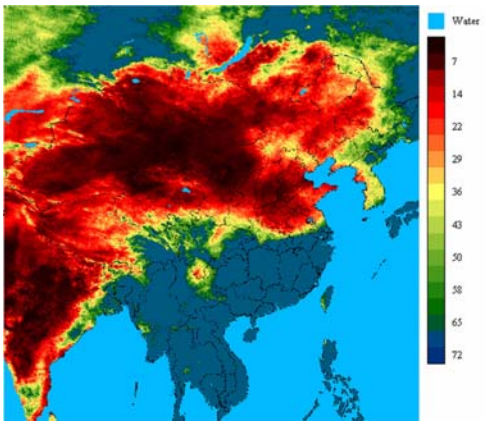


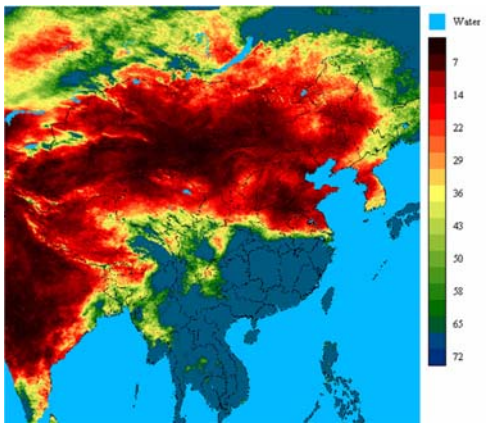


**Figure 4.** CMI Map of Spring Season in 2000.

**Figure 5.** CMI Map of Spring Season in 2001.

From the above maps we could see the different climatic situation in the same season (month) of different years. The same location could have different value in the same season (month) of different year.

## 5.3 Different Season Products Analysis

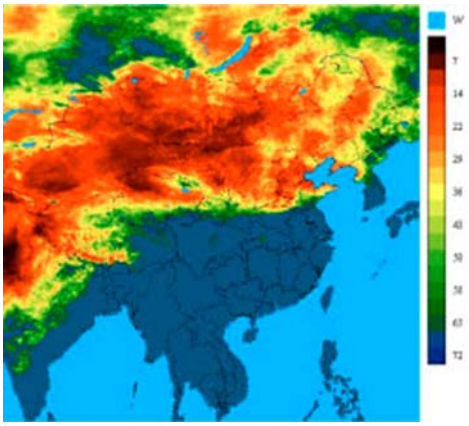

**Figure 6.** CEWBMS CMI Map of Spring in 2000.

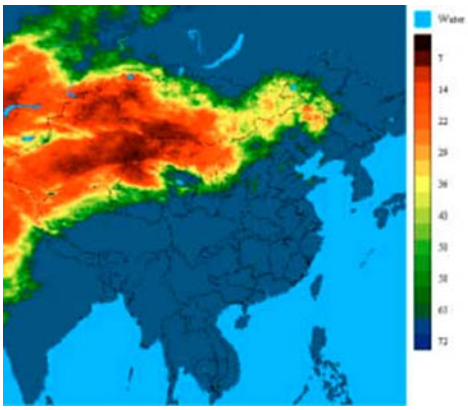

**Figure 7.** CEWBMS CMI of Summer in 2000.

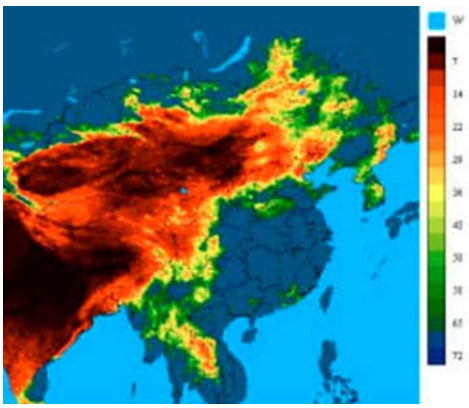

**Figure 8.** CEWBMS CMI Map of Autumn in 2000.

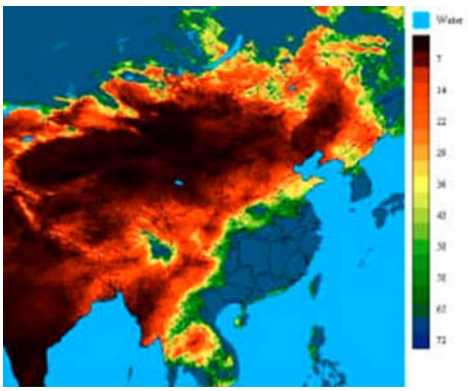

**Figure 9.** CEWBMS CMI of Winter in 2001.

General speaking CMI value in the winter would much less than the summer of the year.

### 5.4 Yearly Products Analysis of SMI

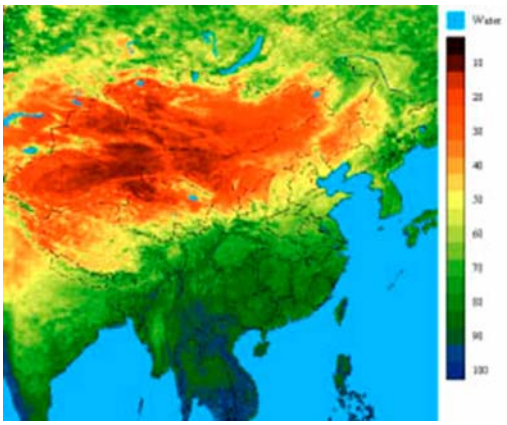


**Figure 10.** SMI Map of CEWBMS by Using 2000 GMS Data.

SMI map could show the real soil moisture situation. SMI could be closer with the water supply status than CMI. It means SMI gives more realistic drought or desertification of land. Therefor the SMI map in different month, season or year will give timely and objective information for drought and desertification early warning.

Both CMI and SMI could scientifically support the decision making of drought and desertification control.

## 6 CONCLUSIONS AND POTENTIAL APPLICATIONS

After the establishment of CEWBMS a scientific committee had examined and evaluated the products of CEWBMS and its sub system Desertification Monitoring System (DMS). The expert committee reached agreement that the China Energy and Water Balance Monitoring System has a very important application value.

CEWBMS, using static meteorology satellite data and covering China completely, can provide distributed information on rainfall, temperature, radiation and actual evapotranspiration at 5km spatial resolution, which can remedy the limited coverage of the network of meteorological ground stations and the actual situation of their uneven distribution. The system may also be used to supplement and improve drought and desertification monitoring and systems already used in China.

Every year the CEWBMS can produce new maps of the national Climatic Moisture Index (CMI). This map can provide important reference data for the Chinese implementation of the United Nations Convention to Combat Desertification (UNCCD). The CMI map currently used by China was generated in the 1990s based on climate data of the 1980s. The system CEWBMS provides a cost-effective technological means of producing nationwide CMI maps for monitoring of annual and long term climate change. Furthermore, the system provides a new Soil Moisture Index (SMI) map, which is directly related to water content in the surface layer of the soil. The system provides pixel by pixel values of CMI and SMI, which for the monitoring and early warning of drought and desertification as well as the prevention and combat of desertification are of considerable practical value.

At the start of this project, using static meteorology satellite data, the system was implemented and operationalized. Especially the national level monitoring with nationwide coverage of such aspects as actual evapotranspiration and the climatic moist index, the soil moist index etc., possesses innovative and internationally advanced level.

The CEWBMS system has many potential application fields in China. In general the CEWBMS system is a useful source of information to support government decision making at local and national level. CEWBMS reveals many elements related to the energy and water balance of climate and soil. These information could be used for the decision making of drought and desertification control, assessment of the ecological construction projects in large scale and the globe change analysis etc.. There are also a large number of potential users for the energy and water balance data generated by the CEWBMS like Environment, Hydrology, Meteorology, Climatology, Agro-meteorology, early warning etc..

## REFERENCES

[1] UNCCD, 1994: United Nations Convention to Combat Desertification in Those Countries Experiencing Serious Drought and/or Desertification, in, Paris.
[2] CCICCD, 1997 China Country Paper to Combating Desertification, Beijing.
[3] SIHENG, S., 1994: China Technical Framework of National Desertification Monitoring, Beijing.
[4] YU, Z., DATONG, N. AND SMIL, V.,1996: An estimate of economic loss for desertification in China, China Population, Resources and Environment, vol.6, no.1.
[5] BUDYKO,M.I ,1974: Climate and Life,ed. D.H.Miller, Academic Press, New York and London, 508 p.

[6] ROSEMA, A, VERHEES, L., VAN PUTTEN, E., GIELEN, H., LACK, T., WOOD, J., LANE, A., FANNON, J., ESTRELA, T.; DIMAS, M., DE BRUIN, H., MOENE, A. AND MEIJNINGER, W., 2001: European Energy and Water Balance Monitoring System, EU FP4 final report, Contract number ENV-CT97-0478.
[7] DE BRUIN, H.A.R., 1993: Analysis of EFEDA and HAPEX-SAHEL remote rensing data, Final report, NRSP-2 93-32. Netherlands.
[8] BASTIAANSEN, W.G.M. AND ROEBELING, R.A., 1993: Analysis of Land Surface exchange Processes in two agricultural Regions in Spain Using Thematic Mapper Simulator Data, Proceedings of IAHS meeting in Jokohama, Japan.
[9] ROSEMA, A. ETC., 1994: Assessment and Monitoring of Desertification in the Mediterranean Area (ASMODE). Final report. ECDG-XII RTD Programme, Project EV5V-CT91-0029.
[10] ROEBELING, R.A. AND ROSEMA, A. ETC., 1999: ACMP Agromet and Crop Monitoring Project in the SADC region-3, NRSP-2 99-15, Netherlands.

# Integrating Remote Sensing and GIS to Monitor Changes in Land use in the Mount Cameroon Region

R. Siwe[a] and B. Koch[a]

[a] Department of Remote Sensing and Landscape Information Systems, Faculty of Forest and Environmental Sciences, University of Freiburg, Tennenbacherstasse 4; 79104 Freiburg; Germany, email: siwerene@felis.uni-freiburg

## ABSTRACT

The once remote and inaccessible forests of the mount Cameroon are currently experiencing conversion to other land use forms, principally agricultural land. Local conservation and planning organisations desire accurate land use/cover data from multi-temporal satellite imagery. It is within this context that the efficacy of five different change detection algorithms in identifying changes in the land use and land cover in the mount Cameroon region were tested using Landsat TM and ETM. The change detection techniques implemented were: change vector analysis, post classification comparison, univariate image differencing, NDVI differencing and post classification using binary mask on date 2.

The efficiency of the methods was compared based on their abilities to provide quantitative (extent of change), qualitative ("from-to" information) and location information (where change has occurred). The ease of implementation of the technique and the interpretation of results were also taken in to consideration since most conservation personnel are still inexperienced with remote sensing approaches.

The highest overall accuracy was achieved by univariate image differencing method using band 5. The technique is straight forward and the results are easily interpretable but had the disadvantage of not providing qualitative change information ("from-to" information). As expected the post classification comparison provided rich qualitative details likewise did the change vector analysis.

**Keywords:** Post classification comparison, change vector analysis, univariate image differencing, land use/cover changes.

## 1 INTRODUCTION

Cameroon like most tropical countries is currently experiencing rapid wide range changes in land use and land cover. Changes in forest ecosystems have attracted attention at both national and international levels due to the effects these changes may have on regional and global climate; forest biodiversity and indigenous rights. The reasons for these changes are numerous and vary according to region. In the mount Cameroon region the changes are principally due to anthropogenic influences in the form of agricultural extension and wood extraction. These changes are at different scales ranging from small scale subsistence farms and fuel wood extraction usually not exceeding 250 m resolution, to large scale agricultural plantations and extraction of industrial wood spanning usually hundreds of hectares. Monitoring these changes constitute indispensable aspects for further understanding of the change mechanism and modelling the impact of the change on the environment. The sustainability requirement of present-day ecosystem management necessitates resource data that are accurate and continuously updated [1] but unfortunately these kinds of information remain a rarity. Terrestrial surveys are inconsistent as a result of the crisis afflicting the nation's economy. To exacerbate this, the remote and inaccessible nature of the mount Cameroon terrain limits the feasibility of ground-based inventory and monitoring methods for extensive land areas. As a result there is an increase in the need to explore alternative methods to monitor the forests of Cameroon and the mount Cameroon region in particular.

Since their inception some three decades ago, Earth observation satellites have demonstrated immense potentials in providing accurate and continuous data on different landscape scenarios. Correspondingly, different algorithms have been developed during this period to interpret these satellite images as well as accomplish change detection. Numerous change detection techniques are currently in application viz: change vector analysis, image differencing, image ratioing, principal component analysis, post classification comparison etc. [10, 1, 2].

The implementation of these algorithms in detecting changes has led to varying results and consequently variable opinions exist about the value and appropriateness of different change detection techniques. This is mainly due to landscape complexities of study areas and data used. The purpose of this review is to analyse the effect of

applying five different change detection algorithms often used in tropical vegetation studies and to evaluate their efficiency in detecting changes in land cover and land use in the mount Cameroon region. Their efficiency will be evaluated based on their capabilities to detect change; its extent, type and nature. The personnel in local management and conservation organisations have limited knowledge on remote sensing and GIS procedures consequently, the ease of implementation of the techniques and the interpretability of the results were considered.

## 2. METHODOLOGY

### 2.1 Study Area

The study area is situated on the west slope of the mount Cameroon in the south west of Cameroon bordering the Atlantic Ocean. The test area comprises approximately 6500 hectares, covering the villages of Kotto 1, Kotto 2, Kosse, Efolofo and Kotakata as shown on figure 1 below.

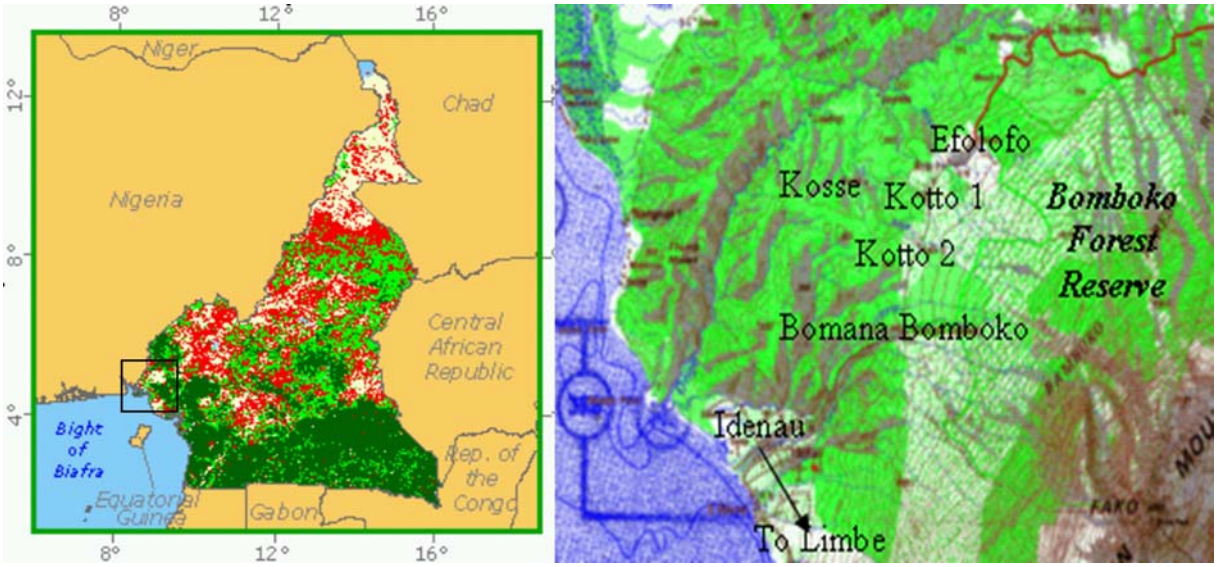


**Figure 1.** The test area.

The major land cover forms comprise subsistence agriculture (principally food crops; for example: colocacia, yams, cassava, maize, beans, Musa species, etc), agricultural plantations (principally Palm, Cocoa and sparsely Musa species), lowland primary forests, scrubs (elephant bush), mono-dominant forest. Part of the study area lies within the Bomboko Forest Reserve. The climate is hot and very humid with annual precipitation ranging from 3000 to 10000 mm and an annual average temperature of approximately 29°C. Based on the precipitation, two distinct seasons can be discerned: a long rainy season from March to November and a short dry season from December to February.

The reasons for the selection of this site are: (1) the floral and faunal variety makes this area a biodiversity hotspot and consequently necessitates conservation and management; (2) continuous change in the land use and cover; (3) the presence of a management and conservation project in the area on whose database access was granted and; (4) fondness of the researcher with the area.

### 2.2 Data Acquisition

The selection of the satellite imagery was based mainly on the availability of cloud free scenes. Initially, the objective was to carry out a multi-temporal analysis using datasets of equal intervals stretching over two decades. Unfortunately, the required satellite data are either not available in the archive or had a bad quality owing to cloud cover. Finally two dates of Landsat imagery were selected: TM 1987 and ETM 2002, path 187, row 57. The scenes were acquired in the month of March and December respectively (corresponding to the dry season), thereby, apparently reducing scene-to-scene variations due to sun angle, atmospheric condition and vegetation phenology. According to [10], the impact of sun angle differences and vegetation phenology differences may be partially reduced by selecting data belonging to the same time of the year.

## 2.3 Pre-processing

Pre-processing of satellite images prior to actual change detection is essential and has as its unique goals the establishment of a more direct linkage between the data and biophysical phenomena, the removal of data acquisition errors and image noise, and the masking of contaminated scene fragments like clouds [2]. Certain techniques were applied to attenuate the effects of geometric and radiometric variations in the images. Even though the images had already been geometrically corrected, ground control points were used to rectify the 2002 image and it was used as the master to co-register the 1987 scene.

Subsequently, the images were topographically normalized to account for extraneous effects caused by terrain related variations. The C-Factor non-Lambertian method, which is based on using a DEM of the same resolution as the image to be corrected, to model illumination conditions was used in this study [7]. The DEM is required to compute the incident angle defined as the angle between the normal to the ground and the sun rays.

The effects of atmospheric interference (scattering and absorbing) on the spectral values were not corrected as the necessary ancillary data (visibility and relative humidity) were not readily available.

## 2.4 Implementation of Change Detection Techniques

The basic premise in applying change detection techniques is that the changes in land cover must result in changes in radiance values and changes in the radiance due to land cover change must be large with respect to radiance change caused by other factors [10]. A wide variety of digital change detection algorithms have been developed over the last decades of which different reviewers have attached definitions that vary in complexity and to a certain extent in coverage. The algorithms selected for this study are those mostly frequently implemented in vegetation canopy studies in the tropics.

### 2.4.1 Univariate Image Differencing

Single bands of registered images (1987 and 2002) are subtracted to produce a residual image representing the change between both dates. Band 5 was preferred because it is least affected by atmosphere and is good for vegetation analysis. Thresholds are calculated from the histogram to differentiate change and no-change areas.

### 2.4.2 NDVI Differencing

This approach is similar to the univariate image differencing method. To begin with, Normalised Difference Vegetation Index (NDVI) is calculated for each date of imagery as in equation (1) below and later, the resultant NDVI images are subtracted from one another to obtain change areas. Lastly, thresholds are then determined to separate change from no-change pixels.

$$NDVI = (TM4 - TM3) / (TM4 + TM3) \quad (1)$$

### 2.4.3 Change Vector Analysis (CVA)

This procedure takes advantage of the fact that multi-spectral remote sensing data can be represented as coordinates of a vector in multi dimensional space. A change vector can be described by a magnitude (vector length) of change from date 1 to date 2 (Jensen 1996) and an angle of change (vector direction). Owing to the potentially large number of possible change vector directions, it is often desirable to simplify the characterisation of change direction. Therefore, to ease implementation, CVA can be applied to multi-temporal data to compare the differences in the time-trajectory of a biophysical indicator for successive time periods [5]. It processes the full dimensionality (spectral and temporal) of the image data and produces two outputs: change magnitude and change direction.

In this study, CVA was applied using the Tasselled Cap as biophysical parameter.

Initially, Tasselled Caps were calculated from bands 1, 2, 3, 4, 5, and 7 of the 1987 and 2002 images respectively. Brightness and greenness images were determined for each year using the first two bands of the Tasselled Cap images. Next, brightness and greenness differences were evaluated for the time interval, from which magnitude and direction images were calculated.

Magnitude was calculated from the difference images shown in the equation (2):

$$|\Delta G| = \sqrt{(\text{brightness diff.})2 + (\text{greenness diff.})2} \quad (2)$$

Afterwards, thresholds were determined for the magnitude image to separate change from no-change pixels. Conventionally, the threshold of the change magnitude is empirically determined (like in other change detection techniques).

Finally, the directions were calculated as indicated in equation (3) and (4):

$$\text{Cos}\theta 1 = \text{brightness diff.} / \text{magnitude} \quad (3)$$

$$\text{Cos}\theta 2 = \text{greenness diff.} / \text{magnitude} \quad (4)$$

The direction images facilitated the discrimination of the change types.

### 2.4.4 Post Classification Comparison (PCC)

It involves rectification and classification of each remotely sensed imagery separately. The two images are classified and the resultant maps are then compared on a pixel by pixel basis using a change detection matrix [3].

### 2.4.5 Post Classification using binary mask on date 2

A base image referred to as date 1 is selected (in this case Landsat 2002). Landsat 1987 (the earlier image) is considered as date 2. Landsat 2002 (date 1) is rectified and classified using maximum likelihood algorithm. Next, band 5 from both dates of imagery is placed in a new dataset. The two-band data set is analysed using image differencing to produce a new file. By analysing the histogram, threshold values were selected to identify areas of change and no-change in the new image (similar to image differencing technique described above).

The change image is then recoded into a binary mask file consisting of areas that have changed between the two dates. The change mask is then overlaid onto date 2 (Landsat 1987) and only those pixels that were detected as having changed are classified in the Landsat 1987 (date 2) imagery.

A post classification comparison is then applied to yield from-to change information.

## 2.5 Accuracy Assessment

Historical reference data for the study area were either inexistent or incomplete. The aerial photograph flights commissioned in 1984 were envisaged to serve as historical reference data but after examining the date it was realised that the entire test site was not surveyed during the flight, presumably due to cloud cover. Consequently, the visual interpretation method was adapted and used to develop reference data for error matrices. Random sample points were selected from ground truth data collected in 2003 and displayed on the TM, RGB colour composite imagery of 1987. The points were then labelled as change or no change by visual interpretation and comparison. Interviews on land use history carried out during the field studies were used to complement the data ("from" information). An error matrix was subsequently developed and plotted against the values of change images.

## 3 RESULTS

The values of the images produced by the differencing procedures (univariate and NDVI differencing) presented a normal distribution with no-change pixels accumulating on the peak and change pixels on the tails. Threshold levels were determined using a one step thresholding method (by testing different standard deviation values from the mean). The best results were obtained using one standard deviation. After assessing the accuracy of the differencing methods in detecting change and no-change areas the univariate image differencing method gave an overall accuracy of 89.61% and a kappa coefficient of 0.7936. The NDVI differencing had an overall accuracy of 72.73% and a kappa coefficient of 0.4829. Both methods have the disadvantage of not providing "from-to" information. Thresholds were also determined for the magnitude image of the CVA method to separate change and no-change areas. The one-step standard deviation approach was also implemented here. The overall accuracy was 70.13% and kappa coefficient was 0.3590.

**Table 1.** Possible change classes from both input components and related types of change.

| Classes | Brightness | Greenness | Probable Descriptions |
|---|---|---|---|
| **Class 1** | - | - | Burning/water |
| **Class 2** | + | - | Deforestation |
| **Class 3** | - | + | Re-growth |
| **Class 4** | + | + | Biomass loss |

"From-to" information was obtained from the direction image. The fact that just the brightness and greenness bands were employed, change classes constituted $2^2$ that is, 4 classes could be discerned as indicated in table 1.

By overlaying the magnitude image on the direction image the change scenario could be visualized. The post classification comparison procedure was carried out by independently classifying the imageries of 2002 and 1987 respectively. The 2002 image was classified using the maximum likelihood algorithm into 7 thematic classes (primary forest, secondary forest, palm plantation, intensive subsistence agriculture, mono-dominant forest, trees and scrubs, and exploited or cleared area) as shown in figure 3. On the other hand the 1987 image was classified into 3 thematic classes (primary forest, secondary forest and trees and scrubs) using unsupervised classification (see figure 2).

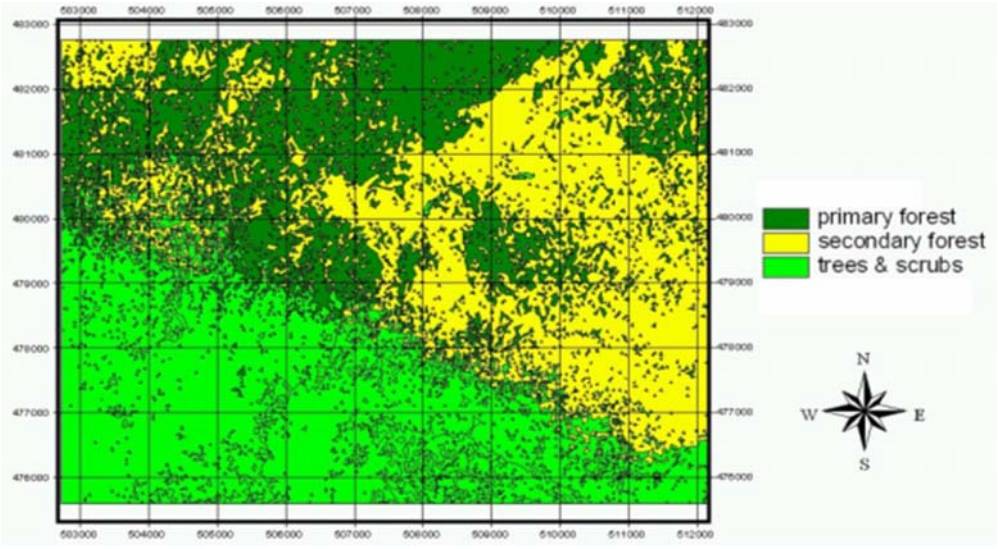


**Figure 2.** Land cover map of the test site for 1987 resulting from unsupervised classification.

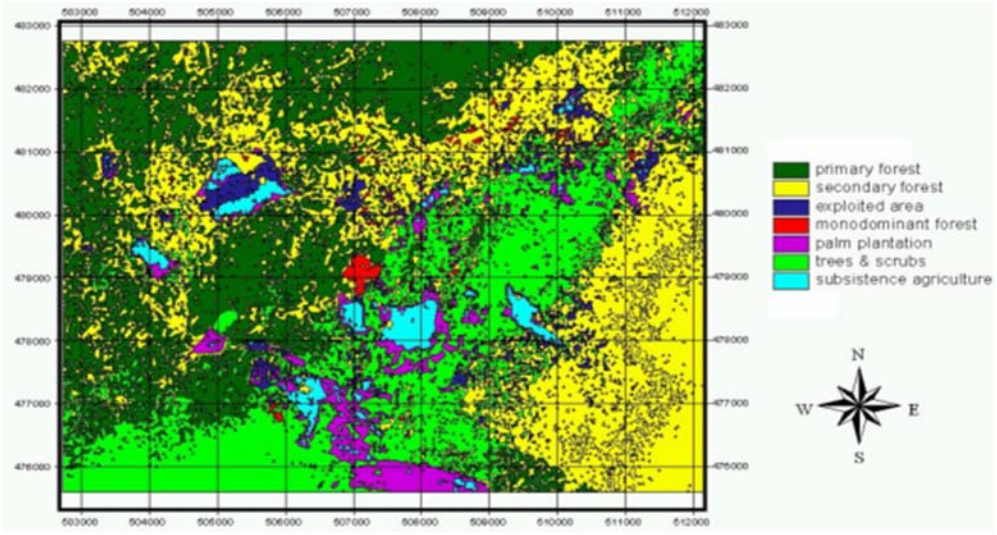


**Figure 3.** Land cover map of the test site for 2002 resulting from supervised classification.

The classified images were then overlaid and a change image generated. 21 change classes were discerned. The overall accuracy was 70.49% and the overall kappa statistics was 0.6614.

**Table 2.** Land cover changes from 1987 to 2002.

| Land Cover | 1987 | | 2002 | | Change | |
|---|---|---|---|---|---|---|
| | Area (ha) | % | Area (ha) | % | Area (ha) | % |
| **Prim forest** | 1430,928 | 21,52 | 1306,807 | 19,65 | 124,121 | 1,87 |
| **Sec. forest** | 2702,258 | 40,64 | 2933,881 | 44,12 | -231,623 | -3,48 |
| **Trees & Scrubs** | 2516,236 | 37,84 | 1815,167 | 27,30 | 701,069 | 10,54 |
| **Palm Plantation** | - | - | 221,564 | 3,33 | 221,564 | 3,33 |
| **Subsistence Agriculture** | - | - | 122,101 | 1,84 | 122,101 | 1,84 |
| **Monodominant forest** | - | - | 64,797 | 0,97 | 64,797 | 0,97 |
| **Exploited Area** | - | - | 185,105 | 2,78 | 185,105 | 2,78 |

The land cover/land use change results were quantified in two ways. First, the totals for each land use/cover change type were tabulated and the trends between the years examined as indicated in table 2. Later, bar graphs were created to illustrate the changes as shown on figure 4.

The post classification comparison using binary mask on date 2 (1987) involved recoding the change image produced from differencing band 5 (had a better overall accuracy than the NDVI differencing) into a binary mask consisting of areas that have changed between the two dates. The change mask was encoded onto date 2 and only the changed pixels were classified. The results obtained by using these five techniques are summarised in table 3 below.

**Table 3.** Comparison of the performances of the change detection procedures.

| Change detection procedure | Kappa Statistics | Overall Accuracy |
|---|---|---|
| **Band 5 Differencing** | 0.7936 | 89.61% |
| **NDVI Differencing** | 0.4829 | 72.73% |
| **Change Vector Analysis** | 0.3590 | 70.13% |
| **Post Classification Comparison** | 0.6614 | 70.49% |
| **Binary Mask & Post Class. Comparison** | 0.7936 | 89.61% |

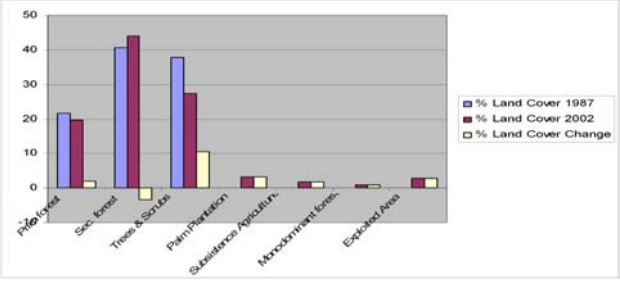


**Figure 4.** Bar chart illustrating percentage change in land cover classes.

## 4 DISCUSSION

The objective of this study was to develop an accurate and efficient change detection method to monitor the conversion of forest to agricultural land from a time-series satellite image database of the mount Cameroon region. It was of utmost importance to generate accuracy assessment data from the visual interpretation and comparison of TM colour composites of the 1987 imagery and terrestrial data acquired in 2003 as no other reliable historical reference data was available for this remote, inaccessible and permanently cloudy study area. The highest accuracy was obtained from the univariate image differencing method confirming the assertion of [10] that post classification comparison was less effective compared to image differencing techniques. In this study, Band 5 was implemented as it is least influenced by the atmosphere and it proved to be effective in evaluating changes from forest land to agricultural plantations. This univariate differencing approach is straight forward and allows an easy identification of large scale change locations. It is worthy to note that the accuracy assessment data were recorded in a stratified random approach in which possible land use/cover classes were identified on printouts (unsupervised classification and image compositing) and the data recorded randomly from targeted areas. Consequently, most of the accuracy assessment data were recorded from large homogenous areas (the areas best detected by the band 5 differencing) thus, the highest accuracy produced by this technique. The most critical aspect of this technique

is the determination of the threshold values, which remains very subjective. After several attempts of testing different threshold values the difference image was established. Large scale homogenous change areas were located but not all types of change were adequately dealt with.Similarly the NDVI technique also detected large scale homogenous changes. An increase in the reflectance of the NDVI highlighted areas where the amount of photosynthesising vegetation had increased and a decrease in reflectance highlighted areas where there was a decrease in green vegetation cover.

Post classification comparison as expected produced relatively good results. The most remarkable land cover changes were identified by this approach – the emergence of palm plantation, extensive subsistence food crop cultivation, exploited areas and mono-dominant forest. The very complex and problematic nature of the vegetation classification accounted for the moderate accuracy assessment result of the 2002 image (70%). Due to the closed canopy of much of the vegetation, and the fact that large numbers of different species are found within a few hectares of vegetation it was very difficult to decipher an appropriate classification scheme. Thus, it turned out to be extremely difficult to distinguish structurally similar communities in the satellite images even when ground surveys indicate differences exist. A typical example is demonstrated by the cocoa plantations; even though they were identified during the ground surveys it was difficult to differentiate them spectrally. Unlike palm, they are shade tolerant species and thrive in a midst of other trees. They were classified either under the scrubs and trees or secondary forest classes.

The dynamic nature of the ecosystem possibly led to a disparity between the ground truth data and the spectral information carried in the images since they were acquired at different time periods (satellite image acquisition and ground truthing). Post classification comparison proved to be effective in expressing the specific nature of change as well as providing statistical information on change in the form of graphs, tables and change maps.

Despite having the lowest accuracy of all the procedures, CVA, nevertheless demonstrated great potentials in monitoring tropical vegetation. The direction images provided qualitative information, which gave an indication as to the trend of evolution of the vegetation. As reported by [4], a general limitation of this technique is that the vectors contain dynamic information and not state information. For example, the vector representing deforestation (increase in brightness and decrease in greenness) neither indicates that the change area was previously forest nor that it has changed to non-forest. This vector was obtained in areas where mono-dominant forest occurred on the 2002 image and not on the 1987 image.

## 5 CONCLUSION

The results reveal that all the techniques proved satisfactory in locating and identifying the extent of change. Each technique has its merits and there apparently is no single best way to perform change detection. Depending on the degree of details set out (location, type and nature of change) different methods will be suitable at different instances. While certain procedures necessitate a high degree of a priori knowledge (Post Classification Comparison) others required a high level of a posteriori information (Univariate differencing, NDVI differencing, and CVA)

The Univariate and NDVI image differencing techniques are straight forward and they identify location changes but give no information as to the type and nature of changes. CVA and post classification comparison on the other hand have the added advantage of providing information pertaining to the type and the nature of changes. The integrated approach of the image differencing and post classification comparison provided good location as well as type and nature information. Uncertainties will still remain as to the best technique with the future of change detection lying in an integrated approach.

The most significant conclusion is that the main land cover changes in the study area (conversion of forest land to agricultural land) can be monitored with a high degree of accuracy even using simple straight forward remote sensing techniques. This is very important considering that management initiatives are now geared towards community forest management. It is thus reassuring when techniques exists that are easy to implement and their results are also easy to interpret. This coupled to the fact that the approaches provide a cost-effective alternative when more information is needed but budgets are limited could only foster the management of resources by communities. Nevertheless, much research needs to be done to improve upon the results of land use/cover change monitoring in this study area and Cameroon at large. The establishment of a national (regional) spatial policy coupled with a GIS database will not only coordinate activities in this field but will also provide valuable historical and contemporary data to researchers. Moreover, continuous monitoring of changes using remote sensing analyses complemented by field surveys at regular intervals is required.

## ACKNOWLEDGEMENTS

This work is carried out in the department of Remote Sensing and Landscape Information Systems, University of Freiburg under the supervision of Professor Koch. The acquisition of the remote sensing and GIS material was funded by the International Promotions Programme (IPP) of the Faculty of Forest and Environmental Sciences, University of Freiburg – Germany. The field trips were partially funded by the IPP, *Wissenschaftliche Gesellschaft* – University of Freiburg and GTZ Cameroon.

## REFERENCES

[1] COPPIN P. R. AND BAUER M. E., 1996: Digital Change Detection in Forest Ecosystems with Remote Sensing Imagery. Remote Sensing Reviews, Volume 13, pp. 207-234.
[2] COPPIN P., JONCKHEERE I., NACKAERTS K., MUYS B. AND LAMBIN E., 2004: Digital change detection methods in ecosystem monitoring: a review. Int. J. Remote Sensing, Vol. 25, No. 9, pp. 1565-1596.
[3] JENSON J. R., 1996: Introductory Digital Image Processing – A Remote Sensing Perspective.
[4] JOHNSON R. D. AND KASISCHKE E. S., 1998: Change Vector Analysis: A technique for the Multispectral Monitoring of Land Cover and Condition. Int. Journal of Remote Sensing, 1998, Vol. 19, No. 3, pp. 411 – 426.
[5] LAMBIN E. F. AND STRAHLER A. H., 1994: Change-Vector Analysis in Multitemporal Space: A Tool to Detect and Categorize Land-Cover Change Processes Using High Temporal-resolution Satellite Data; Remote Sensing of the Environment, 48: pp. 231-244.
[6] MAS J.-F., 1999: Monitoring Land-cover Changes: A comparison of change detection techniques. Int. J. Remote Sensing, Vol. 20. No. 1, pp. 139-152.
[7] MCCORMICK N., 1999: Satellite based forest mapping using the Silvics software – User Manual.
[8] MICHALEK J. L., WAGNER T. W., LUCZKOVICH J. J. AND STOFFLE R. W., 1993: Multispectral Change Vector Analysis for Monitoring Coastal Marine Environments. PE&RS Vol. 59, No. 3, March 1993, pp. 381-384.
[9] SADER S., 2002: Change Detection techniques for Monitoring Forest Clearings and Regrowth in a Tropical Moist Forest.
[10] SINGH, 1989: Digital Change Detection Techniques Using Remotely-sensed Data. Int. J. Remote Sensing, Vol. 10, No. 6, pp. 989-1003.
[11] SOHL T. L., 1999: Change Vector Analysis in the United Arab Emirates: An Investigation of Techniques. PE&RS, Vol. 65, No. 4, April 1999, pp. 475-484.

# Detection of the ground water distribution using thermal remote sensing technique in the Kirya oasis, southern part of the Taklimakan desert, Xinjiang, China

Y. Tashi[a], M.-F. Courel[a] and T. Tiyip[b]

[a] UMR 8586 PRODIG, 2 rue Valette 75005 Paris France, email : tashi@univ-paris1.fr
[b] University of Xinjiang, 14 Shengli road, 830046 Urumqi, China

## ABSTRACT

Kirya oasis, which lies in the southern part of the Taklimakan desert and the north foot of the Kunlun Mountains, is one of the cases that have shown obvious degradation of ecological environment due to the intrusion of human activities in the last 50 years. Therefore, it has become one of the target areas for researching, exploiting and utilizing of water resources in the oasis. The purpose of this study is to determine the depth of occurrence of groundwater and evaluate the ground water level distribution in oasis and desert ecotone using thermal IR image data in combination with the measured groundwater level, soil temperature and auxiliary material of the research area. Based on the field measured groundwater level data and soil temperature, the regressive relationship between the surface temperature and the ground water has been established and the inversion model of groundwater level has been elaborated using the integrative means of remote sensing and mathematical modeling. The result of experimental tests of the model in the oasis and desert ecotone, Kirya County, Xinjiang Uyghur Autonomous Region has shown a good correspondence, the correlation coefficient is 0.893.

**Keywords:** oasis and desert ecotone , thermal IR image data , soil temperature, inversion model of ground water.

## 1 INTRODUCTION

It is 30 years since the first application of remote sensing technique to detection and estimation of groundwater resources. Scientists initially estimated the existence of groundwater resources by using air photos and via topographic and vegetation indices. Along with the development of thermal remote sensing technique, scientists have tried to apply this technique to detection of groundwater, such as the quantitative study of the relationship between the surface temperature of representative land coverage types and groundwater abundance using the thermal IR image data of Landsat TM.

Kirya oasis, which lies in the southern part of the Taklimakan desert and the north foot of the Kunlun Mountains, is one of the cases that have shown the obvious degradation of ecological environment due to the intrusion of human activities in the last 50 years. The purpose of this study is to determine the depth of occurrence of groundwater and evaluate the ground water level distribution in oasis and desert ecotone using thermal IR image data in combination with the measured groundwater level, soil temperature and auxiliary material of the research area.

## 2 NATURAL CONDITIONS AND DATA COLLECTION

### 2.1 Natural condition

Kirya (Yutian) County was founded in 1833, giving it the longest history in Hotan (Hetian) Prefecture. It is located along the south margin of the Taklimakan Desert and in the middle part of the north foot of the Kunlun Mountains. Its eastern part has pebbly terrain, the *gobi* desert adjacent to Niya(Menfeng) County, and its western part has sandy desert terrain and meadows adjacent to Qira (Cele) County. It is located at 81°09′-82.51′ E and 35°14′-39°29′ N, is 30-120km wide from the east to west, 466 km long from the north to the south, and 40,300 $km^2$ in land area of which oasis constitutes $307.99\times10^4$ mu. The town of Kirya is located at 81°40′ E and 36°52′ N, and is 1,427m in altitude. It is one of the highest town and oasis in the Taklimakan Desert, and is 1,329 km from Urumqi, the capital of Xinjiang province, china (Figure 1).

Kirya County is deep in the interior of a typical inland arid land area. Multi-year (1956-1999) average precipitation is 43.7mm. Multi-year average evaporation is 2,420.23mm, and multi year average relative humidity is 42%. Since it is located along the south margin of the Taklimakan Desert, the area surrounding the oasis is very hostile, the ecological system is very fragile, and the condition for human existence are very harsh. Kirya oasis is

one of the cases that have shown the obvious degradation of ecological environment due to the intrusion of human activities in the last 50 years.

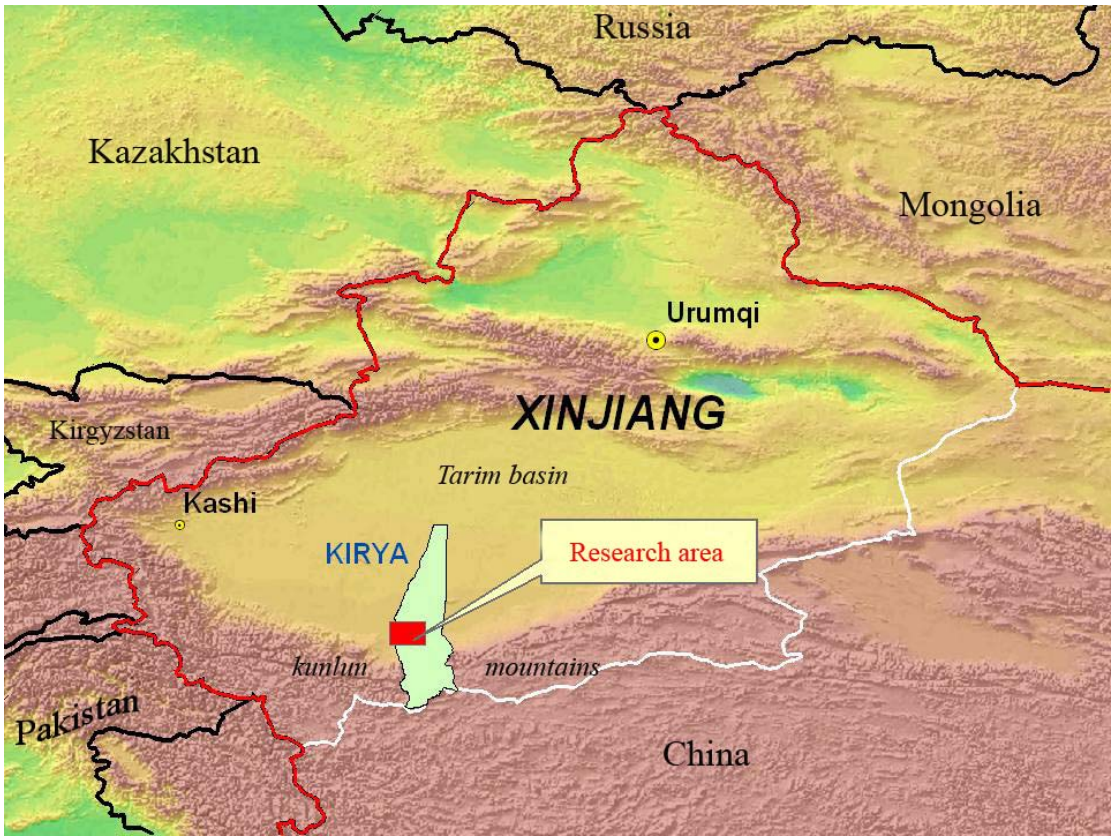


**Figure 1** Geographic position of the research area.

Groundwater is one of the most important natural resources in the arid and semi arid land. Supplying of groundwater has close connection with the terrain and geological conditions and the sources of water.

The groundwater in the piedmont plain originated mainly from surface water, while a part of the surface water in the plain comes from groundwater. There exists such relationship as mutual supply between surface water and ground water, which is called the mutual transformation of surface water and groundwater.

The rivers, which supply water to Kirya oasis, all originate in the mid-mountain belt and the lower part of alpine mountains, the Kunlun Mountains. Kirya River, principal water resources of the oasis, originates from the Kunlun Mountains above 6,000m. In about 200km from the headwaters, Kirya River reaches the fan apex, whose elevation is 1,920m. The fan radius is about 50km. Kirya Oasis is located at 1,420m , below the fan toe, the river flows into the sand dune area of the Taklimakan Desert.

In the southern part of Kirya , the rivers firstly come into diluvial fan in the piedmont plain after coming out of the mountains. The gradient of riverbed declines sharply downstream. Since the riverbed and the stratum under it mainly consist of pebble layer, the river is lost quickly by infiltration. In addition, the level of the surface water is about 10-100m higher than the groundwater level. So a great deal of surface water infiltrates and replenishes the groundwater which turns into the subsurface stream. Furthermore, the rest of surface water is led to irrigation area by canals, excluding the amount lost by evaporation, most of water seeps and form underground water.

When the seeped groundwater reaches the upper part of the oasis, that is a fine soil belt edge of diluvial fan, because of the falling of the elevation, the weakening of the ability in infiltration, the ground level rises. Thus, some subsurface streams formed by infiltration overflow the ground surface in the form spring and become surface water.

## 2.2 Data collection

A Landsat TM image of the research area taken in June 2001 has been selected as the source of the thermal IR remote sensing data for this study.

From 2 to 18 June 2002, we carried out a field survey in Kirya Oasis and collected a lot of information about its natural conditions such as vegetations, groundwater level, soil moisture and soil temperature at different depth, capillary characteristic of the soil etc. In the mean time, the meteorological data of the same period (from 2 to 18 June 2001) were collected, as well as the geographic coordinates, latitude and water level of the 30 sample points that had been chosen for this study. We paid attention to equal distribution and representativeness of the sample points.

## 3 METHODOLOGY

On the same illumination condition, soil moisture is the main factor that affects the change speed of soil temperature. Because of the higher thermal capacity of high soil moisture area, the soil temperature of this area rise slower than that of low soil moisture area from the sunrise to the time when satellite pass overhead, at this period of time. Therefore, the different areas with different soil moisture value have different soil temperatures. At present, some research works have indicated that the capillary and heat exchange function of soil and rock as well as the evaporation lead to change of surface temperature and soil moisture, which can be manifested as the difference of temperature in the thermal IR band image of Landsat TM. The surface temperature of wet soil is 5k higher than that of water body but lower than that of arid soil. This phenomenon has been applied by some researchers to detect the groundwater concentration areas on the basis of the surface temperature calculate by the thermal IR image data of Landsat TM. All these show that some quantitatively relation could be established between ground water and surface temperature.

In the oasis and desert ecotone, as there is no irrigation, few or none precipitation and strong evaporation, the soil moisture is greatly influenced by groundwater level. When the groundwater is at its higher level, the top soil can be supplied with water by the capillary function of soil and the soil moisture will therefore increase. Inversely, along with the drop of the ground water level, the soil moisture and its water evaporation capacity decrease as a result of the reduction of the water amount supplied by the capillary function of soil, and this leads to the changes in the surface temperature. This means that the fluctuation of groundwater level can bring on to the changes in surface temperature by the capillary and thermal function of soil and inversely the changes in surface temperature can reflect the fluctuation of ground water level. Therefore, by measuring the surface temperature we can indirectly detect the change in the upper level of groundwater and the depth of accuracy of groundwater, and in this sense, remote sensing technique would be the most efficient means of getting rapidly the information on the surface temperature over large area.

To avoid the area affected by surface water, the maximum likelihood classification method has been applied to the image of research area. All the original pixel values classified into the classes influenced by the surface water such as croplands and water body have been replaced by the value of zero, and the masked 0 values are not included in the calculations.

### 3.1 Correlation analyse between surface temperature and grounwater

While it is already known that there is a correlation between surface temperature and groundwater level, the main issue is to know how such a relationship will be at different soil depths (e.g., 0cm, 5cm, 10cm, 15cm, 20cm and 40cm). So we have proceeded to a correlation analyses between groundwater level and soil temperature at different depth based on the field measured and the meteorological data obtained at the weather station.

As it is impossible to get the soil temperature data of all the sample points at the same time, the collected data have to be unified to a same time in order to establish a relationship between remote sensing data and ground water. All the collected data must be unified to the time when satellite passes overhead the research area; it is 10:42 local time. This has been done through the credible observation data of weather station and on the assumption that the weather condition of the research area is stable in the observation period (from 2 to 15 June 2002). As the observation period is relatively short and the weather condition in the early summer is relatively stable, furthermore the research area is small enough to ignore the fluctuation of weather in such a short period of time, thus this assumption become acceptable.

The data of weather station include: soil temperature in the depth of 0cm, 5cm, 10cm, 15cm, 20cm, and 40cm. the observation time are: 2:00, 8:00, 14:00, and 20:00, and the date is 2-15 June 2002.

To make the time interval include the satellite overpasses time, 10 minute is fixed as the time interval for the regression analysis equation (Equation 1) which has been used to simulate soil temperature changes in the whole day (Figure 2). The coefficients (Table 1) have been calculated based on the data of weather station mentioned above, then, the field observed values of the sample points at the different soil depth have been brought into the equation respectively to calculate the temperature which correspond to the satellite overpass time.

$$y = a_0 + a_1 x + a_2 x^2 + a_3 x^3 + a_4 x^4 \quad (1)$$

**Table 1** Coefficient calculated by the way of least square method.

| | a0 | a1 | a2 | a3 | a4 | a5 |
|---|---|---|---|---|---|---|
| **0cm** | 0.00E+00 | 3.73E-05 | -1.18E-02 | 1.11E+00 | -2.83E+01 | 2.48E+02 |
| **5cm** | 5.00E+00 | 4.55E-06 | -1.85E-03 | 2.21E-01 | -7.18E+00 | 2.64E+02 |
| **10cm** | 1.00E+01 | -9.75E-07 | -4.20E-05 | 4.71E-02 | -2.80E+00 | 2.80E+02 |
| **15cm** | 1.50E+01 | -2.42E-06 | 5.25E-04 | -1.99E-02 | -7.68E-01 | 2.85E+02 |
| **20cm** | 2.00E+01 | -1.98E-06 | 4.92E-04 | -3.19E-02 | 3.61E-02 | 2.80E+02 |
| **40cm** | 4.00E+01 | -7.83E-08 | 4.67E-05 | -6.22E-03 | 2.17E-01 | 2.52E+02 |

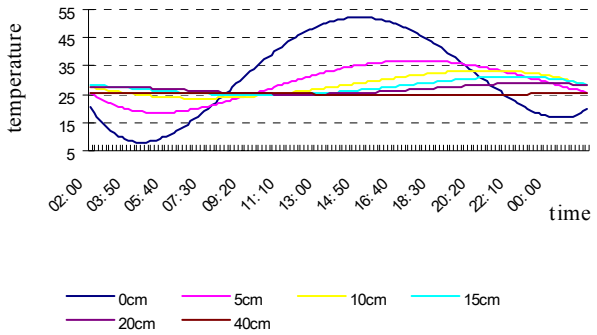


**Figure 2.** Simulation image of soil temperature change in the whole day after data interposition.

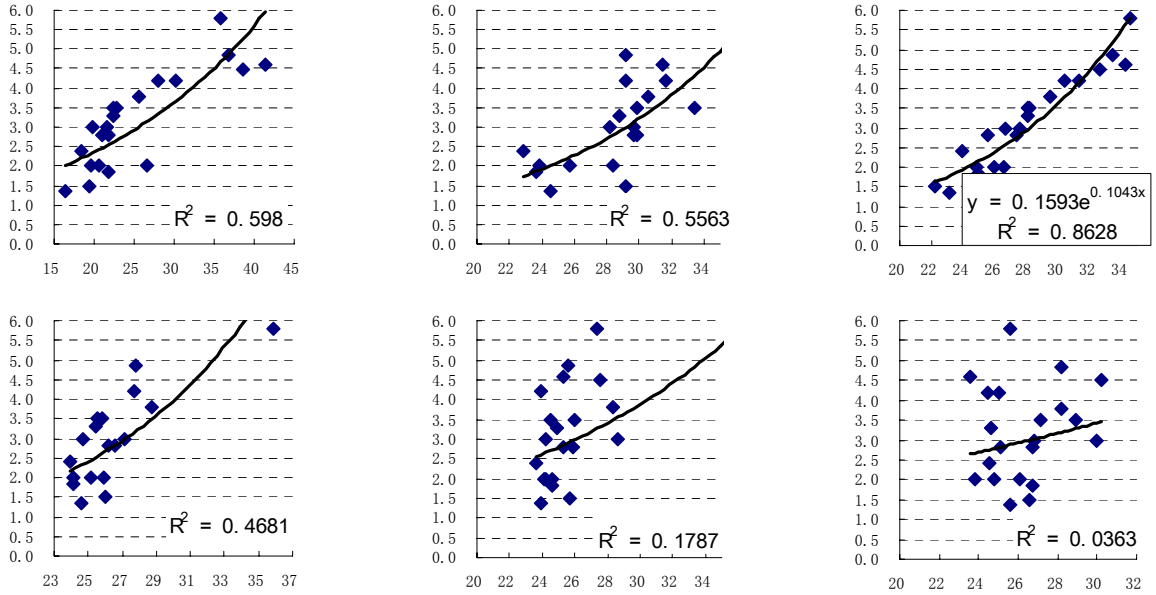


**Figure 3**. correlation charts between land soil temperature and relevant ground water level value.

Be provided with the soil temperature data having the same observation time, we can proceed to a correlation analysis between the soil temperature at each depth and the corresponding groundwater level in order to compare

and find out the soil depth whose temperature could reflect well the occurrence depth of groundwater as a result of a higher correlation value. The result of such analysis is shown as below:

As shown in the Figure 3, the best correlation has appeared in the depth of 10cm with the correlation coefficient $R^2$ =0.8628, the relative equation is:

$$y = 0.1593e^{0.1043x} \tag{2}$$

Where *x* is the soil temperature in the depth of 10cm, *y* is the value of groundwater level.

### 3.2 Surface temperature inversion

The surface temperatures have been calculated from the thermal infrared image data of Landsat TM, using the following algorithm:

$$T_s = \frac{[a_6(1-C_6-D_6)+b_6(1-C_6-D_6)+C_6+D_6]\times T_6 + D_6 T_a}{C_6}$$
$$C_6 = \tau_6 \varepsilon_6 \qquad D_6 = (1-\tau_6)[1+\tau_6(1-\varepsilon_6)] \tag{3}$$

Where $T_s$ is surface temperature, $a_6$ and $b_6$ are coefficient ($a_6$ = -60.3263, $b_6$=0.43436 when the temperature is 0-30 °C), $\tau_6$ is atmospheric transmission, $T_a$ is the mean temperature of the atmosphere, $T_6$ is the brightness temperature (temperature at sensor) $\varepsilon_6$ is surface emissivity. $\tau_6$ and $T_a$ can be estimated respectively with the following equations:

$$Ta = 16.0110+0.92621T0 \tag{4}$$

where $T_0$ is the near surface temperature of the atmosphere;

When the atmosphere moisture falls within 0.4~1.6 in summer, then:

$$\tau_6 = 0.974290-0.08007\ w \tag{5}$$

where $w$(g/cm$^2$) is the atmosphere moisture.

Griend and Owe (1993) have discovered that there is a strong relationship between NDVI and emissivity with the correlation coefficient as high as 0.941, which make it possible to approximately calculate the emissivity value of each image pixel based on the NDVI value of the pixel:

$$\varepsilon_6 = 1.0094 + 0.047 \ln(NDVI) \tag{6}$$

To establish a relationship between the surface temperatures calculated from the thermal IR image data with the Equation 3 and the ground water level, firstly the relationship between the soil temperatures at the depth of 0cm (surface) and that of 10cm has been established with the Equation 7 described below, based on the weather station data mentioned earlier. Then, through the Equation 2, 3, 4,5,6,7, we can set up quantitative relationship between thermal IR remote sensing data and ground water level (Figure 4).

$$y = 20.228e0.0056x \tag{7}$$
$$R2 = 0.9479$$

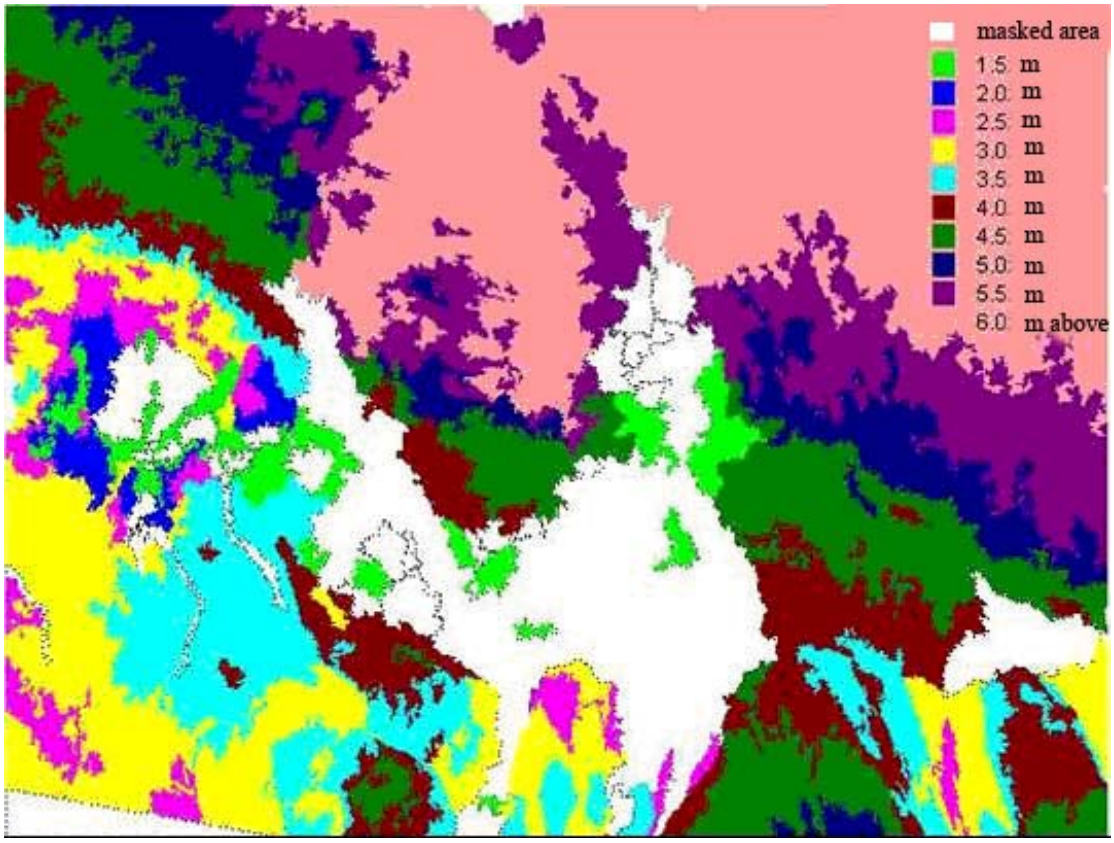


**Figure 4.** The groundwater level map of the research area made through the inversion method.

## 3.3 Accuracy analysis

Table 2 lists the sample points selected both in the field and in the groundwater distribution map for evaluating the accuracy of the inversion model for ground water level. The comparison analysis between the field measured groundwater level values and that estimated through the model shows a good correspondence with the correlation coefficient as high as 0.893, Figure 5.

**Table 2.** sample points and their groundwater value acquired on the field and model.

| № | Geographic position (longitudes and latitudes) | | Field measured groundwater level (m) | Groundwater level estimated through the inverse method (m) |
|---|---|---|---|---|
| **1** | 81.32083ºE | 37.12269ºN | 5.5 | 5.2 |
| **2** | 81.18750ºE | 37.05778ºN | 5.2 | 5.3 |
| **3** | 81.36528ºE | 37.14611ºN | 6.8 | 6.5 |
| **4** | 81.41250ºE | 37.20278ºN | 5.2 | 5.2 |
| **5** | 81.88222ºE | 36.84694ºN | 3.0 | 2.9 |
| **6** | 81.95278ºE | 36.89083ºN | 4.5 | 4.2 |
| **7** | 81.91722ºE | 36.87000ºN | 2.2 | 2 |
| **8** | 81.87139ºE | 36.89194ºN | 4.3 | 4.5 |
| **9** | 81.29556º | 36.89417º | 4.8 | 4.3 |
| **10** | 81.29389º | 36.90889º | 3.8 | 4.1 |
| Correlation coefficient | | | 0.893 | |

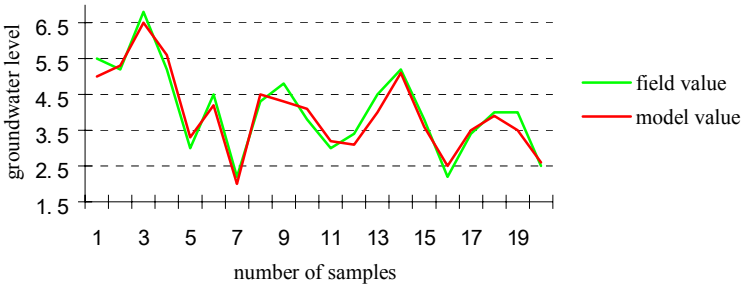


**Figure 5.** comparison charts between the groundwater level values of the field and that of the model.

The result of this study is satisfying in terms of evaluating the ground water level distribution in oasis and desert ecotone using thermal IR image data, but several factors imply the existence of some errors:

1) The Landsat TM image used in this study was taken on 30 June 2001, while all the field measured data were collected from 2 to 15 June 2002, although both in the same month(in June) but not in the same year, so some errors might still exist.
2) The soil types have not been taken into account, the groundwater inversion accuracy could be changing according to the type of soil.

## REFERENCES

[1] SARF, S K AND CHOUDHURY, P R., 1998: Integrated Remote Sensing and GIS for Grondwater Exploration and Identification of Artificial Recharge Sites. *Int J RemoreSensing*, 19(10), 1925-1841.
[2] KAHLE A B AND GOETZ A F H., 1983: Mineralogic Information form a new Airborne Thermal Infrared Multispectral Scanner. *Science*, 222 (4619), 24-27.
[3] KAHLE A B, PALLICONI F., HOOK S, ET AL., 1991: The Advanced Spaceborne Thermal Emission and Reflection Radiometer (ASTER). *Imaging Syst Tech*, 3, 144-156.
[4] YAMGUCHI Y., HASE H. AND OGAWA, K., 1992: .Remote sensing for Geothermal Applicantions. *Episodes* 15(1), 62-67.
[5] WHITING, J.M., 1976: Airborne Thermal Infra-red Sensing Of Soil Moisture and Groundwater. Remote Sensing of Soil Moisture and Groundwater (Collected papers). CANADA: WORKSHOP PROCEEDINGS.
[6] OMAR, A.A., 1990: Use of SIR-A interpretation for under ground water prospecting in southern Iraq. *Remote Sensing: an operational technology for the mining and petroleum industries,* 165-172.
[7] DAS, D., 1991: Extraction of Geomorphic and Geologic Information For Groundwater Exploration Through Satellite Remote Sensing In and Around The WICHITA Mountains, OKLAHOMA. *Eighth Thematic Conference on Geologic Remote Sensing* 1, 171-180.
[8] K.R. KNAPP, K.M. MORGAN. Using SPOT and TM to Map Fractures Related to Ground-Water Resources in the Slick Hills of Oklahoma. Tenth *Thematic Conference on Geologic Remote Sensing* 1, 155-167.
[9] KRISHNAMURTHY，J. AND SRINIVAS, G., 1995: Role of geological and geomorphological factors in ground water exploration: a study using IRS LISS data. *Int. Journal of Remote* Sensing 16 (14), 2595-2618.
[10] MINOR, T.B., CARTER, J.A., CHESTEY, M.A. ETC., 1994: The Use of GIS and Remote Sensing In Groundwater Exploration For Developing Countries. *Tenth Thematic Conference on Geologic Remote Sensing* 1, 168-178.
[11] KRISHNAMURTHY, J., WENKATESA KUMAR, N., JAYARAMAN, V. MANIVEL, M. ETC., 1996: An approach to demarcate ground water potential zones through remote sensing and geographical information system. *Int. Journal of Remote* Sensing, 17 (10), 1867-1884.
[12] SARAF，A.K. AND CHOUDHURY, P.R., 1998: Integrated Remote Sensing and GIS for Groundwater Exploration and Identification of Artificial Recharge Sites. *Int. Journal of Remote* Sensing, 19 (10), 1825-1841.
[13] MURTHY, K.S.R., 2000: Groundwater potential in a semi-arid region of Andhra Pradesh --- a geographical information system approach. *Int. Journal of* Remote Sensing 21 (9), 1867-1884.
[14] SHAHID, S., NATH, S.K. AND ROY J., 2000: Groundwater potential modeling in a soft rock area using GIS. *Int. Journal of Remote* Sensing 21 (9), 1919-1924.
[15] FINCH, J.W., 1990: Location of high yielding groundwater sites in Zimbabwe use of remote sensed data. Remote Sensing: an operational technology for the mining and petroleum industries, 147-152.

[16] WASTON, K.，ROWEN, L.C. AND OFFIELD, T.W., 1971: Application of thermal Modelling in the Geologic Interpretation of IR Images. *Remote Sensing Environment* 3, 2017-2041.
[17] POHN, H.A.，OFFIELD, T.W. AND WASTON, K., 1974: Thermal Inertia Mapping from Satellite Discrimination of Geologic Units in Oman. *J. Res. U.S. Geol. Surv.* 2, 147-158.
[18] PRATT, A. AND ELLYETT, C.D., 1979: Thermal Inertia Approach to Mapping of soil moisture and Geology. *Remote Sensing Environment* 8, 151-168.
[19] PRICE, J.C., 1977: Thermal Inertia Mapping：A View of the Earth. *Journal of Geophysical Research* 82, 2582-2590.
[20] PRICE, J.C., 1982: On The Use of Satellite Data to Infer Surface Fluxes at Meteorological Scales. *Applied Meteorology* 21, 1111-1122.
[21] OWE, M., 1998: Estimating Surface Soil Moisture from Satellite Microwave Measurement and a Satellite Derived Vegetation Index. *Remote Sensing of Environment* 24, 331-345.
[22] SEGUIN, B., 1991: The Assessment of Regional Crop Water Conditions from Meteorological Satellite Thermal Infrared Data. *Remote Sensing of Environment* 35, 141-148.

# Land use changes induced by a hydropower reservoir in Fincha'a watershed, western Ethiopia

B. Tefera[a] and G. Sterk[b]

[a] Oromiya Agriculture and Rural Development Bureau, P.O.Box 21118, Code 1000, A. Ababa, Ethiopia. Tel. +251 1 494694, Fax: +251 1 511141, email: bezuayehto@yahoo.com.
[b] Erosion and Soil & Water Conservation Group, Wageningen University, Nieuwe Kanaal 11, 6709 PA, Wageningen, the Netherlands.

## ABSTRACT

This paper analyses the land use dynamics caused by the hydropower dam construction in 1973 at Fincha'a watershed (1318 km2), tributary of the Blue Nile. Aerial photos (1957 and 1980) and an ASTER satellite image of 2001 were used to make three land use maps of the watershed by means of GIS. The study detected a waterbody of 151 km2 in 1980 and 239.3 km2 in 2001; the increment of 88.3 km2 was due to stream diversion into this reservoir in 1987. The lake has inundated 100 km2 grazing land, 120 km2 swamp, 18 km2 cropland and 1.2 km2 forest. There was a net increase of 50.6% in cropland between 1957 and 2001 due to normal population growth in the area and forced migration caused by inundation. Grazing land has decreased by 51% between 1957 and 1980 due to the reservoir, cropland expansion and a high rainfall amount in 1979, prior to 1980. On the other hand grazing land has increased by 21.7% between 1980 and 2001 mainly due to low rainfall amounts in the area which enabled grazing on previous swamp land. Out of the potentially available land for cropland, grazing, forestry and settlements, cropland has increased from 39% in the year 1957 to 77% following the construction of the dam. Cropland has reached the limit that there is hardly any free land available for further expansion. Implementation of suitable land use options could reduce the undesired land use changes in the area. This requires local and international cooperation.

**Keywords:** Land use, GIS, Remote sensing, Fincha'a hydropower dam, Oromiya, Ethiopia.

## 1 INTRODUCTION

Dams have been built for thousands of years for electricity, irrigation, flood control and water supply. However, they cause losses of agricultural lands, forests and grasslands due to inundation [9], [23] and alter the traditional resource management practices [5], [18]. Ethiopia has about 30,000 MW hydropower potential but it was possible to exploit less than 2% of this by the year 1997 [2], [22] mainly due to financial shortfall [2]. Fincha'a hydropower dam was constructed in 1973 for electricity, irrigation, fishery and tourism [11], [13] and generates 128 MW [2], [5], [6]. The original installed capacity of this scheme was 100 MW but increased to the current level following the diversion of Amarti River into this scheme in 1987. Studies showed that the reservoir has evicted several people from their original places [1], [3], [17]. The displaced people have started agricultural activities on steep areas within Fincha'a watershed, which may have caused undesired land use changes in the upstream part of the watershed.

Land use changes directly impact biotic diversity, contribute to local and regional climate change and are the primary sources of soil degradation [8]. The land use studies in Ethiopia, however, give emphasis to estimation of forest cover and deforestation rates that occur at national level [7], [15], [18]. Recent watershed based land use studies in different parts of the country, however, show that there has been an increase in croplands at the expenses of forests, grassland and bush land due to population growth and the land reform of 1975 [10], [21], [24]. These studies showed that the land use dynamics have environmental implication at local scale and beyond. The objective of this paper was to analyse land use changes in Fincha'a watershed over a period of time that includes the creation of a water reservoir and describe the possible causes and implications of these changes on the community at large and the hydropower dam itself. Comparisons were made with the results of the recent studies conducted elsewhere in the country. It was intended to separate between expected land use changes due to population increases, and the changes caused by the reservoir.

# 2 MATERIALS AND METHODS

## 2.1 The setting

The geographical location of Fincha'a watershed is between 9°10'30" to 9°46'45" North latitude and between 37°03'00" to 37°28'30" East longitude. In administrative terms, it is situated in eastern Wallaga zone, Oromiya region, western Ethiopia (Figure 1). It covers an area of about 1318 km$^2$. The dam has 340 m crest length and 20 m height above the lowest foundation level [14].

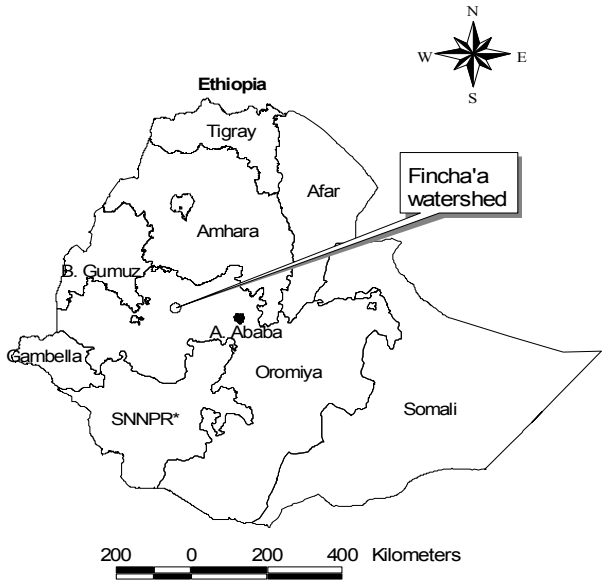


**Figure 1.** Location of Fincha'a watershed. * SNNPR- Southern Nation, Nationalities and Peoples' Region.

Weather data were available from a station at Shambu town, which is situated at the middle part of the watershed. The station has a dataset of daily values of rainfall, temperature, relative humidity, sunshine hours, and wind speed from 1970 till to day. The yearly average rainfall is 1823 mm. About 80% of the annual rain falls between May to September. The monthly mean temperature varies from 14.9°C to 17.5°C (Figure 2). The average annual Reference Evapotranspiration (based on Penman-Monteith) is 1320 mm, with low monthly variations.

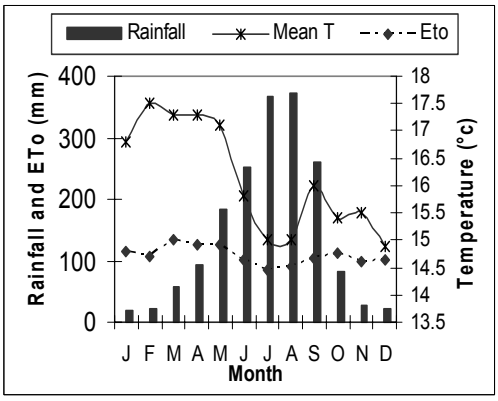


**Figure 2.** Climate conditions at Fincha'a watershed. Source: The National Metrological Service Agency (2004).

In general, elevation in the watershed ranges between 2200 m to 3100 m. Most of the area (80%), which can be described as a wide rolling plateau is within the altitude range between 2200 m and 2400 m. About 18% of the watershed is situated between 2400 and 2800 m: the difference being between 2800 and 3100m. The high rising grounds of the watershed boundary area as well as the middle parts of the watershed which exist as an isolated outcrop are made of Quaternary volcanics. A small part of the watershed at the north eastern part is covered by the Adigrat sandstone formation. The dominant soils are clay loam, clay and loam.

Population density was 98 people/ km$^2$, with average family size of 8.3 people per household. In 2002 the average land holding size was 2.5 ha, with an average per capita land holding size of 0.3 ha [3]. Integrated crop-livestock production is the main agricultural system in this watershed. Land was privately owned before the land reform of 1975. Under this tenure arrangement few landlords owned much land but tenants use the land based on mainly sharecropping arrangement. However, following the land reform of 1975, the tenant-landlord relations were relinquished and farmlands were distributed to the tillers. Since then, land has become state property under which only use right was given to the farmers. On the other hand, the other land

use types such as forests and grazing lands have become open access lands leading to encroachment and overgrazing.

## 2.2 Methodology

The technologies of Geographic Information Systems (GIS) and Remote Sensing (RS) were used to analyse the spatial-temporal status of land use in Fincha'a watershed. A combination of aerial photographs and a satellite remote sensing image was used. Aerial photos of the year 1957 taken in November to December (57 photographs) and 1980 taken in January (60 photographs) with base scales of 1:50,000 were obtained from the Ethiopian Mapping Agency (EMA). An ASTER satellite image of green, red and near-infrared bands of January 2001 (30 m resolution) was obtained from the internet. While the ASTER image was used due to the absence of recent aerial photographs, the aerial photos were the only sources of information for earlier periods. The timing of all three data sources was such that they represented the dry season, with minimal cloud cover, and could be considered comparable in terms of land cover conditions (e.g. bare conditions on cropland).

The aerial photographs were visually interpreted using a mirror stereoscope. Topographic maps of scale 1:50,000 were obtained from EMA and used to delimit and cut out the study watershed by superimposing the view on the spatial databases created from the aerial photographs. The false colour composite of the ASTER image was created and geo-referenced based on the Universal Transverse Mercator, UTM 1983 and Zone 37. The rectified image was then interpreted in Idrisi GIS using the method of supervised classification. In this method spectral signatures were developed from the specified locations that were verified to be of a particular land use type known as "training sites". Then a vector layer was digitized over a raster scene to get different land use types.

Preliminary land use classes were defined prior to aerial photo interpretation but then some modification was made while interpreting the satellite image. Using aerial photographs eight land use classes were identified: waterbody, cropland, swamp, grassland, bush-covered grassland, forest, plantation and town. But the ASTER image was less detailed, which resulted in a poor differentiation between forest and plantation, and between grassland and bush-covered grassland. Hence, we merged forest and plantation to one class and called it forest, and also grassland and bush-covered grassland were combined into grazing land. Finally, six classes, namely, waterbody, cropland, swamp, grazing land, forest and town were used for the aerial photo and ASTER image interpretations (Table 1).

**Table 1.** Land use classes and their description in Fincha'a watershed.

| Land use classes | Description |
|---|---|
| Waterbody | Areas completely inundated by water |
| Cropland | Areas used for cultivation, including fallow plots and a complex units such as homestead |
| Swamp | Areas flat & swampy during both wet & dry seasons & covered with grass. |
| Grazing land | Areas covered with grass, bushes and trees and used for grazing: usually communal |
| Forest | Areas covered with natural and plantation trees forming nearly closed canopy; 70-100%. |
| Town | Areas covered with urban & marketplaces |

Analysis of annual rainfall was carried out to determine the amounts of rainfall in the year prior to the remote sensing datasets of 1980 and 2001. Only rainfall data from 1970 to 2003 were available, so no information on the rainfall prior to the 1957 dataset existed. It was expected that a relatively wet year prior to the land use classification may have resulted in a larger extent of the waterbody and perhaps more swamp land than when the antecedent rainfall was below average. Overlays of the 1980 and 2001 waterbody areas on the 1957 land use map were made to determine the spatial distribution and magnitude of the land use types directly affected by the reservoir. Comparisons were made between the findings of the current study and those of other land use change studies conducted elsewhere in the country [10], [21], [24]. This was done to differentiate between the effects of the reservoir and other land use change drivers, such as population increase. Altogether five elderly people were interviewed and used as a key informant for their past and current knowledge regarding the extent and environmental effects of land use changes in the area.

## 3 RESULTS

**Rainfall:** The mean annual rainfall at Shambu station was 1823 mm, but showed some variation over the period of analysis (1970-2003) (Figure 3). The obtained coefficient of variation was 22.5%, which indicates a relatively low variation. The annual rainfall ranged from 1281 mm in 1994 to 3195 mm in 1980. We assumed a range of 600 mm

around the average (1523-2123 mm) as being normal fluctuations. Years with rainfall above or below this range were considered abnormally wet or dry, respectively. Wet years occurred from 1977 till 1981, and another wet year was experienced in 1985. Dry years occurred around 1975, which coincided with the famine that struck Ethiopia, and again several dry years were experienced since 1987. A general decline in annual rainfall can be observed following the peak rainfall in 1980. But since the number of years with rainfall data analyzed was limited this is not necessarily a trend. The year prior to the aerial photographs of 1980 was very wet, with an annual rainfall of 2347 mm. The year prior to the ASTER satellite image of 2001 was relatively dry, with an annual rainfall of 1484 mm.

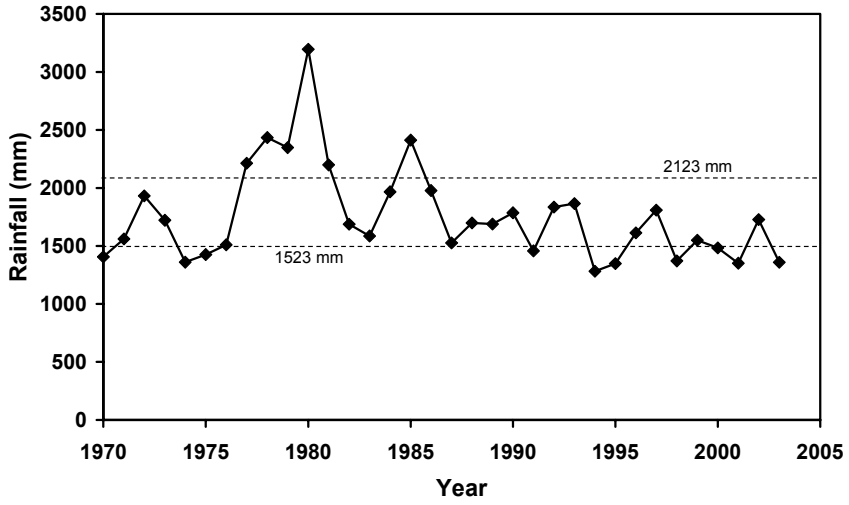


**Figure 3.** Annual rainfall at Fincha'a watershed. Dotted lines indicate the range for assumed normal variation in annual rainfall.

The land use in the three years (1957, 1980 and 2001) was classified according to the classes defined in Table 1. The areas covered by the different classes are shown in Table 2. The same results were plotted in Figure 4, excluding the class 'town' to improve clarity of the maps.

**Table 2.** Land use classes of Fincha'a watershed in 1957, 1980 & 2001.

| Land use | Area in 1957 | | Area in 1980 | | Area in 2001 | | Area change (km2) in | |
|---|---|---|---|---|---|---|---|---|
| | km2 | % | km2 | % | km2 | % | 1957/1980 | 1980/2001 |
| **Waterbody** | 0.0 | 0.0 | 151.1 | 11.5 | 239.3 | 18.2 | +151.1 | +88.2 |
| **Cropland** | 403.3 | 30.6 | 478.8 | 36.3 | 607.1 | 46.1 | +75.5 | +128.3 |
| **Swamp** | 286.1 | 21.7 | 376.6 | 28.6 | 95.5 | 7.2 | +90.5 | -281.1 |
| **Grazing land** | 555.2 | 42.1 | 272.9 | 20.7 | 332.2 | 25.2 | -282.3 | +59.3 |
| **Forest** | 70.5 | 5.4 | 34.1 | 2.6 | 37.9 | 2.9 | -36.4 | +3.8 |
| **Town** | 2.5 | 0.3 | 4.1 | 0.3 | 5.6 | 0.4 | +1.6 | +1.5 |

**Waterbody:** There was no significant waterbody in this watershed before the impoundment period. The interpretations of the 1980 aerial photos, however, show that about 151 $km^2$ was converted to waterbody, which is equivalent to the estimate given in [13]. This value has increased to 239.3 $km^2$ in 2001, a net increase of 88.2 $km^2$. From the 1980 land use map it appeared that there were two major waterbodies (i.e., upper part also called Coomman and lower part also called Doonje) that were physically separated by a ridge (8 m height and 1 km wide) across the lakes and acts as a natural dam [12]. The analysis of the satellite image, however, showed unified waterbodies. This was obviously a result of increased reservoir level following the stream diversion in 1987.

**Cropland:** This category also includes rural villages and homestead plantations because it was practically difficult to treat them as a separate land use type. Most homestead areas are set in such a way that tree plantation and cultivation are intermingled. Generally cropland has increased from 403.3 $km^2$ in 1957 to 478.8 $km^2$ in 1980 and 607.1 $km^2$ in 2001. Overlay analysis of the waterbody in 1980 and the land use map of the 1957 show that 11.5 $km^2$ of croplands that were situated at western, northern and eastern sides of the lower lake were inundated. The waterbody that existed in 2001 has inundated an additional 6.5 $km^2$ areas of croplands. This makes a total of 18 $km^2$

of cropland loss to the farmers due to the creation of the reservoir. Most croplands were situated in relatively flat areas in 1957 and 1980. In 2001, however, many steep lands (as steep as 90%) were converted to cropland.

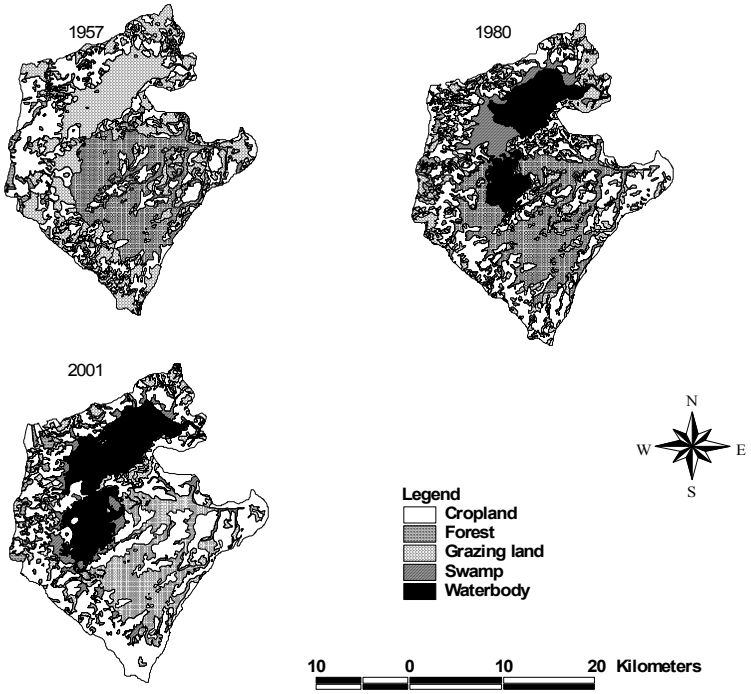


**Figure 4.** Land use maps of Fincha'a watershed in 1957, 1980 and 2001.

**Grazing land:** The area of grazing land has decreased by 50.8% between 1957 and 1980 but increased by 21.7% between 1980 and 2001, i.e., a net decrease of 40.1% between 1957 and 2001. Overlay analysis of the 1957 and the 1980 land use maps show that 94.2 $km^2$ of grazing land have been inundated. An additional 6 $km^2$ of grazing land that was situated in the western sides of the current lake became inundated between 1980 and 2001. This makes a total of 100.2 $km^2$ grazing land that was lost to the farmers due to the reservoir. Grazing lands were situated at depression areas of the watershed where seasonal water logging occurred and along the water divide lines, on the hills and along embankments of streams and rivers.

**Swamp:** Much of the flat areas of the upper part of the reservoir (Coomman) used to be swamp before the creation of the dam. This land cover type has shown a pattern of increase in the first period and a decrease in the second (Table 2). Overlay analysis of the waterbody of the 1980 and 1957 land use maps show that 44.5 $km^2$ of swamp have been inundated. But an additional 75.4 $km^2$ of swamp have been inundated between 1980 and 2001. Consequently, leaving much of its original places for a waterbody, the swamp has engulfed a large area of grazing land and cropland, between 1957 and 1980. The satellite image of 2001, however, detected that the size has considerably reduced in favor of grazing land. The recent decline in the size of swampland is attributable to the generally low amounts of rainfall in the watershed area (Figure 3). The rainfall amount in 1979, prior to the 1980 aerial photographs was abnormally high causing a large area of swamp land. On the other hand, the year prior to the 2001 image was generally a dry year and caused a large area of swamp to become dry, and was classified as grazing land.

**Forest:** There was a general lack of forest cover in the watershed area before 1957. The remaining forest cover has changed from 5.4% in 1957 to 2.6% in 1980 and 2.9% in 2001. Overlay analysis of the waterbody of 1980 and 1957 land use maps show that 0.9 $km^2$ of forests were inundated. An additional 0.3 $km^2$ were inundated between 1980 and 2001. The forests were mainly situated along water divide lines in the western and south-western parts of the watershed, hillsides, along embankments of streams and rivers and adjacent to towns and settlement areas. In general rapid forest reduction was detected between 1957 and 1980 perhaps due to cropland and grazing land expansion. In 2001 the forest cover was increased compared to the amount in 1980. This could be due to the reforestation activities carried out at forest areas, hills and settlements in the 1980s.

**Town:** Urbanization as land cover, in the form of built-up or paved areas, covers 0.3 to 0.4% of the watershed area. The construction of the dam and electrification have created limited job opportunities and attracted people to the towns. Towns showed mixed impacts on land use. On one hand urbanization affects the land use through increasing use of forests for construction and fuel wood but on the other hand plantation activities have been intensified in and around the towns.

# 4 DISCUSSION

## 4.1 Comparison to other watersheds

In this section the results of land use studies conducted in different parts of the country are compared with the situation in Fincha'a watershed. Only the most important land use classes, namely cropland, grazing land and forest were considered. We combined the individual land use classes defined by the authors based on the definition given in Table 1. The studies were conducted at Mettu [21], Denbecha [10] and Chemoga [24] watersheds. The farming system at Mettu is (perennial) coffee based, but those of Denbecha and Chemoga are cereal based. The sizes of those watersheds, study years and relative areas of the land use types are shown in Table 3.

**Table 3.** Major land use classes at Mettu, Denbecha, Chemoga and Fincha'a watersheds in Ethiopia.

| **Land use class** | **Mettu (146 km$^2$)** | | **Denbecha (271 km$^2$)** | | **Chemoga (364 km$^2$)** | | **Fincha'a (1318 km$^2$)** | |
|---|---|---|---|---|---|---|---|---|
| | **1957** | **1982** | **1957** | **1995** | **1957** | **1998** | **1957** | **2001** |
| | % | % | % | % | % | % | % | % |
| **Cropland** | 30.5 | 40.4 | 39.5 | 77.1 | 60.4 | 66.6 | 30.6 | 46.1 (+68.0$^{\dagger}$) |
| **Grazing land** | 32.9 | 18.6 | 32.9 | 17.9 | 14.7 | 6.8 | 42.1 | 25.2 (-37.1$^{\dagger}$) |
| **Forest** | 36.6 | 41.0 | 27.1 | 2.2 | 9.1 | 6.5 | 5.4 | 2.9 (-4.3$^{\dagger}$) |

$^{\dagger}$ *Numbers between brackets show land use changes in Fincha'a watershed between 1957 and 2001.*

Compared to the other study areas the forest cover of Mettu was higher and the amount was increased during the study period. Denbecha had a better forest cover compared to Chemoga and Fincha'a but this value was extremely lowered in 1995. At Denbecha 77% of the area was cropland in 1995 showing a low possibility for further expansion [10]. The proportion of cropland was already very high in Chemoga watershed in 1957 and increased only by 10% in 1998. In Fincha'a watershed it was assumed that the reservoir and swamp will not be used for cropland, grazing and forestry. Based on this assumption cropland was increased by 68% between 1957 and 2001. The cereal based farming systems at Denbecha, Chemoga and Fincha'a demanded more land for cultivation and increased deforestation but the coffee production system at Mettu encouraged forest plantation. Regardless of similar cereal based farming system and the same land reform policy implementation in 1975, the increase in cropland at Denbecha and Fincha'a was extremely high compared to that at Chemoga. The presence of a large area of forest cover at Denbecha and vast grazing land at Fincha'a in 1957 should have created a high possibility for cropland expansion. Grazing land showed a decreasing trend in all the study areas.

## 4.2 Land use changes in Fincha'a watershed

In this section the major land use changes, underlying factors of these changes and opportunities available for the community in the watershed are discussed. The major land use changes in Fincha'a watershed were the creation of 239.3 km$^2$ area of waterbody that inundated 18 km$^2$ cropland, 120 km$^2$ swamps, 100 km$^2$ grazing land and 1.2 km$^2$ forest between 1957 and 2001. In the same period, the area of cropland has increased by 203.8 km$^2$, mainly at the expense of grazing land and forest. Recently the dynamics in the area and location of swamp and grazing land became unusual for the community as well as the power company. Before 2001, many people thought that the reservoir area was expanding but after 2001 it has receded in all directions due to low annual rainfall amounts. The inter-face between swamp and grazing land fluctuates depending on the magnitude of rainfall and the gradient of the reservoir bed. In the inundated area, a low longitudinal gradient of 1:476 m/m was determined between damsite and the remotest part of the reservoir. This could be a reason for a large reservoir area of 239 km$^2$ to be impounded by a low dam of 20 m height and crest length of 340 m.

It was indicated that the annual rainfall amounts together with the dam plays a major role in limiting the suitability of part of the watershed for community utilization such as crop production, forestry, grazing and settlement. Since we do not know the amount of annual rainfall that was occurred before 1970 we assume the

rainfall amount of 1980 as a peak annual amount in the watershed. Therefore, the area of swamp and waterbody in the year 1980 can be used to delimit the potentially available (well drained area) land to the community. There is a probability for such a high annual rainfall amount to occur in the future. Accordingly, the total area that was potentially available for community use was 1032 $km^2$ (78%) in 1957 but reduced to 790 $km^2$ (60%) in 1980 and 2001. This showed that cropland area has increased from 39% in 1957 to 77% in 2001 (Table 4).

**Table 4.** Major land use area compared to the potentially available land in 1957, 1980 and 2001 in Fincha'a watershed.

| **Land use** | **1957 (1032 $km^2$)** | | **1980 (790 $km^2$)** | | **2001 (790 $km^2$)** | |
|---|---|---|---|---|---|---|
| | $km^2$ | % | $km^2$ | % | $km^2$ | % |
| **Cropland** | 403.3 | 39.0 | 478.8 | 60.6 | 607.1 | 76.9 |
| **Grazing land** | 555.2 | 53.8 | 272.9 | 34.5 | 332.2 | 42.1 |
| **Forest** | 70.5 | 6.8 | 34.1 | 4.3 | 37.9 | 4.8 |

This analysis showed that the change in cropland and grazing land was hastened by the construction of the dam. Consequently, there is not much possibility for further expansion. In spite of this, the high population pressure of 98 people/ $km^2$ depends mainly on the extensive cereal based farming system that mounts pressure on the remaining fragile lands. Besides, 20 to 35% of the farm households, who have recently formed their own families, have already become landless [17]. Livestock and crop production activities compete rather than supplementing each other. Crop intensification is still lacking and improved livestock feed sources were not developed in the area either. In spite of these there has been no meaningful policy implementation which either regulates the livestock number or promotes the production of improved feed sources.

### 4.3 Implications of reservoir in Fincha'a watershed

The increase in cropland size in this watershed show that areas potentially subjected to accelerated erosion is increasing. Field observation showed a high sediment influx into the waterbody leading to reduced surface area of the reservoir. Many farmers started to grow potatoes and maize and graze their animals in the currently receded areas. This situation was not detected using the satellite image because this phenomenon must have been evident after the image was taken. Though the dam plays a significant role in supporting the national economy the rural community in Fincha'a watershed is not benefiting from the electricity generated. Besides, the key informants have reported that the reservoir and swamps have caused economic as well as environmental side effects to the community in the watershed area. For instance, often animals and sometimes human beings drowned in the swamps and reservoir. The swamps harbour birds and wild animals that attack agricultural crops and animals. When the watershed was with good vegetation cover, clean water was obtained from streams and springs the whole year round but now a days the water supply from these sources is short-lived. Streams often burst and cause habitat destruction. Hence, the water shortage for human and livestock and famine have become recent phenomena [1], [4].

## 5 CONCLUSION

Generally, the current land use situation of Fincha'a watershed is mainly the effect of the construction of the hydropower dam, population pressure and annual rainfall fluctuations. The reservoir has speeded up land use changes in this watershed. Grazing lands and forests have remained open access because there was no system in place that protects them from encroachment. Most of the available grazing lands are difficult to graze during rainy season because an increase in the reservoir level easily inundates them. The fact that a large proportion of the community is currently landless (others hold low farm sizes) and off-farm activities were not developed show that further undesired land use changes are expected in the future. The cropland expansion into grazing land and forest in Fincha'a watershed is also a common trend in the country [10], [21], [24] and other developing countries [14], [16], [20]. But the magnitude of change in cropland area that has occurred in Fincha'a watershed is very high compared to the many studies done elsewhere. The factors of land use changes in this watershed have been interacting in a very complicated ways, the overall implication being onsite environmental degradation and offsite sedimentation of water reservoir. Therefore, the changes in land use in this watershed could be a threat to the livelihood of the community and will affect the ability of the dam to deliver the planned economic benefits. Since Fincha'a is a tributary of the Blue Nile, the onsite and offsite effects of this watershed would be local and beyond. Therefore, implementation of suitable land use options also calls for the cooperation of all levels. For instance allocation of part of the revenue generated from the power generation on the development initiatives could be justifiable in terms of property rights and equity.

## ACKNOWLEDGEMENTS

Financial support for the study was obtained from International Foundation for Sciences, IFS and Wageningen University, the Netherlands.

## REFERENCES

[1] ASSEFA, K., 1994. Valuing environmental quality changes in Horro-Guduru: Field survey report, Wallaga, Ethiopia.
[2] ASSEFA, T., 2003. Hydropower development in Ethiopia: fact-sheet. Addis Ababa, Ethiopia.
[3] Bezuayehu, T. and de Graaff, J., 2005. Socio-economic impacts of creation of hydropower reservoir on upland farming in Fincha'a watershed, Ethiopia.
[4] DECHASSA, L., 2003: Surplus producing eastern highland parts of eastern Wallagga zone badly hit by current crisis. Assessment report submitted to the Office for the Coordination of Human Affairs, UN, Ethiopia
[5] DE WET, C., 1999: Displacement, resettlement, rehabilitation, reparation and development. Thematic Review, Social Issues 1.3. African Experience, South Africa. http://www.dams.org/.
[6] EEPCO (ETHIOPIA ELECTRIC POWER CORPORATION), 2002: EEPCo in brief. http://www.eepco.gov.et/.
[7] EFAP (ETHIOPIAN FORESTRY ACTION PROGRAM), 1994: The challenge for development. Vol. II. final report. Transitional Government of Ethiopia, Ministry of Natural Resources Development and Environmental Protection, Ethiopia.
[8] EL-SWAIFY, S.A., 2002: Impacts of land use change on soil erosion and water quality-A case study from Hawaii. In: Technology and method of SWC. Proceedings of 12th International Soil Conservation Organization Conference, May 26-31, 2002 Beijing, China. Volume III, Pp 267-270.
[9] FUGGLE, R., AND SMITH, W.T., 2000: Experience with dams in water and energy resources development in the People's Republic of China. Prepared for the World Commission on Dams. http://www.dams.org/.
[10] GETE, Z., 2000: Landscape dynamics and soil erosion process modelling in the North-western Ethiopian Highlands. African Studies Series A16, Geographica Bernensia, Berne, Switzerland. PhD thesis.
[11] HARZA ENGINEERING COMPANY, 1965: Appraisal of potential agricultural development. Fincha'a Project, Ethiopia. Report prepared for Water Resources Department, Ministry of Public Works and Communications, Imperial Government of Ethiopia. Volume III-Appendices.
[12] HARZA ENGINEERING COMPANY, 1966: Fincha'a project feasibility study. Report prepared for Water Resources Department, Ministry of Public Works and Communications, Imperial Government of Ethiopia. Volume II-Appendices.
[13] HARZA ENGINEERING COMPANY, 1975: Fincha'a Hydroelectric Project, Ethiopia. Civil design memorandum C-1. Report by HARZA Engineering Company, Washington D.C., USA.
[14] KAMMERBAUER, J., ARDON, C., 1999: Land use dynamics and landscape change pattern in a typical watershed in the hillside region of central Hunduras. Agriculture, Ecosystems & Environment. 75: 93-100.
[15] MESFIN, W., 1985: "Northern Shewa and Wello. Background paper on development strategy for the problem of vulnerability to famine. FAO, Ethiopia.
[16] MUNGAI, D.N., ONG, C.K., KITEME, B., ELKADUWA, W., SAKTHIVADIVEL, R. 2004: Lessons from two long-term hydrological studies in Kenya and Sri Lanka. Agriculture, Ecosystems and Environment 104:135-143.
[17] OADB (OROMIYA AGRICULTURE DEVELOPMENT BUREAU), 1996: Land resource and socio-economic survey report of Chomman watershed, Oromiya, Ethiopia.
[18] RITLER, A., 1997: Land use, forests and the landscape of Ethiopia, 1699-1865. An enquiry into the historical geography of central-northern Ethiopia. Soil Conservation Research Program and Centre for Development and Environment. Research report 38, Switzerland.
[19] ROODER, W., 1994: Human adjustments to Kainji Reservoir in Nigeria. New York/London: University Press of America.
[20] EMWAL, R.L., NAUTIYAL, S., SEN, K.K., RANA, U., MAIKHURI, R.K., ROA, K.S., SAXENA, K.G. 2004: Patterns and ecological implications of agricultural land-use changes: a case study from central Himalaya, India. 102: 81-92.
[21] SOLOMON, A., 1994: Land use dynamics, soil degradation and potential for sustainable sue in Mettu area, Iluababor region, Ethiopia. African Studies Series A13, Geographica Bernensia, Berne, Switzerland.
[22] SOLOMON, S., 1998: Hydropower of Ethiopia: Status, potential and prospects. Ethiopian Association of Civil Engineers (EACE) Bulletin Vol 1, No 1. Addis Ababa, Ethiopia.
[23] WCD (WORLD COMMISSION ON DAMS), 2000: Dams and development: A new framework for decision-making. An overview. Http://www.dams.org/.
[24] WOLDEAMLAK, B., 2003: Towards integrated watershed management in highland Ethiopia: the Chemoga watershed case study, Tropical Resources Management Papers 44, Wageningen, the Netherlands.

# Combining soil spectral reflectance data and satellite imagery to assess impacts of land use on soil fertility in Tajikistan

B. Wolfgramm[a], B. Seiler[b], D. Guntli[b], H. Liniger[a], K. Shepherd[c], M. Kneubühler[b] and T. Kellenberger[b]

[a] Centre for Development and Environment, Institute of Geography, University of Berne, Steigerhubelstrasse 3, 3008 Berne, Switzerland, email: Bettina.Wolfgramm@cde.unibe.ch
[b] Remote Sensing Laboratories (RSL), University of Zurich, Winterthurerstrasse 190, 8057 Zurich, Switzerland
[c] World Agroforestry Centre (ICRAF), P.O. Box 30677-00100, Nairobi, Kenya

## ABSTRACT

Recent studies showed that soil fertility properties can be predicted from soil spectral reflectance data and in a second step can be combined successfully with information from satellite imagery for rapid assessment of soil quality over large areas. This approach shall be adapted for a test area in the Loess zone of Tajikistan in order to assess the impact of land use on soil fertility. The groundtruth data collected confirms that widespread land use changes have taken place since 1992 (30 % of the area formerly used as grazing land has been cultivated since 1992). The newly cultivated areas are situated on steep slopes (the average slope is 20 %) and show visible signs of water erosion in 60 % of the cases observed. Also 48 % of the plots recorded from grazing land showed signs of water erosion. VIS-NIR measurements of soil samples collected from each sampling plot have been explored for relations between soil reflectance data and commonly used indicators of soil fertility in the study area. First results show that reflectance wavebands are strongly relating to $CaCO_3$ and soil colour. Regression tree modelling has been carried out successfully to calibrate total nitrogen contents determined by chemical analysis against reflectance wavebands (validation $r^2$ for regression was 0.71). A classification tree model predicting areas with water erosion shows the potential of decision tree modelling when combining different datasets. Hierarchical structures can be revealed and thresholds for mapping purposes using raster datasets available (DEM and Landsat 7 satellite imagery) can be determined. Prediction success determined by 10 fold cross-validation was 72 % and 61 % for the classes erosion and no erosion respectively.

**Keywords:** diffuse reflectance spectroscopy, land cover / land use, land degradation / conservation assessment, soil fertility, Tajikistan.

## 1 INTRODUCTION

In the 1990's increasing poverty triggered by the civil war and the transformation of the economy lead to widespread cultivation of steep slopes formerly used as grazing land. The starting point for this development, was March 1992 when the Presidential Decree “On Renting Land” authorized collectives ore state farms to rent and lease land to households for independent cultivation [1]. The foothills of western Tajikistan consist mainly of easily erodable Loess deposits. Water erosion is considered to be the fastest and most widespread degradation process [2]. Examples of farmers searching for alternative land management types with soil and water conservation (SWC) measures such as area closure by fencing, where vegetation cover has been increased several times, give an idea of the potential of the area with regard to sustainable land management [3].

Today governmental offices in Tajikistan lack the resources for monitoring land degradation at the national level and up-to-date information on the state of natural resources in the rainfed areas is not available. Cost and time efficient as well as reliable methods and combinations of methods for generating up-to-date information for assessments over large areas are needed.

The spectral library approach recently developed at the World Agroforestry Centre (ICRAF) in Kenya is designed for rapid determination of soil fertility properties for big numbers of samples, which is opening up opportunities for risk assessments. VIS-NIR measurements of air-dried soil samples carried out under standardized conditions in the laboratory have been calibrated to soil properties determined by chemical analysis for a wide range of African soils [4]. Further it has been shown that soil fertility indexes integrating commonly used agronomic indicators of soil fertility can be developed from reflectance spectral data and be calibrated to local conditions, allowing the spatial representation of soil fertility based on remote sensing satellite imagery [5].

This approach shall be adapted for a test area in the Loess zone of Tajikistan in order to assess the impact of land use on soil fertility. The objectives of this paper are: (i) to give an overview on crucial land cover/land use change and land degradation issues based on groundtruth data collected, (ii) to take first steps in adapting the spectral library approach to predict soil properties from spectral measurements to Tajik conditions and (iii) to test opportunities for mapping land cover/land use and land degradation/conservation classes by combining various datasets using classification tree modelling.

## 2 MATERIALS AND METHODS

### 2.1 The study area – general description

The three test areas of this study are all situated on the Loamy Loess and are defined as calcareous mountain cinnamonic soils by the local Tajik definition system. Typical values for soil particle size distribution are 5 % sand, 60 % silt and 25 % clay. $CaCO_3$ contents vary between 2 to 30 %, depending on the mother rock, but also on the state of erosion. In the topsoil average contents of TN are 0.15-0.25 % and soil organic carbon (SOC) 1-2 % [6]. Rainfall characteristics vary from the South with 400 mm per year to the Northeast with up to 900 mm. Rainfall distribution is alike in all the area and rains are concentrated during November through to April. The main crop is winter wheat. The fields are prepared (ploughed or harrowed) in November before the rains start. In rotation (every 2-4 years) flax, chickpeas and beans are planted. Since tractors cannot be driven along the contours of the steep slopes, fields are ploughed up and down, wherever tractors are available.

### 2.1 Overall study approach

Figure 1 gives an overview on groundtruth collected, materials used, methods applied and first results achieved that will be presented in this paper.

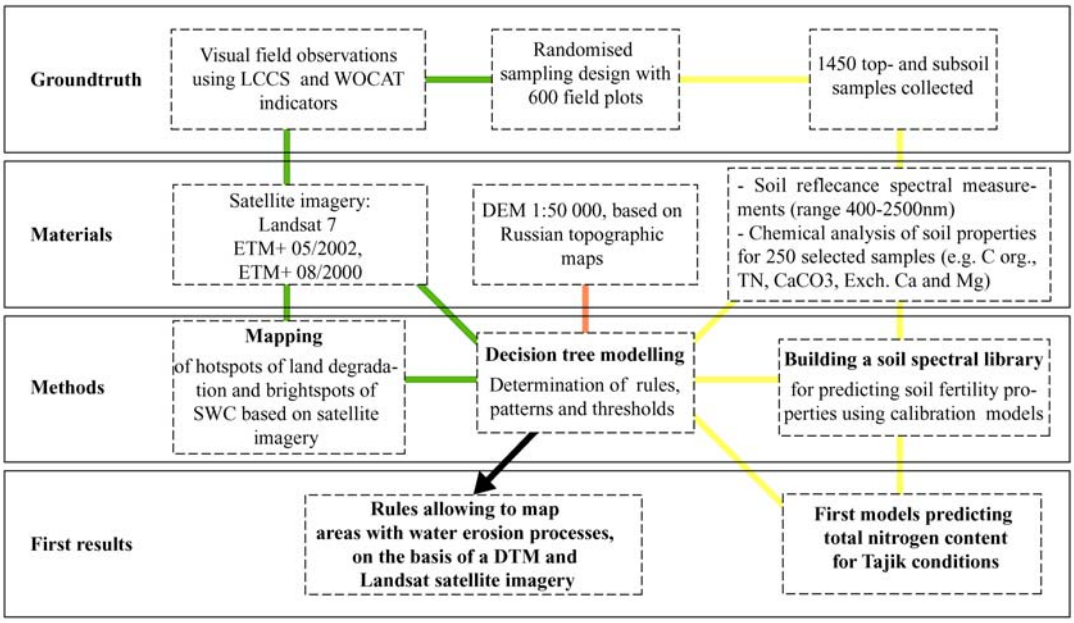


**Figure 1.** Overall approach

## 2.3 Rasterdata sets

The bases for mapping and analysis provide a digital elevation model (DEM) calculated from Russian topographic maps (1:50 000, 20 m equidistance) and Landsat 7 (ETM+) imagery from various years and seasons. Satellite imagery rectification was performed using GPS Ground Control Points measured in the field and additional control points extracted from Russian topographic maps. Differential GPS was not available. Residuals in x direction were for both Landsat 7 images on average 53 m, y-residuals amounted to 11 m for the image from 2002 and 20 m for the one from 2000. The atmospheric correction of the georeferenced images was conducted using ATCOR3 [7]. The main focus so far has been on the land cover/land use situation and the state of the soil in the years 2000. The state of fullest development of vegetation is represented by an image dating from 24.05.2002 and the situation after harvest, during the dry season and best visibility of bare ground is represented by an image dating from 22.08.2000. Given the importance of vegetation characteristics when assessing land degradation, the Optimised Soil Adjusted Vegetation Index (OSAVI) [8] was derived from the Landsat 7 satellite imagery. By adding the soil-adjustment parameter 0.16 it is attempted to minimize brightness-related soil effects. Surface reflectance for each sampling point was extracted from the Landsat 7 scene and from the DEM and served as input into land cover/land use and land degradation models.

## 2.4 Groundtruth

Test areas of 10x10km were selected based on a first assessment of seasonal changes in vegetation, approximated by information derived from the calculated OSAVI layers. This assessment based on the assumption that (i) if during the main vegetation period areas are showing no vegetation, it is a sign of severe degradation (hotspots) and (ii) on the other hand if after harvesting of rainfed crops, during the very dry months of July to October areas show dense vegetation this land use type is likely to conserve the land resources (brightspots). Test areas were placed in regions showing similar distributions of hot- and brightspots and representing different ecological zones.

A randomised sampling design as described by Walsh [9] was chosen for full characterization of the area, allowing geo-statistical and risk assessments. It included 600 plots, clustered in groups of 13 plots. These clusters were again distributed over the 3 test areas, each including 15 clusters. Plots size was approximately 30 by 30 m, corresponding with the pixel size of Landsat 7 scenes.

Groundtruth was collected for visible indicators of land degradation and conservation according to the World Overview on Conservation Approaches and Technologies (WOCAT) [10],[11] and land cover classes according to the FAO land cover classification system [12]. According to WOCAT land degradation characteristics the field protocol included water erosion, sediment deposition, crusting, cracks, compaction and mass movements. Conservation classes recorded were (typical examples from Tajikistan for each conservation class are given in brackets): Agronomic (e.g. contour ploughing), vegetative (e.g. grass strips, windbreaks consisting of poplar trees), structural (e.g. terraces introduced in Soviet times) and management measures (e.g. private area closure by fencing). Land cultivation history types have been determined in the field based on visible observations such as indicator plants, signs of ploughing and former field boundaries. The information noted down in the field was then compared or crosschecked against land use maps at a scale 1:10 000 dating from 1985. On each sampling plot topsoil (0-20 cm) and subsoil (20-50 cm) samples were collected as composite samples from two sampling pits. Soil chemical and physical analysis are being conducted at the laboratories of the World Agroforestry Centre (ICRAF) in Kenya using standard laboratory procedures. The following soil properties, expected to provide the basis for a soil fertility index for the study area, are being determined: C org., TN, pH, $CaCO_3$, Exch. Ca, Mg and K and soil particle size.

## 2.5 Building a Soil Spectral Library

The procedure is based on the method developed by Shepherd and Walsh [4] and includes the following steps: (i) sampling of soil variability within the target area, (ii) measuring of soil spectral reflectance, (iii) sampling of the spectral data space, (iv) acquiring soil attribute data on selected soil samples and (v) calibrating of soil property data to spectra applying multivariate calibration methods.

Air-dried and to 2 mm grinded soil samples were filled into Duran glass Petri-dishes and reflectance spectral readings were measured with a FieldSpec PRO FR spectroradiometer at wavelengths from 350 to 2500 nm at an interval of 1 nm. For standardization the samples were illuminated with an artificial light source from the bottom with a High Intensity Mug Light. In order to reduce differences in light scattering, samples was measured twice at angles differing by 90°.

## 2.6 Statistical methods

Pre-processing of the raw spectral data prior to statistical analysis was also carried out as described by Shepherd and Walsh [4]. The following steps were carried out: (i) resampling of relative reflectance spectra by selecting

every tenth nanometre in order to reduce the volume of data and to match it more closely to the spectral resolution of the instrument, (ii) transformation of the data by first derivative processing using a Savitzky–Golay filter for minimization of variation among samples caused by variation in grinding and (iii) omitting of spectral bands 350 to 380 nm, 970 to 1010 nm and 2460 to 2500 nm, since these bands have low signal to noise ratio or display noise due to splicing between the individual spectrometers [13]. Alternatively to first derivative processing Multiple Scatter Correction (MSC) was tested, but did not improve calibrations.

Selection of samples for chemical analysis was conducted based on principal component analysis on the first derivatives of soil spectral reflectance data using Unscrambler version 7.5 [14]. For each sampling cluster 6-7 samples were selected with regard to an even distribution of the samples over the range of first and second principle components.

Decision tree modelling was carried out using the software CART (Classification And Regression Trees) [15], based on binary recursive partitioning [16]. Decision tree models reveal the hierarchical structures of variables and indicator sets and determine thresholds for classification of data. Decision tree modelling was conducted (i) to build regression models for calibration of TN contents determined by chemical analysis against the 198-reflectance wavebands and (ii) to build classification models for mapping of hotspots and brightspots using information derived from available raster datasets for the plots where groundtruth had been collected. Rules and thresholds determined this way, serve for mapping with knowledge based imagery classification systems.First Results and Discussion

## 3 FIRST RESULTS AND DISCUSSION

### 3.1 Field observations

In a first attempt to gain an overview on the state of the land resources in the study area the data recorded in the field has been assessed focusing on land cover/land use, land use changes as well as water erosion processes. Since a random sampling scheme was applied, it is assumed that the dataset presented here is representative for the situation prevailing in the agricultural land of the test areas. Only the datasets from the test areas Faizabad and Yavan including two thirds of the data collected are being used here.

Land cultivation history has been classified as follows: (i) cultivation for more than 15 years / area being cultivated also during soviet times (ii) cultivation only started after 1992, (iii) cultivation started after 1992 but has been abandoned again and (iv) never cultivated. As can be seen from Table 1, since 1992 considerable land use changes took place: Of the recorded plots only 9 % have been cultivated already during soviet times. Today all in all 27 % of the area is managed, arable area. Additional 12 % of the land has been under cultivation since 1992, but cultivation has now been abandoned again. Therefore it can be assumed that on around 30 % of the total area, formerly used as grazing land (semi-natural and natural areas) ploughing has taken place since 1992.

**Table 1.** Distribution of the average slope steepness and the share of plots showing visible signs of water erosion with regard to major land cover class and land cultivation history type. The total number of observations is 316.

| **Major land cover class according to FAO-LCCS** | **Land Cultivation History Type** | **Distribution of Land Cultivation History Type recorded [%]** | **Average slope steepness, standard deviation in brackets [Slope %]** | **Percentage of plots within the specific LU class showing water erosion [%]** |
|---|---|---|---|---|
| Managed (arable) areas | Cultivated > 15 years | 9 | 14 (8.8) | 10 |
| | Cultivated since 1992 | 18 | 19 (10.1) | 61 |
| | **Total** | **27** | **18 (10.3)** | **43** |
| Semi-natural and natural areas | Abandoned | 12 | 22 (11.3) | 59 |
| | Never cultivated | 61 | 31 (15.5) | 48 |
| | **Total** | **73** | **29 (15.1)** | **50** |

Further more land turned into managed land after 1992 is situated on steep slopes. The figures in Table 1 show that areas still cultivated today are situated on slopes with an average of 19 % steepness, the areas now abandoned on slopes with an average of 22 %. Considering that only in 17 % of the managed land SWC measures such as

contour ploughing were observed, it is not surprising that 61 % of the plots cultivated since 1992 and 59 % of the plots now abandoned show visible signs of soil erosion. However also in 48 % of the semi-natural/natural areas that have never been under cultivation visible signs of erosion were recorded, indicating that pressure on the grazing land is also high.

## 3.2 Applying the soil sensing approach to new conditions

In order to explore relations between the variation in the soil spectra and in soil properties determined in the field or in the laboratory, first principal component (PC1) was plotted against the second (PC2), while the increase in the value of the soil property of interest is displayed by colours (light yellow to black). The principal component analysis was conducted on first derivatives of the soil spectral reflectance data. PC1 explains 52 % and PC2 24 % of the total variance in the spectral data. A thorough analysis for outlier detection should result in even better expressiveness of the principal components.

The left scatter plot in Figure 2 shows relations between principal components and spectral reflection at wavelength 2330 nm. This waveband has been identified as a strong $CaCO_3$ absorption peak [17]. High reflectance in the 2330 nm waveband indicating low $CaCO_3$ contents coincides also with soil samples of a hue value 5 determined by Munsel Colour Code. These soils are of dark red colour and originate from locations where plutonic mother rock is not covered by quaternary loess deposits. The plot shows the presence of systematic variation in the soil spectra that relates to the $CaCO_3$ absorption peak. The strong relationship between the soil spectra and the hue of the soil colour as well as the relationship to $CaCO_3$ content which is also effecting the soil colour is not unexpected, since the wavebands in the visible range are strongly influencing the principle components (apparent by the high loadings of these variables). Further more the 2330 nm waveband is not independent of the principle components, since it is also included in the principle component analysis.

The right scatter plot in Figure 2 shows increasing contents of TN measured in the lab in relation to the first two principle components. The relation for the data plotted here is weak, but thorough outlier detection and data transformations should improve the relationship.

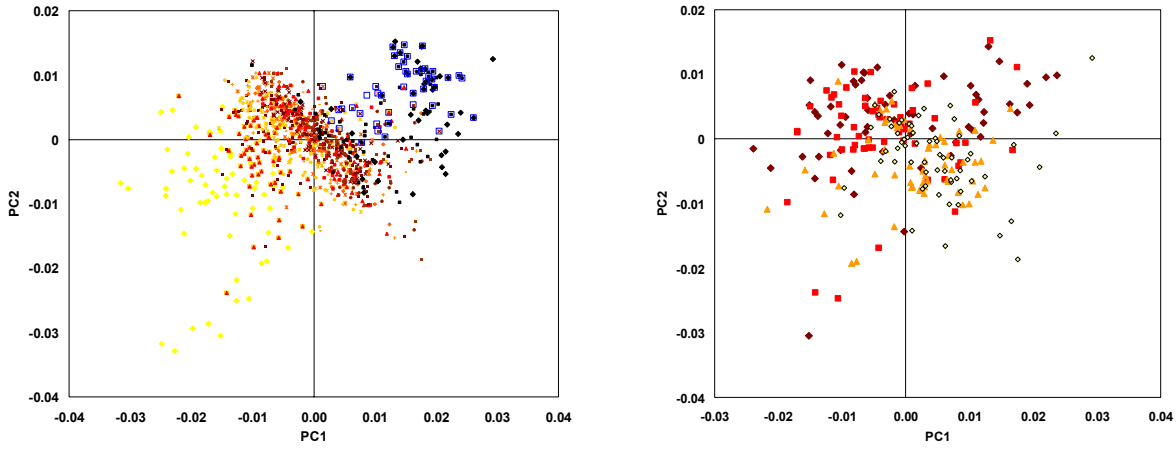


**Figure 2.** Scatter plots showing relations between variation in soil spectra and soil properties: variations in wavelength 2330nm, being a high $CaCO_3$ absorption peak, and hue of Munsel Colour Code (spots marked with a blue square) for 1050 samples on the left and measured contents of TN [%] for 250 soil samples on the right. Light marks indicating high and dark marks low contents of $CaCO_3$ and TN respectively.

First calibration models for prediction of soil properties to soil spectra have been elaborated for TN using the binary recursive partitioning method implemented in the software CART [15]. The scatter plot in Figure 3 shows actual and predicted values for TN calibration and validation datasets. The respective coefficients of determination are $r^2$=0.92 and $r^2$=0.71. 186 samples served for calibration, and 80 randomly selected holdout samples for validation.

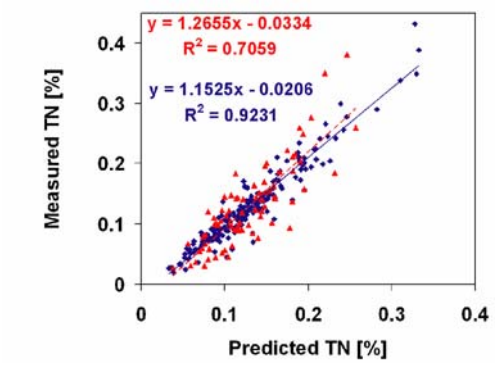


**Figure 3.** Calibration of soil properties to first derivative reflectance spectra using binary recursive partitioning modelling: Predicted values for TN plotted against measured TN contents: calibration (blue) and validation data (red).

As Shepherd and Walsh [4] explain, such level of prediction accuracy is sufficiently high when spatial and temporal variability of the soil property is large relative to the accuracy of its measurement. Moreover with regard to the inaccuracy of analytical results from Tajik laboratories today, it can be expected that the soil library approach will provide a reliable opportunity for accurate determination of soil properties over the long run.

## 3.3 Decision trees revealing rules for water erosion mapping

Characteristics of water erosion processes differ distinctively between semi-natural/natural and managed land cover classes. Therefore models for predicting areas with water erosion and without erosion have been run separately for the two types of land cover/land use classes. Several sets of splitting rules are available with CART. The Gini method typically produces best results [16], which was also true for the modelling conducted in this study. Prediction success was determined by 10 fold cross-validation. For the test data of the model presented in Figure 4 it is 61 % and 72 % for the cases no erosion and erosion respectively. Model input data consisted of (i) topographic information extracted from the DEM (slope, aspect, and curvature) (ii) Landsat 7 spectral information (band 1-5) of scenes dating from May 2002 and August 2000 and (iii) the vegetation index OSAVI calculated from these images. In addition to the raster information, the first principle components (PC1+2) calculated for the soil spectral reflectance data of topsoil samples, so far only available as point data, also fed into this model. From the 17 variables available, five layers were found most effective in splitting the data into nodes where cases of "erosion" or "no erosion" prevailed. Interesting that four of those layers contain mainly information on the presence and state of vegetation. The absence of topographic information supports the assumption that it is the land cover/land use characteristics that are decisive for the occurrence of soil erosion processes. The presence of the variable PC1+2 in this model suggests that soil spectral information is relating to the presence of water erosion in a specific area.

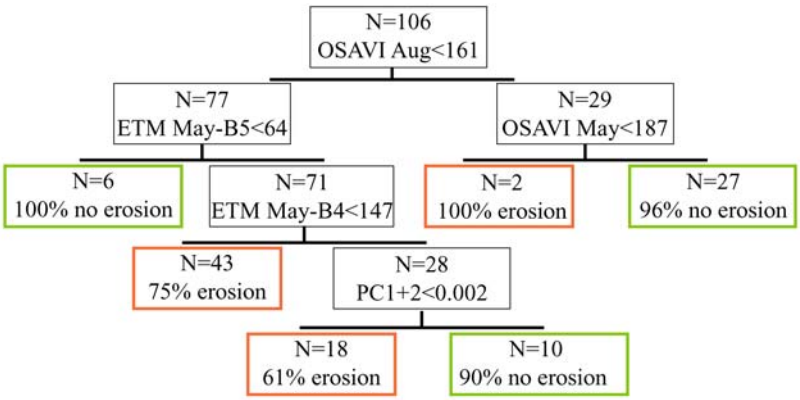


**Figure 4.** Tree model for mapping water erosion on cultivated areas (erosion or no erosion visible). Groundtruth was collected on 106 plots (N=number of plots). The abbreviations for input data used are as follows. Landsat 7 scene from May 2002 (ETM May), from August 2000 (ETM Aug), bands 4,5 (B4, B5), OSAVI (OSAVI), first and second principal components of soil spectral data (PC1+2). Percentages given in the end nodes represent the number of cases observed with regard to the total number of cases in the respective end node.

## 4 CONCLUSIONS

The groundtruth data shows that visible signs of water erosion can be observed in 50 % of the plots recorded. It further indicates that the risk for water erosion processes going on is high in areas that only after 1992 have been turned from grazing land into cultivated areas and are situated on rather steep slopes. It has been shown that variety in soil spectral reflectance data is relating to soil properties important for determination of soil fertility in the region, such as $CaCO_3$. Further a first model allowing to predict TN from soil spectral data shows a coefficient of determination of $r^2$=0.71, which can be considered a sufficient level of accuracy. These results are encouraging for providing efficient, stable and accurate methods for soil property determination in Tajikistan. First results from decision tree modelling for areas with visible signs of water erosion show that an index representing soil properties from spectra will be very helpful in mapping land degradation, especially so if such an index can be calibrated to Landsat 7 satellite imagery data as successfully done by Vagen et.al. [5].

## ACKNOWLEDGMENTS

The Soil Science Research Institute of the Tajik Academy of Agricultural Science has and is contributing to the study in scientific, administrative and organizational questions. The Remote Sensing Laboratory (RSL), Institute of Geography of the University of Zurich, provided the spectroradiometer. The investigations were supported by the National Centre for Competence in Research North-South (NCCR) / Individual Project 'Natural Resources and Ecology' (IP2), financed by the Swiss National Science Foundation (SNSF) and the Swiss Agency for Development and Cooperation (SDC).

## REFERENCES

[1] ADB, 2001: Agricultural Assessment Project (ASAP) Tajikistan. TA 3295 – TAJ. Revised Final Report, pp.48

[2] SADIKOV, KH.R. (ed.), 1999: Abstracts of the International Conference on Mountain regions of Central Asia. Sustainable Development Issues. Dushanbe, Tajikistan.

[3] ERGASHEV, M., WOLFGRAMM, B. AND NEKUSHOEVA, G., 2005: Individual Approach for Improving the Productivity of Grazing Land. In: Critchley W., Liniger H.P. (eds.): Local responses to global land degradation. (Forthcoming).

[4] SHEPHERD, K. AND WALSH, M., 2002: Development of Reflectance Spectral Libraries for Characterization of Soil Properties. *Soil Sci. Soc. Am. J. 66*, pp. 988–998.

[5] VÅGEN, T.-G., SHEPHERD, K. AND WALSH, M., 2004: Vis-Nir spectroscopy for characterisation of landscape level change in soil quality following deforestation and conversion in the highlands of Madagascar. *Geoderma* (submitted).

[6] KUTEMINSKIJ, V.J. AND LEONTEVA, R.S., 1966: Soils of Tajikistan [In Russian]. Dushanbe: Tajik Soil Science Institute, Ministry of Agriculture of Tajikistan.

[7] RICHTER, R., 2005: Atmospheric / topographic correction for satellite imagery", DLR IB 565-01/05, Wessling, Germany.

[8] RONDEAUX, G., STEVEN, M. AND BARET, F., 1996: Optimisation of soil-adjusted vegetation indices. *Remote Sensing of Environment, 55*, pp. 95–107.

[9] WALSH, M., 2004: Baseline and Project Monitoring Plan for the Western Kenya Integrated Ecosystem Management. Paper in progress, World Agroforestry Centre (ICRAF), Nairobi, Kenya.

[10] LINIGER, H.P. AND SCHWILCH, G., 2002: Better decision making based on local knowledge - WOCAT method for stainable soil and water management. *Mountain Research and Development Journal, 22 Vol. 1*

[11] LYNDEN VAN, G.W.J., LINIGER, H.P. AND SCHWILCH, G., 2002: The WOCAT mapping methodology, a standardized tool for mapping degradation and conservation. *Proceedings of ISCO Conference 2002*, Beijing.

[12] DI GREGORIO, A., AND JANSEN, L.J.M., 1998: Land Cover Classification System (LCCS): Classification Concepts and User Manual. FAO, Rome.

[13] ANALYTICAL SPECTRAL DEVICES INC., 1997: FieldSpecTM User's guide. Analytical Spectral Devices Inc., Boulder, CO.

[14] CAMO Inc., 1998: The Unscrambler user manual. CAMO Inc., Corvallis, OR.

[15] Breiman, L., Friedman, J., Olshen, R. and Stone, Ch., 1984: Classification and Regression Trees. Wadsworth, Pacific Grove.

[16] STEINBERG, D. AND COLLA, P., 1995: CART: Tree-Structured Non-Parametric Data Analysis. Salford Systems, San Diego, CA.

[17] GAFFEY, F.Y., 1986: Spectral reflectance of carbonate minerals in the visible and in near infrared (0.35-2.55um): calcite, aragonite and dolomite. *American Minerals 71*, pp. 151-162.

# Land degradation monitoring in the Ordos region, China

W. Wu[a], C. Zucca[a] and G. Enne[a]

[a] NRD, University of Sassari, Italy, email: wuwc@ephe.sorbonne.fr/nrd@uniss.it

## ABSTRACT

This paper presents our study on land degradation and sand-control monitoring by remote sensing in the Ordos region, China, aiming to introduce at the same time the successful experience in sand-control of the Chinese people to the world and draw attention of the international scientists and stakeholders to this arid land, of which 50% is desert and/or desertified land. Multitemporal Landsat images (MSS, TM and ETM+) were used for this monitoring research. The results show that combating desertification has been widely conducted in this region, especially, in the Mu Us Sandy Land and great success has been met with. However, land degradation has still taken place mainly in the non-controlled zones: grassland patches in the marginal areas are in disappearance and engulfed by deserts; deserts are in southeastward extension at a rate of 11-21m/year; degradation caused by overgrazing and collective grazing around water points is observed. It is concluded from this case study that desertification is produced by human activity, mainly grazing in this case and intensified and extended by climatic factors as aridity and wind blowing.

**Key words:** Remote sensing monitoring, Land degradation, Desertification control, Ordos region, China.

## 1 INTRODUCTION

As one of the important arid areas in China, the Ordos region is administratively composed of the whole Ordos Prefecture (8 counties) of Inner Mongolia, a part of the Yulin Prefecture (6 counties) of Shaanxi and a small part (3 counties) of Ningxia (figure 1). Extending from 106°15'E to 110°15'E in longitude and from 37°30'N to 40°50'N in latitude, the region covers around 114,000 $km^2$ of territory including the Mu Us Sandy Land in the south and Kubuqi Desert in the north and involves a population of about 2,890,000. Geomorphologically, it is named the Ordos Plateau surrounded with the Yellow River on the north and west and connected with the Loess Plateau on the south and east (figure 1). The region is located in the transitional belt between the arid grasslands and desert prairies where the vegetation is mainly shrub, semi-shrub and perennial herb.

There is abundant good-quality coal resource as well as natural gas reserve in this region. About 120 billion tones of coal reserve have been explored in the Dongshen-Shen(mu)fu(gu) Coal Field and 750 billion $m^3$ of gas have been measured in the Sulige Gas Field.

The annual precipitation is around 300 mm, 70% of which concentrates in the period July-September. Wind from the north-west blows 230 days, among which the ones exceeding Grade-8 occur more than 40 days per year. The hyper-concentration of rainfall and strong wind provoke soil erosion and water loss. Furthermore, long time human activity in grazing, agriculture, coal mining, deforestation and medicinal herb collection in the plateau has intensified land degradation and desertification [21]. It is said that the desertification is the major factor constraining the economic development in the region. Additionally, sand-dust storms, a process of wind erosion in the arid and hyper-arid zones and transported elsewhere by strong airflow, occur more and more frequently in the North of China in the recent years. This implies an ongoing spread of land degradation and desertification in the North and Northwest of the country, including the Ordos region. To stop these degradations, reduce the loss of economy, protect the security of life and wealth of the people and improve the environment, combating desertification is therefore the overwhelming task for both the governments and rural people.

The first sand-control was spontaneously undertaken in the Xiaotanzi village in Dianbian, Shaanxi by the villagers in 1950s (China Water Conservancy News, Aug.16, 2003). After a lot of failures, the locals finally found a method for sand-control by fixing sand movement using grass and/or shrub buried squarely (so-called sand-barrier) and then planting trees in these squares. In 1958, the first patches of forest miraculously appeared over the previously sand dunes on the village border. This experience was rapidly extended and reproduced in other parts in Mu Us. In the 1960s-70s, sand-control was organized by the central and local governments, especially, by the Bureaus of Forestry. Since 1980s, besides the governments, many individuals and enterprises have joined in this combating and some heroes and heroines, who are especially worthy of mention, occurred in the Ordos region:

NIU Yuqin (f), Jinjisha villager in Jianbian, Shaanxi, National Heroine and winner of an award from FAO in 1993;

SHI Guangyin (m), Haiziliang villager, Dianbian, Shaanxi, National Hero;
WANG Zhilan (f), Anbian villager, Dianbian, Shaanxi, National Heroine;
BAI Chunlan (f), Shabianzi villger, Yanchi, Ningxia, National Heroine;
WANG Youde (m), Farmer, Baijitan, Linwu, Ningxia, National Hero;
YIN Yuzhen (f), Farmer in Uxin, Inner Mongolia, National Heroine; etc.

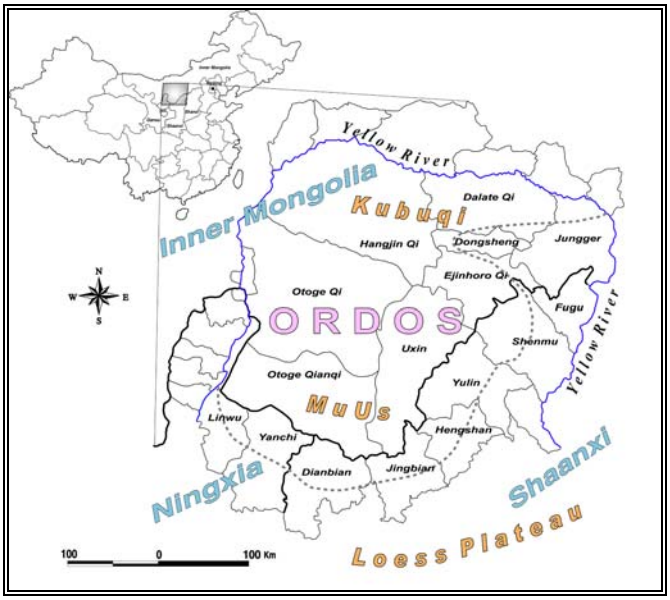


**Figure 1.** Location and administrative units of the study site.

Through near 50 years' efforts of the governments and rural individuals, land degradation has been to large extent controlled in the region, particularly, in the Mu Us Sandy Land and great success has been met with. However, problems as fund shortage for scientific researches and sand-control are encountered and land degradation is still in progress. This study is focused on land degradation and sand-control monitoring and evaluation by remote sensing technique. Another objective of the research is to introduce the successful experience of the Chinese people in combating desertification to the world and attract attention of the international scientists and stakeholders to this aridland.

**Table 1.** Landsat images used in the study.

| Path-Row | Acquisition dates | Haze | Path-Row | Acquisition dates | Haze | Path-Row | Acquisition dates | Haze |
|---|---|---|---|---|---|---|---|---|
| **129-32** | ETM 2000 June 11<br>TM 1989 Aug.24<br>MSS 1977 Sept.22 | 9.87<br>38.66 | **128-32** | ETM 2000 Nov. 11<br>TM 1991 Aug.7<br>MSS 1978 Aug.16 | 12.14<br>45.06 | **127-32** | ETM 2000 June 13<br>TM 1990 Aug.13<br>MSS 1979 Sept.1 | 19.23<br>39 |
| **129-33** | ETM 2001 Oct. 6**<br>ETM 1999 Aug.12*<br>TM 1989 Sep. 17*<br>TM 1987 Sep.20*<br>MSS 1978 Aug.21 | 31.06<br><br>85.54 | **128-33** | ETM 2000 Nov. 11<br>TM 1988 Sep.15<br>MSS 1978 Oct.9 | 9.98<br>36.42 | **127-33** | ETM 2002 Aug.6<br>ETM 2000 July 31*<br>TM 1989 Sep.11<br>TM 1986 Aug.2*<br>MSS 1978 Aug.19 | 17.86<br>19.66<br>45.5<br>68.58 |
| **129-34** | ETM 1999 Aug.12<br>TM 1989 Aug.24<br>MSS 1978 Aug.21 | 9.95<br>40.39 | **128-34** | ETM 1999 Sep.22<br>TM 1991 Aug.23<br>MSS 1978 Aug.20 | 12.92<br>38.75 | **127-34** | ETM 1999 Oct.17<br>TM 1990 Aug.29<br>MSS 1978 Aug.1 | 15.87<br>35.16 |
| **Note: (1) * inherited from the Sino-Belgian cooperation project, ** provided by Dr C. Künzer, others acquired freely from Landsat.org; (2) haze values in DC.** | | | | | | | | |

# 2 METHODOLOGY

## 2.1 Material

Multitemporal Landsat images dated 1970s (MSS), 1990s (TM) and 2000 (ETM+) were utilized in this study (table 1).

## 2.2 Approaches

To monitor land degradation and sand-control is in fact to detect land cover changes. Several change detection techniques such as delta data change detection, image differencing, post-classification comparison, ratioing, and change vector analysis, etc., are at present available [18]. As differencing and thresholding technique provides lower change detection errors when compared against other approaches [11], it is thus applied to this study.

The procedure to monitor changes in land cover is shown as follows:

### 2.2.1 Image-to-image rectification

The images of the frames 129-33, 129-34, 129-33 were geometrically corrected by the topographic maps on the scale of 1/200,000 to 1/300,000 in the datum WGS84 and projection UTM (48, 49) using polynomial model (3rd order) and bilinear re-sampling. The RMS error of the image-to-image rectification comes between 0.23 and 0.58 pixels. Other scenes were already orthorectified when acquired. Afraid of an inconformity of the orthorectified images with terrain, we used topographic maps on the scale of 200,000 and GPS points obtained from the field trips to verify it. It was found that the difference is less than one pixel. These orthorectified images can be made use of directly.

### 2.2.2 Atmospheric correction

An image-based approach was introduced in this study.

Chavez [2, 3] proposed a DOS (dark-object subtraction) model and its ameliorated version — COST model in 1996. A key point in his method is to determine the haze value to be removed. The traditional way to obtain the haze value is to measure the radiance in some deep clear water or shaded areas in image where the radiance in near infrared bands is zero or near zero. Any over-zero value is considered to be a result of scattering and path radiation. Such haze removal often produces over-correction and is not applicable to the image where dark-object does not exist [4]. In this study, the 4th tasselled cap feature [5, 6, 7] was used to estimate the haze value (table 1). The scattering effect was removed from each band according to Chavez [3]. Detailed procedure can be seen in Wu [17, 18]. Then the COST model was followed to correct sun elevation and sun-earth distance effect and at the same time transform the at-satellite radiance into the surface feature reflectance based on the following formula:

$$R_s = \frac{\pi(L_{sat} - L_{haze})}{E_0 \cos^2 \theta} \tag{1}$$

where $R_s$ — spectral reflectance of the surface;
$L_{haze}$ — haze effect, for example, path radiance ($Wm^{-2}\,sr^{-1}\mu m^{-1}$);
$E_o$ — solar spectral irradiance on a surface perpendicular to the sun's rays outside the atmosphere ($Wm^{-2}\,\mu m^{-1}$). $E_o$ contains the Earth-Sun distance term that is in astronomical units (AUs are a function of time of year and range from about 0.983 to 1.017) (see [1].
$\theta$ — solar zenith angle
$L_{sat}$ — at-satellite spectral radiance for the given band ($Wm^{-2}\,sr^{-1}\mu m^{-1}$). It has the following relationship with the digital counts of pixel [4, 14]:
$L_{sat}$ = ((*Lmax* – *Lmin*)/Maximum DC)* DC + *Lmin*

where *Lmax* represents the spectral radiance scaled to the maximum digital number (DC), *Lmin* is the spectral radiance to the minimum DC (see [14, 1]).

### 2.2.3 Multispectral transformation

NDVI and other vegetation indices have been widely used in land cover change detection. The tasseled cap transformation, developed for MSS data by Kauth *et al*[12] and extended to the TM images by Crist *et al*.[5, 6, 7], has been successfully applied in the Sino-Belgian cooperation project (1999-2001) [20, 17, 18, 19]. However, Huang *et al*. [10] reproduced the tasseled cap coefficients for Landsat ETM+ data. Two sets of coefficients produce incompatible features. For prudence, this transformation was out of selection this time and the Soil-Adjusted

Vegetation Index (SAVI) developed by Huete [9] was chosen for highlighting the vegetation cover information. This index is formulated as:

$$SAVI = (1+L)\frac{NIR - R}{NIR + R + L} \tag{2}$$

where, NIR and R are reflectance values of the near-infrared and red bands and L an adjustment factor ranging from 0 to 1. For low vegetation density, L = 1, for intermediate vegetation density L = 0.5 and for higher vegetation density L = 0.25. Huete [9] said that for any adjustment factor from 0.25 to 1, soil influences were considerably reduced in comparison to the NDVI and PVI. For the Ordos region, L can be set to 1.

### 2.2.4 Indicator differencing and thresholding

A differencing processing was applied to the atmospherically corrected SAVI between two dates followed by a thresholding technique. Thus the negative and positive changes of vegetation cover or vigour were distinguished.

For the scenes 128-32, 128-33, the recent images were acquired in November. Any transformation can not amplify the vegetation information. Thus band 7, of a significant difference between vegetated and non-vegetated land cover, was used for differencing and thresholding.

### 2.2.5 Change extraction

Step 2.2.4 produces photosynthetic change information in vegetation cover. These positive and negative changes include a lots of false change such as conversion from cropland to fallow land or from fallow land to farmland. These are not true changes and have been excluded by visual comparison. Finally, vegetation degradation, land salinisation, desert extension, cropland extension and sand-control were identified and mosaicked.

## 3 RESULTS AND DISSCUSION

The remote sensing processing results are shown in figure 2 and depicted as follows:

### 3.1 Sand-control

It is observed that sand-control has been widely undertaken in the Ordos region, especially, in the Mu Us Sandy Land. Not only small patches of sand dunes but also parts of large deserts in Otoge Qianqi, Uxin Qi, and Dianbian, Jianbian and Yulin Counties have been successfully vegetated or controlled. A part of the controlled land has been used for grazing and farming since 1980s (see figures 3 and 4 as zooms 1 and 2 in figure 2).

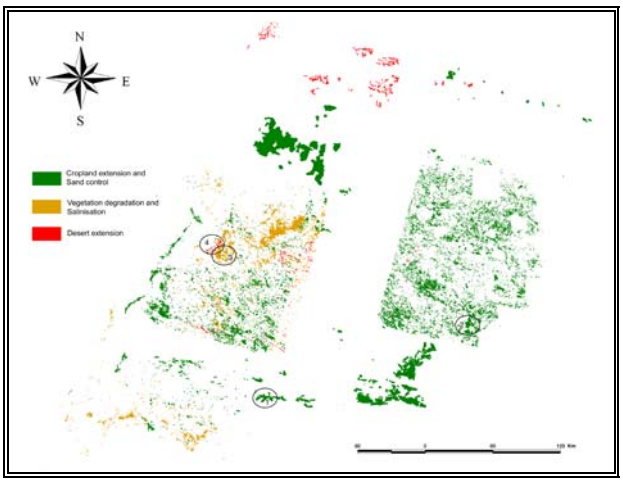


**Figure 2.** Land degradation and sand-control in the Ordos region.

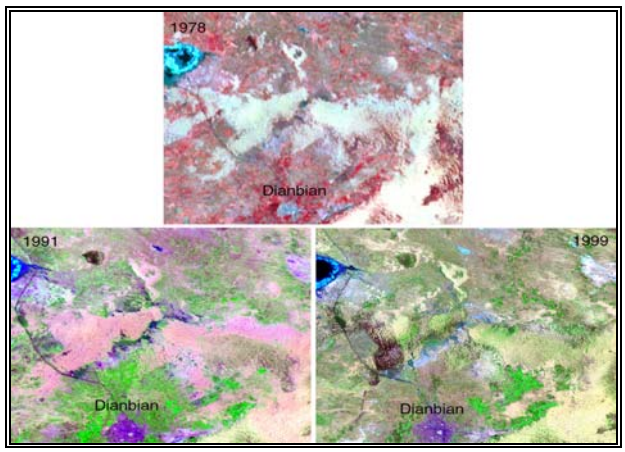


**Figure 3.** Showing sand-control on the sand dunes before 1978 and after 1991 around Dianbian town (zoom 1 in figure 2). Note: Two national hero and heroine namely SHI Guangyin and WANG Zhilan have been contributing themselves to the sand-control enterprise in Dianbian County since 1983.

Totally, 3421km$^2$ of desert and desert patches have been identified as a photosynthetically controlled areas (scenes 128-32, 128-33 are not included). In fact, lots of recent combating management can not be revealed by vegetation indicator differencing due to its weak greenness or low density. In addition, many parts of deserts had been already managed before 1980. An example can be seen in figure 3. Both these two cases can not be reflected by this change detection. The real controlled area since 1950s would be much larger than the one detected. If some earlier aerial photos and more recent images dated 2004 and 2005 were available, the monitoring would be more pertinent.

In sand-control, local people plant trees (particularly poplar and Chinese pine) and shrub such as sand-willows, ningtiao (in Chinese pronunciation), sand-artemisia, seabuckthorn, ephedra, licorice and so on, on the sand squares fixed by the buried straw, namely sand-barrier. Such netlike tree-shrub-grass belts together with some arid-resistant techniques have played a good part in combating desertification. The shrub e.g., sand-willow, can be used as fuel and also for production of artificial boards. Ephedra is the major material for refining ephedrine. Licorice is a general Chinese medicinal herb. **Therefore sand-control not only stops desertification, desert extension and improves the environment but also produces economic value**.

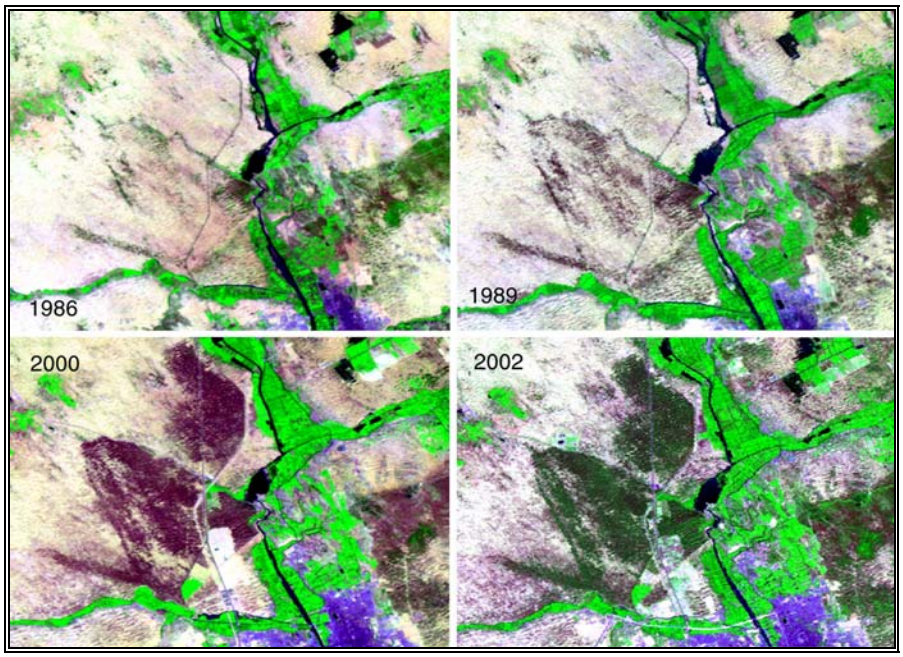


**Figure 4.** Success in desert control since 1980s — vegetation cover development on the sand dunes from 1986 to 2002 near Yulin city, Shaanxi (zoom 2 in figure 2).

## 3.2 Land degradation

Although desertification has been largely combated in the whole region, several kinds of land degradation were observed, especially, in the west parts of the Mu Us Sandy Land and Kubuqi Desert:

### 3.2.1 Grassland in degradation

Some small pieces of grassland on the marginal belts in Otoge Qianqi and Otoge Qi are in degradation and engulfed gradually by desert (figures 5 and 6) and a large surface of grassland becomes nude (brown color in figure 2). Some round bare patches occurred in the grassland (figure 5).

Besides the practice in desertification control, some land use policy as “grazing rotation in zoned areas” is also implemented so as to protect the pastoral land. The photosynthetic vegetation degradation does not seem to be a climate-related phenomenon but a result of overgrazing in these zoned areas and collective grazing around water points. This remains to be further verified later.

### 3.2.2 Deserts in extension

The southward encroachment of the Mu Us Desert at a velocity of several km/year as reported by the media in China in 1990s was not observed in the geomorphologically transitional zones between the deserts and the Loess Plateau. However, it is noted that the **deserts or patches of sand dunes especially in the non-controlled zones are in southeastward extension** (red color in figure 2). Taking the west margin of the Mu Us Sandy Land for

example (figure 5), in the periods 1978-1987 and 1987-1999, the deserts and small patches of sand dunes extended respectively 4-8 pixels and 3-6 pixels (1 pixel = 28.5m) and swallowed the grassland in the mentioned direction. We used the ETM+ image dated 2001 to verify whether such extension still continues or not in the recent years. The result is that they advanced again 1-2 pixels from 1999 to 2001. Clearly, this extension is due to the wind action from northwest. As shown in section 1, the wind from this direction blows 230 days per year. Driven by the wind, the deserts have encroached 250-480m in the past 23 years, at an advancing rate of 11-21m/year.

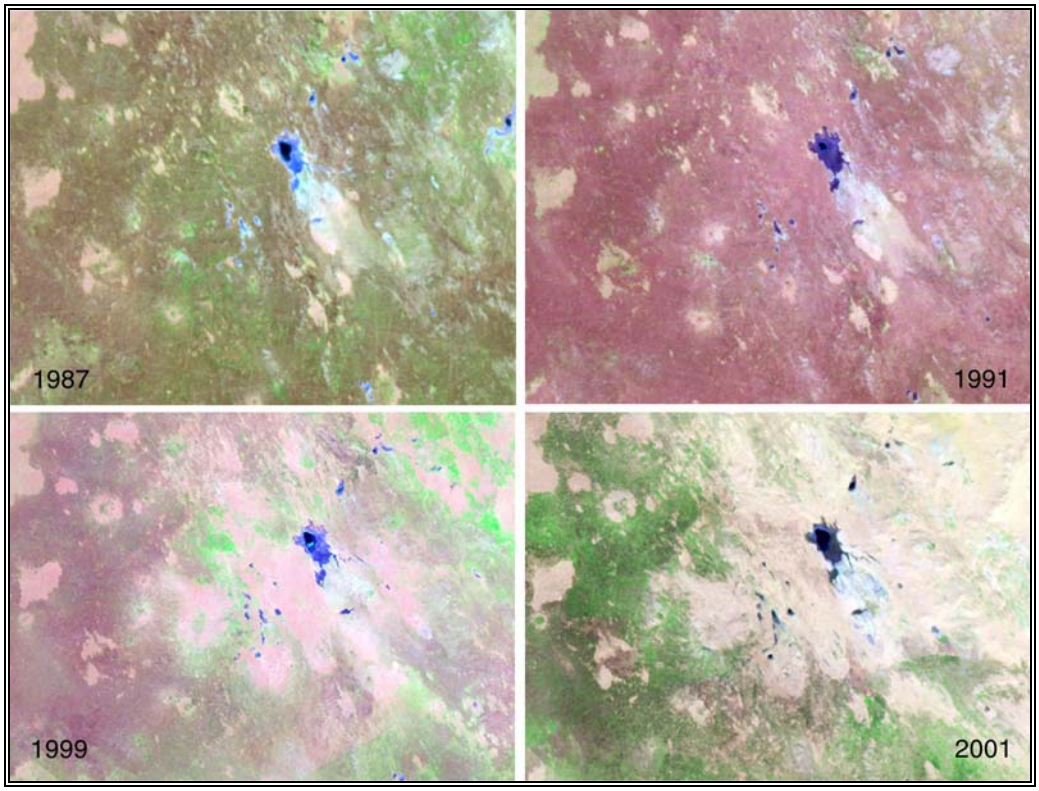


**Figure 5.** Grassland in degradation and round bare patches in extension in west Mu Us (zoom 3 in figure 2).

It is also observed that such extension of deserts and sand dune patches are even more rapid in the marginal zones of the Kubuqi Desert (figure 2). However, such advancement was not detected in Yulin, Jianbian in north Shaanxi. This implies the great success in sand-control in these counties.

### 3.2.3 Salinisation

From the Landsat images, salinisation (brown color in figure 2) was observed but mainly in Yanchi, Linwu, and Dianbian counties, where grassland has been converted into farmland. It is thus an agricultural activity related degradation phenomenon.

Some other analyses on land use changes such as farmland extension, urbanization and coal mining and their driving forces in North Ningxia and North Shaanxi have been reported [20, 17, 18, 19].

## 3.3 Discussion

This research is an effective attempt on land desertification monitoring by remote sensing. Unfortunately, the recent images of the scenes 128-32 and 128-33 were acquired in winter so that much information in land degradation and sand-control in the Kubuqi Desert could not be extracted. This shortcoming is expected to be improved later when a financial support is available. Moreover, the desertification in progress and sand-control work completed in the recent years are “subtle changes” in land cover and can not be reflected by Landsat images due to the 30m resolution and weak vegetation vigor. This has to certain extent reduced the monitoring accuracy. Some polite sites are suggested to use higher resolution images like SPOT or airphotos to distinguish such changes.

Out of remote sensing, some serious problems have been confronted with in sand-control. Sand-control itself, to plant shrub or tree or grass in the sand dunes, is a hard practice. Some incredibly intentional forest destroy events

have happened in this region. Almost all the national heroes and heroines mentioned above have suffered such problem due to a conflict with other local people's interests.

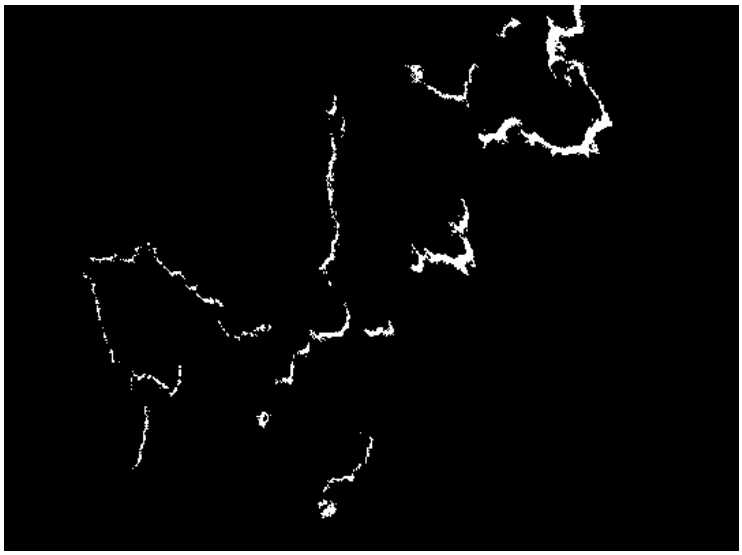

**Figure 6.** Showing desert southeastward extension (zoom 4 in figure 2).

Furthermore, sand-control is faced with a difficulty to go ahead for both the local governments and the individual heroes or heroines owing to a lack of financial support, especially for the latter, who have invested heavily in this combating enterprise and brought wealth to the villagers but themselves as loanees of banks have run into debt. Through long time of practice, it is found that some cheap species of trees as poplar are not suitable for combating desert owing to poor land quality. Some other types as zhangzisong (in Chinese) are effective for this purpose but expensive. Without aid, sand-control becomes hard. The improvement of this situation depends on whether there are some other funding sources.

## 4 CONCLUSIONS AND PROSPECTS

(1) Sand-control has been widely conducted and environment to certain degree improved in the region, especially, in the Mu Us Sandy Land.

(2) Land degradation in the following forms was observed mainly in the non-controlled zones but also in the earlier managed land:

- Grassland patches in the marginal areas are in disappearance and engulfed by deserts;
- Deserts are in southeastward extension at a rate of 11-21m/year, along the wind blowing direction;
- Degradation caused by overgrazing in zoned areas and collective grazing around water points is noted. This conclusion is different from that of Hanan *et al* [8], who carried out a desertification assessment in Sahel, Africa.

(3) The Ordos region is one of the best sites for desertification and sand-control study in the world.

(4) It is concluded from this case study that desertification is produced by human activity, mainly grazing in this case, and intensified and extended by climatic factors as wind blowing.

This is a tentative monitoring by remote sensing. If there is a continuation of financial support, the monitoring will be conducted at depth; more field investigations and verification will be undertaken; better understanding on the driving forces of land degradation will be reached by linking remote sensing with human activity; socio-economic and biophysical indicators for assessing desertification [15, 16] will be produced; a multidisciplinary monitoring system will be established and the sustainable development will be assessed.

## ACKNOWLEDGMENTS

A part of Landsat images were inherited from the Sino-Belgian cooperation project on land use and land cover changes (1999-2001) in the University of Louvain, Louvain-La-Neuve, Belgium. Other scenes were acquired from

## REFERENCES

[1] CHANDER, G. and MARKHAM, B., 2003: Revised Landsat 5 TM radiometric calibration procedures and post-calibration dynamic ranges, http://landsat7.usgs.gov/documents/L5TMCal2003.pdf.

[2] CHAVEZ, P. S., Jr., 1975: Atmospheric, solar and M.T.F. corrections for ERTS digital imagery, *Proceedings of American Society of Photogrammetry Fall Conference,* Phoenix, Arizona, pp.69.

[3] CHAVEZ, P. S., Jr., 1988: An improved Dark-Object Subtraction Technique for Atmospheric Scattering Correction of Multispectral Data, *Remote Sensing of Environment*, Vol. 24, pp.459-479.

[4] CHAVEZ, P. S., Jr, 1996: Image-Based Atmospheric Correction — Revisited and Improved, *Photogrammetric Engineering and Remote Sensing,* Vol. 62, No., 9, pp.1025-1036.

[5] CRIST, E. P., CICONE R. C., 1984a: Aplication of the Tasseled Cap Concept to Simulated Thematic Maper Data, *Photogrammetric Engineering & Remote Sensing*, Vol.50, No.3, pp.343-352.

[6] CRIST, E. P., CICONE, R. C., 1984b: A Physically-Based Transformation of Thematic Mapper Data — The TM Tasseled Cap, *IEEE Transaction on Geoscience and Remote Sensing*, Vol. GE22, No.3, pp.256-263.

[7] CRIST, E. P., LAURIN, R., and CICONE, R. C., 1986: Vegetation and soil information contained in transformed Thematic Maper data, in *Proceedings of IGARSS'86 Symposium,* p.1465-1470, Ref. ESA SP-254, European Space Agency, Paris.

[8] HANAN, N. P., PREVOST, Y., DIOUF, A., and O. DIALLO, 1991: Assessment of desertification around deep wells in the Sahel using satellite imagery, *Journal of Applied Ecology*, Vol. 28, pp.173-186.

[9] HUETE, A. R., 1988: A Soil-Adjusted Vegetation Index (SAVI), *Remote Sensing of Environment,* 25, pp.295-309.

[10] HUANG C., WYLIE B., YANG L., HOMER, C. and ZYLSTRA, G., 2002: Derivation of a Tasseled Cap transformation based on Landsat 7 at-satellite reflectance, USGS (http://landcover.usgs.gov/pdf/tasseled.pdf.)

[11] JENSEN, J.R and TOLL, D.R., 1982: Detecting residential land use development at the urban fringe, *Photogrammetric Engineering and Remote Sensing*, 48, pp.629-643

[12] KAUTH, R. J. and THOMAS, G. S., 1976: The Tasseled Cap — a graph description of the spectral-temporal development of agricultural crops as seen by Landsat. *Proceedings of the 2nd International Symposium on Machine Processing of Remote Sensed Data*, Purdue University, West Lafayette, Indiana, p.4B41-4B51.

[13] LAMBIN, E. F., 1994: *Modelling deforestation processes* (A Review). Tropical ecosystem environment observations by satellites, TREES series B: Research Report n°1, EUR15744EN, pp.45-101.

[14] NASA*, Landsat 7 Science data Users Handbook*, 2000 (http://Itpwww.gsfc.nasa.gov/IAS/handbook).

[15] PULINA, G., D'ANGELO, M., MADRAU, S., ZUCCA, C. AND ENNE, G., 1998: Indicators of land use intensity in agropastoral ecosystem. In: Enne, G., D'Angelo, Zannolla, C. (ed.): Indicators for assessing desertification in the Mediterranean, pp.177-185, Università di Sassari, Italy.

[16] PULINA, G., D'ANGELO, M., ZUCCA, C., 2000: Methdologies to prevent and mitigate land degradation phenomena in Mediterranean agrosilvopastoral systems. In Enne, G., Zanolla, Ch. And Peter, D. (ed.): Desertification in Europe: mitigation strategies, land-use planning, pp.199-205, European Commission.

[17] WU, W., 2003a: Evaluation on land use and land cover changes in north Shaanxi, China. *Photo-Interpretation,* 36(2), pp.15-29, plates pp.35-45.

[18] WU, W., 2003b: Application de la géomatique au suivi de la dynamique de l'environnement en zones arides, PhD dissertation, Université de Paris 1, France.

[19] WU, W., 2004: Land use and cover changes in the critical areas in northwestern China. In: O. Manfred, D. Guido (ed): *Remote Sensing for Agriculture, Ecosystems, and Hydrology V*, Proceedings of the SPIE, 5232, pp. 245-256.

[20] WU, W., LAMBIN, E. F. and COUREL, M.-F., 2002: Land use and cover change detection and modeling for North Ningxia, China, *Proceedings of Map Asia 2002*, Bangkok, Thailand, Aug.6-9, 2002.
http://www.gisdevelopment.net/application/environment/overview/envo0008.htm

[21] WU, W. and ZHANG, W., 2003: Present land use and cover patterns and their development potential in North Ningxia, China, *Journal of Geographical Sciences*, 13 (1), pp.54-62.